MycoKeys 75: 1–29 (2020)
doi: 10.3897/mycokeys.75.53673
https://mycokeys.pensoft.net

RESEARCH ARTICLE

A peer-reviewed open-access journal
MycoKeys
Launched to accelerate biodiversity research

Taxonomic revision of *Russula* subsection *Amoeninae* from South Korea

Komsit Wisitrassameewong[1,2], Myung Soo Park[1], Hyun Lee[1,9], Aniket Ghosh[3], Kanad Das[4], Bart Buyck[5], Brian P. Looney[6], Miroslav Caboň[7], Slavomír Adamčík[7], Changmu Kim[8], Chang Sun Kim[9], Young Woon Lim[1]

1 *School of Biological Sciences and Institute of Microbiology, Seoul National University, Seoul 08826, South Korea* **2** *National Biobank of Thailand (NBT), National Science and Technology Development Agency (NSTDA), Thailand Science Park, Thanon Phahonyothin, Tambon Khlong Neung, Amphoe Klong Luang, Pathum Thani 12120, Thailand* **3** *Department of Botany & Microbiology, H.N.B. Garhwal University (A Central University), Srinagar, Garhwal, 246174, Uttarakhand, India* **4** *A.J.C. Bose Indian Botanic Garden, Botanical Survey of India, P.O. Botanic Garden, Howrah 711103, India* **5** *ISYEB (CNRS, Sorbonne Université, EPHE) Institut de Systématique, Évolution, Biodiversité, Muséum national d'Histoire naturelle, case postale 39, 57 rue Cuvier, F-75231 Paris cedex 05, France* **6** *Department of Biology, Duke University, Durham, NC 27708, USA* **7** *Plant Science and Biodiversity Centre, Slovak Academy of Sciences, Dúbravská cesta 9, SK-845 23, Bratislava, Slovakia* **8** *Microorganism Resources Division, National Institute of Biological Resources, Incheon 22689, South Korea* **9** *Forest Biodiversity Division, Korea National Arboretum, Pocheon-si, Gyeonggi-do 11186, South Korea*

Corresponding author: Young Woon Lim (ywlim@snu.ac.kr)

Academic editor: Zai-Wei Ge | Received 27 April 2020 | Accepted 9 October 2020 | Published 9 November 2020

Citation: Wisitrassameewong K, Park MS, Lee H, Ghosh A, Das K, Buyck B, Looney BP, Caboň M, Adamčík S, Kim C, Kim CS, Lim YW (2020) Taxonomic revision of *Russula* subsection *Amoeninae* from South Korea. MycoKeys 75: 1–29. https://doi.org/10.3897/mycokeys.75.53673

Abstract

Russula subsection *Amoeninae* is morphologically defined by a dry velvety pileus surface, a complete absence of cystidia with heteromorphous contents in all tissues, and spores without amyloid suprahilar spot. Thirty-four species within subsection *Amoeninae* have been published worldwide. Although most *Russula* species in South Korea have been assigned European or North American names, recent molecular studies have shown that *Russula* species from different continents are not conspecific. Therefore, the present study aims to: 1) define which species of *Russula* subsection *Amoeninae* occur on each continent using molecular phylogenetic analyses; 2) revise the taxonomy of Korean *Amoeninae*. The phylogenetic analyses using the internal transcribed spacer (ITS) and multilocus sequences showed that subsection *Amoeninae* is monophyletic within subgenus *Heterophyllidiae* section *Heterophyllae*. A total of 21 *Russula*

subsection *Amoeninae* species were confirmed from Asia, Australia, Europe, North America, and Central America, and species from different continents formed separate clades. Three species were recognized from South Korea and were clearly separated from the European and North American species. These species are *R. bella*, also reported from Japan, a new species described herein, *Russula orientipurpurea*, and a new species undescribed due to insufficient material.

Keywords
Amoeninae, *Heterophyllae*, multilocus phylogeny, *Russula orientipurpurea*, species delimitation

Introduction

Russula Pers. is the largest genus in the family Russulaceae, with at least 2,000 described species worldwide (Adamčík et al. 2019). Compared to most other genera of Basidiomycetes, *Russula* has complex morphological and chemical features (Buyck et al. 2018). The initial period of diversification of the genus has been inferred as occurring in temperate regions of the Northern hemisphere, though there is some debate as to its origin given its high diversity in tropical areas (Looney et al. 2016; Buyck et al. 2018). Recent molecular studies have recognized eight subgenera within the genus: *Russula* subg. *Archaeae* Buyck & V. Hofst., *R.* subg. *Brevipedum* Buyck & V. Hofst., *R.* subg. *Compactae* (Fr.) Bon, *R.* subg. *Crassotunicatae* Buyck & V. Hofst., *R.* subg. *Glutinosae* Buyck & X.H. Wang, *R.* subg. *Heterophyllidiae* Romagnesi, *R.* subg. *Malodorae* Buyck & V. Hofst., and *R.* subg. *Russula* (Buyck et al. 2018; Buyck et al. 2020).

In the field, specimens of *Russula* subsection *Amoeninae* Buyck are identified by their velvety pileus surface and stipe, white spore print, mild taste, and stipe flushed with pink, red, or purple. Microscopically, species of *Amoeninae* display subglobose spores, typically with prominent amyloid and reticulate ornamentation but without amyloid suprahilar spot. Moreover, the basidiomes completely lack gloeocystidia, and both pileipellis and lamellar edges have large subulate hyphal terminations often arising from short unbranched cells (Buyck 1988, 1994). Because of the complete absence of gloeocystidia, Sarnari (1998) altered the rank of this subsection to subgenus, proposing *Russula* subg. *Amoenula* Sarnari. Recent multilocus phylogenetic studies, however, have shown that *Amoeninae* is in fact a small part of *R.* subg. *Heterophyllidiae* section *Heterophyllae* (see position of *R. violeipes* Quél. and *R. mariae* Peck in Buyck et al. 2018).

To date, 34 species have been published worldwide within *Russula* subsection *Amoeninae* (Suppl. material 1: Table S1), some of which were not originally placed in this group (e.g. *R. diversicolor* Pegler, *R. epitheliosa* Singer, and *R. variegata* Romagn.). However, their microscopic features are very similar to those of other *Amoeninae* species. Three species have been reported from Europe: *R. amoena* Quél., *R. amoenicolor* Romagn., and *R. violeipes* Quél. (Sarnari 1998). Although no relevant molecular studies have been performed that include species from North America, previous studies using morphological data have listed 14 species for this area (Suppl. material 1: Table S1). Regarding the tropics, *R. diversicolor* and *R. epitheliosa* were reported from neotropical

areas of Latin America (Buyck 1988), as were six species from tropical areas of Africa (Buyck 1994; Buyck and Sharp 2007) and Madagascar (Heim 1938), and two species from arid areas of Australia (Lebel and Tonkin 2007, Hyde et al. 2016). Finally, six species native to Asia have been described, two from East Asia (Chiu 1945; Hongo 1968), and four from India (Das et al. 2005, 2017; Crous et al. 2016; Hyde et al. 2016).

Historically, taxonomic studies of *Russula* in Asia have been influenced by European or North American literature. That is why *Russula* species from Asia were often assigned names of morphologically similar counterparts from Europe or North America. However, recent molecular studies have revealed that many Asian *Russula* species are in fact not conspecific with European or North American species (Park et al. 2014; Lee et al. 2017; Paloi et al. 2018; Song et al. 2018). Although molecular data can provide additional information that may result in more robust phylogenies (Hebert et al. 2003; Savolainen et al. 2005; Hibbett et al. 2016; Adamčík et al. 2019), the use of this type of data may be hampered by misidentifications when there are limited reference databases or when low-resolution markers are used (Hofstetter et al. 2019).

The present study aims to: 1) clearly distinguish species of *Russula* subsection *Amoeninae* from different continents through a phylogenetic analysis using updated sequence data; and 2) revise the taxonomy of Korean *Amoeninae* based on materials obtained from recent collections from different habitats and areas of the Korean peninsula. Four *Amoeninae* species were reported in South Korea: *R. amoena*, *R. bella*, *R. mariae*, and *R. violeipes* (Park et al. 2013; Lee et al. 2015). *Russula amoena* and *R. violeipes* were described from Europe, *R. bella* from Japan, and *R. mariae* from North America. With the increase in available *Russula* sequence data, taxonomists can investigate more precisely the boundaries and distribution of Korean species. Therefore, the present study also aims to verify whether species are conspecific between continents using internal transcribed spacer (ITS) sequences from GenBank and generated for this study in a first analysis and, in a second analysis, using a concatenated dataset of other molecular markers including the second largest subunit of RNA polymerase II (*rpb2*), mitochondrial small subunit ribosomal DNA region (mtSSU), and the translation elongation factor 1-alpha (*tef1a*).

Methods

Sampling

A total of 15 collections from the Korean peninsula were included in this study. All Korean specimens were deposited in the Seoul National University Fungus Collection (SFC) and The Herbarium Conservation Center of the National Academy of Agricultural Science (HCCN). Because of a paucity of available sequence data from other continents, eight additional specimens from USA, four from Europe, and one from India were sequenced; all non-Asian samples are from the Herbarium of Plant Science and Biodiversity Centre of the Slovak Academy of Sciences (SAV) (Table 1 and Suppl. material 2: Table S2).

Table 1. Specimens used for the multi-locus analyses in this study. Sequences produced in this study are presented in boldface.

Taxon	Herbarium no.	Locality	GenBank accession no.		
			rpb2	mtSSU	*tef1α*
Outgroup					
R. aff. *delica*	1119/BB 12.086	Italy	KU237879	KU237442	KU238020
R. chloroides	572/BB 07.209	Slovakia	KU237845	KU237407	KU237990
R. herrerae	239/BB 06.532	Mexico	KU237772	KU237330	KU237915
Other subgenera					
R. aff. *griseobrunnea*	741/BB 09.344	New Caledonia	KU237877	KU237440	KU238018
R. cfr. *liberiensis*	91/BB 06.184	Madagascar	KU237760	KU237318	KU237905
R. compacta	228/B 06.295	USA	KU237766	KU237324	–
R. edulis	579/BB 08.167	Madagascar	KU237850	KU237412	KU237993
Russula sp.	569/BB 06.066	Madagascar	KU237842	KU237404	KU237987
Russula sp.	570/BB 08.178	Madagascar	KU237843	KU237405	KU237988
Closely related groups in subg. *Heterophyllidiae*					
R. aff. *crustosa*	31/BB 06.616	Canada	KU237747	KU237305	KU237896
R. aff. *madagassensis*	93/BB 06.255	Madagascar	KU237761	KU237319	KU237906
R. aff. *virescens*	721/BB 09.021	New Caledonia	KU237868	KU237430	KU238009
R. amoenolens	577/ BB 08.675	Italy	KU237410	KU237848	–
R. cfr. *annulata*	75/BB 06.048	Madagascar	KU237756	KU237314	KU237902
R. cfr. *illota*	36/ BB 06.380	Mexico	KU237750	KU237308	KU237898
R. cfr. *pseudocarmesina*	6/BB 06.030	Madagascar	KU237739	KU237296	–
R. cfr. *roseoalba*	82/BB 06.105	Madagascar	KU237758	KU237316	–
R. cfr. *vesca*	45/BB 06.525	Mexico	KU237751	KU237309	KU237899
R. flavobrunnea var. *violaceotincta*	71/ BB 06.050	Madagascar	KU237754	KU237312	KU237901
R. grisea	449/BB 07.184	Slovakia	KU237795	KU237355	KU237939
R. ionochlora	448/BB 07.338	Slovakia	KU237794	KU237354	KU237938
R. langei	450/ BB 07.792	France	KU237796	KU237356	KU237940
R. madagassensis	21/BB 06.146	Madagascar	KU237742	KU237300	KU237891
R. maguanensis	XHW4765	China	MH939989	–	MH939983
R. medullata	555/BB 07.252	Slovakia	KU237832	KU237392	KU237976
R. mustelina	1176/SA 09.88	Slovakia	KU237881	KU237444	KU238022
R. oleifera	254/BB 98.024	Tanzania	KU237776	KU237334	KU237919
R. ornaticeps	46/BB 06.530	Mexico	KU237752	KU237310	–
R. prolifica	18/BB 06.161	Madagascar	KU237741	KU237299	KU237890
R. pulverulenta	578/ BB 05.160	USA	KU237849	KU237411	–
Russula sp.	545/BB 08.061	Madagascar	KU237823	KU237383	KU237967
R. substriata	XHW4785	China	MH939994	–	MH939988
Subsect. *Amoeninae*					
R.* aff. *mariae	**SAV F–4484**	**USA, New York State**	**–**	**MT417192**	**–**
R.* aff. *mariae	**SAV F–4493**	**USA, New York State**	**–**	**MT417193**	**MT417213**
R.* aff. *mariae	**SAV F–4564**	**USA, New York State**	**–**	**MT417194**	**MT417214**
R. alachuana	**SAV 1252**	**USA, Florida**	**MT417198**	**MT417186**	**MT417204**
R. alachuana	**SAV F–20108**	**USA, Florida**	**MT417199**	**MT417187**	**MT417206**
R. amoena	**SAV F–1352**	**Slovakia**	**MT417200**	**MT417185**	**–**
R. amoena	**SAV F–3147**	**Slovakia**	**MT417202**	**MT417190**	**MT417211**
R.* cf. *amoenicolor	**SAV F–20302**	**Greece**	**MT417196**	**MT417188**	**MT417209**
R.* cf. *amoenicolor	**SAV F–20324**	**Greece**	**MT417197**	**MT417189**	**MT417210**
R. bella	**SFC20120722–03**	**South Korea**	**MT199642**	**MT196930**	**–**
R. bella	**SFC20170819–05**	**South Korea**	**MT199643**	**MT196931**	**MT199655**
R. bella	**SFC20170819–10**	**South Korea**	**MT199644**	**MT196932**	**MT199656**
R. bella	**HCCN16818**	**South Korea**	KF361734	**MT196933**	**–**
R. bella	**HCCN15410**	**South Korea**	**–**	**MT196934**	**–**
R. bella	**HCCN21655**	**South Korea**	KF361736	**MT196935**	**MT199657**
R. bella	**SFC20170731–02**	**South Korea**	**MT199645**	**MT196936**	**MT199658**
R. mariae	546/BB 07.038	USA	KU237824	KU237384	KU237968
***R. orientipurpurea* sp. nov.**	**HCCN19111**	**South Korea**	KF361712	**MT196923**	**MT199648**
***R. orientipurpurea* sp. nov.**	**HCCN18725**	**South Korea**	KF361710	**MT196924**	**MT199649**

Taxon	Herbarium no.	Locality	GenBank accession no.		
			rpb2	mtSSU	*tef1α*
***R. orientipurpurea* sp. nov.**	**HCCN21685**	**South Korea**	KF361714	**MT196925**	**MT199650**
***R. orientipurpurea* sp. nov.**	**SFC20170819–08**	**South Korea**	**MT199638**	**MT196926**	**MT199651**
***R. orientipurpurea* sp. nov.**	**SFC20170725–37**	**South Korea**	**MT199639**	**MT196927**	**MT199652**
***R. orientipurpurea* sp. nov.**	**SFC20170821–22b**	**South Korea**	**MT199640**	**MT196928**	**MT199653**
***R. orientipurpurea* sp. nov.**	**SFC20170726–47**	**South Korea**	**MT199641**	**MT196929**	**MT199654**
R. pseudoamoenicolor		**India**	**MT199646**	**MT196937**	**MT199659**
R. violeipes	542/BB 07.273	Slovakia	KU237820	KU237380	KU237964
***Russula* sp.**	**SFC20160726–13**	**South Korea**	**MT199647**	**MT196938**	**MT199660**
***Russula* sp.**	**SAV F–20134**	**USA, Florida**	–	–	**MT417205**
***Russula* sp.**	**SAV F–20117**	**USA, Florida**	**MT417195**	–	**MT417208**
***Russula* sp.**	**SAV F–4063**	**USA, Tennessee**	**MT417203**	**MT417191**	**MT417212**

Morphological study

Macromorphological characters were described from fresh specimens using the terminology of Vellinga (1988). The color standard codes in Kornerup and Wanscher (1978) were followed for describing the colour of the basidiomes. All microscopic characters were measured from dried herbarium samples using an Eclipse 80i light microscope (Nikon, Japan) with immersion lenses at the magnification of 1000× and using the software NIS ELEMENT BR v3.2 (Nikon, Japan). The description templates and terminology of Adamčík et al. (2019) were used for the observations of microscopic structures. The exception is that the sterile elements in hymenium have no distinct heteromorphous contents unlike hymenial cystidia of majority of *Russula* members, i.e. gloeocystidia. Because it is not certain if they correspond to "true gloeocystidia", we refer to them as hymenial cystidia when observed on lamellae sides and marginal cells in case of lamellar edges. Spore ornamentation was observed using a light microscope, and a scanning electron microscope (SEM, SUPRA 55VP, Carl Zeiss, Germany) at 5,000× and 10,000× magnification. For each collection, statistics of the measurements of microscopic characters were based on 20 measurements per character. Spore measurements excluded ornamentation. We followed the protocols of chemical tests for micro-morphological observation in Adamčik et al. (2019). Statistics of microscopic characters are expressed as the mean ± standard deviation with extreme values in parenthesis. The mean values are indicated by underline. When multiple samples were available, individual measurements of all microscopic characters of a species were obtained from at least three samples and diagnostic characters of species were further used to compare with the remaining samples.

Molecular studies

DNA was extracted from fresh or dried basidiomes using a modified CTAB extraction method (Roger and Bendich 1994). Four molecular markers were used for species-level identification and to infer evolutionary relationships among species. The following primer pairs were used in the amplifications: NSI1 and NLB4 for the ITS

region (Martin and Rygiewicz 2005), bRBP2-6F1 and RPB2-7R for the partial *rpb2* locus (Matheny et al. 2007), MS1 and MS2 for part of the mtSSU region (White et al. 1990), and EF1-983F and EF1-2218R for the partial *tef1a* locus (Matheny et al. 2007). The PCR conditions were: initial denaturation of 5 min at 95 °C, 35 cycles that varied for each marker (60 s at 95 °C, 40 s at 50 °C, and 60 s at 72 °C for ITS; 40 s at 95 °C, 40 s at 58 °C, and 60 s at 72 °C for *rpb2*; 30 s at 94 °C, 30 s at 55 °C, and 60 s at 72 °C for mtSSU; 30 s at 94 °C, 30 s at 56 °C, and 60 s at 72 °C for *tef1a*), and final incubation of 7 min at 72 °C. All PCR products were checked on 1% agarose gel stained with EcoDye DNA staining solution (SolGent Co., Daejeon, South Korea) and purified with the Expin PCR purification kit (GeneAll Biotechnology, Seoul, South Korea) following the manufacturer's instructions. DNA sequencing was conducted using an ABI3730 automated DNA Sequencer by Macrogen (Seoul, South Korea). The obtained sequences were checked and manually edited using the software FINCHTV v1.4 (Geospiza, Inc.), and then assembled manually using MEGA 7 (Kumar et al. 2016).

Phylogenetic analysis

For species delimitation of the Korean samples, ITS sequences of *R.* subsect. *Amoeninae* were downloaded from GenBank and aligned with the newly generated ITS sequences using MAFFT v7, with the E-INS-I strategy (Katoh and Standley 2013). *Russula grisea* and *R. virescens* were used as outgroup based on the results of previous studies (Buyck et al. 2008; Park et al. 2013). Maximum Likelihood (ML) analyses were conducted using RAxML 8.2.10 (Stamatakis 2014) and the GTR + G model with 1000 rapid bootstrap replicates. For *rpb2*, mtSSU, and *tef1a* regions, sequences of each locus were separately aligned and analyzed after introns were excluded. Seven partitions were assigned; mtSSU, *rpb2*pos1, *rpb2*pos2, *rpb2*pos3, *tef1a*pos1, *tef1a*pos2, and *tef1a*pos3. Substitution models of all partitions were tested using ModelTest-NG (Darriba et al. 2020). The best substitution models for the different loci under BIC were GTR+I+G for mtSSU, K80+I+G for *rpb2* partitions, and TrN+I+G for *tef1a* partitions. Bayesian inference (BI) analysis was performed with MRBAYES v. 3.2.6 (Ronquist and Huelsenbeck 2003), with four independent runs of four chains each. The TrN substitution model for *tef1a* was replaced by the GTR model for this analysis. The analysis was run for 20 million generations, with sampling every 1,000th generation. At the end of the run, the average standard deviation of split frequency of runs was 0.001412. The convergence and burn-in values of runs were then checked in Tracer 1.6 (Rambaut et al. 2014). We considered clades with the bootstrap values and posterior probabilities exceeding 70% and 0.95 as well-supported. The ITS dataset and the combined dataset (*rpb2*-mtSSU-*tef1a*) are available in TreeBase (http://treebase.org/treebaseweb/; submission ID 26896 and 22640, respectively). All phylogenetic analyses were executed on the CIPRES Science Gateway (Miller et al. 2010). Three species of *R.* subg. *Malodorae* were chosen as outgroup.

Results

Phylogenetic analysis

The ITS region was amplified and sequenced from 22 specimens for this study. A total of 152 ITS sequences belonging to *Amoeninae* were downloaded from GenBank and used in the analysis (Suppl. material 2: Table S2). The phylogenetic analysis of the ITS sequences indicated the existence of more than 21 *Russula* species-level clades: eight Asian species (two names undetermined), five European (one undetermined), five North American (three undetermined), two Australian, and one Central American (undetermined) (Fig. 1). However, none of the African or Malagasy species were included in this analysis as no ITS sequences were available. The Korean samples represented three phylogenetic species, and they were grouped with Asian samples and clearly separated from specimens of Australia, Europe, and North America.

A total of 72 ITS sequences were confirmed as *R. bella*: 5 from this study and 67 from GenBank. All of these sequences are from specimens in East Asia, i.e. from South Korea, China, and Japan. Of the ITS sequences in the *R. bella* clade, 31 were initially misidentified as the European *R. violeipes*, 35 ambiguously labelled as "*Russula* sp.", and one labelled as *Russula* cf. *violeipes*. A total of 33 specimens for which ITS sequences were newly generated or retrieved from GenBank belonged to a new species clade, *R. orientipurpurea.* The twenty nine ITS sequences from GenBank originated from South Korea, China, and Japan. Of these, 22 were mislabelled as the North American *R. mariae* and seven were labelled as "*Russula* sp." (Suppl. material 1: Table S1). The *R. orientipurpurea* clade was closely related to *R. mariae*, but they were clearly separated (Figs 1, 2). One specimen (SFC20160726-13) formed a unique clade with three Chinese specimens and we define it as an undetermined species. Two Indian species were positioned as a sister clade of the *Russula* sp. clade.

Russula amoena, *R. amoenicolor*, *R. andaluciana*, and *R. violeipes* were monophyletic (Fig.1). The European Mediterranean samples have similar morphology with *R. amoenicolor*. However, phylogenetic analysis showed that they are likely not conspecific. Therefore, we named them as "*R.* cf. *amoenicolor*" in this study. The North American samples formed five clades. Of these, only two clades are labelled with species names (*R. mariae* and *R. alachuana*). The four Australian samples formed two well-supported clades that do not overlap with samples from other continents.

Sequences of three loci (*rpb2*, mtSSU, and *tef1a*) were obtained for 28 samples (Table 1) and combined with 102 sequences of 34 samples obtained from GenBank. Two short introns were detected only in *tef1a* and they were excluded in the phylogenetic analysis. The results of this multilocus phylogenetic analysis were similar to those of the ITS analysis. Subsection *Amoeninae* formed a well-supported monophyletic group (Fig. 2). Three species were found for South Korea, and the East Asian *Russula* species were clearly separated from European and North American species.

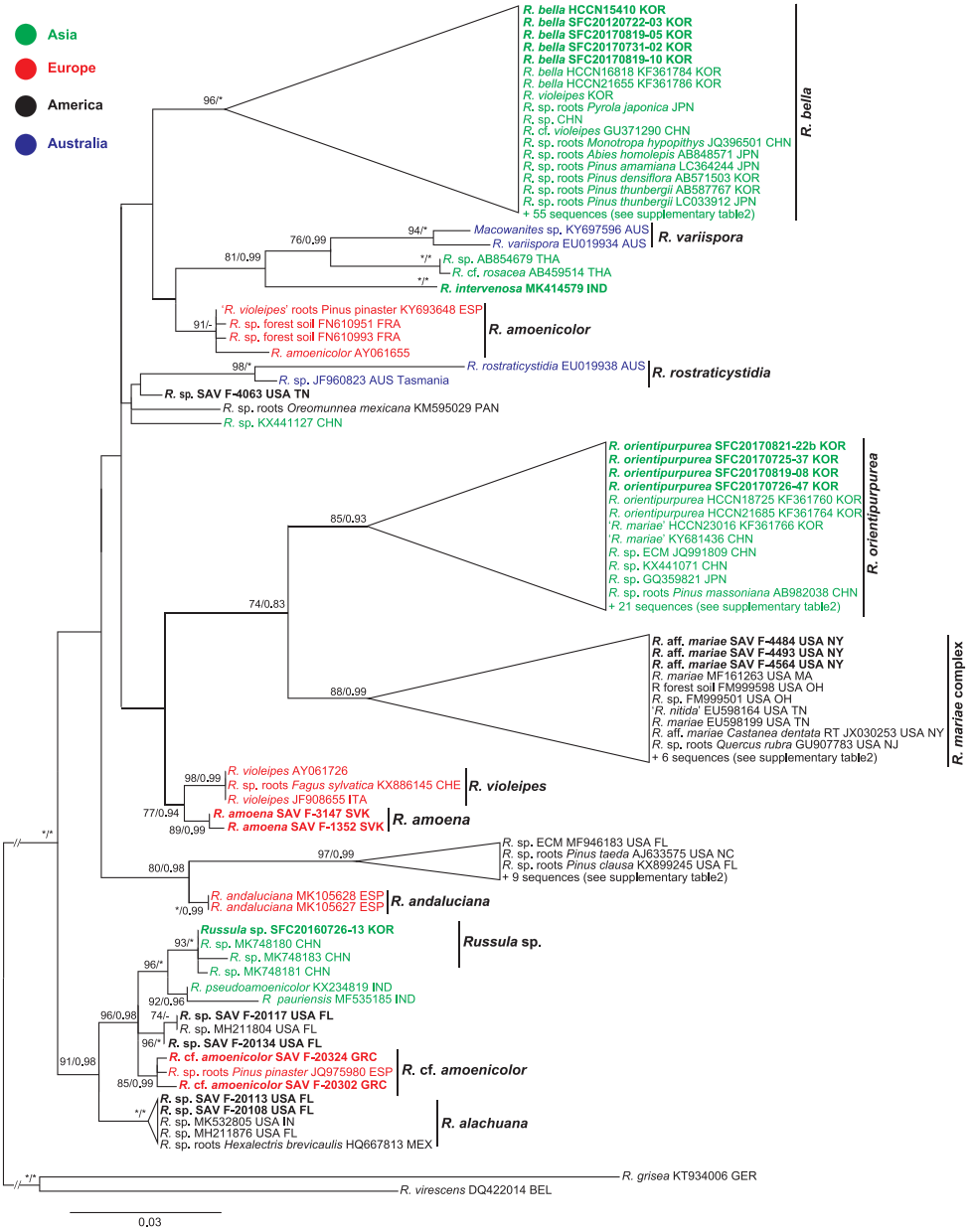

Figure 1. Maximum Likelihood (ML) tree based on internal transcribed spacer (ITS) sequences of most *Russula* subsect. *Amoeninae* and closely related species. Species in boldface are described in this study. ML bootstrap values >70 and Bayesian Inference posterior probability >0.90 are shown. Stars indicate clades with 100 ML bootstrap values and 1.0 Bayesian posterior probabilities.

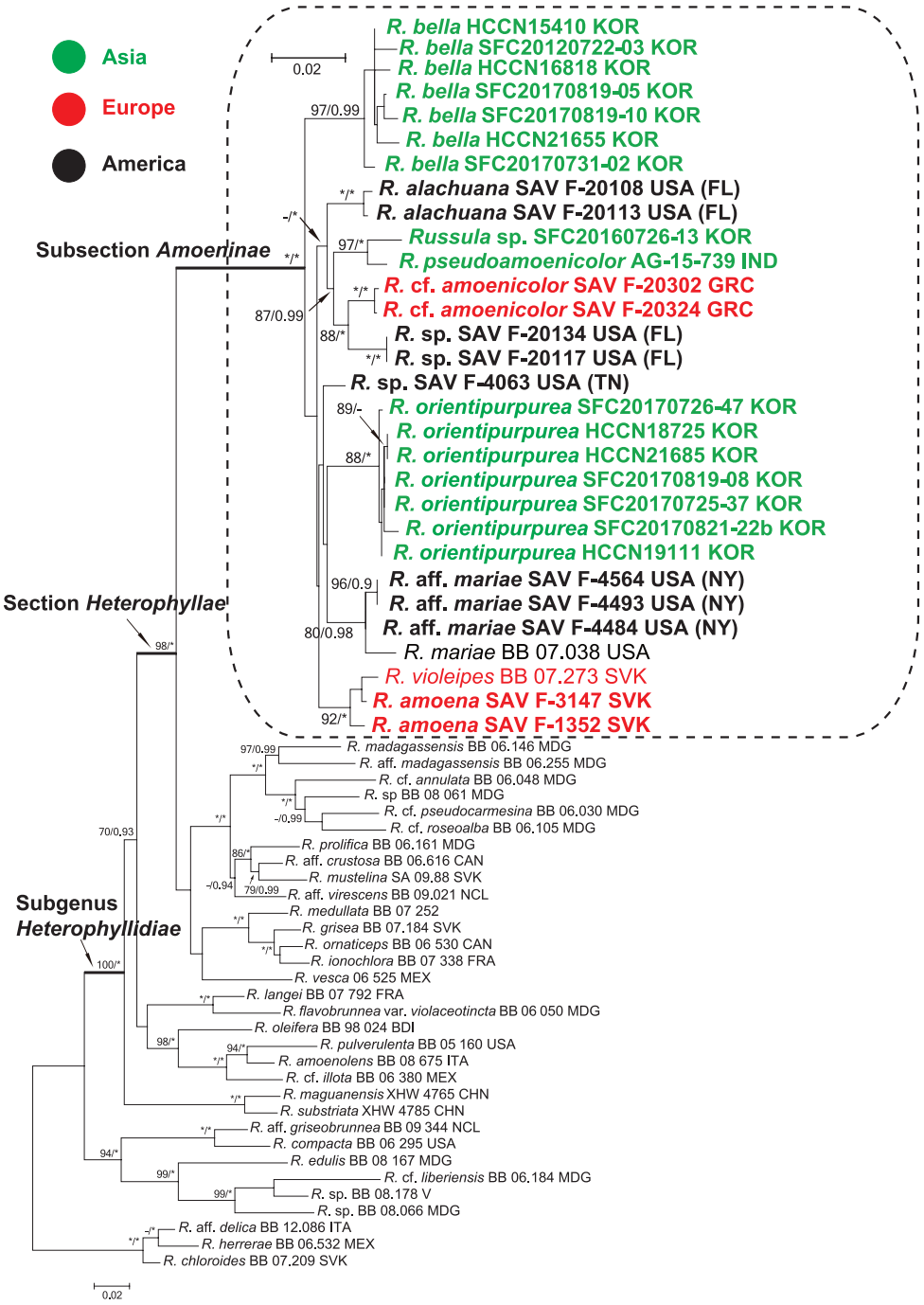

Figure 2. Maximum Likelihood (ML) tree based on the second largest subunit of RNA polymerase II (*rpb2*), mitochondrial small subunit ribosomal DNA region (mtSSU), and the translation elongation factor 1-alpha (*tef1a*) sequences of *Russula* subsect. *Amoeninae* species and representatives from closely related subgenera. Species in boldface are described in this study. ML bootstrap values >70 and Bayesian Inference posterior probability >0.90 are shown. Stars indicate clades with 100 ML bootstrap values and 1.0 Bayesian posterior probabilities.

Morphological analysis

The three species found in South Korea have the typical morphological characters of subsection *Amoeninae*: pruinose dry pileus surface, mild taste, and stipe flushed with pink, red, or purple. In fact, they have almost completely white stipes, usually with only a faint pink color (Fig. 3). Microscopically, these species display moderately large spores with crested and subreticulate to reticulate ornamentation (Fig. 4), an absence of cystidia with well-defined contents reactant with sulfovanillin, and a pileipellis comprising mainly attenuated terminal cells of hyphae usually subtended by one or two shorter ellipsoid or subglobose cells. The pileipellis of all three species have dimorphous hyphal terminations, some with long subulate or lageniform terminal cells and others with shorter, cylindrical, or ellipsoid terminal cells (Figs 5–7). The three Korean species were easily distinguished in the field. The morphological features of the Korean *R. bella* are consistent with the original description of the species (Table 2). The other two Korean species, however, do not entirely agree with the description of any previously described *Russula* species.

Taxonomy

Russula bella **Hongo, Memoirs of Shiga University 18:50 (1968)**
Figs 3A, B, 4A, B, 5

Diagnosis. Pileus medium-sized, 20–50 mm diam., plano-convex to convex when young, applanate with depressed center to infundibuliform when mature, often lobate, margin with short striation, sometimes cracking in age; cuticle smooth, pruinose, viscid and shiny when wet, cuticle peeling approximately to half of the pileus radius or sometimes almost to the center, color variable, typically darker at the disk, greyish red (11D5), brownish violet (11D6) to bluish red (12A6-A8, 12B7), few with yellowish brown spots, margin pink (11A5) to greyish rose (11B5). **Lamellae** 2–3 mm deep, brittle, adnate, approximately 11–19 per cm near the pileus margin, moderately distant to crowded, yellowish white to pale cream; lamellulae absent; edge entire and concolorous. **Stipe** 17–34 × 5–9 mm, centrally attached or eccentric, cylindrical to slightly tapered towards the base, surface dry, longitudinally striate, whitish with a pinkish flush; solid when young, becoming hollow in age. **Context** 1–3 mm thick near the stipe, white, unchanging after cutting, turning greenish with $FeSO_4$, turning quickly yellow with KOH, pale violet with PDAB; taste mild; odor slightly fruity. **Spore print** pale cream to white.

Basidiospores (n = 60, 3, 3) (6–)6.5–7.1–7.7(–8.8) × (5–)5.3–5.7–6(–6.6) µm, broadly ellipsoid, Q = (1.11–)1.17–1.25–1.33(–1.49), ornamentation thin, 0.4–1 µm high ridges forming an incomplete reticulum (2–7 in a 3 µm circle) with some dispersed isolated warts (0–2 warts in a 3 µm circle), suprahilar spot not amyloid, smooth. **Basidia** (25.1–)30–35.3–40.5(–48) × (7–)8.5–9.4–10.5(–11.5) µm,

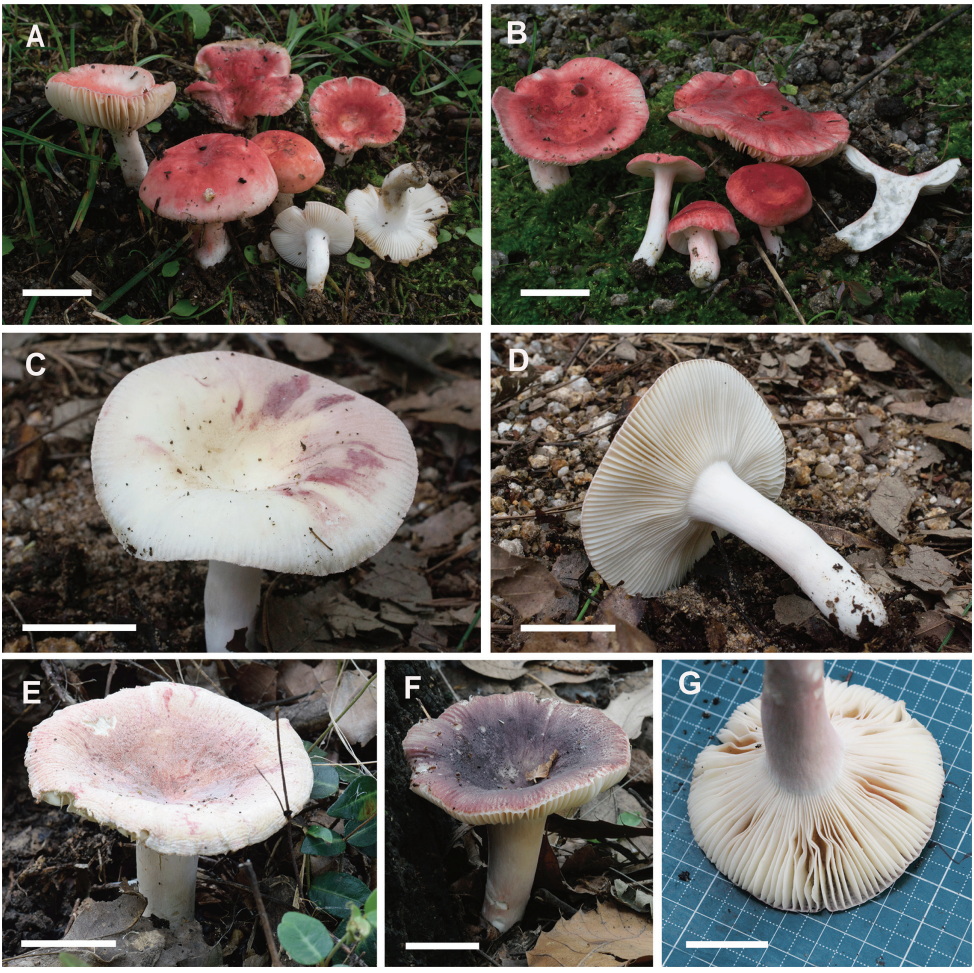

Figure 3. Basidiomes of Korean *Amoeninae* from this study. **A, B** *Russula bella* (A-SFC20170802-03, B-SFC20170819-05) **C–E** *R. orientipurpurea* (SFC20170819-08) **F, G** *Russula* sp. (SFC20160726-13). Scale bars: 20 mm.

4-spored, narrowly clavate, with guttate or granular contents. **Basidiola** (27.3–)28.4–32–35.5(–41.7) × (8.1–)8.7–9.4–10.3(–10.6) µm, narrowly clavate, with guttate or granular contents. **Hymenial cystidia on lamellae sides** inconspicuous, widely dispersed, up to 100 per mm^2, (37.5–)52–63.5–75(–90) × (5.5–)7.5–9–10.5(–11.5) µm, clavate to subcylindrical, originating from subhymenium, apically obtuse, thick-walled with walls up to 0.8 µm; contents optically empty, negative in sulfovanillin. **Lamellar edge** with dispersed basidia, true gloeocystidia (with differentiated contents) absent; marginal cells very abundant, resembling terminal cells in the pileus, typically narrowly lageniform or subulate (24–)38.5–50.8–63(–83) × (4–)5.5–6.8–7.5(–9.5) µm; shorter clavate to subcylindrical with obtuse apex present, (9–)12.5–15.7–18.5(–23.5) × (3.5–)4.5–5.7–7(–7.5) µm. **Pileipellis** orthochromatic in Cresyl blue, trichoderm, sharply

Table 2. Morphological characteristics of Asian *R.* subsect. *Amoeninae* species.

		R. bella[a]	***R. bella***	*R. intervenosa*[b]	*R. muteshwarica*[c]	***R. orientipurpurea***	*R. pavriensis*[d]	*R. pseudoamoenicolor*[e]	*R. punicea*[f]	***Russula* sp.**
Pileus size (mm)		20–45	20–50	26–49	65–130	52–60	53–63	50–100	25–60	60
Pileus colour	bright red	√	√	√				√		
	pink	√	√	√					√	
	grey					√	√			√
	brown									
	purple				√	√		√		
	violet				√		√	√		√
	green				√		√			
	bright yellow			√	√					
	cream or pale yellow					√	√			
Stipe colour	almost white		√			√			√	√
	partly pink	√	√	√	√			√		
	partly purple			√	√		√	√		
	partly violet						√			
Spore size	length (µm)	6.5–7.5	6.5–7.7	7–8	7.6–9.3	6.9–7.8	6–8	6–9.5	6.5–7	6.5–7
	width (µm)	5.5–6	5.3–6.0	6.5–7	7.3–8.2	6–6.9	5.5–7	5–8	5–6	5.6–6.2
	mean (length × width)		7.1 × 5.7	7.5 × 6.7		7.3 × 6.4	6.9–6.3	7.3–6.3		6.8 × 5.9
	Q value		1.17–1.33	1.07–1.19	1.00–1.15	1.09–1.19	1.00–1.17	1.03–1.33		1.10–1.19
Spore ornamentation	subreticulate	√	√	√	√	√	√	√	√	√
	reticulate					√			√	
	height (µm)		0.4–1.0	0.6–0.9	0.75	0.6–1	-2	-2		0.7–1.2
Cystidia on lamellae sides	length (µm)	44–55	52–75	29–34	80–110	74.5–101	55–135	90–117	45–60	66.5–91.5
	width (µm)	5.5–7	7.5–10.5	10–12.5	11–17	10.5–15	12–22	10–21	9–12	12.5–16.5
	cylindrical or clavate	√	√						√	
	subulate or lageniform									√
	fusiform			√	√	√	√	√	√	√
	obtuse		√			√	√	√	√	
	acute			√			√		√	√
Cystidia on lamellae edges	length (µm)	37–65	38.5–63	32–39	70–100	48–88	36–68	30–85		42.5–56.5
	width (µm)	5.5–7	5.5–7.5	5.5–7	11–17	5.5–10.5	8–15	7–10		5.5–7
	different from sides	√	√	√						
TC (margin)	length (µm)	44–80	47–76	39–47		55.5–89	9–64	11–65		60–85
	width (µm)	5.3–8	5–7	2.5–4.5	5–11	5–7	4–10	4–10	6–9	4.5–6
Short cells	number		1–2		2–4	0–2	2–4			1–2
	subterminal width (µm)						-12	-14		
TC centre	width (µm)		4.5–7.5			4.5–7.5				3–4

References: a-Hongo 1968, b-Crous et al. 2016, c-Das et al. 2005, d-Das et al. 2017, e-Hyde et al. 2016, f-Chiu 1945, Size unit of pileus is mm and the other microscopic characters are µm. Species in boldface are described in this study.

delimited from the underlying context, 280−400 µm thick, with a well-defined, gelatinized, 150−200 µm thick suprapellis of ascending or erect hyphal terminations forming a trichoderm, subpellis 130–200 µm thick, dense, horizontally oriented, sldender and gelatinized hyphae; acid-resistant incrustrations absent. Hyphal terminations near the pileus margin unbranched, often slightly flexuous, either long and attenuated or subcylindrical and obtuse, the attenuated ones more abundant, with terminal cells (20.5–)47–61.4–76(–85) × (3.5–)5–5.9–7(–8) µm, subulate or narrowly lageniform, rarely fusiform, apically acute to subacute, thin-walled, usually followed by 1–2 shorter and often more inflated cells before the branching; subcylindrical ones shorter, with terminal cells (7.5–)33.5–51.2–69(–107.5) × (2–)3.5–4.7–6(–7) µm, frequently

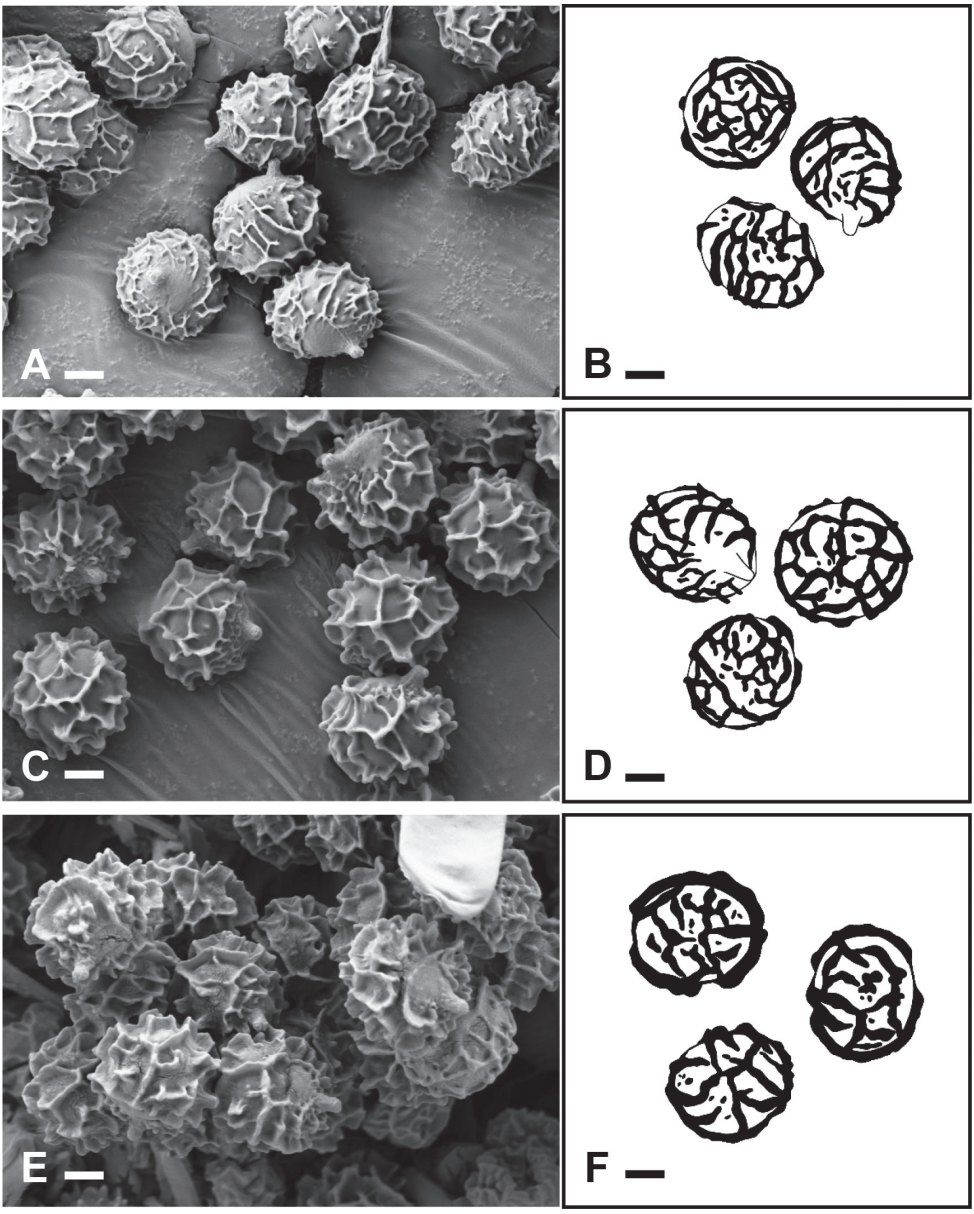

Figure 4. Basidiospores with scanning electron microscopy images (**A, C, E**) and drawing images (**B, D, F**) **A, B** *Russula bella* (SFC20170819-05) **C, D** *R. orientipurpurea*; (SFC20170821-22b) **E, F** *Russula* sp. (SFC20160726-13). Scale bars: 2 μm.

originate from branched cells, sometimes with one shorter unbranched subterminal cell. Hyphal termination near the pileus center also dimorphous, the attenuated ones with terminal cells (10.5–)18.5–50.5–82.5(–104.5) × (3.5–)4.5–6.0–7.5(–10) μm, mainly subulate, occasionally narrowly fusiform, apically acute and sometimes acute-pointed, often with thickened walls (up to 0.8 μm), shorter cylindrical hyphae with

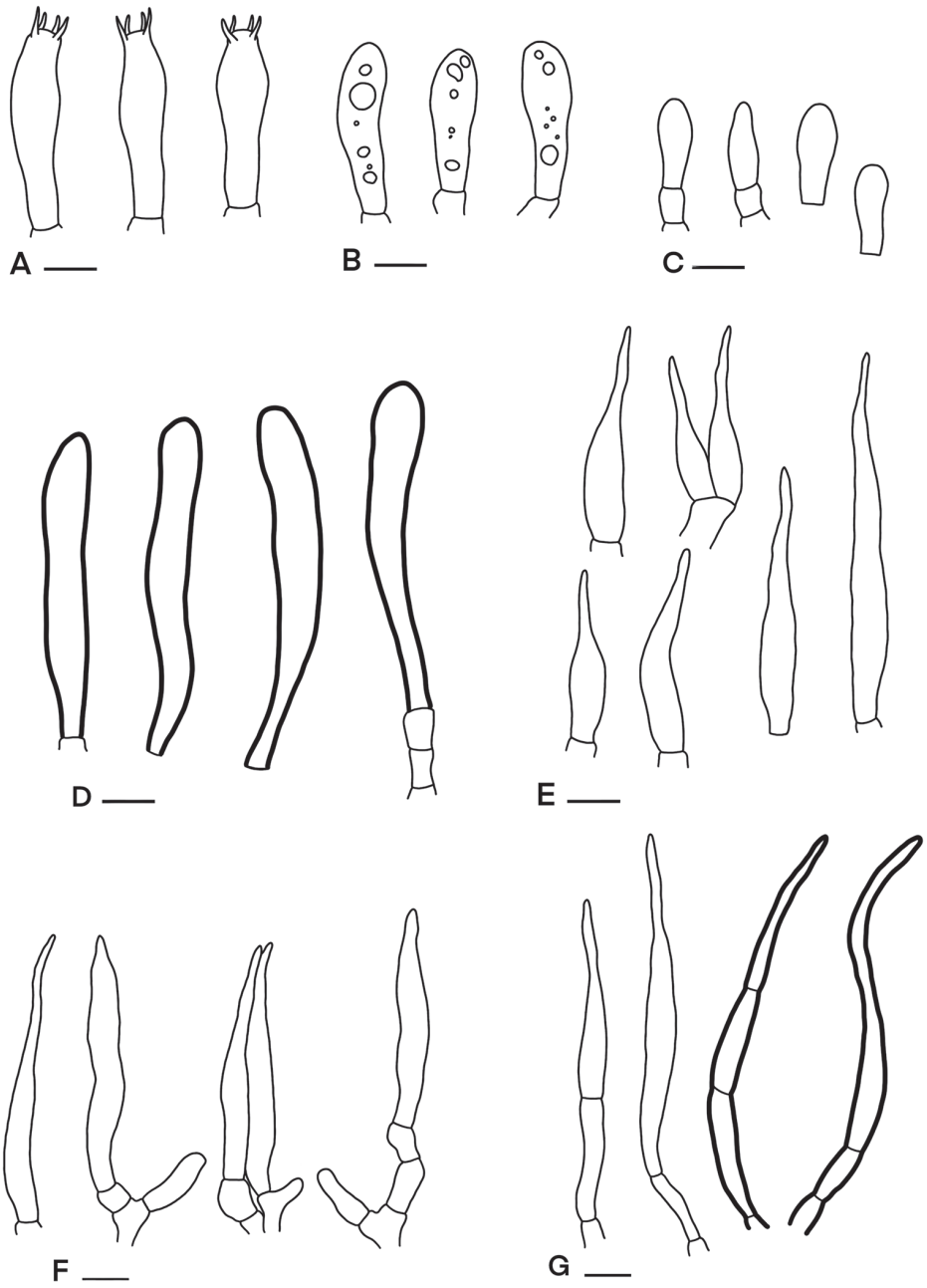

Figure 5. Microscopic features of *Russula bella* (SFC20170819-05) **A** basidia **B** basidiola **C** clavate marginal cells **D** hymenial cystidia on lamellae sides **E** subulate marginal cells **F** hyphal termination at pileus margin **G** hyphal termination at pileus centre. Scale bars: 10 μm.

terminal cells (9–)12.5–18.6–24.5(–32) × (2.5–)3–4–5(–6) μm; followed by 1–3 unbranched shorter cells, subterminal cells not usually not distinctly wider. **Pileocystidia** absent. Cystidioid or oleipherous hyphae in subpellis or context absent.

Ecology. gregarious to scattered on soil in mixed forest with *Quercus aliena*, *Pinus densiflora*, and *Populus* sp.

Studied materials. South Korea. Jeollanam-do, Haenam-gun, Mt. Duryun, 614 m elev., 34°27'24"N, 126°37'07"E, Yang Seop Kim, 5 September 1985, HCCN1457A (HCCN!); Chungcheongbuk-do, Danyang-gun, Mt. Sobaek, 790 m elev., 36°57'29"N, 128°26'35"E, Soon Ja Seok, 13 July 2007, HCCN15410 (HCCN!); Gyeonggi-do, Suwon-si, Seonggyungwan University, 58 m elev., 37°17'42"N, 126°58'22"E, Soon Ja Seok, 1 August 2008, HCCN16735 (HCCN!); Gangwon-do, Wonju-si, 275 m elev., 37°19'59"N, 127°54'35"E, Soon Ja Seok, 6 August 2008, HCCN16818 (HCCN!); Gyeonggi-do, Suwon-si, Seonggyungwan University, 48 m elev., 37°17'28"N, 126°58'24"E, Hye Yeong Choi, 5 August 2011, HCCN21655 (HCCN!); Daejeon-si, Yuseong-gu, 105 m elev., 36°23'48"N, 127°20'13"E, Myung Soo Park, 31 July 2012, SFC20120731-02 (SFC!); Gyeongsangbuk-do, Ulleung-gun, Mt. Seonginbong, 420 m elev., 37°30'50"N, 130°52'10"E, Seung-Yoon Oh, Won Ju Kim, Young Woon Lim, 14 August 2012, SFC20120814-23 (SFC!); Chungcheongnam-do, Seosan-si, Yonghyeon Natural Recreation Forest, 151 m elev., 36°45'53"N, 126°36'10"E, Young Ju Min, Won Ju Kim, Hyun Lee, 10 October 2012, SFC20121010-06 (SFC!); Seoul, Gwanak-gu, Seoul National University, 103 m elev., 37°27'26"N, 126°56'59"E, Komsit Wisitrassameewong, 31 July 2017, SFC20170731-02 (SFC!); ibid., 19 August 2017, SFC20170819-05 (SFC!).

Comments. *Russula bella* is morphological similar to *R. pseudoamoenicolor*, *R. punicea*, and *R. violeipes*. *Russula pseudoamoenicolor* has a more vividly colored pileus and a larger basidiome and hymenial cystidia than those of *R. bella* (Hyde et al. 2016). *Russula punicea* differs from *R. bella* in the shape of hymenial cystidia; the former has acute cystidia, whereas the latter has obtuse cystidia (Chiu 1945; Hongo 1968). *Russula violeipes* differs from *R. bella* in the yellowish to greenish smeared violet color of the pileus (Kränzlin 2005). Moreover, *R violeipes* has larger basidia (45–65 × 11–14 μm) and pleurocystidia (80–115 × 12–15 μm) than those of *R. bella* (Kränzlin 2005).

Russula orientipurpurea **Wisitr., H. Lee & Y.W. Lim, sp. nov.**
MycoBank No: 835272
Figs 3C–E, 4C, D, 6

Material examined. ***Holotype***. South Korea. Jullanam-do, Yeosu-si, Dolsando islands, 202 m elev., 34°35'24"N, 127°47'57"E, Komsit Wisitrassameewong, Jae Young Park, 25 July 2017, SFC20170725-37 (Holotype, SFC!).

Etymology. 'orientipurpurea' refers to the origin of the species, East Asia, and its typical purple color of pileus.

Diagnosis. Pileus surface with pale cream with flushed pale purple to purple stains; spores with almost complete to complete reticulum; subfusiform to fusiform hymenial cystidia.

Pileus medium-sized, 52–60 mm diam., plano-convex to applanate with the deeply depressed center, margin inconspicuously striate up to 2 mm, acute, even; surface smooth, pruinose, slightly waxy, matt, slightly viscid when wet, cuticle peeling 1/2

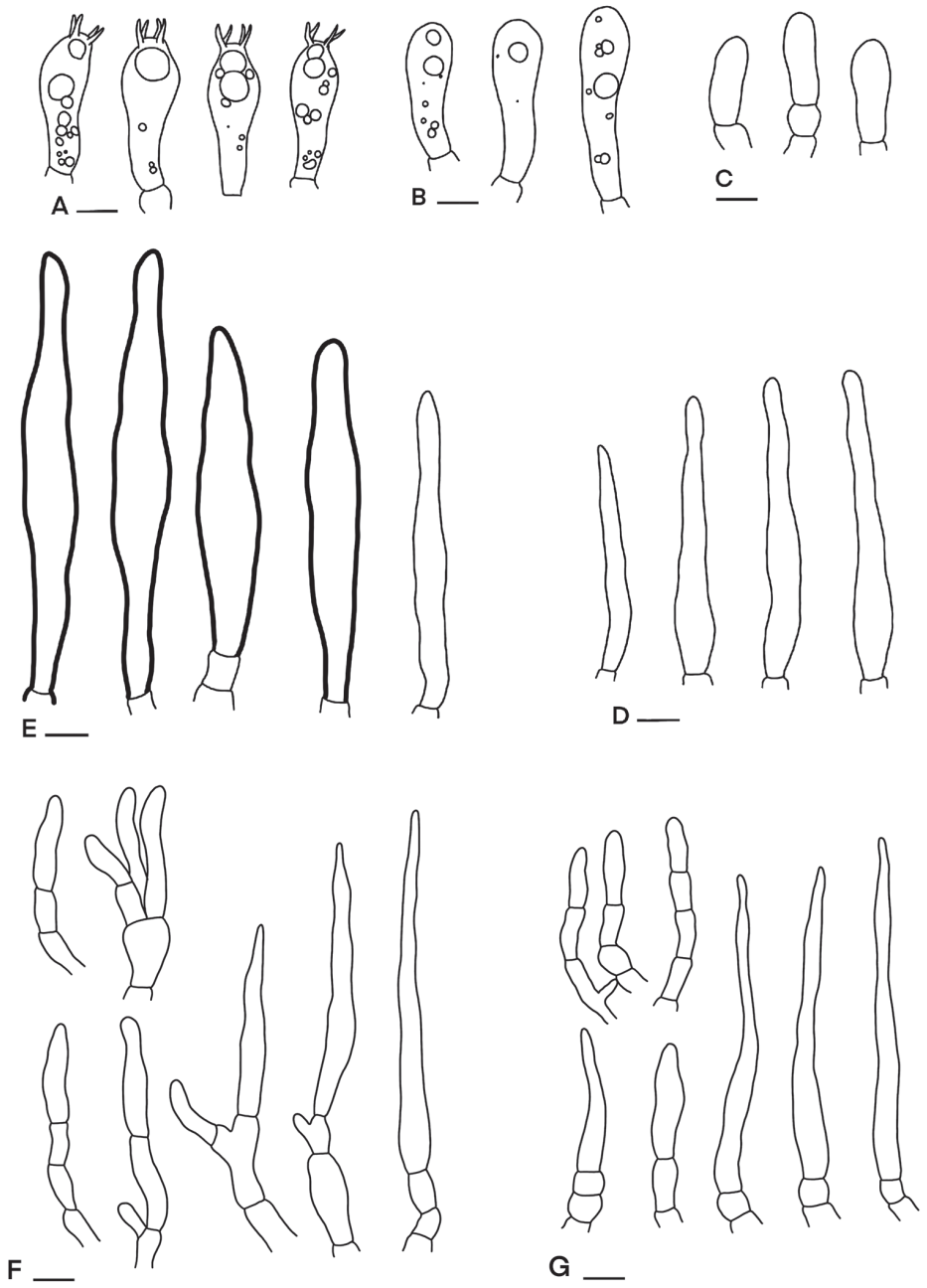

Figure 6. Microscopic features of *Russula orientipurpurea* (SFC20170725-37) **A** basidia **B** basidiola **C** clavate marginal cells **D** hymenial cystidia on lamellae sides **E** subulate marginal cells **F** hyphal termination at pileus margin **G** hyphal termination at pileus centre. Scale bars: 10 μm.

to 3/4 of the pileus radius, color pale cream to cream, with darker shade of cream towards the center, typically flushed with pale or darker purple stains, sometimes with radial stripes of greyish ruby (12E5). **Lamellae** 4–5 mm deep, adnate, moderately

distant, approximately 11–18 per cm near the pileus margin, white to pale yellow (3A3), furcations sometimes present near the stipe, lamellulae occasional, edge even. **Stipe** 40–50 × 11–13 mm, centrally attached, cylindrical, surface smooth, longitudinally striate, color white and sometimes with a greyish red (11D4-D5) flush; hollow. **Context** 2–3 mm thick at half of the pileus radius, white, rather firm but fragile in stipe when mature, turning slowly greenish with $FeSO_4$ and pale orange to orange white with KOH; taste mild; odor slightly fruity. **Spore print** cream white to white.

Basidiospores (n = 80, 4, 4) (6.3–)6.9–7.3–7.8(–8.6) × (5.4–)6–6.4–6.9(–7.6) µm, subglobose to broadly ellipsoid, Q = (1.06–)1.09–1.14–1.19(–1.28), ornamentation of thin to moderately thick, 0.6–1.4 µm high ridges forming an incomplete or complete reticulum (3–7 in a 3 µm circle), in a 3 µm circle isolated warts rare (0–1 in a 3 µm circle), suprahilar spot not amyloid, small, surrounded by fine and less prominent reticulation. **Basidia** (28–)32–36.2–40(–45) × (7.5–)9.5–10.9–12.5(–14.5) µm, 4-spored, clavate. **Basidiola** (27.8–)33.4–37.7–42.1(–43.4) × (9–)9.7–10.5–11.4(–12.2) µm, narrowly clavate, with guttate or granular contents. **Hymenial cystidia on lamellae sides** widely dispersed to dispersed, 200–700 per mm^2, (64–)74.5–87.9–101(–131) × (8.5–)10.5–12.8–15(–18.5) µm, mostly fusiform or narrowly fusiform, occasionally clavate, originating from subhymenium, emergent or not beyond basidia, apically constricted but obtuse, usually with thickened walls (up to 0.8 µm), contents optically empty, negative in sulfovanillin. **Lamellar edge** with dispersed basidia, true gloeocystidia (with differentiated contents) absent; marginal cells very abundant, resembling terminal cells in the pileus, usually narrowly lagenifom or subfusiform, apically narrowed but obtuse (28.5–)48–67.8–88(–121) × (3–)5.5–8.2–11(–14.5) µm; shorter narrowly clavate to clavate, (10.5–)13.5–18–22.5(–27.5) × (3.5–)5–6.5–8(–10.5) µm. **Pileipellis** orthochromatic in Cresyl blue, sharply delimited from the underlying context, 170–240 µm thick, with a well-defined, gelatinized, 30–60 µm thick suprapellis of ascending or erect hyphal terminations forming a trichoderm, subpellis 180–250 µm thick, dense, horizontally oriented, gelatinized and branched cylindrical to inflated hyphae; acid-resistant incrustrations absent. Hyphal terminations near the pileus margin unbranched, apically often flexuous, either long and attenuated or subcylindrical, short and obtuse, the attenuated ones (39.0–)55.5–72.3–89.0(–112.0) × (2.5–)5.0–6.1–7.2(–8.5) µm, subulate or narrowly fusiform, sometimes slightly moniliform, apically subacute, thin-walled, subterminal cells shorter, cylindrical ones with terminal cells (10–)16.5–25.3–34(–57) × (3–)4–5.2–6(–7.5) µm, apically sometimes slightly constricted, apically obtuse; followed by 0–2 unbranched short, equally wide cells, sometimes originate from branched cells. Hyphal termination near the pileus center also dimorphous, the attenuated ones prevailing with terminal cells (10.5–)18.5–50.5–82.5(–104.5) × (3.5–)4.5–6.0–7.5(–10) µm, subulate, thin-walled, apically subacute, cylindrical ones with terminal cells (13.5–)19–42.9–66.5(–85.5) × (3.5–)4.5–5.6–6.5(–9.0) µm. **Pileocystidia** absent. Cystidioid or oleipherous hyphae in subpellis or context absent.

Ecology. solitary to scattered on soil in mixed forest with *Quercus* and *Pinus* trees.

Studied materials. South Korea. Chungcheongnam-do, Gongju-si, Mt. Museong, 341 m elev., 36°35'52"N, 127°01'59"E, Hyun Lee, Seung-Yoon Oh, 26

July 2012, SFC20120726-37 (Paratype SFC!); Incheon-si, Gangwha-gun, Mt. Goryeo, 228 m elev., 37°44'54"N, 126°26'01"E, Young Woon Lim, 4 August 2012, SFC20120804-09 (Paratype, SFC!); Seoul, Gwanak-gu, Mt. Gwanak, 154 m elev., 37°27'06"N, 126°56'34"E, Hyun Lee, Won Ju Kim, 25 August 2012, SFC20120825-02 (Paratype SFC!); ibid, 202 m elev., 37°27'34"N, 126°56'19"E, Hyun Lee, Myung Soo Park, 31 August 2012, SFC20120831-04 (Paratype SFC!); ibid, 238 m elev., 37°26'53"N, 126°54'11"E, Hyun Lee, Komsit Wisitrassameewong, 19 August 2017, SFC20170819-08 (Paratype SFC!); Gyeongsangnam-do, Hapcheon-gun, Mt. Gaya, 631 m elev., 35°47'59"N, 128°05'46"E, Jae Young Park, Komsit Wisitrassameewong, Ki Hyeong Park, 26 July 2017, SFC20170726-47 (Paratype SFC!); Gyeongsangbuk-do, Ulleung-gun, Nari basin, 395 m elev., 37°31'03"N, 130°52'11"E, Jae Young Park, Nam Kyu Kim, 21 August 2017, SFC20170821-22b (Paratype SFC!).

Comments. *Russula orientipurpurea* is common in mixed forests in South Korea. This species was misidentified as the North American *R. mariae* (Park et al. 2013). The spores in *R. orientipurpurea* have more complete ridge connections (3–7 lines in the 3 µm circle) and a smaller number of warts (0–1 warts in the 3 µm circle) than those in *R. mariae* (lines 1–4, warts 4–6). *Russula orientipurpurea* is morphologically similar to *R. intervenosa*. However, the dark red pileus centere, broader hymenial cystidia (up to 18 µm), and the thicker pileipellis (250–600 µm) of *R. intervenosa* (Crous et al. 2016) distinguishes this species from *R. orientipurpurea* (see Table 2).

***Russula* sp.**

Figs 3F, G, 4E, F, 7

Diagnosis. Pileus medium-sized, 60 mm diam., applanate with deeply depressed center, margin distinctly striate, crenulate, radially cracking; cuticle dry, viscid when moist, pruinose, peeling to 1/2 of the pileus radius, color greyish violet (18E5-E6), with dark violet (18F4-F6) patches, towards margin violet grey (18D2) to dull violet (18D3). **Lamellae** 3 mm deep, adnate, dense, pale cream; lamellulae rare, forked near the stipe; edge smooth and concolorous. **Stipe** 55 × 8–10 mm, centrally attached, tapering downwards base, surface dry, longitudinally-striated, white and flushed with purple. **Context** 2 mm thick at half of the pileus radius, white, unchanging; taste and odor not recorded. **Spore print** cream white.

Basidiospores (n = 20, 1, 1) (6.4–)6.5–6.8–7(–7.2) × (5.5–)5.6–5.9–6.2(–6.5) µm, Q = (1.08–)1.1–1.14–1.19(–1.24), subglobose to broadly ellipsoid, ornamentation of thin to moderately thick, 0.8–1.4 µm high ridges forming an incomplete reticulum (2–6 in a 3 µm circle), isolated warts rare (0–2 in a 3 µm circle), suprahilar spot not amyloid, small. **Basidia** (32–)34–36.2–38.5(–40) × (9–)9.5–10.5–11(–11.5) µm, 4-spored, clavate. **Basidiola** (24–)25.8–31–35(–42.5) × (8.3–)8.9–9.9–10.8(–11.4) µm, narrowly clavate, with guttate or granular contents. **Hymenial cystidia on lamellae sides** widely dispersed to dispersed, 100–500 per mm^2, (63)66.5–79–91.5(–109) × (10.5–)12.5–14.5–16.5(–18) µm, narrowly fusiform or lageniform, originating from subhymenium and emergent beyond basidia, apically acute or obtuse

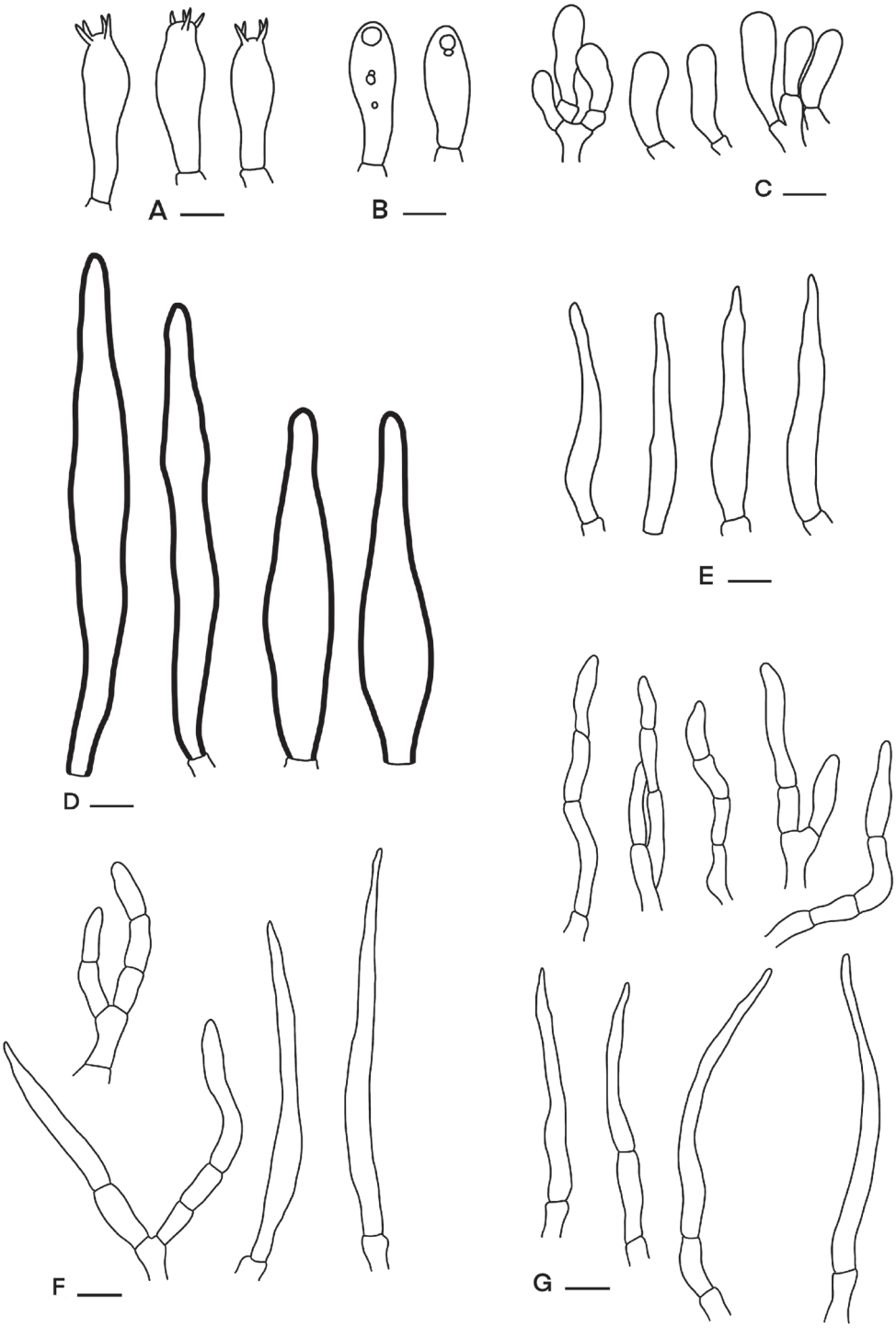

Figure 7. Microscopic features of *Russula* sp. (SFC20160726-13) **A** basidia **B** basidiola **C** clavate marginal cells **D** hymenial cystidia on lamellae sides **E** subulate marginal cells **F** hyphal termination at pileus margin **G** hyphal termination at pileus centre. Scale bars: 10 μm.

but narrowed, thick-walled (walls up to 0.9 µm), contents optically empty, negative in sulfovanillin. **Lamellar edge** with dispersed basidia, true gloeocystidia (with differentiated contents) absent; marginal cells very abundant, resembling terminal cells in the pileus, narrowly lageniform or subulate (36.5–)42.5–49.6–56.5(–70.1) × (5–)5.5–6.3–7(–7.5) µm, narrowly lageniform or subulate, apically acute; narrowly clavate to clavate with optuse apex, (11.5–)14.5–17.8–21.2(–23.2) × (4–)5.2–6.2–7(–7.5) µm. **Pileipellis** orthochromatic in Cresyl blue, sharply delimited from the underlying context, 250–400 µm thick, with gelatinous matter, cystidoid hyphae prevailing, shorter cylindrical terminal hyphae present, parallel or repent scattered, pileocystidia absent, with a well-defined, gelatinized, 70–120 µm thick suprapellis of ascending or erect hyphal terminations forming a trichoderm, subpellis 230–350 µm thick, dense, horizontally oriented, gelatinized and branched cylindrical hyphae; acid-resistant incrustrations absent. Hyphal terminations near the pileus margin unbranched, usually only slightly flexuous, either long and attenuated or subcylindrical, short and obtuse; the attenuated ones more frequent, with terminal cells (45.0–)60.0–72.6–85.0(–96.5) × (3.5–)4.5–5.1–6.0(–6.5) µm, subulate, apically acute, thin-walled, shorter ones with terminal cells (18–)20.5–28.7–37.0(–48.0) × (3.0–)3.5–4.4–5.0(–6.0) µm, cylindrical or subcylindrical, apically obtuse but often constricted, thin walled; followed by (0–)1–2(–3) unbranched shorter and equally wide cells. Hyphal termination near the pileus center similar but shorter and narrower, attenuated longer ones with terminal cells (38.5–)43.5–53.4–63.0(–73.0) × (2.5–)3–3.5–4.0(–4.5) µm; shorter cylindrical ones with terminal cells (11.5–)13.5–16.4–19.0(–22.0) × (3.0–)3.5–4.1–4.5(–5.5) µm. **Pileocystidia** absent. Cystidioid or oleipherous hyphae in subpellis or context absent.

Ecology. solitary on soil in deciduous forest, near *Quercus mongolica*.

Material examined. South Korea. Incheon-si, Ongjin-gun, Jangbongdo islands, 72 m elev., 37°31'55"N, 126°21'10"E, Jae Young Park, Nam Kyu Kim, Suldbold Jargalmaa, 26 July 2016, SFC20160726-13 (Holotype, SFC!).

Comments. This species is morphologically similar to *R. mukteshwarica*, but phylogenetically close to *R. pseudoamoenicolor* and *R. pauriensis*. *Russula mukteshwarica* and *R. pauriensis* differ from *Russula* sp. in the greenish yellow region at the pileus center, which is present in the first two species but absent in the latter (Das et al. 2005, 2017). *Russula pseudoamoenicolor* has a discolorous lamella edge (Hyde et al. 2016), whereas *Russula* sp. has a concolorous lamellae edge. *Russula* sp. has a purple pileus similar to that of *R. violeipes*; however, spore ornamentation height (up to 0.7 µm) and pleurocystidia size (80–115 × 12–15 µm) distinguishes *Russula* sp. from *R. violeipes* (Kränzlin 2005).

Key characters to Asian species in *R.* subsect. *Amoeninae*

1	Basidiome with pinkish pileus	**2**
–	Basidiome with violet or purple pileus	**4**
2	Obtuse hymenial cystidia, subreticulate spore ornamentation, in mixed *Pinus* and *Quercus* forests	***R. bella***
–	Acute hymenial cystidia, subreticulate to reticulate spore ornamentation	**3**

3 Reticulate spore ornamentation, large hymenial cystidia (46–60 × 9–12 µm), broad hyphal terminations (6–9 µm wide) in the pileipellis ..... ***R. punicea***

– Subreticulate spore ornamentation, small hymenial cystidia (29–34 × 10–12.5 µm), narrow hyphal termination (2.5–4.5 µm wide) in the pileipellis ..... ***R. intervenosa***

4 Reticulate spore ornamentation, pileus with pale cream to yellowish grey color and purplish tinges..... ***R. orientipurpurea***

– Subreticulate spore ornamentation, pileus with vivid color **5**

5 Pileus with violet/greenish/yellowish shades, stipe with purplish flush, large and broad hymenial cystidia **6**

– Pileus without greenish or yellowish shades..... **7**

6 Small spores with high ornamentation (up to 2 µm), lamellae yellowish, lamellulae absent..... ***R. pauriensis***

– Large spores with low ornamentation (up to 0.75 µm), lamellae yellowish to greenish, lamellulae present..... ***R. mukteswarica***

7 Lamellar edge discolorous (pastel violet), spore ornamentation up to 2 µm high ..... ***R. pseudoamoenicolor***

– Lamellar edge concolorous, spore ornamentation up to 1.2 µm high ..... ***Russula* sp.** (SFC20160726-13)

Discussion

The phylogenetic analyses showed that subsection *Amoeninae* forms a well-supported monophyletic group. Moreover, the species of Asian, Australian, European, and North American origin form separate clades. Similar results have been reported for other species groups in the various ectomycorrhizal genera of Russulaceae, which are often endemic to specific geographical regions or a single continent (Cho et al. 2018; De Crop et al. 2018; Wang et al. 2018; Lee et al. 2019; Looney et al 2020). Their host plants may have acted as bridges for species dispersal and diversification (Looney et al. 2018), and geographic distance and climate disjunctions may have caused species divergence (Caboň et al. 2019; Lee et al. 2019). The present study included recently obtained sequences of well-known species from different continents except Africa, which will provide useful information for understanding the diversity in this section.

Four *Amoeninae* species had been previously reported from South Korea based on morphological characteristics: two European, one North American, and one Japanese species (Lee et al. 2015). Based on ITS, large ribosomal subunit (LSU), and *rpb2* data, Park et al. (2013) found that the Korean *Amoeninae* species were *R. mariae* (North American) and *R. violeipes* (European). The differences between those results and the present study may be traced back to the limited amount of sequences available at the time. The dramatic increase in the number of sequences available in public databases and the data obtained in the present study allow us to conclude that the species previously identified as *R. mariae* and *R. violeipes* in South Korea are in fact *R. orientipurpurea* and *R. bella*, respectively. We also showed that *R. orientipurpurea* forms a distinct

clade that is quite distantly related to North American species, *R. mariae*. Moreover, the color of the pileus and geographical disjunction distinguishes *R. orientipurpurea* from *R. mariae*.

Phylogenetic analysis of LSU sequence data showed a close relationship among *R. bella*, *R. mariae*, and *R. violeipes* (Shimono et al. 2004). Although there are no ITS sequences available of *R. bella* from Japan, one LSU sequence of *R. bella* was identical to that of Korean samples (Park et al. 2013). The European *R. violeipes* is clearly distinguished from *R. bella* (Figs 1, 2). Therefore, considering the available morphological and molecular information, we conclude that all Korean samples previously designated as *R. violeipes* are in fact *R. bella*.

Russula sp. (SFC20160726-13) was confirmed to be identical to the three unidentified Chinese samples. The Chinese samples are from Taishan of Shandong Province, which is geographically close to South Korea. They formed a distinct clade and might be a new species. However, there are limited specimens to describe it as a new species. It would be better to introduce this new species after observing more specimens.

The occurrence of a previously reported species from South Korea (Lee et al. 2015), *R. amoena*, was not confirmed in this study. This species was originally described from Europe (Sarnari 1998). Two European specimens of *R. amoena* were included in our phylogenetic analyses, but none of the Korean samples match with these European collections. Thus, so far, *R. amoena* has not been confirmed in South Korea.

Most Korean specimens of *R. bella* and *R. orientipurpurea* were collected from mixed forests with pine and oak trees, which are very common in South Korea. Previous studies have reported that *R. bella* is commonly found as ectomycorrhizal root tips of the conifer species *Abies homolepsis* (Miyamoto et al. 2014), *Pinus amamiana* (Sugiyama et al. 2019), *P. densiflora* (direct GenBank submission), *P. thenderbergii* (Obase et al. 2011; Nakashima et al. 2016), and *P. yunnanensis* (Xie et al. 2010). Some sequences of *R. orientipurpurea* were also obtained from the roots of other *Pinus* spp. (Wen et al. 2015). This indicates that these two species are associated with conifers, but symbiotic relationships with deciduous trees cannot be excluded as the information available in the literature is scarce. *Russula* sp. (SFC20160726-13) seems rare and was collected in a forest dominated by *Quercus mongolica*. Since we have limited sample and data, additional specimens are needed to complete a morphological and ecological characterization of the species. Ecological information can be useful for the identification of morphologically similar ectomycorrhizal fungi species (Nuytinck and Verbeken 2003; Lee et al. 2019). Further investigations focused on ecological information are necessary to obtain a better understanding of the three Korean *Russula* species.

In conclusion, the East Asian *Russula* species in subsection *Amoeninae* are distinct from the European and North American species. Three species were identified from South Korea based on molecular and morphological data. However, the molecular data available in GenBank are still limited and comprise only some *Russula* species in subsection *Amoeninae*. The amount of ITS data for this group has continuously increased, but protein-coding gene sequences are still insufficient. An overall increase in sequence information would allow for a better understanding of the phylogenetic relationships and global diversity of this group.

Acknowledgements

This study was supported by the National Institute of Biological Resources (NIBR 201801105), Korea National Arboretum (KNA1-1-25, 19-2), and the Korean government (NRF-2015M3A9B8029237). The research of Miroslav Caboň and Slavomír Adamčík was funded by Slovak Grant APVV 15-0210.

References

Adamčik S, Jančovičová BB (2018) The Russulas described by Charles Horton Peck. Cryptogamie Mycologie 39(1): 3–110. https://doi.org/10.7872/crym/v39.iss1.2018.3

Adamčík S, Looney B, Caboň M, Jančovičová S, Adamčíková K, Avis PG, Barajas M, Bhatt RP, Corrales A, Das K, Hampe F, Ghosh A, Gates G, Kälviäinen V, Khalid AN, Kiran M, De Lange R, Lee H, Lim YW, Kong A, Manz C, Ovrebo C, Saba M, Taipale T, Verbeken A, Wisitrassameewong K, Buyck B (2019) The quest for a globally comprehensible *Russula* language. Fungal Diversity 99: 369–449. https://doi.org/10.1007/s13225-019-00437-2.

Beeli M (1936) Contribution a l'étude la flore mycologique de Congo. XI. Fungi Geossensiani XII. Bulletin du Jardin Botanique de l'État à Bruxelles 14: 83–91. https://doi.org/10.2307/3666668

Bills GF, Miller OK (1984) Southern Appalachian Russulas. I. Mycologia 76: 975–1002. https://doi.org/10.1080/00275514.1984.12023944

Buyck B (1987) Trois Russules nouvelles du Zaïre. Bulletin du Jardin Botanique National de Belgique 57(3–4): 385–387. https://doi.org/10.2307/3668111

Buyck B (1988) Etude microscopique des specimens-types de Russules tropicales de la sous-section *Diversicolores*. Mycotaxon 33: 57–70.

Buyck B (1992) Checklist of tropical *Russulae* and their type specimens. Russulales News special issue 1, 99 pp.

Buyck B (1994) Flore illustrée des champignons d'Afrique Centrale. Fascicule 16. *Russula* II (Russulaceae). Ministère de l'Agriculture, Jardin Botanique National de Belgique, 411–542.

Buyck B (1995) *Russula* subsection *Amoeninae* in tropical African miombo woodland. Documents Mycologiques 98–100: 103–112.

Buyck B, Sharp C (2007) Two new species and first records for 13 other *Russula* (Russulales) from Zimbabwe. Cryptogamie Mycologie 28(1): 13–27.

Buyck B, Hofstetter V, Eberhardt U, Verbeken A, Kauff F (2008) Walking the thin line between *Russula* and *Lactarius*: the dilemma of *Russula* subsect. *Ochricompactae*. Fungal Diversity 28: 15–40.

Buyck B, Zoller S, Hofstetter V (2018) Walking the thin line… ten years later: the dilemma of above- versus below-ground features to support phylogenies in the Russulaceae. Fungal Diversity 89(1): 267–292. https://doi.org/10.1007/s13225-018-0397-5

Buyck B, Wang XH, Adamčíková K, Caboň M, Jančovičová S, Hofstetter V, Adamčík S (2020) One step closer to unravelling the origin of *Russula*: subgenus *Glotinosae* subg. Nov. Mycosphere 11(1): 285−304. https://doi.org/10.5943/mycosphere/11/1/6

Caboň M, Li G-J, Saba M, Kolařík M, Jančovičová S, Khalid AN, Moreau P-A, Wen H-A, Pfister DH, Adamčík S (2019) Phylogenetic study documents different speciation mechanisms

within the *Russula globispora* lineage in boreal and arctic environments of the Northern Hemisphere. IMA fungus 10: e5. https://doi.org/10.1186/s43008-019-0003-9

Chiu WF (1945) The Russulaceae of Yunnan. Lloydia 8(1): 31−59.

Cho HJ, Park MS, Lee H, Oh S-Y, Wilson AW, Mueller GM, Lim YW (2018) A systematic revision of the ectomycorrhizal genus *Laccaria* from Korea. Mycologia 110(5): 948–961. https://doi.org/10.1080/00275514.2018.1507542

Crous PW, Wingfield MJ, Richardson DM, Le Roux JJ, Strasberg D, Edwards J, Roets F, Hubka V, Taylor PWJ, Heykoop M, Martín MP, Moreno G, Sutton DA, Wiederhold NP, Barnes CW, Carlavilla JR, Gené J, Giraldo A, Guarnaccia V, J Guarro, Hernández-Restrepo M, Kolařík M, Manjón JL, Pascoe IG, Popov ES, Sandoval-Denis M, Woudenberg JHC, Acharya K, Alexandrova AV, Alvarado P, Barbosa RN, Baseia IG, Blanchette RA, Boekhout T, Burgess TI, Cano-Lira JF, Čmoková A, Dimitrov RA, Dyakov MYu, Dueñas M, Dutta AK, Esteve-Raventós F, Fedosova AG, Fournier J, Gamboa P, Gouliamova DE, Grebenc T, Groenewald M, Hanse B, Hardy GEStJ, Held BW, Jurjević Ž, Kaewgrajang T, Latha KPD, Lombard L, Luangsa-Ard JJ, Lysková P, Mallátová N, Manimohan P, Miller AN, Mirabolfathy M, Morozova OV, Obodai M, Oliveira NT, Ordóñez ME, Otto EC, Paloi S, Peterson SW, Phosri C, Roux J, Salazar WA, Sánchez A, Sarria GA, Shin HD, Silva BDB, Silva GA, Smith MTh, Souza-Motta CM, Stchigel AM, Stoilova-Disheva MM, Sulzbacher MA, Telleria MT, Toapanta C, Traba JM, Valenzuela-Lopez N, Watling R, Groenewald JZ (2016) Fungal Planet description sheets 400−468: *Russula intervenosa* S. Paloi, A.K. Dutta & K. Acharya sp. nov. Persoonia: Molecular Phylogeny and Evolution of Fungi 36: 316−458. https://doi.org/10.3767/003158516X692185

Das K, Ghosh A, Chakraborty D, Li J, Qiu L, Baghela A, Halama M, Hembrom ME, Mehmood T, Parihar A, Pencakowski B, Bielecka M, Recyńska K, Sasiela D, Singh U, Song Y, Świerkoz K, Szczęśniak K, Uniyal P, Zhang J, Buyck B (2017) Fungal biodiversity profile 31–40. Cryptogamie Mycologie 38(3): 353–406. https://doi.org/10.7872/crym/v38.iss3.2017.353

Das K, Miller SL, Sharma JR, Sharma P, Bhatt RP (2005) *Russula* in Himalaya 1: A new species of subgenus *Amoenula*. Mycotaxon 94: 85–88.

Darriba D, Posada D, Kozlov AM, Stamatakis A, Morel B, Flouri T (2020) ModelTest-NG: A new and scalable tool for the selection of DNA and protein evolutionary models. Molecular Biology and Evolution 37(1): 291−294. https://doi.org/10.1093/molbev/msz189

De Crop E, Hampe F, Wisitrassameewong K, Stubbe D, Nuytinck J, Verbeken A (2018) Novel diversity in *Lactifluus* section *Gerardii* from Asia: five new species with pleurotoid or small agaricoid basidiocarps. Mycologia 110: 962–984. https://doi.org/10.1080/00275514.2018.1508979

Härkönen M, Buyck B, Saarimäki T, Mwasumbi L (1993) Tanzanian mushrooms and their uses 1. *Russula*. Karstenia 33: 11–50. https://doi.org/10.29203/ka.1993.297

Hebert PDN, Cywinska A, Ball SL, deWaard JR (2003) Biological identifications through DNA barcodes. Proceedings of the Royal Society of London. Series B: Biological Sciences 270: 313–321. https://doi.org/10.1098/rspb.2002.2218

Heim R (1938) Diagnoses latines d'espèces et variétés nouvelles de Lactario-Russulés du domaine oriental de madagascar. Candollea (7): 375–393.

Hibbett D, Abarenkov K, Kõljalg U, Öpik M, Chai B, Cole J , Wang Q, Crous P, Robert V, Helgason T, Herr JR, Kirk P, Lueschow S, O'Donnell K, Nilsson RH, Oono R, Schoch C, Smyth C, Walker DM, Porras-Alfaro A, Taylor JW, Geiser DM (2016) Sequence-based classification and identification of Fungi. Mycologia 108(6): 1049–1068.

Hofstetter V, Buyck B, Eyssartier G, Schnee S, Gindro K (2019) The unbearable lightness of sequenced-based identification. Fungal Diversity 96(1): 243–284. https://doi.org/10.1007/s13225-019-00428-3

Hongo T (1968) Notulae Mycologicae (7). Memoir of Shiga University 18: 47–52. https://doi.org/10.2307/1293963

Hyde KD, Hongsanan S, Jeewon R, Bhat DJ, McKenzie EHC, Jones EBG, Phookamsak R, Ariyawansa HA, Boonmee S, Zhao Q, Abdel-Aziz FA, Abdel-Wahab MA, Banmai S, Chomnunti P, Cui B-K, Daranagama DA, Das K, Dayarathne MC, de Silva NI, Dissanayake AJ, Doilom M, Ekanayaka AH, Gibertoni TB, Góes-Neto A, Huang S-K, Jayasiri SC, Jayawardena RS, Konta S, Lee HB, Li W-J, Lin C-G, Liu J-K, Lu Y-Z, Luo Z-L, Manawasinghe IS, Manimohan P, Mapook A, Niskanen T, Norphanphoun C, Papizadeh M, Perera RH, Phukhamsakda C, Richter C, de Santiago ALCMA, Drechsler-Santos ER, Senanayake IC, Tanaka K, Tennakoon TMDS, Thambugala KM, Tian Q, Tibpromma S, Thongbai B, Vizzini A, Wanasinghe DN, Wijayawardene NN, Wu H-X, Yang J, Zeng X-Y, Zhang H, Zhang J-F, Bulgakov TS, Camporesi E, Bahkali AH, Amoozegar MA, Araujo-Neta LS, Ammirati JF, Baghela A, Bhatt RP, Bojantchev D, Buyck B, da Silva GA, de Lima CLF, de Oliveira RJV, de Souza CAF, Dai Y-C, Dima B, Duong TT, Ercole E, Mafalda-Freire F, Ghosh A, Hashimoto A, Kamolhan S, Kang J-C, Karunarathna SC, Kirk PM, Kytövuori I, Lantieri A, Liimatainen K, Liu Z-Y, Liu X-Z, Lücking R, Medardi G, Mortimer PE, Nguyen TTT, Promputtha I, Raj KNA, Reck MA, Lumyong S, Shahzadeh-Fazeli SA, Stadler M, Soudi MR, Su H-Y, Takahashi T, Tangthirasunun N, Uniyal P, Wang Y, Wen T-C, Xu J-C, Zhang Z-K, Zhao Y-C, Zhou J-L, Zhu L (2016) Fungal diversity notes 367–490: taxonomic and phylogenetic contribution to fungal taxa. Fungal Diversity 80(1): 1–270. https://doi.org/10.1007/s13225-016-0373-x

Katoh K, Standley DM (2013) MAFFT multiple sequence alignment software version 7: improvement in performance and usability. Molecular Biology and Evolution 30(4): 772–780. https://doi.org/10.1093/molbev/mst010

Kibby G, Fatto R (1990) Keys to the species of *Russula* in Northeastern North America, 3rd edition. Kibby-Fatto Enterprises, Somerville, 61 pp.

Kornerup A, Wanscher JH (1978) Metheun handbook of colour, 3rd edn. Eyre Metheun Ltd., London, 252 pp.

Kränzlin F (2005) Fungi of Switzerland, vol 6, Russulaceae: *Lactarius*, *Russula*. Verlag Mykologia, Luzern, 320 pp.

Kumar S, Stecher G, Tamura K (2016) MEGA7: Molecular Evolutionary Genetics Analysis Version 7.0 for bigger datasets. Molecular Biology and Evolution 33: 1870−1874. https://doi.org/10.1093/molbev/msw054

Lebel T, Tonkin J (2007) Australian species of *Macowanites* are sequestrate species of *Russula* (Russulaceae, Basidiomycota). Australian Systematic Botany 20: 355–381. https://doi.org/10.1071/SB07007

Lee YS, Lim YW, Kim JJ, Yun HY, Kim C, Park JY (2015) National list of species of Korea: Basidiomycota. National Institute of Biological Resources, South Korea, 364 pp.

Lee H, Park MS, Jung PE, Eimes JA, Seok SJ, Lim YW (2017) Re-evaluation of the taxonomy and diversity of *Russula* section *Foetentinae* (Russulales, Basidiomycota) in Korea. Mycoscience 58(5): 351–360. https://doi.org/10.1016/j.myc.2017.04.006

Lee H, Wissitrassameewong K, Park MS, Verbeken A, Eimes J, Lim YW (2019) Taxonomic revision of the genus *Lactarius* (Russulales, Basidiomycota) in Korea. Fungal Diversity 95(1): 275–335. https://doi.org/10.1007/s13225-019-00425-6

Looney BP (2015) Molecular annotation of type specimens of *Russula* species described by W.A. Murrill from the southeast United States. Mycotaxon 129(2): 255–268. https://doi.org/10.5248/129.255

Looney BP, Ryberg M, Hampe F, Sánchez-García M, Matheny PB (2016) Into and out of the tropics: global diversification patterns in a hyperdiverse clade of ectomycorrhizal fungi. Molecular Ecology 25: 630–647. https://doi.org/10.1111/mec.13506

Looney BP, Meidl P, Piatek MJ, Miettinen O, Martin FM, Matheny PB, Labbé JL (2018) Russulaceae: a new genomic dataset to study ecosystem function and evolutionary diversification of ectomycorrhizal fungi with their tree associates. New Phytologist 218(1): 54–65. https://doi.org/10.1111/nph.15001

Looney BP, Adamčík S, Matheny PB (2020) Coalescent-based delimitation and species-tree estimations reveal Appalachian origin and Neogene diversification in *Russula* subsection *Roseinae*. Molecular Phylogenetics and Evolution 147: e106787. https://doi.org/10.1016/j.ympev.2020.106787

Maire R (1910) Les bases de la classification dan le genre *Russula*. Bulletin de la Société Mycologique de France 26: 49–125.

Martin KJ, Rygiewicz PT (2005) Fungal-specific PCR primers developed for analysis of the ITS region of environmental DNA extracts. BMC Microbiology 5(28): 1–11. https://doi.org/10.1186/1471-2180-5-28

Matheny PB, Wang Z, Binder M, Curtis JM, Lim YW, Nilsson RH, Hughes KW, Hofstetter V, Ammirati JF, Schoch CL, Langer E, Langer G, McLaughlin DJ, Wilson AW, Frøslev T, Ge ZW, Kerrigan RW, Slot JC, Yang ZL, Baroni TJ, Fischer M, Hosaka K, Matsuura K, Seidl MT, Vauras J, Hibbett DS (2007) Contributions of *rpb2* and *tef1* to the phylogeny of mushrooms and allies (Basidiomycota, Fungi). Molecular Phylogenetics and Evolution 43: 430–451. https://doi.org/10.1016/j.ympev.2006.08.024

Miller MA, Pfeiffer W, Schwartz (2010) Creating the CIPRES science gateway for inference of large phylogenetic trees. Proceeding of the Gateway Computing Environments Workshop (GCE): 1–8. https://doi.org/10.1109/GCE.2010.5676129

Miyamoto Y, Nakano T, Hattori M, Nara K (2014) The mid-domain effect in ectomycorrhizal fungi: range overlap along an elevation gradient on Mount Fuji, Japan. The ISME Journal 8(8): 1739–1746. https://doi.org/10.1038/ismej.2014.34

Murrill WA (1940) Additon to Florda fungi: 1. Bulletin of the Terrey Botanical Club 67(1): 57–66. https://doi.org/10.2307/2485361

Murrill WA (1941) More Florida novelties. Mycologia 33: 434–448. https://doi.org/10.1080/00275514.1941.12020837

Murrill WA (1943) More new fungi from Florida. Lloydia 6: 207–228. https://doi.org/10.1056/NEJM194302112280612

Nakashima H, Eguchi N, Uesugi T, Yamashita N, Matsuda Y (2016) Effect of ectomycorrhizal composition on survival and growth of *Pinus thunbergii* seedlings varying in resistance to the pine wilt nematode. Mycorrhiza 30(2): 475–481. https://doi.org/10.1007/s00468-015-1217-0

Nuytinck J, Verbeken A (2003) *Lactarius sanguifluus* versus *Lactarius vinosus*–molecular and morphological analyses. Mycological Progress 2(3): 227–234. https://doi.org/10.1007/s11557-006-0060-5

Obase K, Lee JK, Lee SY, Chun KW (2011) Diversity and community structure of ectomycorrhizal fungi in *Pinus thunbergii* coastal forests in the eastern region of Korea. Mycoscience 52: 383–391. https://doi.org/10.1007/S10267-011-0123-6

Paloi S, Das K, Acharya K (2018) *Russula darjeelingensis*, a new species from Eastern Himalaya, India. Phytotaxa 358(1): 83–90. https://doi.org/10.11646/phytotaxa.358.1.6

Park MS, Fong JJ, Lee H, Oh SY, Jung PE, Min YJ, Seok SJ, Lim YW (2013) Delimitation of *Russula* subgenus *Amoenula* in Korea using three molecular markers. Mycobiology 41(4): 191–201. https://doi.org/10.5941/MYCO.2013.41.4.191

Park MS, Lee H, Oh SY, Jung PE, Seok SJ, Fong JJ, Lim YW (2014) Species delimitation of three species within the *Russula* subgenus *Compacta* in Korea: *R. eccentrica*, *R. nigricans*, and *R. subnigricans*. Journal of Microbiology 52(8): 631–638. https://doi.org/10.1007/s12275-014-4168-z

Peck CH (1872) Report of the botanist (1870). Annual report on the New York state museum of natural history 24: 41–108.

Posada D (2008) jModelTest: Phylogenetic model averaging. Molecular Biology and Evolution 25(7): 1253–1256. https://doi.org/10.1093/molbev/msn083

Quélet L (1880) Quelques especes critique ou nouvelles de la Flore Mycologique de France. Comptes Rendus de l'Association Française pour l'Avancement des Sciences 9: 661–675.

Quélet L (1898) Quelques espèces critiques ou nouvelles pour la Flore mycologique de France. Comptes Rendus de l'Association Française pour l'Avancement des Sciences 26(2): 446–452.

Rambaut A, Suchard MA, Xie D, Drummond AJ (2014) Tracer 1.6. http://beast.bio.ed.ac.uk

Roger SO, Bendich AJ (1994) Extraction of total cellular DNA from plants, algae and fungi. In: Gelvin SB, Schilperport RA (Eds) Plant molecular biology manual. Kluwer Academic Publisher, Boston, 183–190. https://doi.org/10.1007/978-94-011-0511-8_12

Romagnesi H (1962) Taxa nova ex genere *Russula*. Bulletin Mensuel de la Société Linnéenne de Lyon 31(1): 172–177. https://doi.org/10.3406/linly.1962.7058

Romagnesi H (1985) *Russula amoena* Quél. Var. acystidiata n.f. Bulletin de la Société Mycologique de France 101: 2–5.

Ronquist F, Huelsenbeck JP (2003) MrBayes 3: Bayesian phylogenetic inference under mixed models. Bioinformatics 19: 1572–1574. https://doi.org/10.1093/bioinformatics/btg180

Sarnari M (1998) Monographia Illustrata del Genere Russula in Europa tomo primo. Associazioni Micologica Bresadola, Trento, 800 pp.

Savolainen V, Cowan RS, Vogler AP, Roderick GK, Lane R (2005) Towards writing the encyclopaedia of life: an introduction to DNA barcoding. Philosophical Transactions of the Royal Society B – Biological Sciences 360: 1805–1811. https://doi.org/10.1098/rstb.2005.1730

Shimono Y, Kato M, Takamatsu S (2004) Molecular phylogeny of Russulaceae (Basidiomycetes; Russulales) inferred from the nucleotide sequences of nuclear large subunit rDNA. Mycoscience 45: 303–316. https://doi.org/10.1007/S10267-004-0189-5

Singer R (1932) Monographie der Gattung Russula. Beihefte zum Botanischen Centralblatt 49(2): 205–380.

Singer R (1942a) Type studies on Basidiomycetes. I. Mycologia 34: 64–93. https://doi.org/10.1080/00275514.1942.12020874

Singer R (1942b) Das system der Agaricales. II. Annales Mycologici 40: 1–108.

Singer R (1958) New and interesting species of Basidiomycetes. V. Sydowia 11: 141–374. https://doi.org/10.2307/3756045

Singer R (1975) *The Agaricales in modern taxonomy*. 3rd edn. J. Cramer, Vaduz, 912 pp.

Song Y, Li J, Buyck B, Zheng J, Qiu L (2018) *Russula verrucospora* sp. nov. and *R. xanthovirens* sp. nov., two novel species of *Russula* (Russulaceae) from southern China. Cryptogamie Mycologie 39(1): 129–142. https://doi.org/10.7872/crym/v39.iss1.2018.129

Stamatakis A (2014) RAxML Version 8: A tool for phylogenetic analysis and post-analysis of large phylogenies. Bioinformatics 30(9): 1312–1313. https://doi.org/10.1093/bioinformatics/btu033

Sugiyama Y, Murata M, Kanetani S, Nara K (2019) Towards the conservation of ectomycorrhizal fungi on endangered trees: native fungal species on *Pinus amamiana* are rarely conserved in trees planted ex situ. Mycorrhiza 29(3): 195–205. https://doi.org/10.1007/s00572-019-00887-1

Vellinga EC (1988) Glossary. In: Bas C, Kuyper TW, Noordeloos ME, Vellinga EC (Eds) Flora Agaricana Neerlandica, vol.1 A.A. Balkema, Rotterdam, 1–182.

Wang X-H, Halling RE, Hofstetter V, Lebel T, Buyck B (2018) Phylogeny, biogeography and taxonomic re-assessment of *Multifurca* (Russulaceae, Russulales) using three-locus data. PLoS ONE 13(11): e0205840. https://doi.org/10.1371/journal.pone.0205840

Wen Z, Murata M, Xu Z, Chen Y, Nara K (2015) Ectomycorrhizal fungal communities on the endangered Chinese Douglas-fir (*Pseudotsuga sinensis*) indicating regional fungal sharing overrides host conservatism across geographical regions. Plant and Soil 387: 189–199. https://doi.org/10.1007/s11104-014-2278-3

White TJ, Bruns T, Lee S, Taylor J (1990) Amplification and direct sequencing of fungal ribosomal RNA genes for phylogenetics. In: Innis MA, Gelfand DH, Sninsky JJ, White TJ (Eds) PCR protocols: a guide to methods and applications. Academic Press, San Diego, 315–322. https://doi.org/10.1016/B978-0-12-372180-8.50042-1

Xie X D, Liu PG, Yu FQ (2010) Species diversity of russuloid mycorrhizae-forming fungi on *Pinus yunnanensis* seedlings and the mycorrhizal morphology. Acta Botanica Yunnanica 32: 211–220. https://doi.org/10.3724/SP.J.1143.2010.10001

Supplementary material 1

Table S1. List of validly published names classified in *R.* subsect. *Amoeninae* and allied species around the world

Authors: Komsit Wisitrassameewong, Myung Soo Park, Hyun Lee, Aniket Ghosh, Kanad Das, Bart Buyck, Brian P. Looney, Miroslav Caboň, Slavomír Adamčík, Changmu Kim, Chang Sun Kim, Young Woon Lim

Data type: species list

Explanation note: List of validly published names classified in *R.* subsect. *Amoeninae* and allied species around the world.

Link: https://doi.org/10.3897/mycokeys.75.53673.suppl1

Supplementary material 2

Table S2. Sequences used for the ITS analyses in this study

Authors: Komsit Wisitrassameewong, Myung Soo Park, Hyun Lee, Aniket Ghosh, Kanad Das, Bart Buyck, Brian P. Looney, Miroslav Caboň, Slavomír Adamčík, Changmu Kim, Chang Sun Kim, Young Woon Lim

Data type: ITS sequences

Explanation note: Sequences used for the ITS analyses in this study. ITS sequences generated in this study are presented in boldface. (T) indicates the type specimen. Species names in bracket are the original species epithet in GenBank or Park et al. (2013).

Link: https://doi.org/10.3897/mycokeys.75.53673.suppl2

MycoKeys 75: 31–49 (2020)
doi: 10.3897/mycokeys.75.57192
https://mycokeys.pensoft.net

RESEARCH ARTICLE

A peer-reviewed open-access journal
MycoKeys
Launched to accelerate biodiversity research

Five new additions to the genus *Spathaspora* (Saccharomycetales, Debaryomycetaceae) from southwest China

Shi-Long Lv[1], Chun-Yue Chai[1], Yun Wang[1], Zhen-Li Yan[2], Feng-Li Hui[1]

1 *School of Life Science and Technology, Nanyang Normal University, Nanyang 473061, China* **2** *State Key Laboratory of Motor Vehicle Biofuel Technology, Henan Tianguan Enterprise Group Co. Ltd., Nanyang 473000, China*

Corresponding author: Feng-Li Hui (fenglihui@yeah.net)

Academic editor: K.D. Hyde | Received 3 August 2020 | Accepted 25 October 2020 | Published 9 November 2020

Citation: Lv S-L, Chai C-Y, Wang Y, Yan Z-L, Hui F-L (2020) Five new additions to the genus *Spathaspora* (Saccharomycetales, Debaryomycetaceae) from southwest China. MycoKeys 75: 31–49. https://doi.org/10.3897/mycokeys.75.57192

Abstract

Spathaspora is an important genus of D-xylose-fermenting yeasts that are poorly studied in China. During recent yeast collections in Yunnan Province in China, 13 isolates of *Spathaspora* were obtained from rotting wood and all represent undescribed taxa. Based on morphological and phylogenetic analyses (ITS and nuc 28S), five new species are proposed: *Spathaspora elongata*, *Sp. mengyangensis*, *Sp. jiuxiensis*, *Sp. parajiuxiensis* and *Sp. rosae*. Our results indicate a high species diversity of *Spathaspora* waiting to be discovered in rotting wood from tropical and subtropical southwest China. In addition, the two *Candida* species, *C. jeffriesii* and *C. materiae*, which are members of the *Spathaspora* clade based on phylogeny, are transferred to *Spathaspora* as new combinations.

Keywords

Five new species, Debaryomycetaceae, Saccharomycetales, yeast taxonomy, D-xylose-fermenting yeast

Introduction

Spathaspora N.H. Nguyen, S.O. Suh & M. Blackw (2006) (Saccharomycetales, Debaryomycetaceae) was introduced, based on a single species, *Spathaspora passalidarum*, which was isolated from a passalid beetle in Louisiana, USA (Nguyen et al. 2006). This species produces asci containing elongate ascospores with curved ends, a unique trait of this

genus (Nguyen et al. 2006; Nguyen et al. 2011). Subsequently, *Spathaspora arborariae*, *Sp. boniae*, *Sp. brasiliensis*, *Sp. girioi*, *Sp. gorwiae*, *Sp. hagerdaliae*, *Sp. piracicabensis*, *Sp. roraimanensis*, *Sp. suhii* and *Sp. xylofermentans* were introduced. These were from rotting wood (Cadete et al. 2009, 2013; Lopes et al. 2016; Morais et al. 2017; Varize et al. 2018) and *Sp. allomyrinae* from insects (Wang et al. 2016). *Spathaspora* has been shown to be a polyphyletic group, containing members placed throughout the larger *Spathaspora*/*Candida albicans*/*Lodderomyces* clade of Debaryomycetaceae (Morais et al. 2017; Varize et al. 2018). Several *Candida* species, such as *C. blackwellae*, *C. jeffriesii*, *C. lyxosophila*, *C. materiae*, *C. parablackwellae* and *C. subhashii*, are closely related to *Spathaspora*, based on a phylogenetic analysis of the D1/D2 domain of the nuclear 28S rDNA (nuc 28S) sequences (Cadete et al. 2013; Daniel et al. 2014; Morais et al. 2017; Varize et al. 2018).

Most species of *Spathaspora*, including *Sp. arborariae*, *Sp. brasiliensis*, *Sp. passalidarum*, *Sp. roraimanensis*, *Sp. suhii* and *Sp. xylofermentans*, are economically important because of their ability to ferment D-xylose, the second most abundant sugar in lignocellulosic feedstocks (Nguyen et al. 2011; Cadete et al. 2013; Lopes et al. 2016; Morais et al. 2017). These xylose-fermenting species can be used directly for ethanol production or may provide a source of genes, enzymes and/or sugar transporters to engineer industrial strains for the efficient production of bioethanol from renewable biomass (Wohlbach et al. 2011; Cadete et al. 2013).

Spathaspora species are associated with rotting-wood substrates and the insects that occupy this ecological niche (Cadete et al. 2009, 2013; Nguyen et al. 2011; Lopes et al. 2016; Wang et al. 2016; Morais et al. 2017; Varize et al. 2018). They can be found in tropical, subtropical and temperate regions on different continents, but most species are presently known from Brazilian regions (Cadete et al. 2009, 2013; Lopes et al. 2016; Morais et al. 2017; Varize et al. 2018). In China, the genus is underexplored with only three published reports of the species *Sp. allomyrinae*, *Sp. gorwiae* and *Sp. passalidarum* (Ren et al. 2013; Wang et al. 2016). Here, we describe five new species of *Spathaspora* discovered in tropical and subtropical areas of southwest China, based on their morphological characters and molecular phylogenetic analyses.

Materials and methods

Sample collection and isolation

Rotting wood samples were collected in two areas of Yunnan Province, China. The areas are located in the Xishuangbanna Primeval Forest Park of Jinghong (21°98'N, 100°88'E) and Jiuxi Mountain Forest Park of Honghe (24°40'N, 103°68'E). The predominant vegetation is characterised as a tropical and subtropical forest biome. The climate is hot and humid, with annual precipitation between 1,100 to 1,600 mm and an average temperature that ranges from 17.2 to 26.4 °C. Sixty decayed wood samples were collected, thirty from each area, during July to August in 2016–2018. The samples were stored in sterile plastic bags and transported under refrigeration to the

laboratory over a period of no more than 24 h. The yeast strains were isolated from rotting wood samples in accordance with the methods described by Lopes et al. (2016). Each sample (1 g) was added to 20 ml sterile D-xylose medium (yeast nitrogen base 0.67%, D-xylose 0.5%, chloramphenicol 0.02%, pH 5.0 ± 0.2) in a 150 ml Erlenmeyer flask and then cultured for 3–10 days on a rotary shaker. Subsequently, 0.1 ml aliquots of the enrichment culture and appropriate decimal dilutions were spread on D-xylose agar plates and then incubated at 25 °C for 3–4 days. Different yeast colony morphotypes were then isolated by repeated plating on yeast extract-malt extract (YM) agar (1% glucose, 0.5% peptone, 0.3% yeast extract and 0.3% malt extract, pH 5.0 ± 0.2) and stored on YM agar slants at 4 °C or in 15% glycerol at –80 °C.

Morphological, physiological and biochemical studies

Morphological and physiological properties were determined according to Kurtzman et al. (2011). Induction of the sexual stage was tested by incubating single or mixed cultures of each of the two strains on cornmeal (CM) agar, 5% malt extract (ME) agar, dilute (1:9 and 1:19) V8 agar or yeast carbon base plus 0.01% ammonium sulphate (YCBAS) agar at 25 °C for 2 months (Cadete et al. 2013; Lopes et al. 2016). Assimilation of carbon and nitrogen compounds and growth requirements were tested at 25 °C. The effects of temperature from 25–40 °C were examined in liquid culture and on agar plates. Ethanol was determined with alcohol oxidase (Sangon Biotech, China) and peroxidase (Sangon Biotech, China), as described previously (Alves et al. 2007).

DNA extraction, PCR amplification and nucleotide sequencing

Genomic DNA was extracted from the yeasts using the Ezup Column Yeast Genomic DNA Purification Kit, according to the manufacturer's protocol (Sangon Biotech, China). The nuc rDNA ITS1-5.8S-ITS2 (ITS) region was amplified using the primer pair ITS1/ITS4 (White et al. 1990). The D1/D2 domain of the nuc 28S rDNA was amplified using the primer pair NL1/NL4 (Kurtzman and Robnett 1998). The following thermal profile was used to amplify the ITS and nuc 28S regions: an initial denaturation step of 2 min at 95 °C, followed by 35 cycles of 30 s at 95 °C, 30 s at 51 °C and 40 s at 72 °C, with a final extension of 10 min at 72 °C (Liu et al. 2016). PCR products were directly purified and sequenced by Sangon Biotech Inc. (Shanghai, China). We determined the identity and accuracy of the newly-obtained sequences by comparing them to sequences in GenBank and assembled them using BioEdit (Hall 1999). Newly-obtained sequences were then submitted to GenBank (https://www.ncbi.nlm.nih.gov/genbank/; Table 1).

Phylogenetic analyses

The sequences obtained from this study and the reference sequences downloaded from GenBank (Table 1) were aligned using MAFFT v. 6 (Katoh and Toh 2010) and

Table 1. DNA sequences used in the molecular phylogenetic analysis. Entries in bold are newly generated in this study.

Species	Strain	ITS	D1/D2
Candida albicans	NRRL Y-12983^T	HQ876043	U45776
Candida argentea	CBS 12358^T	JF682350/	JF682353
Candida baotianmanensis	CBS 13915^T	KM586743	KM586733
Candida blackwellae	CBS 10843^T	EU402940/	EU402939
Candida bohiensis	NRRL Y-27737^T	FJ172255	AY520317
Candida buenavistaensis	NRRL Y-27734^T	FJ623627	AY242341
Candida cetoniae	CBS 12463^T	KC118129	KC118128
Candida chauliodes	NRRL Y-27909^T	FJ623621	DQ655678
Candida coleopterorum	CBS 14180^T	KU128707	KU128722
Candida corydalis	NRRL Y-27910^T	FJ623622	DQ655679
Candida dubliniensis	NRRL Y-17841^T	KY102055	U57685
Candida frijolesensis	NRRL Y-48060^T	EF658666	EF120596
Candida hyderabadensis	NRRL Y-27953^T	AM180949	AM159100
Candida jeffriesii	CBS 9898^T	NR_111398	NG_042498
Candida jiufengensis	CBS 10846^T	EU402936	EU402935
Candida kantuleensis	CBS 15219^T	LC317101	LC317097
Candida labiduridarum	NRRL Y-27940^T	EF658664	DQ655687
Candida lyxosophila	NRRL Y-17539^T	KY102184	HQ263370
Candida maltosa	NRRL Y-17677^T	NR_138346	U45745
Candida margitis	CBS 14175^T	KU128708	KU128721
Candida materiae	CBS 10975^T	FJ154790	FJ154790
Candida metapsilosis	CBS 10907^T	FJ872019	DQ213057
Candida morakotiae	NBRC 105009^T	AB696987	DQ400364
Candida neerlandica	NRRL Y-27057^T	EF658662	AF245404
Candida oleophila	NRRL Y-2317^T	AJ539374/	U45793
Candida orthopsilosis	ATCC MYA-96139^T	FJ545241	DQ213056
Candida oxycetoniae	CBS 10844^T	KY102281	EU402933
Candida parablackwellae	NYNU 17763^T	MG255731	MG255702
Candida parachauliodis	CBS 13928^T	KP054272	KP054271
Candida parapsilosis	NRRL Y-12969^T	AJ635316	U45754
Candida pseudojiufengensis	CBS 10847^T	EU402938	EU402937
Candida pseudoviswanathii	CBS 13916^T	KM586736	KM586735
Candida sanyaensis	CBS 12637^T	JQ647915	JQ647914
Candida sakaeoensis	CBS 12318^T	AB696985	AB617978
Candida sojae	NRRL Y-17909^T	KJ722419	U71070
Candida subhashii	CBS 10753^T	NR_073356	EU836708
Candida tetrigidarum	NRRL Y-48142^T	FJ623630	EF120599
Candida theae	ATCC MYA-4746^T	JQ812707	JQ812701
Candida tropicalis	NRRL Y-12968^T	AF287910	U45749
Candida verbasci	CBS 12699^T	JX515982	JX515981
Candida viswanathii	CBS 4024^T	KY102515	U45752
Candida xiaguanensis	CBS 13923^T	KM586732	KM586731
Candida yunnanensis	NYNU 17948^T	MG255721	MG255709
Lodderomyces beijingensis	CBS 14171^T	KU128709	KU128720
Lodderomyces elongisporus	NRRL YB-4239^T	AY391848	U45763
Nematodospora anomalae	CBS 13927^T	KP054270	KP054269
Nematodospora valgi	CBS 12562^T	KM386993	HM627112
Scheffersomyces stipitis	NRRL Y-7124^T	JN943257/	U45741
Spathaspora allomyrinae	CBS 13924^T	KP054268	KP054267
Spathaspora arborariae	ATCC MYA-4684^T	NR_111592	NG_042574
Spathaspora boniae	CBS 13262^T	NR_158910	KT276332
Spathaspora brasiliensis	CBS 12679^T	JN099271	JN099271
Spathaspora elongata	**NYNU 18115^T**	**MK682770**	**MK682796**
Spathaspora elongata	**NYNU 181112**	**MT276033**	**MT274662**

Species	Strain	ITS	D1/D2
Spathaspora elongata	**NYNU 181120**	**MT276034**	**MT276036**
Spathaspora elongata	**NYNU 181158**	**MT276035**	**MT276032**
Spathaspora girioi	CBS 13476^{T}	NR_155783	NG_059955
Spathaspora gorwiae	CBS 13472^{T}	NR_155784	NG_059956
Spathaspora hagerdaliae	CBS 13475^{T}	NR_155800	KU556168
Spathaspora jiuxiensis	**NYNU 17416^{T}**	**MG255706**	**MG255718**
Spathaspora jiuxiensis	**NYNU 17417**	**MT276035**	**MT276032**
Spathaspora mengyangensis	**NYNU 17741^{T}**	**KY213816**	**KY213819**
Spathaspora mengyangensis	**NYNU 17705**	**MT272353**	**MT272351**
Spathaspora parajiuxiensis	**NYNU 16747^{T}**	**MG255728**	**MG255705**
Spathaspora parajiuxiensis	**NYNU 16632**	**MT272352**	**MT272350**
Spathaspora passalidarum	NRRL Y-27907^{T}	NR_111397	DQ109807
Spathaspora piracicabensis	CBS 15054^{T}	KR864907	KR864906
Spathaspora rosae	**NYNU 17934^{T}**	**MG255725**	**MG255701**
Spathaspora rosae	**NYNU 17903**	**MT274659**	**MT274661**
Spathaspora rosae	**NYNU 17909**	**MT274664**	**MT274663**
Spathaspora roraimanensis	CBS 12681^{T}	JN099269	JN099269
Spathaspora suhii	CBS 12680^{T}	JN099270	JN099270
Spathaspora xylofermentans	CBS 12682^{T}	JN099268	JN099268
Wickerhamia fluorescens	JCM 1821^{T}	NR_111311/	NG_054831

Abbreviations: **ATCC**: American Type Culture Collection, Manassas, VA, USA; **CBS**: CBS-KNAW Collections, Westerdijk Fungal Biodiversity Institute, Utrecht, The Netherlands; **JCM**: RIKEN BioResource Research Center-Japan Collection of Microorganisms, Takao, Japan; **NRRL**: the ARS Culture Collection, National Center for Agricultural Utilization Research, Peoria, IL, USA; **NYNU**: Microbiology Lab, Nanyang Normal University, Henan, China; **T**: type strain.

manually edited using MEGA v. 7 (Kumar et al. 2016). The best-fit nucleotide substitution models for each gene were selected using jModelTest v2.1.7 (Darriba et al. 2012), according to the Akaike Information Criterion.

Phylogenetic analyses of the combined gene regions (ITS and nuc 28S) were performed using the Maximum Likelihood (ML) and Bayesian Inference (BI) methods. *Candida argentea* CBS 12358 was chosen as the outgroup. ML analysis was performed using MEGA v7 with the GTR+I+G model (Nei and Kumar 2000) and 1,000 rapid bootstrap replicates to estimate branch confidence. BI analysis was performed using a Markov Chain Monte Carlo (MCMC) algorithm in MrBayes v. 3.0b4 (Ronquist and Huelsenbeck 2003). Two MCMC chains, started from random trees for 1,000,000 generations and trees, were sampled every 100th generation, resulting in a total of 10,000 trees. The first 25% of the trees were discarded as burn-in of each analysis. Branches with significant Bayesian Posterior Probabilities (BPP) were estimated in the remaining 7,500 trees. The phylogenetic trees from the ML and BI analyses were displayed using Mega 7 and FigTree v1.4.3 (Rambaut 2016), respectively.

Results

Phylogenetic analyses

The combined nuclear dataset (ITS and nuc 28S) was analysed to infer the interspecific relationships within the larger *Spathaspora*/*Candida albicans*/*Lodderomyces* clade

of Debaryomycetaceae. The dataset consisted of 72 sequences including the outgroup, *Candida argentea* (culture CBS 12358). A total of 944 characters including gaps (391 for ITS and 553 for nuc 28S) were included in the phylogenetic analysis. The best nucleotide substitution model for ITS and nuc 28S was GTR+I+G. ML and BI analyses of the combined dataset resulted in phylogenetic reconstructions with similar topologies and the average standard deviation of split frequencies was 0.011210 (BI). In the ML phylogenetic tree (Figure 1), thirteen strains formed five single clades with high to full support (100% in ML and 0.99 or 1.00 in BI) and clustered in the clade that comprised most species of *Spathaspora*. Phylogenetically, *S. elongata* and *S. mengyangensis* clustered together with high support (84% in ML and 0.91 in BI), while *S. jiuxiensis* and *S. parajiuxiensis* clustered together with strong support (100% in ML and 1.00 in BI). Two strains of *S. rosae* formed a unique lineage with *S. allomyrinae*, but with low support.

Taxonomy

Spathaspora elongata **C.Y. Chai & F.L. Hui, sp. nov.**
MycoBank: 836444
Figure 2

Type. China, Yunnan Province, Jinghong City, Mengyang Town, in rotting wood from a tropical rainforest, August 2018, K.F. Liu & Z.W. Xi (holotype, NYNU 18115^{T} preserved in a metabolically-inactive state), ex-holotype: CICC 33353; CBS 16002.

Etymology. *Elongata* refers to the elongate ascospores of this yeast.

Description. After 3 days of culture in YM broth at 25 °C, the cells are ovoid (3–4 × 3–7 μm) and occur singly or in pairs (Fig. 2a). Budding is multilateral. Sediment is formed after a month, but a pellicle is not observed. After 3 days of growth on YM agar at 25 °C, colonies are white to cream-coloured, butyrous and smooth with entire margins. After 14 days at 25 °C, on Dalmau plate culture on CM agar, pseudohyphae are present, but true hyphae are not formed (Fig. 2b). Sporulation occurs on dilute (1:19) V8 agar after 14 days at 25 °C. Unconjugated asci are formed from single cells with one elongated ascospore which are tapered and curved at the ends (Fig. 2c). Glucose, galactose, maltose and sucrose are weakly fermented. Xylose fermentation is absent using Durham tubes, but ethanol is produced from xylose when determined with alcohol oxidase and peroxidase tests. Glucose, D-ribose, D-xylose, D-arabinose, sucrose, maltose, trehalose, methyl α-D-glucoside, cellobiose, salicin, arbutin, inulin, ribitol, D-glucitol, D-mannitol, 2-keto-D-gluconate, succinate, citrate and ethanol are assimilated. No growth occurs with galactose, L-sorbose, D-glucosamine, L-arabinose, L-rhamnose, melibiose, lactose, raffinose, melezitose, glycerol, erythritol, xylitol, galactitol, *myo*-inositol, D-glucono-1, 5-lactone, 5-keto-D-gluconate, D-gluconate, D-glucuronate, DL-lactate or methanol. For the assimilation of nitrogen compounds, growth on ethylamine, L-lysine, glucosamine or D-tryptophan is present, whereas growth on nitrate, nitrite, cadaverine, creatine, creatinine or imidazole is absent. Growth is observed at 37 °C but not at 40 °C. Growth in the presence of 1% acetic acid is present,

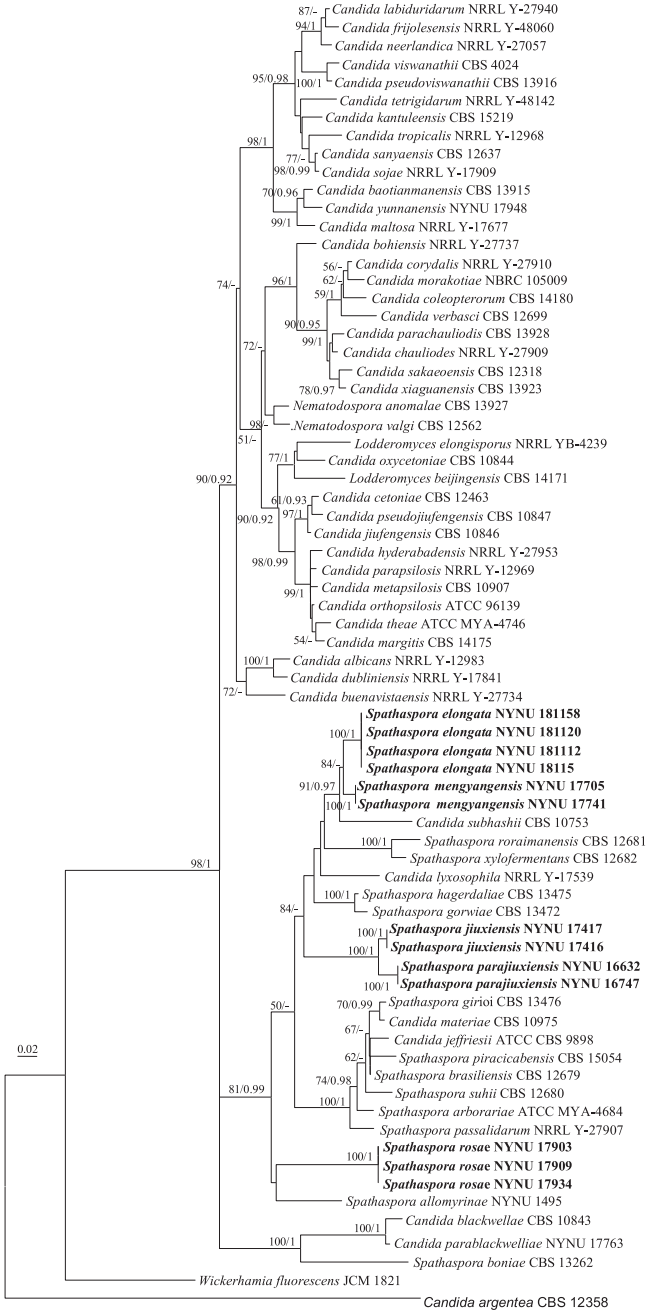

Figure 1. Phylogenetic tree, based on an ML analysis of a combined DNA dataset of ITS and nuc 28S rDNA sequences for *Spathaspora* species and related taxa in the Debaryomycetaceae. Numbers above the branches indicate ML bootstraps (left, MLBS ≥ 50%) and Bayesian Posterior Probabilities (right, BPP ≥ 0.90). The tree is rooted with sequences from *Candida argentea* CBS 12358. Isolates from the current study are shown in bold letters. "-" indicates MLBS < 50% or BPP < 0.90. The scale bar indicates the number of substitutions per site.

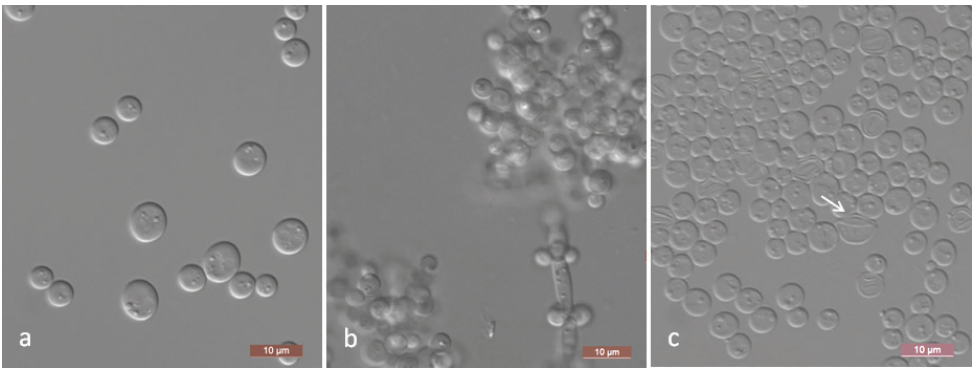

Figure 2. Morphology of *Spathaspora elongata* (NYNU 18115, holotype) **a** budding cells on YM broth after 3 d **b** Pseudohyphae on CM agar after 14 d **c** ascus and ascospore (arrow) on dilute V8 agar after 14 d. Scale bars: 10 µm.

but growth in the presence of 10% sodium chloride (NaCl) plus 5% glucose and 0.01% cycloheximide is absent. Starch-like compounds are not produced. Urease activity and diazonium blue B reactions are negative.

Additional isolates examined. China, Yunnan Province, Jinghong City, Mengyang Town, in rotting wood from a tropical rainforest, August 2018, K.F. Liu & Z.W. Xi, NYNU 181112, NYNU 181120 and NYNU 181158.

Notes. Four strains, representing *Sp. elongata*, clustered in a well-supported phylogenetic clade that is closely related to *Sp. mengyangensis*, another new species proposed in this paper and *C. subhashii*. The nucleotide differences between *Sp. elongata* and *Sp. mengyangensis* were 2.5% substitutions in the D1/D2 domain and 5.2% substitutions in the ITS region (Groenewald et al. 2016). Similarly, *Sp. elongata* and *C. subhashii* showed differences of 3.9% substitutions in the D1/D2 domain and 5.9% substitutions in the ITS region (Groenewald et al. 2016). Physiologically, *Sp. elongata* can be differentiated from its close relative, *Sp. mengyangensis*, based on its growth in citrate and the presence of 1% acetic acid, which are present for *Sp. elongata* and absent for *Sp. mengyangensis*. Moreover, *Sp. elongata* weakly ferments glucose, galactose, maltose and sucrose and grows at 37 °C, but *Sp. mengyangensis* does not.

***Spathaspora mengyangensis* C.Y. Chai & F.L. Hui, sp. nov.**
MycoBank: 836445
Figure 3

Type. China, Yunnan Province, Jinghong City, Mengyang Town, in rotting wood from a tropical rainforest, July 2017, K.F. Liu & L. Zhang (holotype, NYNU 17741^{T} preserved in a metabolically-inactive state), ex-holotype: CICC 33267; CBS 15227.

Etymology. *Mengyangensis* refers to the geographical origin of the type strain of this species.

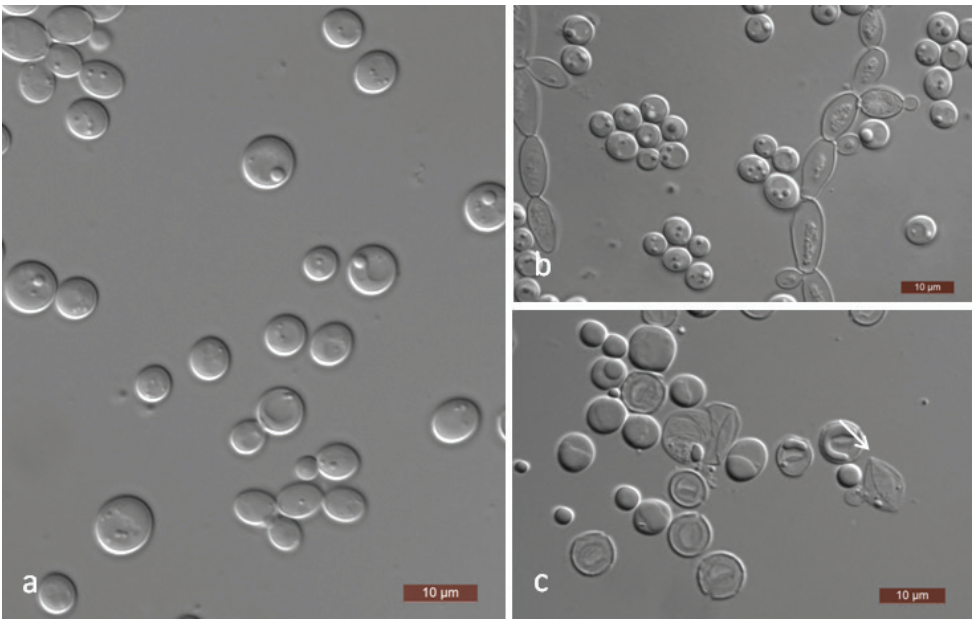

Figure 3. *Spathaspora mengyangensis* (NYNU 17741, holotype) **a** budding cells on YM broth after 3 d **b** simple pseudohyphae on CM agar after 14 d **c** ascus and ascospore (arrow) on CM agar after 14 d. Scale bars: 10 µm.

Description. In YM broth after 3 days at 25 °C, cells are ovoid (3–7 × 5–7.5 µm) and occur singly or in pairs (Fig. 3a). Budding is multilateral. Sediment is formed after a month, but a pellicle is not observed. After 3 days of growth on YM agar at 25 °C, colonies are white to cream-coloured, butyrous and smooth with entire margins. After 14 days at 25 °C on Dalmau plate culture on CM agar, pseudohyphae are present, but true hyphae are not formed (Fig. 3b). Sporulation occurs on CM agar after 14 days at 25 °C. Unconjugated asci are formed from single cells with one elongated ascospore which are tapered and curved at the ends (Fig. 3c). Xylose fermentation is negative using Durham tubes, but ethanol is produced from xylose when determined with alcohol oxidase and peroxidase tests. Glucose, D-ribose, D-xylose, sucrose, maltose, trehalose, methyl α-D-glucoside, cellobiose, salicin, arbutin, inulin, ribitol, D-glucitol, D-mannitol, 2-keto-D-gluconate, succinate and ethanol are assimilated. No growth occurs with galactose, L-sorbose, D-glucosamine, L-arabinose, D-arabinose, L-rhamnose, melibiose, lactose, raffinose, melezitose, glycerol, erythritol, xylitol, galactitol, *myo*-inositol, D-glucono-1, 5-lactone, 5-keto-D-gluconate, D-gluconate, D-glucuronate, DL-lactate, citrate or methanol. For the assimilation of nitrogen compounds, growth on ethylamine, L-lysine, glucosamine or D-tryptophan is present, whereas growth on nitrate, nitrite, cadaverine, creatine, creatinine or imidazole is absent. Growth is observed at 30 °C, but not at 35 °C. Growth in the presence of 10% NaCl plus 5% glucose, 0.01% cycloheximide and 1% acetic acid is absent. Starch-like compounds are not produced. Urease activity and diazonium blue B reactions are negative.

Additional isolate examined. China, Yunnan Province, Jinghong City, Mengyang Town, in rotting wood from a tropical rainforest, July 2017, K.F. Liu & L. Zhang, NYNU 17705.

Notes. Phylogenetic analyses show that *Sp. mengyangensis* is closely related to *Sp. elongata* and *C. subhashii*; however, the independent phylogenetic position and different physiological characters can distinguish *Sp. mengyangensis* from its sister species *Sp. elongata* (as mentioned above). Similarly, *Sp. mengyangensis* differed from *C. subhashii* by 2.8% substitutions in the D1/D2 domain and 7.8% substitutions in the ITS region (Groenewald et al. 2016). Physiologically, *Sp. mengyangensis* can be differentiated from *C. subhashii* by the ability to assimilate D-ribose, trehalose, D-glucitol and D-mannitol and the inability to assimilate galactose, L-arabinose and melezitose. In addition, *C. subhashii* can grow at 40 °C, but *Sp. mengyangensis* cannot.

***Spathaspora jiuxiensis* C.Y. Chai & F.L. Hui, sp. nov.**

MycoBank: 836446

Figure 4

Type. China, Yunnan Province, Honghe Prefecture, Luxi County, in rotting wood in Jiuxi Mountain Forest Park, July 2017, K.F. Liu & L. Zhang (holotype, NYNU 17416^{T} preserved in a metabolically-inactive state), ex-holotype: CICC 33264; CBS 15226.

Etymology. *Jiuxiensis* refers to Jiuxi Mountain, the mountain from which it was collected.

Description. In YM broth after 3 days at 25 °C, cells are ovoid to elongate (3–6 × 3.5–9 μm) and occur singly or in pairs (Fig. 4a); pseudohyphae are present. Budding is multilateral. Sediment is formed after a month, but a pellicle is not observed. After 3 days of growth on YM agar at 25 °C, colonies are white to cream-coloured, butyrous and smooth with entire margins. After 12 days at 25 °C on Dalmau plate culture on CM agar, pseudohyphae and true hyphae are formed (Fig. 4b). Asci or signs of conjugation were not seen on the sporulation media used. Glucose and maltose are weakly fermented. Xylose fermentation is negative using Durham tubes, but ethanol is produced from xylose when determined with alcohol oxidase and peroxidase tests. Glucose, D-glucosamine, D-ribose, D-xylose, sucrose, maltose, trehalose, methyl α-D-glucoside, cellobiose, salicin, arbutin, melezitose, inulin, ribitol, D-glucitol, D-mannitol, 2-keto-D-gluconate, DL-lactate, succinate and ethanol are assimilated. No growth occurs with galactose, L-sorbose, L-arabinose, D-arabinose, L-rhamnose, melibiose, lactose, raffinose, glycerol, erythritol, xylitol, galactitol, *myo*-inositol, D-glucono-1, 5-lactone, 5-keto-D-gluconate, D-gluconate, D-glucuronate, citrate, L-arabinitol or methanol. For the assimilation of nitrogen compounds, growth on L-lysine, glucosamine or D-tryptophan is present, whereas growth on nitrate, nitrite, ethylamine, cadaverine, creatine, creatinine or imidazole is absent. Growth is observed at 35 °C, but not at 37 °C. Growth in the presence of 0.01% cycloheximide is present, but growth in the presence of 0.1% cycloheximide, 10% NaCl plus 5% glucose and 1% acetic acid is

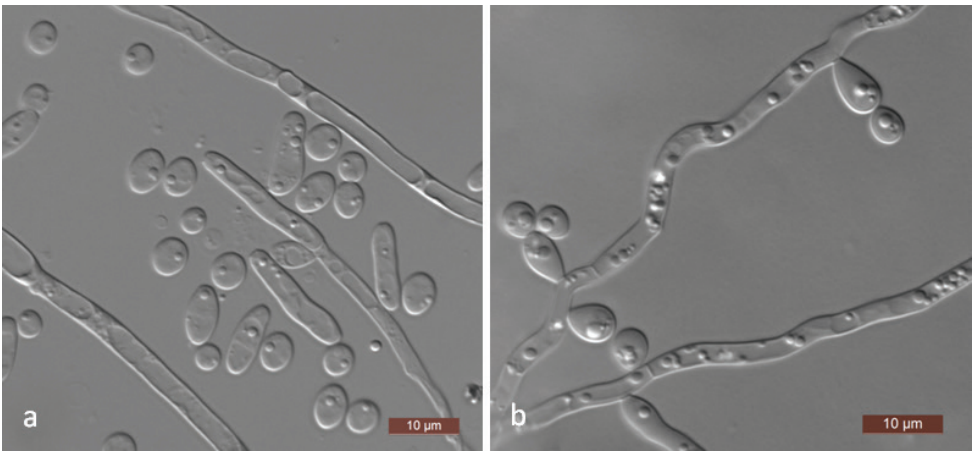

Figure 4. Morphology of *Spathaspora jiuxiensis* (NYNU 17416, holotype) **a** budding cells and pseudohyphae on YM broth after 3 d **b** true hyphae with blastoconidia on CM agar after 14 d. Scale bars: 10 µm.

absent. Starch-like compounds are not produced. Urease activity and diazonium blue B reactions are negative.

Additional isolate examined. China, Yunnan Province, Honghe Prefecture, Luxi County, in rotting wood in Jiuxi Mountain Forest Park, July 2017, K.F. Liu & L. Zhang, NYNU 17417.

Notes. The two strains, both representing *Sp. jiuxiensis*, cluster in a well-supported clade in the phylogenetic analysis and are closely related to *Sp. parajiuxiensis*. The nucleotide differences between these two new species were 1.4% substitutions in the D1/D2 domain and 4.6% substitutions in the ITS region (Groenewald et al. 2016). These two sister species can also be differentiated by a few physiological characteristics; *Sp. jiuxiensis* can assimilate DL-lactate and *Sp. parajiuxiensis* can grow at 37 °C.

***Spathaspora parajiuxiensis* C.Y. Chai & F.L. Hui, sp. nov.**
MycoBank: 836447
Figure 5

Type. China, Yunnan Province, Honghe Prefecture, Luxi County, in rotting wood in Jiuxi Mountain Forest Park, July 2016, R.C. Ren & L. Zhang (holotype, NYNU 16747^{T} preserved in a metabolically-inactive state), ex-holotype: CICC 33162; CBS 14691.

Etymology. *Paraluxiensis* refers to its close phylogenetic relationship to *Sp. luxiensis*.

Description. In YM broth after 3 days at 25 °C, cells are ovoid to elongate (3.5–4 × 7–15 µm) and occur singly or in pairs (Fig. 5a); pseudohyphae are present. Budding is multilateral. Sediment is formed after a month, but a pellicle is not observed. After 3 days of growth on YM agar at 25 °C, colonies are white to cream-coloured, butyrous

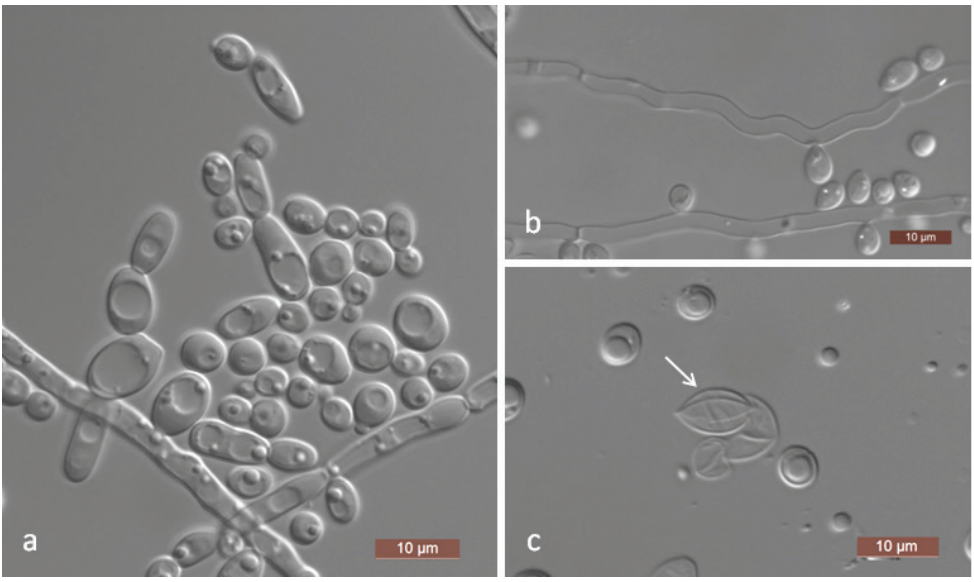

Figure 5. Morphology of *Spathaspora parajiuxiensis* (NYNU 16747, holotype) **a** budding cells and pseudohyphae on YM broth after 3 d **b** true hyphae with blastoconidia on CM agar after 14 d **c** ascus and ascospore (arrow) on 5% ME agar after 14 d. Scale bars: 10 µm.

and smooth with entire margins. After 12 days at 25 °C on Dalmau plate culture on CM agar, pseudohyphae and true hyphae are formed (Fig. 5b). Sporulation occurs on 5% ME agar after 14 days at 25 °C. Unconjugated asci are formed from single cells with one elongated ascospores which are tapered and curved at the ends (Fig. 5c) Glucose and maltose are weakly fermented. Xylose fermentation is negative using Durham tubes, but ethanol is produced from xylose when determined with alcohol oxidase and peroxidase tests. Glucose, D-glucosamine, D-ribose, D-xylose, sucrose, maltose, trehalose, methyl α-D-glucoside, cellobiose, salicin, arbutin, melezitose, inulin, ribitol, D-glucitol, D-mannitol, 2-keto-D-gluconate, succinate and ethanol are assimilated. No growth occurs with galactose, L-sorbose, L-arabinose, D-arabinose, L-rhamnose, melibiose, lactose, raffinose, glycerol, erythritol, xylitol, galactitol, *myo*-inositol, D-glucono-1, 5-lactone, 5-keto-D-gluconate, D-gluconate, D-glucuronate, DL-lactate, citrate, L-arabinitol or methanol. For the assimilation of nitrogen compounds, growth on L-lysine, glucosamine or D-tryptophan is present, whereas growth on nitrate, nitrite, ethylamine, cadaverine, creatine, creatinine or imidazole is absent. Growth is observed at 37 °C, but not at 40 °C. Growth in the presence of 0.01% cycloheximide is present, but growth in the presence of 0.1% cycloheximide, 10% NaCl plus 5% glucose and 1% acetic acid is absent. Starch-like compounds are not produced. Urease activity and diazonium blue B reactions are negative.

Additional isolate examined. China, Yunnan Province, Honghe Prefecture, Luxi County, in rotting wood in Jiuxi Mountain Forest Park, July 2016, R.C. Ren & L. Zhang, NYNU 16632.

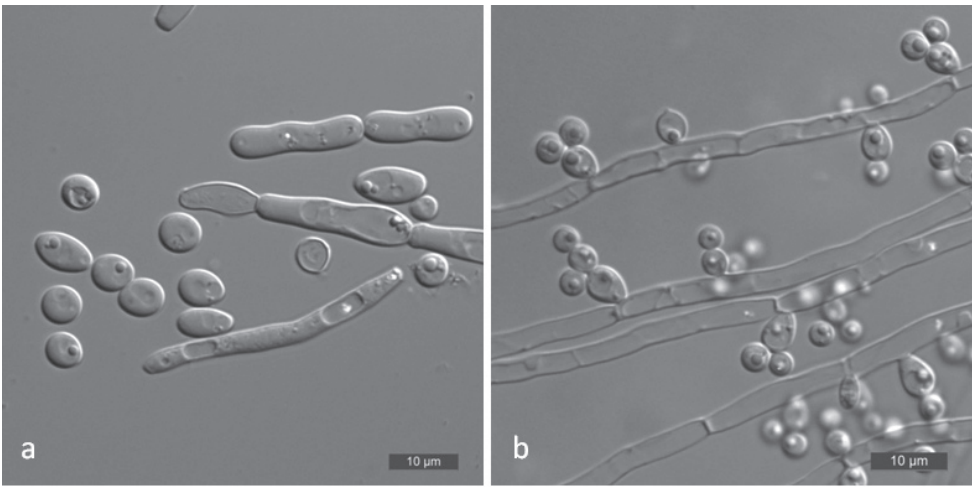

Figure 6. Morphology of *Spathaspora rosae* (NYNU 17934, holotype) **a** budding cells and elongated vegetative cells on YM broth after 3 d **b** true hyphae with blastoconidia on CM agar after 14 d. Scale bars: 10 µm.

Spathaspora rosae **C.Y. Chai & F.L. Hui, sp. nov.**
MycoBank: 836448
Figure 6

Type. China, Yunnan Province, Jinghong City, Mengyang Town, in rotting wood in a tropical rainforest, July 2017, Z.W. Xi & L. Zhang (holotype, NYNU 17934^{T} preserved in a metabolically-inactive state), ex-holotype: CICC 33271; CBS 15231.

Etymology. *Rosae* was named in honour of Carlos A. Rosa for his contributions in yeast taxonomy.

Description. In YM broth after 3 days at 25 °C, cells are ovoid to elongate (4–7 × 5–16 µm) and occur singly or in pairs (Fig. 6a). Budding is multilateral. Sediment is formed after a month, but a pellicle is not observed. After 3 days of growth on YM agar at 25 °C, colonies are white to cream-coloured, butyrous and smooth with entire margins. After 7 days at 25 °C, on Dalmau plate culture on CM agar, pseudohyphae and true hyphae are formed (Fig. 6b). Asci or signs of conjugation are not seen on sporulation media used. Xylose fermentation is negative using Durham tubes, but ethanol is produced from xylose when determined with alcohol oxidase and peroxidase tests. Glucose, D-glucosamine, D-xylose, sucrose, maltose, trehalose, methyl α-D-glucoside, cellobiose, salicin, arbutin, inulin, ribitol, D-glucitol, D-mannitol, 2-keto-D-gluconate, DL-lactate, succinate, citrate and ethanol are assimilated. No growth occurs with galactose, L-sorbose, D-ribose, L-arabinose, D-arabinose, L-rhamnose, melibiose, lactose, raffinose, melezitose, glycerol, erythritol, xylitol, galactitol, *myo*-inositol, D-glucono-1, 5-lactone, 5-keto-D-gluconate, D-gluconate, D-glucuronate, L-arabinitol or methanol. For the assimilation of nitrogen compounds, growth on ethylamine, L-lysine, glucosamine or D-tryptophan is present,

whereas growth on nitrate, nitrite, cadaverine, creatine, creatinine or imidazole is absent. Growth is observed at 35 °C, but not at 37 °C. Growth in the presence of 0.01% cycloheximide is present, but growth in the presence of 0.1% cycloheximide, 10% NaCl plus 5% glucose and 1% acetic acid is absent. Starch-like compounds are not produced. Urease activity and diazonium blue B reactions are negative.

Additional isolates examined. China, Yunnan Province, Jinghong City, Mengyang Town, in rotting wood in a tropical rainforest, July 2017, Z.W. Xi & L. Zhang NYNU 17903, NYNU 17909.

Notes. Three strains, representing *Sp. rosae*, grouped in a well-supported clade and appear to be most closely related to *Sp. allomyrinae* (Wang et al. 2016). The nucleotide differences between *Sp. rosae* and its close relative, *Sp. allomyrinae*, were 10.2% substitutions in the D1/D2 domain and 11% substitutions in the ITS region (Groenewald et al. 2016). Physiologically, *Sp. rosae* can be differentiated from *Sp. allomyrinae*, based on growth in galactose, melezitose, xylitol and 5-keto-D-gluconate, which are positive for *Sp. allomyrinae* and negative for *Sp. rosae*. Moreover, *Sp. allomyrinae* weakly ferments glucose, galactose, maltose and cellobiose, but *Sp. rosae* does not.

Two new combinations

In addition to the previously-described taxa, two new combinations are proposed herein and their descriptions refer to relevant protologues.

Spathaspora materiae **(Barbosa, Cadete, Gomes, Lachance & Rosa) C.Y. Chai & F.L. Hui, comb. nov.**
MycoBank: 836449

Basionym. *Candida materiae* Barbosa, Cadete, Gomes, Lachance & Rosa, International Journal of Systematic and Evolutionary Microbiology 59(8): 2015 (2009).

Spathaspora jeffriesii **(N.H. Nguyen, S.-O. Suh & M. Blackwell) C.Y. Chai & F.L. Hui, comb. nov.**
MycoBank: 836450

Basionym. *Candida jeffriesii* N.H. Nguyen, S.-O. Suh & M. Blackwell, Mycological Research 110(10): 1239 (2006).

Discussion

Spathaspora is distributed worldwide with 12 species identified from rotting wood and insects. In China, three species of *Spathaspora* have been previously reported (Ren et

al. 2013; Wang et al. 2016). In the present study, five additional species, *Sp. elongata*, *Sp. jiuxiensis*, *Sp. mengyangensis*, *Sp. parajiuxiensis* and *Sp. rosae* (Fig. 1), were recorded in addition to previously-known species. Thus, to our knowledge, eight species of *Spathaspora* are currently known from China. Of these eight species, only two species, *Sp. gorwiae* and *Sp. passalidarum*, were reported in China up until 2013 (Ren et al. 2013). The remaining six species, namely *Sp. allomyrinae*, *Sp. elongata*, *Sp. jiuxiensis*, *Sp. mengyangensis*, *Sp. parajiuxiensis* and *Sp. rosae*, were recorded from 2016 to 2018. Given this history, it is most likely that more species will be found. Nonetheless, this number is significant when compared to the total diversity of 11 species of *Spathaspora* reported for South America (Cadete et al. 2009, 2013; Lopes et al. 2016; Morais et al. 2017; Varize et al. 2018). Further studies are needed to document the overall diversity of species of *Spathaspora* in China, especially in the southwest regions.

The phylogenetic relationship of *Spathaspora* has been unclear until now, mainly due to its polyphyletic nature (Daniel et al. 2014; Morais et al. 2017; Varize et al. 2018). In this article, we used more available type strains to revise this genus, based on a phylogenetic analysis of the combined ITS and nuc 28S rDNA sequences. As shown in Figure 1, three main groups were reconstructed and the results showed that *Spathaspora* is not a monophyletic group, but rather is polyphyletic with several *Candida* species included. *Sp. passalidarum*, the type species of the genus, *C. jeffriesii*, *C. materiae*, *Sp. arborariae*, *Sp. brasiliensis*, *Sp. girioi* and *Sp. suhii* form a core group that is well supported by phylogeny. This result is similar to the results of previous phylogenetic analyses of nuc 28S rDNA sequences (Morais et al. 2017; Varize et al. 2018). Therefore, two *Candida* species, *C. materiae* and *C. jeffriesii*, are transferred to *Spathaspora* as new combinations because of their phylogenetic placement within that genus.

The second group is composed of ten distinct species, including the four species *Sp. elongata*, *Sp. mengyangensis*, *Sp. jiuxiensis* and *Sp. parajiuxiensis* described in this study. Typical ascospores are formed by *Sp. elongata*, *Sp. mengyangensis*, *Sp. parajiuxiensis* and *Sp roraimanensis*, but other members of the group are known from their asexual cycle only.

The species *Sp. allomyrinae*, which shares the unique ascospore morphology of the genus, fell outside a larger *Spathaspora* clade, as in the nuc 28S-based phylogeny proposed by Morais et al. (2017). However, this species is joined by *Sp. rosae*, which is described in the current study, in a third cluster consisting of *Spathaspora* in our phylogenetic analysis (Fig. 1). Placement of *Sp. allomyrinae* and *Sp. rosae* is only weakly supported and continued assignment to the genus will require verification from more robust datasets, such as whole genome sequences.

Morais et al. (2017) described the species *Sp. boniae*, based on two strains producing asci containing elongate ascospores with curved ends typical of the genus *Spathaspora*. Our phylogenomic analysis showed that *Sp. boniae* clusters with *C. blackwellae* and *C. parablackwellae* to form a distinct clade outside a larger *Spathaspora* clade. This result was also supported by previous phylogenetic analyses on this clade using nuc 28S rDNA sequences (Morais et al. 2017; Varize et al. 2018; Zhai et al. 2019)**.** These results suggest that the genus *Spathaspora* should be limited to species in the group comprising

the type species *Sp. passalidarum*. This clade, which has been treated previously as members of *Spathaspora*, may represent a separate genus, despite the morphological characteristics of the included species and isolates are similar to *Spathaspora*. Therefore, whole genome sequencing of all *Spathaspora* species and those of related genera, combined with the discovery of new species of the clade, is needed to clarify the possible heterogeneity of this genus.

Spathaspora is a cosmopolitan genus, but most known species have relatively-distinct habitats or regional locations. Currently, most *Spathaspora* species are known from East Asia (mainly in China) and South America. Although the taxonomy of *Spathaspora* has received much attention in recent years, many regions in the world are under-sampled and more under-described indigenous *Spathaspora* species will undoubtedly be discovered in the future as with most microfungal genera (Hyde et al. 2020). Our study indicates that there is a high species diversity of *Spathaspora* waiting to be discovered in rotting wood in tropical and subtropical southwest China and nearby areas as with other genera (Hyde et al. 2018).

Acknowledgements

We sincerely thank Dr. Lin Zhang, Dr. Kai-Fang Liu and Dr. Zhi-Wen Xi for their kind help with collecting specimens. This project was supported by Grant No. 31570021 from the National Natural Science Foundation of China (NSFC), P. R. China, and No. 2018001 from the State Key Laboratory of Motor Vehicle Biofuel Technology, Henan Tianguan Enterprise Group Co. Ltd., China.

References

Alves Jr SL, Herberts RA, Hollatz C, Miletti LC, Stambuk BU (2007) Maltose and maltotriose active transport and fermentation by *Saccharomyces cerevisiae*. Journal of the American Society of Brewing Chemists 65: 99–104. https://doi.org/10.1094/ASBCJ-2007-0411-01

Barbosa AC, Cadete RM, Gomes FC, Lachance MA, Rosa CA (2009) *Candida materiae* sp. nov., a yeast species isolated from rotting wood in the Atlantic Rain Forest. International Journal of Systematic and Evolutionary Microbiology 59: 2104–2106. https://doi.org/10.1099/ijs.0.009175-0

Cadete RM, Santos RO, Melo MA, Mouro A, Goncalves DL, Stambuk BU, Gomes FCO, Lachance MA, Rosa CA (2009) *Spathaspora arborariae* sp. nov., a D-xylose-fermenting yeast species isolated from rotting wood in Brazil. FEMS Yeast Research 9: 1338–1342. https://doi.org/10.1111/j.1567-1364.2009.00582.x

Cadete RM, Melo MA, Dussán KJ, Rodrigues RCLB, Silva SS, Zilli JE, Vital MJS, Gomes FCO, Lachance MA, Rosa CA (2012) Diversity and physiological characterization of D-xylose-fermenting yeasts isolated from the Brazilian Amazonian Forest. PLoS One 7: e43135. https://doi.org/10.1371/journal.pone.0043135

Cadete RM, Melo MA, Zilli JE, Vital MJ, Mouro A, Prompt AH, Gomes FCO, Stambuk BU, Lachance MA, Rosa CA (2013) *Spathaspora brasiliensis* sp. nov., *Spathaspora suhii* sp. nov., *Spathaspora roraimanensis* sp. nov. and *Spathaspora xylofermentans* sp. nov., four novel D-xylose-fermenting yeast species from Brazilian Amazonian forest. Antonie van Leeuwenhoek International Journal of General and Molecular Microbiology 103: 421–431. https://doi.org/10.1007/s10482-012-9822-z

Cadete RM, de Las Heras AM, Sandström AG, Ferreira C, Gírio F, Gorwa-Grauslund MF, Rosa CA (2016) Exploring xylose metabolism in *Spathaspora* species: XYL1.2 from *Spathaspora passalidarum* as the key for efficient anaerobic xylose fermentation in metabolic engineered *Saccharomyces cerevisiae*. Biotechnology Biofuels 9: e167. https://doi.org/10.1186/s13068-016-0570-6

Daniel HM, Lachance MA, Kurtzman CP (2014) On the reclassification of species assigned to *Candida* and other anamorphic ascomycetous yeast genera based on phylogenetic circumscription. Antonie van Leeuwenhoek International Journal of General and Molecular Microbiology 106: 67–84. https://doi.org/10.1007/s10482-014-0170-z

Darriba D, Taboada GL, Doallo R, Posada D (2012) jModelTest 2: more models, new heuristics and parallel computing. Nature Methods 9: 772–772. https://doi.org/10.1038/nmeth.2109

Groenewald DVM, Szöke S, Cardinali G, Eberhardt U, Stielow B, Vries M de, Verkleij MJM, Crous PW, Boekhout T, Robert V (2016) DNA barcoding analysis of more than 9 000 yeast isolates contributes to quantitative thresholds for yeast species and genera delimitation. Studies in Mycology 85: 91–105. https://doi.org/10.1016/j.simyco.2016.11.007

Hall TA (1999) Bioedit: a user-friendly biological sequence alignment editor and analysis program for Windows 95/98/NT. Nucleic acids symposium series 41: 95–98.

Hyde KD, Norphanphoun C, Chen J, Dissanayake AJ, Doilom M, Hongsanan S, Jayawardena RS, Jeewon R, Perera RH, Thongbai B, Wanasinghe DN, Wisitrassameewong K, Tibpromma S, Stadler M (2018) Thailand's amazing diversity: up to 96% of fungi in northern Thailand are novel. Fungal Diversity 93: 215–239. https://doi.org/10.1007/s13225-018-0415-7

Hyde KD, Jeewon R, Chen YJ, Bhunjun CS, Calabon MS, Jiang HB, Lin CG, Norphanphoun C, Sysouphanthong P, Pem D, Tibpromma S, Zhang Q, Doilom M, Jayawardena RS, Liu JK, Maharachchikumbura SSN, Phukhamsakda C, Phookamsak R, Al-Sadi AM, Naritsada Thongklang N, Wang Y, Gafforov Y, Jones EBG, Lumyong S (2020) The numbers of fungi: is the descriptive curve flattening? Fungal Diversity 103: 219–271. https://doi.org/10.1007/s13225-020-00458-2

Katoh K, Toh H (2010) Parallelization of the MAFFT multiple sequence alignment program. Bioinformatics 26: 1899–1900. https://doi.org/10.1093/bioinformatics/btq224

Kumar S, Stecher G, Tamura K (2016) MEGA7: molecular evolutionary genetics analysis version 7.0 for bigger datasets. Molecular Biology and Evolution 33: 1870–1874. https://doi.org/10.1093/molbev/msw054

Kurtzman CP, Robnett CJ (1998) Identification and phylogeny of ascomycetous yeasts from analysis of nuclear large subunit (26S) ribosomal DNA partial sequences. Antonie van Leeuwenhoek International Journal of General and Molecular Microbiology 73: 331–371. https://doi.org/10.1023/A:1001761008817

Kurtzman CP, Fell JW, Boekhout T, Robert V (2011) Methods for isolation, phenotypic characterization and maintenance of yeasts. In: Kurtzman CP, Fell JW, Boekhout T (Eds) The Yeasts – a Taxonomic Study, 5th edn, vol. 1. Amsterdam, Elsevier, 87–110. https://doi.org/10.1016/B978-0-444-52149-1.00007-0

Lachance MA, Boekhout T, Scorzetti G, Fell JW, Kurtzman CP (2011) *Candida* Berkhout (1923). In: Kurtzman CP, Fell JW, Boekhout T (Eds) The Yeasts – a Taxonomic Study, 5th edn, vol. 2. Amsterdam, Elsevier, 987–1278. https://doi.org/10.1016/B978-0-444-52149-1.00090-2

Lopes MR, Morais CG, Kominek J, Cadete RM, Soares MA, Uetanabaro APT, Fonseca C, Lachance MA, Hittinger CT, Rosa CA (2016) Genomic analysis and D-xylose fermentation of three novel *Spathaspora* species: *Spathaspora girioi* sp. nov., *Spathaspora hagerdaliae* fa, sp. nov. and *Spathaspora gorwiae* fa, sp. nov. FEMS Yeast Research 16: 1–12. https://doi.org/10.1093/femsyr/fow044

Morais CG, Batista TM, Kominek J, Borelli BM, Furtado C, Moreira RG, Franco GR, Rosa LH, Fonseca C, Hittinger CT, Lachance MA, Rosa CA (2017) *Spathaspora boniae* sp. nov., a D-xylose-fermenting species in the *Candida albicans–Lodderomyces* clade. International Journal of Systematic and Evolutionary Microbiology 67: 3798–3805. https://doi.org/10.1099/ijsem.0.002186

Nei M, Kumar S (2000) Molecular Evolution and Phylogenetics. Oxford University Press, New York.

Nguyen NH, Suh SO, Marshall CJ, Blackwell M (2006) Morphological and ecological similarities: wood-boring beetles associated with novel xylose-fermenting yeasts, *Spathaspora passalidarum* gen. sp. nov. and *Candida jeffriesii* sp. nov. Mycological Research 110: 1232–1241. https://doi.org/10.1016/j.mycres.2006.07.002

Nguyen NH, Suh S-O, Blackwell M (2011) *Spathaspora* N.H. Nguyen, S.-O. Suh & M. Blackwell. In: Kurtzman CP, Fell JW, Boekhout T (Eds) The Yeasts – a Taxonomic Study, 5th edn, vol. 2. Amsterdam, Elsevier, 795–797. https://doi.org/10.1016/B978-0-444-52149-1.00068-9

Rambaut A (2016) FigTree, version 1.4.3. University of Edinburgh, Edinburgh.

Ren YC, Chen L, Niu QH, Hui FL (2013) Description of *Scheffersomyces henanensis* sp. nov., a new D-xylose-fermenting yeast species isolated from rotten wood. PLoS One 9: e92315. https://doi.org/10.1371/journal.pone.0092315

Ronquist F, Huelsenbeck JP (2003) MrBayes 3: Bayesian phylogenetic inference under mixed models. Bioinformatics 19: 1572–1574. https://doi.org/10.1093/bioinformatics/btg180

Varize CS, Cadete RM, Lopes LD, Christofoleti-Furlan RM, Lachance MA, Rosa CA, Basso LC (2018) *Spathaspora piracicabensis* f. a., sp. nov., a D-xylose fermenting yeast species isolated from rotting wood in Brazil. Antonie van Leeuwenhoek International Journal of General and Molecular Microbiology 111: 525–531. https://doi.org/10.1007/s10482-017-0974-8

Wang Y, Ren YC, Zhang ZT, Ke T, Hui FL (2016) *Spathaspora allomyrinae* sp. nov., a D-xylose-fermenting yeast species isolated from a scarabeid beetle *Allomyrina dichotoma*. International Journal of Systematic and Evolutionary Microbiology 66: 2008–2012. https://doi.org/10.1099/ijsem.0.000979

White TJ, Bruns TD, Lee S, Taylor J (1990) Amplification and direct sequencing of fungal ribosomal RNA genes for phylogenetics. In: Innis MA, Gelfand DH, Sninsky JJ, White TJ (Eds) PCR protocols, a guide to methods and applications. Academic, San Diego, 315–322. https://doi.org/10.1016/B978-0-12-372180-8.50042-1

Wohlbach DJ, Kuo A, Sato TK, Potts KM, Salamov AA, Labutti KM, Sun H, Clum A, Pangilinan JL, Lindquist EA, Lucas S, Lapidus A, Jin M, Gunawan C, Balan V, Dale BE, Jeffries TW, Zinkel R, Barry KW, Grigoriev IV, Gasch AP (2011) Comparative genomics of xylose-fermenting fungi for enhanced biofuel production. Proceedings of the National Academy of Sciences of the United States of America 108: 13212–13217. https://doi.org/10.1073/pnas.1103039108

Zhai YC, Huang LN, Xi ZW, Chai CY, Hui FL (2019) *Candida yunnanensis* sp. nov. and *Candida parablackwellae* sp. nov., two yeast species in the *Candida albicans*/*Lodderomyces* clade. International Journal of Systematic and Evolutionary Microbiology 69: 2775–2780. https://doi.org/10.1099/ijsem.0.003552

MycoKeys 75: 51–69 (2020)
doi: 10.3897/mycokeys.75.55968
http://mycokeys.pensoft.net

RESEARCH ARTICLE

A peer-reviewed open-access journal
MycoKeys
Launched to accelerate biodiversity research

The taxonomy of the model filamentous fungus *Podospora anserina*

S. Lorena Ament-Velásquez[1], Hanna Johannesson[1], Tatiana Giraud[2], Robert Debuchy[3], Sven J. Saupe[4], Alfons J.M. Debets[5], Eric Bastiaans[5], Fabienne Malagnac[3], Pierre Grognet[3], Leonardo Peraza-Reyes[6], Pierre Gladieux[7], Åsa Kruys[8], Philippe Silar[9], Sabine M. Huhndorf[10], Andrew N. Miller[11], Aaron A. Vogan[1]

1 *Systematic Biology, Department of Organismal Biology, Uppsala University, Norbyvägen 18D, 752 36 Uppsala, Sweden* **2** *Ecologie Systématique Evolution, CNRS, Université Paris-Saclay, AgroParisTech, 91400, Orsay, France* **3** *Université Paris-Saclay, CEA, CNRS, Institute for Integrative Biology of the Cell (I2BC), 91198, Gif-sur-Yvette, France* **4** *IBGC, UMR 5095, CNRS Université de Bordeaux, 1 rue Camille Saint Saëns, 33077, Bordeaux, France* **5** *Laboratory of Genetics, Wageningen University, Arboretumlaan 4, 6703 BD, Wageningen, Netherlands* **6** *Instituto de Fisiología Celular, Departamento de Bioquímica y Biología Estructural, Universidad Nacional Autónoma de México, Mexico City, Mexico* **7** *UMR BGPI, Université de Montpellier, INRAE, CIRAD, Institut Agro, F-34398, Montpellier, France* **8** *Museum of Evolution, Botany, Uppsala University, Norbyvägen 18, 752 36, Uppsala, Sweden* **9** *Université de Paris, Laboratoire Interdisciplinaire des Energies de Demain (LIED), F-75006, Paris, France* **10** *Botany Department, The Field Museum, Chicago, Illinois 60605, USA* **11** *Illinois Natural History Survey, University of Illinois, Champaign, IL 61820, USA*

Corresponding author: Aaron A. Vogan (aaron.vogan@ebc.uu.se)

Academic editor: T. Lumbsch | Received 29 June 2020 | Accepted 11 August 2020 | Published 25 November 2020

Citation: Ament-Velásquez SL, Johannesson H, Giraud T, Debuchy R, Saupe SJ, Debets AJM, Bastiaans E, Malagnac F, Grognet P, Peraza-Reyes L, Gladieux P, Kruys Å, Silar P, Huhndorf SM, Miller AN, Vogan AA (2020) The taxonomy of the model filamentous fungus *Podospora anserina*. MycoKeys 75: 51–69. https://doi.org/10.3897/mycokeys.75.55968

Abstract

The filamentous fungus *Podospora anserina* has been used as a model organism for more than 100 years and has proved to be an invaluable resource in numerous areas of research. Throughout this period, *P. anserina* has been embroiled in a number of taxonomic controversies regarding the proper name under which it should be called. The most recent taxonomic treatment proposed to change the name of this important species to *Triangularia anserina*. The results of past name changes of this species indicate that the broader research community is unlikely to accept this change, which will lead to nomenclatural instability and confusion in literature. Here, we review the phylogeny of the species closely related to *P. anserina* and provide evidence that currently available marker information is insufficient to resolve the relationships amongst many of the lineages. We argue that it is not only premature to propose a new name for *P. anserina* based on current data, but also that every effort should be made to retain *P. anserina*

as the current name to ensure stability and to minimise confusion in scientific literature. Therefore, we synonymise *Triangularia* with *Podospora* and suggest that either the type species of *Podospora* be moved to *P. anserina* from *P. fimiseda* or that all species within the Podosporaceae be placed in the genus *Podospora*.

Keywords
phylogenetics, Podospora, Podosporaceae, taxonomy

Introduction

Podospora anserina is a model filamentous fungus that has been at the forefront of molecular biology and genetics for over 100 years (Silar 2020). It has been instrumental in numerous important biological breakthroughs, such as the discovery of eukaryotic plasmids and prions and has been monumental in furthering the fields surrounding aging/senescence, meiotic drive, allorecognition (known as heterokaryon incompatibility in fungi), sexual reproduction and genome defence (Esser 1974; Saupe et al. 2000; Saupe 2007; Silar 2013, 2020; Grognet et al. 2019; Vogan et al. 2019). Along with its role in basic research, *P. anserina* has also caught the attention of industry, where it is used as a source of enzymes that play various roles in the degradation of plant material (Couturier et al. 2016). More recently, *P. anserina* has burst into the genomics era with one of the first published fungal genomes (Fitzpatrick et al. 2006), released in 2008 (Espagne et al. 2008). In the last year, 10 additional chromosome level assemblies of *P. anserina* have been released in concert with the genome of the closely-related species, *P. comata* and *P. pauciseta* (Silar et al. 2019; Vogan et al. 2019). Future projects will expand on this role even further. Wageningen University hosts a collection of strains isolated from the same locale, spanning 30 years of sampling (van der Gaag et al. 1998, 2000; Vogan et al. 2020), which have now all been sequenced and chromosome level assemblies (in preparation) have been produced for the remaining four species of the *Podospora anserina* species complex (Boucher et al. 2017). Therefore, the role of *P. anserina* will continue to be central to many fields in biology and, indeed, likely see use in new fields as new data become public.

The taxonomic history of *Podospora anserina* has been a long and complex one (reviewed in Silar 2020). *Podospora* is a member of the Sordariales and has been traditionally grouped within the family Lasiosphaeriaceae, which itself is an artificial assemblage of genera whose main diagnostic is that they do not belong to the Sordariaceae (Lundqvist 1972). Species within the Lasiosphaeriaceae were divided into genera, based primarily on ascospore morphology, but molecular phylogenies have revealed that these characters do not represent synapomorphies and that most of the genera are polyphyletic (Huhndorf et al. 2004; Miller and Huhndorf 2005). A broad phylogenetic treatment of coprophilous Lasiosphaeriaceae defined four separate clades, with species of *Podospora* represented in all clades, exemplifying the lack of informative morphology amongst these fungi (Kruys et al. 2015). Moreover, the taxon *P. anserina* itself has survived multiple attempts to rename it in the past, which were unsuccessful in part due to how deeply ingrained the name is in the genetics and molecular biology research community (Boucher et al. 2017;

Silar 2020). Recently, this taxonomic mess was stumbled upon by researchers attempting to clean up the distantly-related genus *Thielavia* (Wang et al. 2019). The authors defined the clade containing the type species of *Podospora* (*P. fimiseda*, incorrectly referred to as *P. fimicola* in Wang et al. 2019) as the Podosporaceae (formerly Lasiosphaeriaceae IV) based on a four-marker phylogeny and further divided this clade into three genera: *Podospora*, *Triangularia* and *Cladorrhinum*. As their analyses suggested that *P. anserina* is more closely related to the type species of *Triangularia* (*T. bambusae*), they proposed the new combination, *Triangularia anserina* (Wang et al. 2019).

It is the opinion of the authors here that the taxonomic change of *P. anserina* is both premature and against the ideals of the International Code of Nomenclature for algae, fungi and plants (ICN), as stated in the preamble (Turland et al. 2018). Foremost, it is unlikely that *T. anserina* will be adopted by many of the researchers that rely on it as a model organism, leading to instability of the name. Furthermore, the phylogeny upon which the change was based has a sparse sampling of the diversity of the family and used only four markers. Here, we demonstrate that there is a lack of information amongst the markers currently sequenced in this group and argue that more data are needed before formal taxonomic changes are made for *Podospora*. Ultimately, the best solution for taxonomic stability in the Podosporaceae will be to change the type species of *Podospora* from *P. fimiseda*, which was conserved in 1972 (Nicolson et al. 1984), to *P. anserina* and to only define new genera once more sequence data are available, likely in the form of whole genome sequences.

Methods

Sequences and strains

We generated sequences of 29 strains from 27 species in the Podosporaceae family for markers typically used in molecular phylogenetic studies of Sordariomycetes (including Wang et al. 2019): the ribosomal large subunit (LSU), beta-tubulin (Btub) and RNA polymerase II (rpb2) (Table 1). Sequences were generated as per Huhndorf et al. 2004 and Miller and Hundorf 2005. In brief, DNA was extracted from dried ascomata or multispore isolates of growing cultures using a DNeasy Mini Plant extraction kit (Qiagen Inc., Valencia, California), following manufacturer's recommendations with the exception that tissues were ground in 100 ml AP1 buffer rather than liquid nitrogen. Markers were amplified with the primers listed in Suppl. material 4: Table S1 and sequenced on an Applied Biosystems 3100 automated DNA sequencer. Sequences were deposited in GenBank with accession numbers MT731502–MT731583. In addition, we collected available sequences from GenBank and the NBRC culture collection for all strains suspected to fall within the Podosporaceae for the above markers, as well as the fungal barcode ITS (Schoch et al. 2012). For Btub, two regions are often used in phylogenetic analyses. We sequenced the C-terminal domain of Btub with only a single intron (Btub2), but included sequences from databases that correspond to

Table 1. Strains and markers included in this study. Sequences generated in this study are in bold.

Strain	Species	Clade	ITS	LSU	BTub1	BTub2	RPB2
CBS 539.89**T**	*Apiosordaria backusii*	A	MK926866	**MT731508**	MK926966	**MT731549**	**MT731570**
CBS 106.77	*Apiosordaria backusii*	A	MK926867	AY780051	MK926967	AY780085	AY780149
CBS 304.81**T**	*Apiosordaria effusa*	A	3086201[b]	3086201[b]			
CBS 390.84**T**	*Apiosordaria longicaudata*	A	954801[b]	**MT731505**		**MT731544**	**MT731580**
CBS 244.71**T**	*Apiosordaria stercoraria*	A	MH860096	968201[b]			
CBS 629.82**T**	*Apiosordaria tenuilacunata*	A	MH861532	**MT731507**		**MT731548**	**MT731569**
CBS 363.84**T**	*Apiosordaria tetraspora*	A		**MT731506**		**MT731545**	**MT731581**
NBRC 30422	*Apiosordaria verruculosa*[a]	A	3042201[b]	3042201[b]			
NBRC 30423	*Apiosordaria verruculosa*[a]	A	3042301[b]	3042301[b]			
CBS 148.77	*Apiosordaria verruculosa*[a]	A	MK926874	**MT731510**	MK926974	**MT731546**	**MT731577**
F-152365	*Apiosordaria verruculosa*[a]	A		AY346258		AY780086	AY780150
CBS 550.66	*Apiosordaria verruculosa*[a]	A		**MT731511**		**MT731547**	**MT731579**
CBS 432.64	*Apiosordaria verruculosa*[a]	A	MH858479	MH870111			
CBS 433.64	*Apiosordaria verruculosa*[a]	A	MH858480	MH870112			
CBS 268.67	*Apiosordaria verruculosa*[a]	A	MH858965				
NBRC 31170**T**	*Apiosordaria yaeyamensis*	A	LC146720	LC146720			
CBS 120.289	*Arnium arizonense*	A	KU955584	KF557671		**MT731535**	**MT731563**
S 18211-c	*Arnium arizonense*	A		KF557668		KF557706	
UPS 724	*Arnium arizonense*	A		KF557669		KF557707	
E00204509	*Arnium arizonense*	A		KF557670		KF557708	
CBS 307.81**T**	*Cercophora samala*	A	MH861345	MH873104			
CBS 109.93	*Cercophora samala*	A	AY999134	AY999111	AY999140		
CBS 125293**T**	*Cercophora squamulosa*	A	MH863506				
JF 06314**T**	*Cercophora aquatica*	A	JN673038	JN673038			
SMH 3431	*Cercophora striata*	A		AY780065		AY780108	AY780169
SMH 4036	*Cercophora striata*	A	KX348038	AY780066			
CBS 290.75**T**	*Cladorrhinum microsclerotigenum*	A	FN662475	FN662476			
CBS 301.90**T**	*Cladorrhinum phialophoroides*	A	FM955444	FR692344	KT291718/ MK926971		MK876833
S**T**	*Podospora anserina*	A	Genomic	Genomic	Genomic	Genomic	Genomic
CBS 455.64	*Podospora anserina*	A		**MT731521**		**MT731540**	**MT731564**
CBS 533.73	*Podospora austroamericana*	A		**MT731509**		**MT731539**	**MT731582**
CBS 724.68**T**	*Podospora austroamericana*	A	MK926865	AY999101	MK926965		MK876827
CBS 405.72	*Podospora platensis*	A	MH860505	**MT731514**		**MT731550**	**MT731571**
CBS 251.71**T**	*Podospora praecox*	A	MH860101	MH871877			
FMR 12787	*Podospora setosa*	A		KP981441		KP981569	KP981624
CBS 435.50	*Podospora setosa*	A	GQ922533	MH868219			
CBS 311.58	*Podospora setosa*	A	MK926872	MK926872	MK926972		MK876834
CBS 369.59	*Podospora setosa*	A	MK926873	**MT731515**	MK926973	**MT731551**	**MT731572**
CBS 265.70	*Podospora tarvisina*	A	MH859600	**MT731516**		**MT731552**	**MT731573**
CBS 313.58**T**	*Podospora unicaudata*	A	MH857799	**MT731513**		**MT731554**	**MT731575**
CBS 240.71	*Podospora unicaudata*	A	MH860093	MH871871			
CBS 165.74	*Triangularia angulispora*	A		**MT731517**		**MT731543**	**MT731568**
NBRC 30009	*Triangularia bambusae*[a]	A	3000901[b]	3000901[b]			
CBS 352.33**T**	*Triangularia bambusae*[a]	A	MK926868	**MT731518**	MK926968	**MT731541**	**MT731578/** MK876830
CBS 381.68**T**	*Triangularia batistae*	A	MH859162	**MT731519**		**MT731542**	**MT731576**
IFO 30296	*Zopfiella longicaudata*	A	AY999131	AY999109			
FMR 12365	*Zopfiella longicaudata*	A		KP981448		KP981574	KP981631
FMR 12782	*Zopfiella longicaudata*	A		KP981449		KP981575	KP981632
CBS 252.57**T**	*Zopfiella longicaudata*	A	MK926869	**MT731503**	MK926969	**MT731536**	**MT731567**
CBS 256.71	*Zopfiella longicaudata*	A	MH860106	MH871881			
CBS 257.78	*Zopfiella longicaudata*	A		**MT731504**		**MT731537**	**MT731565**
CBS 971.73	*Zopfiella longicaudata*	A		**MT731502**		**MT731538**	**MT731566**
CBS 671.82**T**	*Zopfiella ovina*	A	MH861539	**MT731512**		**MT731553**	**MT731574**
CBS 127120	*Zopfiella* sp.	A	MH864427	MH875865			
IFO 32904	*Zopfiella tetraspora*	A	AY999130	AY999108	AY999139		
CBS 245.71	*Zopfiella tetraspora*	A	MH860097	**MT731520**			**MT731583**

Strain	Species	Clade	ITS	LSU	BTub1	BTub2	RPB2
CBS 120012	*Arnium olerum*[a]	B		**MT731522**		KF557718	**MT731561**
SMH3253	*Arnium olerum*[a]	B		KF557690			
FMR 13412	*Arnium* sp.	B		KP981428		KP981555	KP981610
S	*Arnium tomentosum*	B		KF557691		KF557720	
SMH 4089	*Cercophora coprophila*	B		KF557692			
IFO 32091	*Cercophora coprophila*	B	AY999136	AY999112	AY999141		
SMH 3794	*Cercophora coprophila*	B		AY780058		AY780102	AY780162
CBS 120013**T**	*Cercophora grandiuscula*	B	GQ922544	**MT731524**		**MT731530**	**MT731562**
ATCC 200395	*Cercophora terricola*	B		AY780067		AY780109	AY780170
CBS 180.66**T**	*Cladorrhinum foecundissimum*[a]	B	MK926856	FR692343	KT291717/ MK926956		MK876818
CBS 182.66	*Cladorrhinum foecundissimum*[a]	B	MH858768				
BCCM 6980	*Cladorrhinum foecundissimum*[a]	B	KT321080	KT312993	KT291721		
CGMCC3.17921	*Cladorrhinum globisporum*	B					KY883234
LC5415	*Cladorrhinum globisporum*	B	KU746680	KU746726	KU746771		
TTI-313	*Podospora australis*	B	KX015765	KX015765			
LyRS93415	*Podospora australis*	B		KF557696			
LyRS92471	*Podospora australis*	B		KF557695			
CBS 322.70**T**	*Thielavia hyalocarpa*	B	MK926857	MK926857	MK926957		MK876819
CBS 102198	*Thielavia hyalocarpa*	B	MK926858	MK926858	MK926958		MK876820
CBS 433.96**T**	*Thielavia intermedia*	B	MK926859	MK926859	MK926959		MK876821
CBS 100257	*Thielavia intermedia*	B	MK926860	MK926860	MK926960		MK876822
CBS 389.84	*Zopfiella leucotricha*	B	982801[b]	**MT731523**			**MT731560**
CBS 463.61	*Zopfiella leucotricha*	B	MH858107	MH869684			
CGMCC 3.15230	*Apiosordaria hamata*	C	KP878306	KP878304			
NBRC 30406	*Apiosordaria jamaicensis*	C	3040601[b]	3040601[b]			
CBS 672.70**T**	*Apiosordaria jamaicensis*	C	MH859895	**MT731527**		**MT731534**	**MT731556**
FMR 6363	*Apiosordaria nigeriensis*	C	AJ458184				
CBS 713.70**T**	*Apiosordaria sacchari*	C	MH859915	KP981425		KP981552	KP981607
CBS 259.71**T**	*Apiosordaria spinosa*	C		MH877809			
CBS 154.77	*Apiosordaria striatispora*	C	MH861043	**MT731529**			**MT731559**
CBS 258.71**T**	*Apiosordaria tuberculata*	C	MH860107	MH871882			
SMH 4021	*Cercophora costaricensis*	C		AY780059		AY780103	AY780163
SMH 3200	*Cercophora* sp.	C		AY780055		AY780098	AY780159
INTA-AR 70**T**	*Cladorrhinum australe*	C	KT321062	KT312976	KT291700		
CBS 304.90**T**	*Cladorrhinum bulbillosum*	C	MK926861	MK926861	MK926961		MK876823
CBS 126090**T**	*Cladorrhinum flexuosum*	C	MH864075	FN662477			
CBS 303.90	*Cladorrhinum samala*	C	FM955447	FR692338			
CBS 302.90	*Cladorrhinum samala*	C		KT312992	KT291719		
NBRC 107619	*Cladorrhinum* sp.	C	12744402[b]	12744401[b]			
CBS 482.64**T**	*Podospora fimiseda*[a]	C	MK926862	**MT731525**	MK926962	**MT731531**	**MT731557**
CBS 990.96	*Podospora fimiseda*[a]	C	AY515361	AY346296	MK926963	AY780133	AY780190
CBS 257.71	*Zopfiella inermis*	C		**MT731526**		**MT731533**	**MT731555**
CBS 286.86**T**	*Zopfiella macrospora*	C	MH861958	**MT731528**		**MT731532**	**MT731558**
CBS 643.75A**T**	*Cladorrhinum brunnescens*		FM955446	FR692346			
Outgroups							
CBS 148.51	*Chaetomium globosum*[a]	Out	Genomic	Genomic	Genomic	Genomic	Genomic
CBS 160.62	*Chaetomium globosum*[a]	Out	KT214565	KT214596	KT214742		KT214666
FMR 13414	*Diplogelasinospora princeps*[a]	Out		KP981431		KP981559	KP981614
SMH 1538	*Lasiosphaeria ovina*[a]	Out		AF064643		AF466046	AY600287
SMH 4106	*Sordaria fimicola*[a]	Out		AY780079		AY780138	AY780194
CBS 230.78	*Zopfiella tabulata*[a]	Out	MK926854	MK926854	MK926954		MK876816
CBS 120402	*Cercophora mirabilis*[a]	Out		KP981429		KP981556	KP981611

T Strain is the Type of the species; [a] Type species of genus; [b] Sequences taken from NBRC

the upstream intron-rich GTPase domain (Btub1) to maximise the number of taxa. When available sequences of markers overlapped with ones that were generated for this study exactly, but had longer flanks, those sequences were merged (two GenBank codes in Table 1). Finally, we included representative strains of the type species of the other families within the Sordariales, as well as the type species of *Zopfiella* and *Cercophora*, which have many representatives within the Podosporaceae, as outgroups. The alignment of all concatenated markers is deposited in TreeBase (http://purl.org/phylo/treebase/phylows/study/TB2:S26777).

Phylogenetic analyses

Each locus was aligned using the online server of MAFFT v. 7.467 (https://mafft.cbrc.jp/alignment/server/; (Katoh et al. 2019) with default settings, followed by manual curation adjusting for the coding frame of the protein-coding markers. We concatenated all alignments and performed a Maximum Likelihood analysis using IQ-TREE v 1.6.8 (Nguyen et al. 2015; Kalyaanamoorthy et al. 2017) with an extended model selection (-m MFP) and 100 standard bootstrap pseudo-replicates. In addition, each individual marker and combinations of markers were analysed as above, but only including sequences that were at least 45% as long as the locus alignment and/or larger than 250 bp. Only strains that consistently showed membership to the Podosporaceae are presented here. The isolates *Podospora brasiliensis* CBS 892.96, *Podospora inflatula* CBS 412.78 and *P. inflatula* CBS 413.82 likely belong to the family, but were excluded due to inconsistent affinities of markers.

Evaluating phylogenetic signal

To evaluate the phylogenetic signal in our datasets, we followed the approach of Shen et al. (2017), which quantifies the amount of support of particular sites or entire genes for two alternative topologies with respect to a particular branch (termed T1 and T2). We set T1 as the Maximum Likelihood topology produced with the concatenated alignment of all markers and T2 as a topology inferred in the same way but constrained to maintain the Clades A and C (see Results) as sisters. To determine what topology is the most supported for each site of each marker, we calculated the site-wise log-likelihood score using RAxML v. 8.2.12 (Stamatakis 2014) with the options *-f G -m GTRGAMMA.* The output was processed with the scripts *1_sitewise_analyzer.pl* and *2_genewise_analyzer.pl* (Shen et al. 2017) and additional custom scripts available as a full Snakemake (Köster and Rahmann 2018) pipeline at https://github.com/SLAment/Podosporaceae. As a result, we obtained the gene-wise log-likelihood score of each gene for either T1 or T2 and compared them by calculating their difference in likelihood (ΔGLS) following Shen et al. (2017).

Results

Our complete dataset contains 107 taxa and 5895 sites, of which 2110 are variable and 1654 are parsimony informative (Suppl. material 5: Table S2: Supplementary_Table2_Markers). However, combined datasets have a considerable amount of missing data due to the sparse availability of markers for most species. In agreement with previous studies, Maximum Likelihood analyses of all markers reveal that three well-supported clades are resolved within the family, referred to here as Clade A, Clade B and Clade C (Fig. 1; see also Suppl. material 1: Fig. S1 ITSLSU.min0.45–250, Suppl. material 2: Fig. S2 Btub1_and_2.min0.45–250 and Suppl. material 3: Fig. S3 rpb2.min0.45–250). The exception is Btub1 and Btub2, alone or combined, which tend to place members of the outgroup within the ingroup (Suppl. material 2: Fig. S2 Btub1_and_2.min0.45–250).

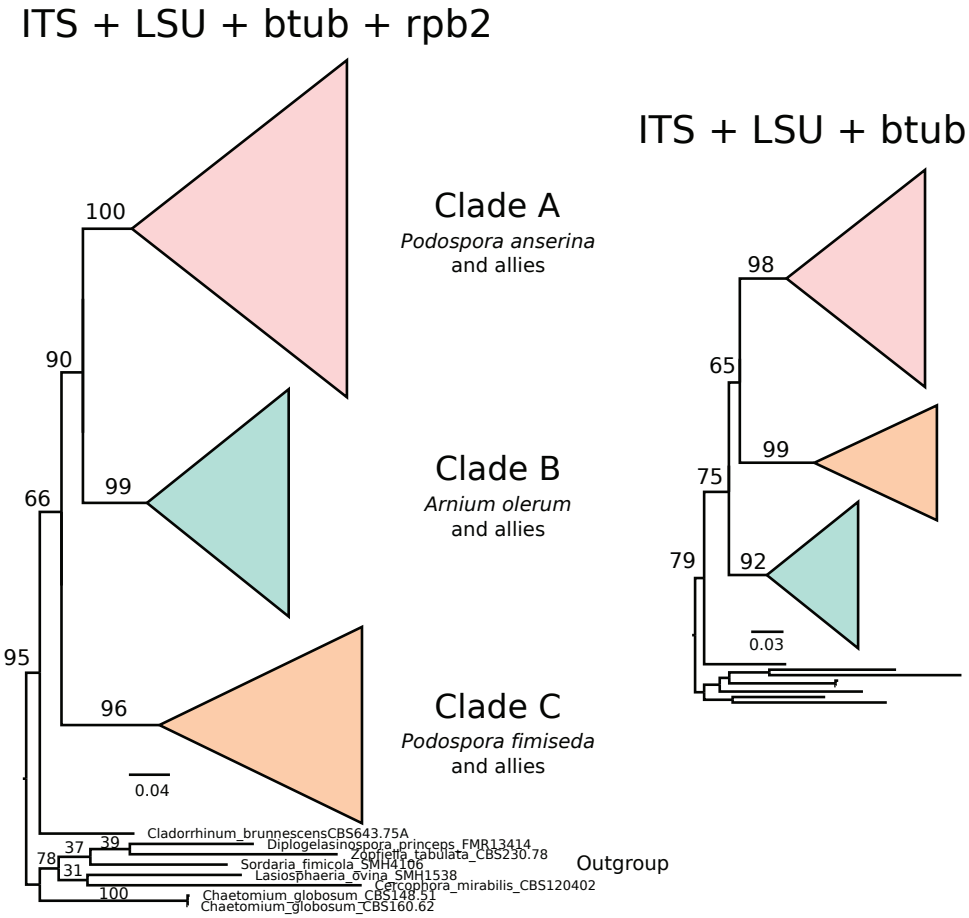

Figure 1. Schematic phylogenetic relationships of the main clades within the Podosporaceae based on Maximum Likelihood analyses of concatenated markers. The three main clades (A, B and C) are strongly supported (bootstrap support values next to relevant branches), but their particular relationship changes depending on the presence of the rpb2 marker. Branches proportional to the scale bar (nucleotide substitutions per site).

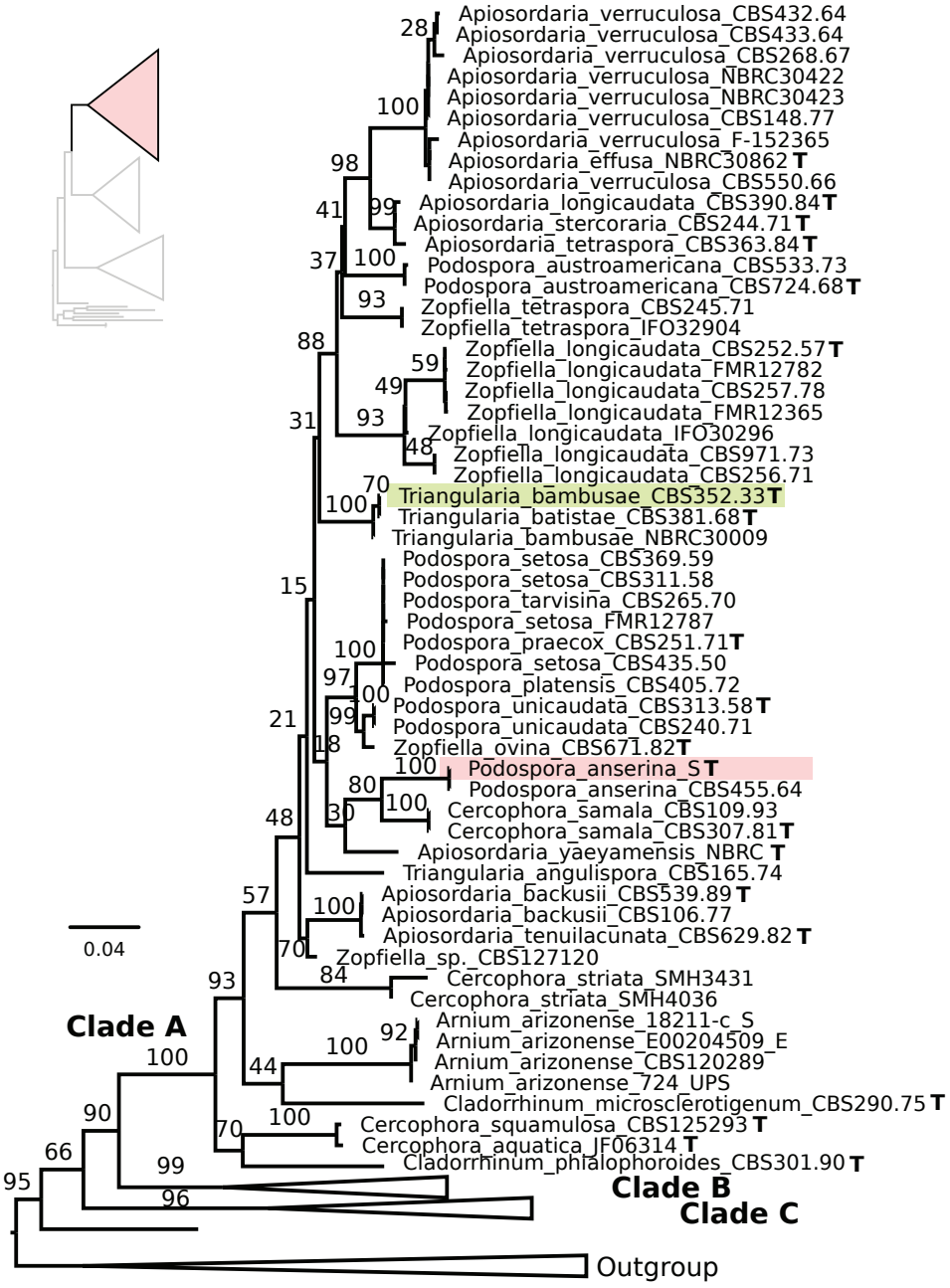

Figure 2. Maximum Likelihood phylogeny of the concatenated analysis of ITS, LSU, Btub and rpb2 for the Podosporaceae, with an emphasis on Clade A. Type strains are indicated with a bold T and those of the focal species *Podospora anserina* and *Triangularia bambusae* are highlighted with coloured boxes. Bootstrap support values are depicted next to their respective branches, but values corresponding to nearly identical sequences are removed for clarity. Branches are proportional to the scale bar (nucleotide substitutions per site).

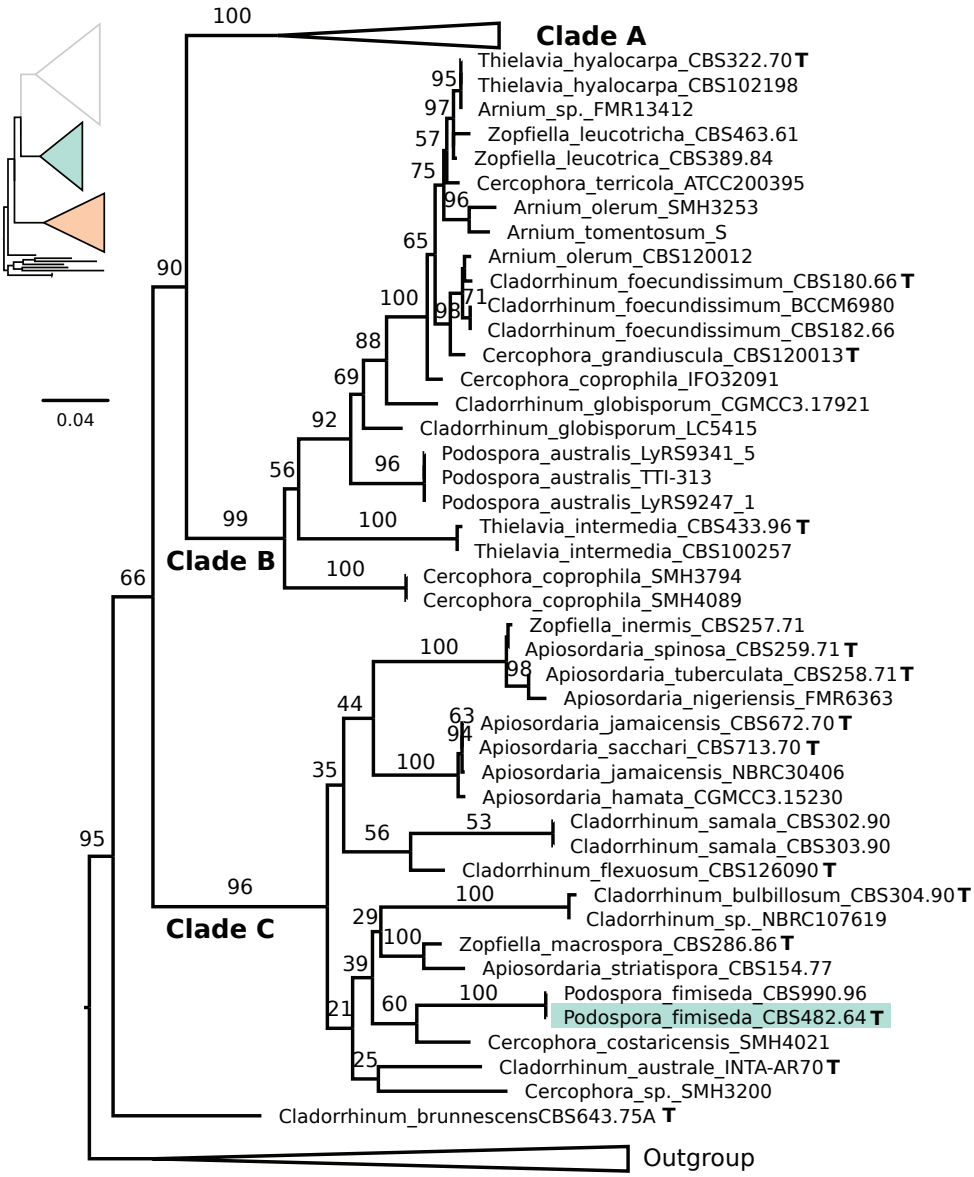

Figure 3. Maximum Likelihood phylogeny of the concatenated analysis of ITS, LSU, Btub and rpb2 for the Podosporaceae, with an emphasis on the clades B and C. Type strains are indicated with a bold T and that of the focal species *Podospora fimiseda* is highlighted with a coloured box. Bootstrap support values are depicted next to their respective branches, but values corresponding to nearly identical sequences are removed for clarity. Branches are proportional to the scale bar (nucleotide substitutions per site).

The taxon *Cladorrhinum brunnescens* appears to represent a distinct lineage within the family, but this finding is only based on the rDNA markers, as no other markers are available for this taxon. None of the main clades of the combined dataset shows mono-

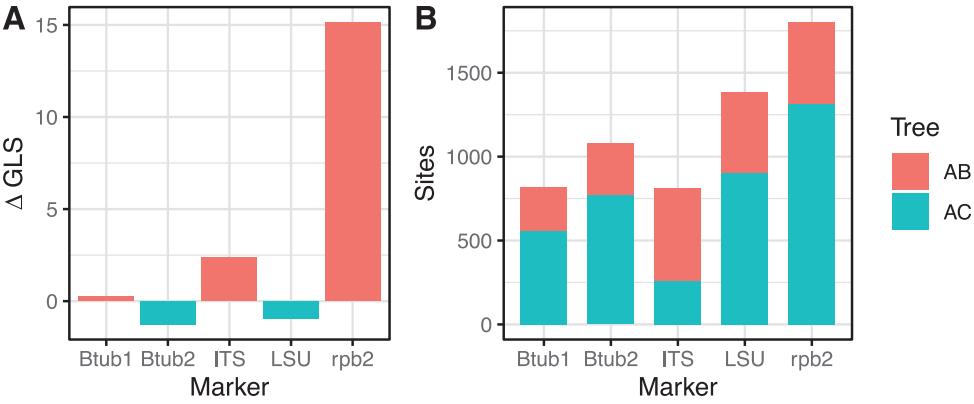

Figure 4. Phylogenetic signal in the available molecular markers for the relationship between clade A and either clade B or C of the Podosporaceae **A** differences in the gene-wise log-likelihood scores (ΔGLS) for each marker, where 0 implies equal support for either of the two alternative sister relationships (A and B or A and C), positive values mean higher support for A and B and negative values higher support for A and C **B** proportion of sites that support each of the two sister relationships within each marker.

phyly for any genera included in the analyses and, for some species, like *Arnium olerum*, representative strains appear to be highly divergent. The focal species of this paper, *P. anserina*, falls within Clade A (Fig. 2), whereas the type species of *Podospora*, *P. fimiseda*, is in Clade C (Fig. 3). While each clade itself is generally well supported for individual markers and combinations of markers, the relationships between the clades are not (Suppl. material 1: Fig. S1 ITSLSU.min0.45–250, Suppl. material 2: Fig. S2 Btub1_and_2.min0.45–250 and Suppl. material 3: Fig. S3 rpb2.min0.45–250). The combined analysis of all markers shows support for the sister relationship of Clades A and B, as reported previously by Wang et al. (2019), but this topology seems to be driven exclusively by the rpb2 marker (Fig. 1). A concatenated analysis of all markers, excluding rpb2, recovers a sister relationship between Clades A and C instead, albeit poorly supported. Except for rpb2, individual markers have generally low ΔGLS values (that is, the difference in likelihood between competing topologies is small), indicating that they have relatively low support for either potential sister relationship (AB or AC). By contrast, rpb2 is strongly biased towards the AB hypothesis (Fig. 4A). Notably, the majority of sites for most markers have higher support for the AC relationship, including rpb2 (Fig. 4B). This suggests that the AC clustering is often favoured by any given site, but only weakly (i.e. the difference in likelihood is very small). Although less frequent, the sites in rpb2 that do support the AB relationship have a large likelihood difference between topologies and likely drive the overall positive ΔGLS value of this gene. Thus, the strong degree of conflict between markers for this internode seems to be driven by a single gene with strong phylogenetic signal (rpb2) and for several other markers without sufficient phylogenetic signal.

Discussion

With the widespread use of molecular markers to determine the phylogenetic relationships among species, numerous important fungal groups have faced taxonomic challenges including *Cryptococcus* (Hagen et al. 2015; Kwon-Chung et al. 2017), *Zymoseptoria* (Quaedvlieg et al. 2011), *Fusarium* (Geiser et al. 2013), *Magnaporthe* (Zhang et al. 2016) and *Ustilago* (McTaggart et al. 2016; Thines 2016), many of which remain unresolved. Fungi are, of course, not the only group whose phylogenetic and taxonomic concepts are in conflict; the model insect genus, *Drosophila*, is still embroiled in a nomenclatural controversy that has yet to be satisfactorily resolved (O'Grady and Markow 2009; Johnson 2018). In the case presented before us, the issue is, in fact, not so complex as most of these other examples. The taxonomic assignments amongst species and strains of the Sordariales has long been recognised as a difficult problem, with various authors seeking to provide some clarity (Huhndorf et al. 2004; Miller and Huhndorf 2005; Félix 2015; Kruys et al. 2015). It is clear that previous use of morphological characters to designate genera has failed to resolve monophyletic groups, as all genera represented here are not only distributed amongst the three clades within the Podosporaceae, but can also be found in the much more distantly-related clades (Lasiosphaeriacceae I–III *sensu* Kruys et al. (2015)). It is thus apparent that the way forward is to define the genera based on molecular phylogenies.

While previous phylogenetic analyses on the Sordariales in general have been informative, the lack of resolution remains a pervasive issue (e.g. Kruys et al. 2015). Our results suggest that the molecular markers, typically used for the study of this group, have a relatively low phylogenetic signal for a number of key internodes. Within Podosporaceae, in particular, the relationship between the clades containing *P. anserina* and *P. fimiseda* (clades A and C) is crucial to decide on an optimal naming scheme that minimises taxonomic and practical conflict. Additionally, throughout the phylogeny, there are a number of strains that have been assigned to different species and genera, but likely belong to the same species (e.g. *Thielavia hyalocarpa* and *Zopfiella leucotricha* strain CBS389.84 are identical for ITS and LSU). Additionally, there appears to be undiscovered sexual states of the anamorphic *Cladorrhinum* species, like *C. foecundissimum* with the *A. olerum strain* CBS120012. Taxonomic re-assignments of these groups should be undertaken; however, without a strong phylogenetic backbone, based on multiple genes and an expanded taxonomic sampling, it seems premature to propose nomenclatural changes.

In recent years, a number of authors have established the use of time-calibrated phylogenies to define ranks from genus up to class for various groups of fungi, although this approach has not been without controversy (Lücking 2019). For the Sordariomycetes, intervals of 150–250 MYA for orders and 50–150 MYA for families have been recommended (Hyde et al. 2017). Both the Sordariales and the Podosporaceae agree well with these values with estimated divergence times of 109.69 MYA and < 76.58 MYA, respectively (Lutzoni et al. 2018), although a comprehensive investigation of divergence amongst the Lasiosphaeriaceae has yet to be conducted. The use of time-calibrated trees

to define genera is less common, but a divergence time of ~30 MYA has been suggested previously (Divakar et al. 2017). In this regard, it would be appropriate to define the three clades presented herein as genera as Wang et al. (2019) have done, based on divergence times between *Lasiosphaeria ovina* and *Anopodium ampullaceum* (Hyde et al. 2017), which show similar phylogenetic distances between each other as the three clades of Podosporaceae (Félix 2015). However, time-calibrated phylogenies need not and often should not, set the standard for taxonomic delimitation. One telling example comes from the field of *Fusarium* research. When the 'one name one fungus' edict came into effect, it threatened to divide a cosmopolitan group of plant pathogenic fungi that are united in their vegetative morphology and pathophysiology into several genera. To combat this issue, the field pushed for the usage of *Fusarium* for the entire group, despite considerable phylogenetic distance (Geiser et al. 2013). As a result, *Fusarium* encompasses species which diverged more than ~70 MYA (Lutzoni et al. 2018), yet this move ensured the nomenclatural stability of the organisms in question.

When proposing new combinations, one should always ensure to make decisions that will cause the least amount of confusion in literature. In this case, it is clear that, for this goal, the name *P. anserina* should be preserved. Google Scholar returns ~11500 hits to the search query *Podospora anserina*, yet only ~2110 hits for *Triangularia*, the majority of which are due to the use of the word "triangularia" in Latin and have no relation to the genus. There are currently 62967 sequences in Genbank with *Podospora anserina* in the title, while only 76 contain *Triangularia* in the title and lastly, the English Wikipedia page for *Podospora anserina* has had 13897 page views from July 2015 to May 2020, while the English Wikipedia *Triangularia* page has had only 705 views over the same period. The best possible way forward to prevent the re-naming of *P. anserina* or the subsequent instability it will cause in literature is to transfer the type of *Podospora* from *P. fimiseda* to *P. anserina*, despite *P. fimiseda* having been conserved over *Schizothecium fimicola* Corda (Proposal 119). Unfortunately, this process can take many years of debate and the re-assignment of *P. anserina* to *Triangularia* already threatens a peaceful transition. At the very least, if *P. anserina* needs to be assigned to another genus, it should be the type species of that genus in order to prevent further potential nomenclatural changes. Thus, we propose, for the interim, to synonymise *Triangularia* with *Podospora* until a more satisfactory resolution can be made. Once more data are available, it will hopefully be possible to resolve the relationships amongst the three clades. If, in the end, Clade A and B are found to be sisters, then it would require that *Cladorrhinum* sensu Wang et al. (2019) (Clade B here) be synonymised with *Podospora* as well. Alternatively, if Clade A and C are sisters, then *Podospora* could be restricted to these two clades and fewer taxonomic changes would be required. As we ultimately aim to move the type species of *Podospora* to *P. anserina*, we will refrain from making any new combinations at the moment.

In the previous example with *Fusarium*, a divergent group of fungi were classified under one name precisely because the researchers in that field desired unity. In the case of *Podospora*, the only factor necessitating that disparate species fall under one genus is the need to operate within the confines of the ICN. The ultimate goal of the code is to provide taxonomic stability and conformity to the organisms it cov-

ers. The nature of studying microscopic fungi has resulted in numerous names with dubious origins and, while obvious fixes are sometimes evident, they are not always possible to enact according to the ICN. It is understandable why the current code is as rigid as it is, but the current editions have seen it become more flexible, which has been advantageous to many fields seeking to solidify tumultuous taxonomy. In the future, we hope that additional data and a permissive code will allow us to enshrine the name *Podospora anserina* indefinitely, settling over a century of nomenclatural friction between taxonomists and other researchers.

Taxonomy

***Podospora* Ces., *Hedwigia* 1(15): 103 (1856)**
MycoBank No: 4284

Type species. *Podospora fimiseda* (Ces. & De Not.) Niessl, *Hedwigia* 22: 156 (1883).
Syn: *Apiosordaria* Arx & W. Gams, *Nova Hedwigia* 13: 201 (1967).
Syn: *Triangularia* Boedijn, *Annls mycol.* 32(3/4): 302 (1934).
Syn: *Lacunospora* Cailleux, *Cahiers de La Maboké* 6(2): 93 (1969) [1968].
Syn: *Tripterospora* Cain, *Can. J. Bot*. 34: 700 (1956).
Syn: *Philocopra* Speg., *Anal. Soc. cient. argent.* 9(4): (1880).
Syn: *Malinvernia* Rabenh., *Hedwigia* 1: 116 (1857).
Syn: *Pleurage* Fr., *Summa veg. Scand.*, Sectio Post. (Stockholm): 418 (1849).

Acknowledgements

We would like to thank Lymari Ruiz for their assistance in generating the sequence data, to Iker Irisarri for his guidance with the phylogenetic analysis, and Martin Ryberg and Mats Thulin for their advice on taxonomic issues. We would like to thank the Swedish Research Council and Formas for research funds. We would also like to acknowledge past and present researchers who have devoted much of their time to the study of *Podospora anserina* to elevate it to the status of model organism.

References

Boucher C, Nguyen T-S, Silar P (2017) Species delimitation in the *Podospora anserina*/ *P. pauciseta*/*P. comata* species complex (Sordariales). Cryptogamie, Mycologie 38: 485–506. https://doi.org/10.7872/crym/v38.iss4.2017.485

Couturier M, Tangthirasunun N, Ning X, Brun S, Gautier V, Bennati-Granier C, Silar P, Berrin J-G (2016) Plant biomass degrading ability of the coprophilic ascomycete fungus *Podospora anserina*. Biotechnology Advances 34: 976–983. https://doi.org/10.1016/j.biotechadv.2016.05.010

Divakar PK, Crespo A, Kraichak E, Leavitt SD, Singh G, Schmitt I, Lumbsch HT (2017) Using a temporal phylogenetic method to harmonize family- and genus-level classification in the largest clade of lichen-forming fungi. Fungal Diversity 84: 101–117. https://doi.org/10.1007/s13225-017-0379-z

Espagne E, Lespinet O, Malagnac F, Da Silva C, Jaillon O, Porcel BM, Couloux A, Aury J-M, Ségurens B, Poulain J, Anthouard V, Grossetete S, Khalili H, Coppin E, Déquard-Chablat M, Picard M, Contamine V, Arnaise S, Bourdais A, Berteaux-Lecellier V, Gautheret D, de Vries RP, Battaglia E, Coutinho PM, Danchin EG, Henrissat B, Khoury RE, Sainsard-Chanet A, Boivin A, Pinan-Lucarré B, Sellem CH, Debuchy R, Wincker P, Weissenbach J, Silar P (2008) The genome sequence of the model ascomycete fungus *Podospora anserina*. Genome Biology 9: R77. https://doi.org/10.1186/gb-2008-9-5-r77

Esser K (1974) *Podospora anserina*. Bacteria, Bacteriophages, and Fungi: 531–551. https://doi.org/10.1007/978-1-4899-1710-2_28

Félix YM (2015) Soil ascomycetes from different geographical regions. Universitat Rovira i Virgili, Spain.

Fitzpatrick DA, Logue ME, Stajich JE, Butler G (2006) A fungal phylogeny based on 42 complete genomes derived from supertree and combined gene analysis. BMC Evolutionary Biology 6: 1–99. https://doi.org/10.1186/1471-2148-6-99

Geiser DM, Aoki T, Bacon CW, Baker SE, Bhattacharyya MK, Brandt ME, Brown DW, Burgess LW, Chulze S, Coleman JJ, Correll JC, Covert SF, Crous PW, Cuomo CA, De Hoog GS, Di Pietro A, Elmer WH, Epstein L, Frandsen RJN, Freeman S, Gagkaeva T, Glenn AE, Gordon TR, Gregory NF, Hammond-Kosack KE, Hanson LE, del Mar Jímenez-Gasco M, Kang S, Corby Kistler H, Kuldau GA, Leslie JF, Logrieco A, Lu G, Lysøe E, Ma L-J, McCormick SP, Migheli Q, Moretti A, Munaut F, O'Donnell K, Pfenning L, Ploetz RC, Proctor RH, Rehner SA, Vincent AR, Rooney AP, Salleh BB, Scandiani MM, Scauflaire J, Short DPG, Steenkamp E, Suga H, Summerell BA, Sutton DA, Thrane U, Trail F, Van Diepeningen A, VanEtten HD, Viljoen A, Waalwijk C, Ward TJ, Wingfield MJ, Xu J-R, Yang X-B, Yli-Mattila T, Zhang N (2013) One fungus, one name: defining the genus *Fusarium* in a scientifically robust way that preserves longstanding use. Phytopathology 103: 400–408. https://doi.org/10.1094/PHYTO-07-12-0150-LE

Grognet P, Timpano H, Carlier F, Aït-Benkhali J, Berteaux-Lecellier V, Debuchy R, Bidard F, Malagnac F (2019) A RID-like putative cytosine methyltransferase homologue controls sexual development in the fungus *Podospora anserina*. PLoS genetics 15: e1008086. https://doi.org/10.1371/journal.pgen.1008086

Hagen F, Khayhan K, Theelen B, Kolecka A, Polacheck I, Sionov E, Falk R, Parnmen S, Lumbsch HT, Boekhout T (2015) Recognition of seven species in the *Cryptococcus gattii*/*Cryptococcus neoformans* species complex. Fungal Genetics and Biology: FG & B 78: 16–48. https://doi.org/10.1016/j.fgb.2015.02.009

Huhndorf SM, Miller AN, Fernández FA (2004) Molecular systematics of the Sordariales: the order and the family Lasiosphaeriaceae redefined. Mycologia 96: 368–387. https://doi.org/10.1080/15572536.2005.11832982

Hyde KD, Maharachchikumbura SSN, Hongsanan S, Samarakoon MC, Lücking R, Pem D, Harishchandra D, Jeewon R, Zhao R-L, Xu J-C, Liu J-K, Al-Sadi AM, Bahkali AH, El-

gorban AM (2017) The ranking of fungi: a tribute to David L. Hawksworth on his 70th birthday. Fungal Diversity 84: 1–23. https://doi.org/10.1007/s13225-017-0383-3

Johnson N (2018) Phylogeny of the genus *Drosophila*. Genetics. 209(1): 1–25. https://doi.org/10.1534/genetics.117.300583

Kalyaanamoorthy S, Minh BQ, Wong TKF, von Haeseler A, Jermiin LS (2017) ModelFinder: fast model selection for accurate phylogenetic estimates. Nature Methods 14: 587–589. https://doi.org/10.1038/nmeth.4285

Katoh K, Rozewicki J, Yamada KD (2019) MAFFT online service: multiple sequence alignment, interactive sequence choice and visualization. Briefings in Bioinformatics 20: 1160–1166. https://doi.org/10.1093/bib/bbx108

Köster J, Rahmann S (2018) Snakemake – a scalable bioinformatics workflow engine. Bioinformatics 34: 1–3600. https://doi.org/10.1093/bioinformatics/bty350

Kruys Å, Huhndorf SM, Miller AN (2015) Coprophilous contributions to the phylogeny of Lasiosphaeriaceae and allied taxa within Sordariales (Ascomycota, Fungi). Fungal Diversity 70: 101–113. https://doi.org/10.1007/s13225-014-0296-3

Kwon-Chung KJ, Bennett JE, Wickes BL, Meyer W, Cuomo CA, Wollenburg KR, Bicanic TA, Castañeda E, Chang YC, Chen J, Cogliati M, Dromer F, Ellis D, Filler SG, Fisher MC, Harrison TS, Holland SM, Kohno S, Kronstad JW, Lazera M, Levitz SM, Lionakis MS, May RC, Ngamskulrongroj P, Pappas PG, Perfect JR, Rickerts V, Sorrell TC, Walsh TJ, Williamson PR, Xu J, Zelazny AM, Casadevall A (2017) The case for adopting the "species complex" nomenclature for the etiologic agents of cryptococcosis. mSphere 2. https://doi.org/10.1128/mSphere.00357-16

Lücking R (2019) Stop the abuse of time! Strict temporal banding is not the future of rank-based classifications in Fungi (Including lichens) and other organisms. Critical Reviews in Plant Sciences 38: 199–253. https://doi.org/10.1080/07352689.2019.1650517

Lundqvist N (1972) Nordic Sordariaceae s. lat. Symbolae Botanicae Upsalienses 20: 1–374.

Lutzoni F, Nowak MD, Alfaro ME, Reeb V, Miadlikowska J, Krug M, Arnold AE, Lewis LA, Swofford DL, Hibbett D, Hilu K, James TY, Quandt D, Magallón S (2018) Contemporaneous radiations of fungi and plants linked to symbiosis. Nature Communications 9: 1–5451. https://doi.org/10.1038/s41467-018-07849-9

McTaggart AR, Shivas RG, Boekhout T, Oberwinkler F, Vánky K, Pennycook SR, Begerow D (2016) *Mycosarcoma* (Ustilaginaceae), a resurrected generic name for corn smut (*Ustilago maydis*) and its close relatives with hypertrophied, tubular sori. IMA Fungus 7: 309–315. https://doi.org/10.5598/imafungus.2016.07.02.10

Miller AN, Huhndorf SM (2005) Multi-gene phylogenies indicate ascomal wall morphology is a better predictor of phylogenetic relationships than ascospore morphology in the Sordariales (Ascomycota, Fungi). Molecular Phylogenetics and Evolution 35: 60–75. https://doi.org/10.1016/j.ympev.2005.01.007

Nguyen L-T, Schmidt HA, von Haeseler A, Minh BQ (2015) IQ-TREE: a fast and effective stochastic algorithm for estimating maximum-likelihood phylogenies. Molecular Biology and Evolution 32: 268–274. https://doi.org/10.1093/molbev/msu300

Nicolson D, Greuter W, Demoulin V, Brummitt R (1984) On changes made in Appendix III (Sydney code). Taxon 33: 310–316. https://doi.org/10.2307/1221177

O'Grady PM, Markow TA (2009) Phylogenetic taxonomy in *Drosophila*: Problems and prospects. Fly 3: 10–14. https://doi.org/10.4161/fly.3.1.7748

Quaedvlieg W, Kema GHJ, Groenewald JZ, Verkley GJM, Seifbarghi S, Razavi M, Mirzadi Gohari A, Mehrabi R, Crous PW (2011) *Zymoseptoria* gen. nov.: a new genus to accommodate *Septoria*-like species occurring on graminicolous hosts. Persoonia – Molecular Phylogeny and Evolution of Fungi 26: 57–69. https://doi.org/10.3767/003158511X571841

Saupe SJ (2007) A short history of small s. Prion 1: 110–115. https://doi.org/10.4161/pri.1.2.4666

Saupe SJ, Clavé C, Bégueret J (2000) Vegetative incompatibility in filamentous fungi: *Podospora* and *Neurospora* provide some clues. Current opinion in microbiology 3: 608–612. https://doi.org/10.1016/S1369-5274(00)00148-X

Schoch CL, Seifert KA, Huhndorf S, Robert V, Spouge JL, Levesque CA, Chen W, Fungal Barcoding Consortium, Fungal Barcoding Consortium Author List (2012) Nuclear ribosomal internal transcribed spacer (ITS) region as a universal DNA barcode marker for Fungi. Proceedings of the National Academy of Sciences of the United States of America 109: 6241–6246. https://doi.org/10.1073/pnas.1117018109

Shen X-X, Hittinger CT, Rokas A (2017) Contentious relationships in phylogenomic studies can be driven by a handful of genes. Nature Ecology & Evolution 1. https://doi.org/10.1038/s41559-017-0126

Silar P (2013) *Podospora anserina*: from laboratory to biotechnology. Soil Biology: 283–309. https://doi.org/10.1007/978-3-642-39339-6_12

Silar P (2020) *Podospora anserina*. 978-2-9555841-2-5. https://hal.archives-ouvertes.fr/hal-02475488

Silar P, Dauget J-M, Gautier V, Grognet P, Chablat M, Hermann-Le Denmat S, Couloux A, Wincker P, Debuchy R (2019) A gene graveyard in the genome of the fungus *Podospora comata*. Molecular Genetics and Genomics 294: 177–190. https://doi.org/10.1007/s00438-018-1497-3

Stamatakis A (2014) RAxML version 8: a tool for phylogenetic analysis and post-analysis of large phylogenies. Bioinformatics 30: 1312–1313. https://doi.org/10.1093/bioinformatics/btu033

Thines M (2016) (2467) Proposal to conserve the name *Ustilago* (Basidiomycota) with a conserved type. Taxon 65: 1170–1171. https://doi.org/10.12705/655.20

Turland NJ, Greuter W, Turland NJ, Wiersema JH, Kusber W-H, Barrie FR, Hawksworth DL, Herendeen PS, Knapp S, Marhold K, Li D-Z, McNeill J, May TW, Munro AM, Prado J, Price MJ, Smith G (2018) International code of nomenclature for algae, fungi, and plants (Shenzhen code): adopted by the nineteenth international botanical congress, Shenzhen, China, July, 2017, 254 pp. https://doi.org/10.12705/Code.2018

van der Gaag M, Debets AJ, Oosterhof J, Slakhorst M, Thijssen JA, Hoekstra RF (2000) Spore-killing meiotic drive factors in a natural population of the fungus *Podospora anserina*. Genetics 156: 593–605.

van der Gaag M, Debets AJ, Osiewacz HD, Hoekstra RF (1998) The dynamics of pAL2-1 homologous linear plasmids in Podospora anserina. Molecular & General Genetics 258: 521–529. https://doi.org/10.1007/s004380050763

Vogan AA, Lorena Ament-Velásquez S, Bastiaans E, Wallerman O, Saupe SJ, Suh A, Johannesson H (2020) The *Enterprise*: A massive transposon carrying *Spok* meiotic drive genes. BioRxiv. https://doi.org/10.1101/2020.03.25.007153

Vogan AA, Lorena Ament-Velásquez S, Granger-Farbos A, Svedberg J, Bastiaans E, Debets AJM, Coustou V, Yvanne H, Clavé C, Saupe SJ, Johannesson H (2019) Combinations of *Spok* genes create multiple meiotic drivers in *Podospora*. eLife 8. https://doi.org/10.7554/eLife.46454

Wang XW, Bai FY, Bensch K, Meijer M, Sun BD, Han YF, Crous PW, Samson RA, Yang FY, Houbraken J (2019) Phylogenetic re-evaluation of *Thielavia* with the introduction of a new family Podosporaceae. Studies in Mycology 93: 155–252. https://doi.org/10.1016/j.simyco.2019.08.002

Zhang N, Luo J, Rossman AY, Aoki T, Chuma I, Crous PW, Dean R, de Vries RP, Donofrio N, Hyde KD, Lebrun M-H, Talbot NJ, Tharreau D, Tosa Y, Valent B, Wang Z, Xu J-R (2016) Generic names in Magnaporthales. IMA fungus 7: 155–159. https://doi.org/10.5598/imafungus.2016.07.01.09

Supplementary material 1

Figure S1

Authors: S. Lorena Ament-Velásquez, Hanna Johannesson, Tatiana Giraud, Robert Debuchy, Sven J. Saupe, Alfons J.M. Debets, Eric Bastiaans, Fabienne Malagnac, Pierre Grognet, Leonardo Peraza-Reyes, Pierre Gladieux, Åsa Kruys, Philippe Silar, Sabine M. Huhndorf, Andrew N. Miller, Aaron A. Vogan

Data type: statistical data

Explanation note: Maximum Likelihood phylogeny of the concatenated analysis of ITS and LSU. Type strains of the focal species are highlighted with coloured boxes. Bootstrap support values are depicted next to their respective branches, but values corresponding to nearly identical sequences are removed for clarity. Branches are proportional to the scale bar (nucleotide substitutions per site). Clades are marked with lateral bars following the topology in Figure 1.

Link: https://doi.org/10.3897/mycokeys.75.55968.suppl1

Supplementary material 2

Figure S2

Authors: S. Lorena Ament-Velásquez, Hanna Johannesson, Tatiana Giraud, Robert Debuchy, Sven J. Saupe, Alfons J.M. Debets, Eric Bastiaans, Fabienne Malagnac, Pierre Grognet, Leonardo Peraza-Reyes, Pierre Gladieux, Åsa Kruys, Philippe Silar, Sabine M. Huhndorf, Andrew N. Miller, Aaron A. Vogan

Data type: statistical data

Explanation note: Maximum Likelihood phylogeny of Btub1 and Btub2 separately. The outgroup taxa are not resolved as monophyletic and, hence, the rooting was arbitrarily chosen. Type strains of the focal species are highlighted with coloured boxes. Bootstrap support values are depicted next to their respective branches, but values corresponding to nearly identical sequences are removed for clarity. Branches are proportional to the scale bar (nucleotide substitutions per site). Clades are marked with lateral bars, following the topology in Figure 1.

Link: https://doi.org/10.3897/mycokeys.75.55968.suppl2

Supplementary material 3

Figure S3

Authors: S. Lorena Ament-Velásquez, Hanna Johannesson, Tatiana Giraud, Robert Debuchy, Sven J. Saupe, Alfons J.M. Debets, Eric Bastiaans, Fabienne Malagnac, Pierre Grognet, Leonardo Peraza-Reyes, Pierre Gladieux, Åsa Kruys, Philippe Silar, Sabine M. Huhndorf, Andrew N. Miller, Aaron A. Vogan

Data type: statistical data

Explanation note: Maximum Likelihood phylogeny of rpb2. Type strains of the focal species are highlighted with coloured boxes. Bootstrap support values are depicted next to their respective branches, but values corresponding to nearly identical sequences are removed for clarity. Branches are proportional to the scale bar (nucleotide substitutions per site). Clades are marked with lateral bars, following the topology in Figure 1.

Link: https://doi.org/10.3897/mycokeys.75.55968.suppl3

Supplementary material 4

Table S1

Authors: S. Lorena Ament-Velásquez, Hanna Johannesson, Tatiana Giraud, Robert Debuchy, Sven J. Saupe, Alfons J.M. Debets, Eric Bastiaans, Fabienne Malagnac, Pierre Grognet, Leonardo Peraza-Reyes, Pierre Gladieux, Åsa Kruys, Philippe Silar, Sabine M. Huhndorf, Andrew N. Miller, Aaron A. Vogan

Data type: molecular data

Explanation note: List of primers used to generate sequence data.

Link: https://doi.org/10.3897/mycokeys.75.55968.suppl4

Supplementary material 5

Table S2

Authors: S. Lorena Ament-Velásquez, Hanna Johannesson, Tatiana Giraud, Robert Debuchy, Sven J. Saupe, Alfons J.M. Debets, Eric Bastiaans, Fabienne Malagnac, Pierre Grognet, Leonardo Peraza-Reyes, Pierre Gladieux, Åsa Kruys, Philippe Silar, Sabine M. Huhndorf, Andrew N. Miller, Aaron A. Vogan

Data type: statistical data

Explanation note: Analysed data matrices.

Link: https://doi.org/10.3897/mycokeys.75.55968.suppl5

MycoKeys 75: 71–143 (2020)
doi: 10.3897/mycokeys.75.59872
https://mycokeys.pensoft.net

RESEARCH ARTICLE

A peer-reviewed open-access journal
MycoKeys
Launched to accelerate biodiversity research

A global meta-analysis of ITS rDNA sequences from material belonging to the genus *Ganoderma* (Basidiomycota, Polyporales) including new data from selected taxa

Vassiliki Fryssouli[1], Georgios I. Zervakis[1], Elias Polemis[1], Milton A. Typas[2]

1 *Agricultural University of Athens, Laboratory of General and Agricultural Microbiology, Iera Odos 75, 11855 Athens, Greece* **2** *National and Kapodistrian University of Athens, Department of Genetics and Biotechnology, Faculty of Biology, Panepistemiopolis, Athens 15701, Greece*

Corresponding author: Georgios I. Zervakis (zervakis@aua.gr)

Academic editor: M.P. Martín | Received 20 October 2020 | Accepted 26 October 2020 | Published 1 December 2020

Citation: Fryssouli V, Zervakis GI, Polemis E, Typas MA (2020) A global meta-analysis of ITS rDNA sequences from material belonging to the genus *Ganoderma* (Basidiomycota, Polyporales) including new data from selected taxa. MycoKeys 75: 71–143. https://doi.org/10.3897/mycokeys.75.59872

Abstract

Ganoderma P. Karst. is a cosmopolitan genus of white-rot fungi which comprises species with highly-prized pharmaceutical properties, valuable biotechnological applications and of significant phytopathological interest. However, the status of the taxonomy within the genus is still highly controversial and ambiguous despite the progress made through molecular approaches. A metadata analysis of 3908 nuclear ribosomal internal transcribed spacer (ITS) rDNA sequences obtained from GenBank/ENA/DDBJ and UNITE was performed by targeting sequences annotated as *Ganoderma*, but also sequences from environmental samples and from material examined for the first time. *Ganoderma* taxa segregated into five main lineages (Clades A to E). Clade A corresponds to the core of laccate species and includes *G. shanxiense* and three major well-supported clusters: Cluster A.1 ('*G. lucidum* sensu lato') consists of taxa from Eurasia and North America, Cluster A.2 of material with worldwide occurrence including *G. resinaceum* and Cluster A.3 is composed of species originating from all continents except Europe and comprises *G. lingzhi*. Clade B includes *G. applanatum* and allied species with a Holarctic distribution. Clade C comprises taxa from Asia and Africa only. Clade D consists of laccate taxa with tropical/subtropical occurrence, while clade E harbours the highest number of non-laccate species with a cosmopolitan distribution. The 92 *Ganoderma*-associated names, initially used for sequences labelling, correspond to at least 80 taxa. Amongst them, 21 constitute putatively new phylospecies after our application of criteria relevant to the robustness/support of the terminal clades, intra- and interspecific genetic divergence and available biogeographic data. Moreover, several other groups or individual sequences seem to represent distinct taxonomic entities and merit

further investigation. A particularly large number of the public sequences was revealed to be insufficiently and/or incorrectly identified, for example, 87% and 78% of entries labelled as *G. australe* and *G. lucidum*, respectively. In general, ITS demonstrated high efficacy in resolving relationships amongst most of the *Ganoderma* taxa; however, it was not equally useful at elucidating species barriers across the entire genus and such cases are outlined. Furthermore, we draw conclusions on biogeography by evaluating species occurrence on a global scale in conjunction with phylogenetic structure/patterns. The sequence variability assessed in ITS spacers could be further exploited for diagnostic purposes.

Keywords
Biogeography, fungal diversity, ITS, medicinal mushroom, phylogeny, taxonomy

Introduction

The genus *Ganoderma* P. Karst. (Basidiomycota, Polyporales) is characterised by a cosmopolitan distribution and high species diversity, especially in the tropics and subtropics. It comprises white-rot fungi that possess an efficient ligninolytic mechanism which is exploited in various biotechnological applications (Ntougias et al. 2012; Zhou et al. 2013; Coelho-Moreira et al. 2018). Many species cause severe diseases (root and butt rots and basal stem rot, differing in terms of invasiveness and host specificity) in economically-important agricultural and forest crops (Elliott and Broschat 2001; Coetzee et al. 2015; Sahebi et al. 2017). *Ganoderma* basidiomes and mycelium biomass have been used for many centuries in traditional medicine mainly in Asia since they are sources of a wide spectrum of bioactive compounds, including polysaccharides, proteins and terpenoids (e.g. ganoderic and lucideric acids) with significant health-promoting and medicinal properties, for example, anti-aging, immunomodulating, anti-cancer, anti-inflammatory, antimicrobial and prebiotic activity (Paterson 2006; Boh et al. 2007; Gargano et al. 2017; Hapuarachchi et al. 2018a; Hsu and Cheng 2018; Khan et al. 2018; Koutrotsios et al. 2019). Nowadays, pertinent *Ganoderma*-derived products are popular worldwide and their development and trade include approximately 800 "ling-zhi products" with a global distribution which are associated with a multibillion-dollar industry (Lai et al. 2004; Li et al. 2016).

Ganoderma was erected to include only one species, *G. lucidum* (Curtis: Fr.) P. Karst. (Karsten 1881). Patouillard (1889) added several other laccate taxa with pigmented spores and adhering tubes and subsequent key studies by Murrill (1908), Imazeki (1939) Donk (1948), Steyaert (1972), Corner (1983) and Gilbertson and Ryvarden (1986) discussed the diversity of the genus extensively. The main discriminating character of *Ganoderma* (with respect to other polypores) is the production of double-walled ellipsoid to ovoid basidiospores with truncate or umbonate apex and a coloured endospore with columnar or crest ornamentations (Moncalvo and Ryvarden 1997). The appearance of crust in the upper surface of the basidiome was traditionally used for separating *Ganoderma* species at the subgenus rank, i.e. subgenus *Ganoderma* for taxa with laccate-shiny pilei possessing a palisade of inflated hyphae at their upper surface and subgenus *Elfvingia* for taxa with non-laccate (dull) pilei (Imazeki 1952).

Species identification was, until recently, mainly based on the morphology of basidiomes, as well as on ecology and geographical distribution (Corner 1983; Gilbertson and Ryvarden 1986; Ryvarden 2000; Ryvarden 2004; Wasser et al. 2006). However, molecular phylogenetic analyses evidenced that several morphological and cultural characteristics widely used in *Ganoderma* taxonomy were polyphyletic (Moncalvo et al. 1995a; Gottlieb et al. 2000), while the delimitation of various *Ganoderma* species – initially circumscribed using morpho-anatomic and ecological features only – was refined by a range of recent molecular studies (Cao et al. 2012; Zhou et al. 2015; Hennicke et al. 2016; Loyd et al. 2018).

Still, the species concept in *Ganoderma* is not universally accepted and remains inadequately established (Corner 1983; Moncalvo et al. 1995a; Richter et al. 2015; Papp et al. 2017). For many species, phylogenetic and mating data are missing or are fragmentary and not properly documented. In addition, morphological criteria are largely affected by pleomorphic and environmentally-influenced characters and hence their use often leads to unclear and obsolete species descriptions (high phenetic plasticity of morpho-anatomic characters often hinders correct assessment of specimen identity) and subsequently to misidentifications. In addition, the loss or bad condition of type specimens and the failure of lecto-, neo- or epitypification for important taxa have resulted in inconsistencies in taxonomy. Therefore, it comes as no surprise that 456 *Ganoderma* names appear in Mycobank (http://www.mycobank.org/) (Richter et al. 2015), which are estimated to represent from 80 to 290 species worldwide (Ryvarden 2000; Kirk et al. 2008).

The internal transcribed spacer (ITS: ITS1-5.8S-ITS2) region of the nuclear ribosomal RNA was erected as the formal DNA barcode in Fungi since it demonstrates a clear barcoding gap for a wide range of lineages and is often in good agreement with morphological/biological species concepts and could, therefore, be exploited for identification purposes (Schoch et al. 2012; Badotti et al. 2017). Unfortunately, the quality of publicly available fungal ITS sequences varies signifantly and their reliability is often dubious due to mislabelling of the material collected, nomenclatural errors and technical issues, while a large number of submissions are not fully determined or annotated (Nilsson et al. 2006; Bidartondo et al. 2008; Nilsson et al. 2012; Schoch et al. 2012; Kõljalg et al. 2013; Nilsson et al. 2017; Hofstetter et al. 2019). As a consequence, the use of online search tools (e.g. BLAST) is often not helpful and can be misleading. Moreover, the adoption of a specific taxonomic threshold with respect to ITS sequence similarity values (e.g. 97%; Geml et al. 2014; Gweon et al. 2015) deriving from comparisons between species is of questionable usefulness in the case of genera like *Ganoderma*, consisting of numerous taxa with high variability and diverse evolutionary background.

Although the ITS region has been used in more *Ganoderma* studies than any other marker for proposing new taxa (Douanla-Meli and Langer 2009; Kinge and Mih 2011; Cao and Yuan 2013; Coetzee et al. 2015; Li et al. 2015; Xing et al. 2018; Hapuarachchi et al. 2019) and for determining relationships amongst species (Moncalvo 2000; Moncalvo and Buchanan 2008; Wang et al. 2012; Wang et al. 2014; Zhou et al. 2015), published *Ganoderma* phylogenies often show weak support and/or resolution in certain clades (Moncalvo et al. 1995a; Smith and Sivasithamparam 2000; Kinge and Mih 2011; Mohanty et al. 2011; Xing et al. 2016). In addition, limited phylogenetic

information is available for many taxa (e.g. the *G. australe* and *G. gibbosum* complexes or as regards species occurring in the Neotropics), thus complicating attempts at resolving their dubious status and relationships. Recent multigene approaches (Zhou et al. 2015; Loyd et al. 2018; Cabarroi-Hernández et al. 2019; Tchotet Tchoumi et al. 2019) provided valuable data towards resolving phylogenetic patterns in *Ganoderma* and mitigated limitations of previous methodologies based mainly (or entirely) on morphological criteria and on the use of single-genetic marker approaches. However, such studies are still confined to a rather low number of species and/or specific geographic regions. In addition, improperly validated material and misidentifications in the records existing in public databases are surfacing and constitute major obstacles at drawing robust taxonomic/phylogenetic conclusions. As a consequence, the distribution patterns for many taxa of the genus remain undefined, species concepts are unclear and interspecific relationships are ambiguous.

On the basis of the discrepancies and shortcomings noted before, the objectives of this study were: (i) to perform a thorough metadata analysis on the basis of a global dataset of *Ganoderma* ITS sequences, (ii) to evaluate the accuracy of specimen identifications to species, (iii) to determine not fully assessed (i.e. "*Ganoderma* sp.") or erroneously labelled sequences in GenBank (www.ncbi.nlm.nih.gov/genbank/) and other relevant databases, in order to associate taxonomic names with phylogenetic lineages, (iv) to expand the knowledge on distribution and biogeography of *Ganoderma* species, (v) to examine controversial boundaries amongst existing species and complexes and (vi) to contribute to the development of quick and efficient sequence-based tools suitable for identification of *Ganoderma* species through the large-scale assessment of molecular information existing in public databases.

Methods

Abbreviations

5.8S: ribosomal DNA 5.8S gene; ASV: amplicon sequence variant; BI: Bayesian Inference phylogenetic analysis; BPP: Bayesian Posterior Probability; BS: Bootstrap Support; DDBJ: DNA Data Bank of Japan; DOI: digital object identifier; DS: dataset; ENA: European Nucleotide Archive, ITS: ribosomal DNA internal transcribed spacer region; ML: Maximum Likelihood phylogenetic analysis; NCBI: National Center for Biotechnology Information.

Biological material

Dried specimens were obtained on loan from the fungaria of the Bulgarian Academy of Sciences (**FBE**), the Catholic University of Louvain (**MUCL**), the University of Palermo (**PAL**) and the Agricultural University of Athens (**ACAM**). In addition, several specimens were collected from various areas of Greece and pure cultures established are maintained in the fungal cultures collection of the Laboratory of General and

Agricultural Microbiology (Agricultural University of Athens), while dried material is preserved in the fungarium of the same institution (ACAM).

We studied 54 specimens in the form of either dried material or pure cultures. They represented well-established *Ganoderma* taxa with European distribution, i.e. four laccate taxa [*G. lucidum* (11 specimens), *G. carnosum* (5), *G. resinaceum* (18) and *G. pfeifferi* (3)] and two non-laccate/dull taxa [*G. adspersum* (8) and *G. applanatum* (5)]. In addition, material not fully identified (*Ganoderma* sp.; 2), together with commercial strains labelled as *G. lucidum* (1) and *G. tsugae* (1), was examined. Initial species labelling was in accordance with the identification made by the respective collector; however, at the end of our study, some of them were re-assessed. Details on their identity appear in Suppl. material 1: Table S1.

Culture conditions and DNA extraction

Mycelia for DNA extraction were produced in static potato dextrose (Difco, USA) cultures. Following a 10–15 day incubation period at 25 °C, the mycelia were harvested by filtration and either directly processed for DNA extraction or stored at -20 °C. Mycelium or dried basidiome samples were pulverised by a micropestle in the presence of sterile sand and liquid nitrogen. Total genomic DNA was subsequently extracted through the silica Plant II DNA Extraction Miniprep System (Macherey and Nagel, Germany) by following the standard CTAB protocol provided by the manufacturer with minor modifications, i.e. the lysis step was extended to 1 h at 65 °C and the precipitation step to 1 h at room temperature, while the final elution step was performed at 65 °C for 1 h (Zervakis et al. 2014). DNA was quantified by using a Nanodrop ND-1000 spectrometer (Nanodrop Technologies, USA) after which it was adjusted to a final concentration of 50 ng μl^{-1} prior to PCR. DNA extracts were stored in aliquots at -20 °C.

PCR amplification, sequencing and data assembly

Sequences of the ITS region were generated for phylogenetic analyses. DNA samples were subjected to PCR amplification of the ITS region by using the primer pairs ITS1/ITS4 (White et al. 1990) or ITS1F/ITS4b (Gardes and Bruns 1993). PCR reactions were prepared from genomic DNA in 50 µl PCR reagent containing 1.5 U Takara HiFi (High Fidelity PCR system, Takara Bio USA, Inc.) and 0.25 µM of each primer. The amplification reactions were conducted on a MiniAmp Plus Thermal Cycler (Applied Biosystems, CA, USA). The PCR conditions were as follows: initial denaturation at 95 °C for 3 min followed by 35 cycles of denaturation at 95 °C for 30 sec, annealing at 50 °C for ITS1/ITS4 and 55 °C for ITS1f/ITS4b for 30 sec and elongation/extension at 72 °C for 1 min. A final extension at 72 °C for 10 min was included to complete the reaction. The required controls (positive and negative) were included in all reactions.

Amplified fragments were examined by electrophoresis on 1% agarose gels. PCR products of the expected size were purified by microcentrifugation using the PureLink PCR purification kit (Invitrogen/Thermo Fisher Scientific, USA), according to manufacturer's protocol. Purified amplicons were processed for bidirectional Sanger

sequencing at CEMIA (University of Thessaly, Greece; https://cemia.eu/) using the forward ITS1 and reverse ITS4 primers. The resulting chromatograms were proofread and assembled using Unipro UGENE v.31 (Okonechnikov et al. 2012). Validated sequences were submitted to GenBank and the following accession numbers were obtained: MG706203 to MG706256 (Suppl. material 1: Tables S1, S2).

Sequence alignment and phylogenetic analyses

An initial dataset was compiled by retrieving and examining all publicly available ITS sequences assigned to the genus *Ganoderma* (followed either by a species epithet or not fully identified and labelled as "*Ganoderma* sp."), as well as associated environmental samples and misidentified entries, appearing in GenBank/ENA/DDBJ (The International Nucleotide Sequence Database Collaboration; Karsch-Mizrachi et al. 2012) and UNITE (http://unite.ut.ee; Nilsson et al. 2019) until 31 July 2020 (Suppl. material 1: Tables S2–S5). Data derived from 555 batch submissions including 3970 entries were examined by a preliminary BLAST analysis (Altschul et al. 1997) after excluding sequences of short length (< 350 bases). At an initial stage, 62 sequences were excluded since they were erroneously assigned to the genus *Ganoderma* or their identity could not be reliably resolved (Suppl. material 1: Table S3). The rest (3908 entries, including the newly-generated sequences obtained from this study) were compared pairwise for similarity by using the assembly algorithm in Geneious Prime version 11.1.4 (Kearse et al. 2012). Each set of identical sequences was termed as "amplicon sequence variant" (ASV) (Callahan et al. 2017); gaps and degenerated sites were considered as differences. Sequences not grouped in ASVs were those presenting unique sequence profiles (singletons or "singleton ASVs"). All relevant information appears in Table 1, Suppl. material 1: Tables S2, S4, and in Fig. 1a.

The principal phylogenetic analysis of ITS sequences, spanning the entire genus, was based on the construction of the main dataset ('DS'), which was prepared by preferably using ASVs since they were considered more reliable. Selected singletons were also included in the DS when they corresponded to type material, when representing material of diverse origin or under various taxonomic names and in the absence of adequate number of ASVs (four was set as minimum and ten as maximum) for a particular clade. On the basis of the outcome of the phylogenetic analysis performed on the DS, six additional partial datasets (designated as 'pDS') were constructed in order to examine in more detail relationships within each of the main phylogenetic groups of the genus as they derived from the analyses performed by including all additional entries available (Table 2). The outgroup taxa *Pycnoporus cinnabarinus* and *Trametes versicolor* were included, as well as 13 additional sequences of seven species representing several closely-related clades (Table 2) selected on the basis of the outcome of a recent study (Costa-Rezende et al. 2017), i.e. *Tomophagus cattienensis* and *T. colossus*, *G. subresinosum*, *G. tsunodae*, *G. ramosissimum* and *G. shandongense*, *Humphreya coffeata* and *G. sandunense*.

Hence, multiple alignments of seven different matrices (Table 2) were performed with the aid of the online version of MAFFT v. 7 (Katoh and Standley 2013; https://

mafft.cbrc.jp/alignment/software/) by using the progressive method G-INS-1 and were finally inspected and manually optimised in MEGA X (Kumar et al. 2018). The 5' end and the 3' end of ITS1 and ITS2 were determined, based on hidden Markov models (HMMs), localisation deriving from the ITSoneDB (Santamaria et al. 2018) and ITS2 Database (Ankenbrand et al. 2015). Oligonucleotides marking the start and end of ITS regions are: TATCGA to ATATAC for ITS1, AACTTT to TCATGA for 5.8S and AATCTT to TTATGA for ITS2. The ITS alignments were partitioned into ITS1, 5.8S and ITS2 and a substitution model for each partition was selected with jModeltest v. 2.0 (Darriba et al. 2012) by using the corrected Akaike Information Criterion (cAIC; Hurvich and Tsai 1989). The best-fit models of evolution are included in Table 2. The number of variable and parsimony informative characters of each dataset was obtained using PAUP* v4.0b10 (Swofford 2003) (Table 2).

Phylogenetic analyses were based on Maximum Likelihood (ML) and Bayesian Inference (BI). The ML analyses were conducted with RaxML HPC BlackBox running on XSEDE (Stamatakis et al. 2014) under the general time-reversible (GTR) model of nucleotide substitution with gamma distributed rate heterogeneity (GTR-GAMMA) for branch confidence with non-parametric bootstrap support (BS) according to MRE-based bootstrapping criteria assessed through the CIPRES Science Gateway-web portal/platform (Miller et al. 2010; http://www.phylo.org/) (Table 2). The BI analyses were conducted in MrBayes v. 3.2.6 (Ronquist et al. 2012). Two analyses using four independent chains (one cold and three heated) were run from a random starting tree and sampled every 1000 generations. Potential scale reduction factors (PSRF) were set to 1.0 for all parameters; each dataset was run for a (total) number of generations which permitted us to obtain values for standard deviation of split frequencies below 0.005 (Table 2). Subsequently, the sampled trees were summarised after omitting the first 25% as burn-in. Bayesian Posterior Probabilities (BPP) of each node were obtained with the majority rule and all compatible partitions were calculated from the remaining trees through a 50% majority rule consensus tree. Resulting trees were visualied using iTOL v. 5.5 (Letunic and Bork 2019). Alignments and phylogenetic trees were deposited in TreeBASE (http://treebase.org) under the submission ID 25723 (http://purl.org/phylo/treebase/phylows/study/TB2:S25723).

ITS sequence variation, diagnostic regions and phylogenetic species in *Ganoderma*

Elaboration of ITS metadata made it possible to assess the phylogeny of *Ganoderma* species under study and the support it received; values of bootstrap support (BS) in ML and Bayesian Posterior Probability (BPP) in BI analyses were considered significant and retained when equal or higher than 65% and 0.95 in ML and BI analyses, respectively. Moreover, inter- and intra-specific pairwise genetic distances (on the basis of uncorrected p-values) within and between allied *Ganoderma* taxa were calculated in MEGA X as the proportion (p) of nucleotide sites at which two sequences was different and was obtained by dividing the number of nucleotide differences by the total number of nucleotides. In addition, ITS sequence similarities were computed in MAFFT

Table 1. Summarised information on the *Ganoderma* ITS sequences used in this study. Species marked in bold appear as they are presented in Clades and/or Clusters according to the outcome of the phylogenetic analysis (Fig. 3), followed by sequences original labelling in GenBank/ENA/DDBJ and UNITE, the number of sequences examined per taxon name (in parentheses), the geographic origin of the sequenced material, the type of associated host (when available) and the support values the respective terminal clades received (BS in ML and BPP in BI analyses; Figures 4–7). Names marked with asterisk (*) include sequences deriving from type material. A detailed presentation of the pertinent material is provided in Suppl. material 1: Tables S2, S4.

CLADES/Species (no. of sequences per taxon)	Sequences original labelling (no. of sequences per taxon)	Geographic origin of sequenced material	Host type	BS/BPP values
CLADE A				**69%/-**
***G. shanxiense* (2)**	*G. shanxiense* (2)	China	AD	100%/1.00
CLADE A, Cluster A.1				**100%/1.00**
***G. tsugae* (57)**	*G. tsugae* (46)*, *G. lucidum* (3), uncultured *Ganoderma* (3), *G. ahmadii* (1)*, *G. carnosum* (1), *G. valesiacum* (1), *Ganoderma* sp. (1), *Polyporus tsugae* (1)	Canada, Germany, India, Pakistan, UK, USA	AD, GS	
***G. oregonense* (27)**	*G. oregonense* (15), *G. carnosum* (5), *G. tsugae* (4), *G. lucidum* (2), uncultured soil fungus (1)	Canada, Estonia, USA	GS	
***G. carnosum* (26)**	*G. carnosum* (22), *G. lucidum* (4)	Belgium, Czech Republic, France, Greece, Poland, Slovakia, Slovenia	GS	
***G.* aff. *carnosum* (4)**	uncultured soil fungus (2), *G. carnosum* (1), *G. lucidum* (1)	Estonia, UK		93%/1.00
***G. lucidum* (153)**	*G. lucidum* (107), uncultured soil fungus (28), *G. tsugae* (12), *G. oerstedii* (3), *G. oregonense* (1), *G. valesiacum* (1), *Ganoderma* sp. (1)	Algeria, Argentina, Armenia, Belgium, Bulgaria, China, Czech Republic, Finland, France, Greece, India, Iran, Italy, Norway, Russia, Slovakia, Spain, South Korea, Sweden, Thailand, UK, USA, commercial	AD, GS	
***G. leucocontextum* – *G. weixiensis* (33)**	*G. leucocontextum* (24)*, *G. lucidum* (3), *Ganoderma* sp. (3), *G. weixiensis* (2)*, *G. carnosum* (1)	China (Tibet), Nepal, Pakistan	AD, GS	81%/1.00
CLADE A, Cluster A.2				**94%/1.00**
***G. austroafricanum* (2)**	*G. austroafricanum* (1)*, *G.* aff. *austroafricanum* (1)	South Africa	AD	89%/-
***G. hoehnelianum* (14)**	*G. hoehnelianum* (9), *Ganoderma* sp. (5)	China, Gabon, Myanmar		99%/1.00
***G. weberianum* (12)**	*G. weberianum* (9), *G. microsporum* (1)*, *G. sichuanense* (1), *Ganoderma* sp. (1)	Philippines, Taiwan	AD	91%/0.99
***G. sichuanense* (19)**	*G. sichuanense* (9)*, *G. weberianum* (4), *G. lucidum* (2), *G. tenue* (2), *Ganoderma* sp. (1), uncultured soil fungus (1)	Australia, China, India	AD	
***G. carocalcareum* (13)**	*Ganoderma* sp. (8), *G. weberianum* (3), *G. carocalcareum* (2)*	Gabon, Cameroon	AD	-/0.98
***Ganoderma* sp. A1 (17)**	*G. weberianum* (17)	India	AD	100%/1.00
***G.* aff. *weberianum* (5)**	*G. weberianum* (2), *G.* cf. *weberianum* (1), *G. subamboinense* (1), *Ganoderma* sp. (1)	Brazil, China, India	AD	
***G. mexicanum* (17)**	*G. mexicanum* (6), *G. subamboinense* var. *laevisporum* (5)*, *G. subamboinense* (2), *G. weberianum* (2), *G. sessiliforme* (1), *G. tuberculosum* (1)	Argentina, Brazil, Martinique, Mexico, USA	AD	
***G. parvulum* (23)**	*G. parvulum* (10), *G. weberianum* (5), *Ganoderma* sp. (4), *G. subamboinense* var. *laevisporum* (2), *G. stipitatum* (1), *G. subamboinense* (1)*	Brazil, Colombia, Costa Rica, Cuba, French Guiana, Mexico, USA	AD	77%/-
***Ganoderma* sp. A2 (2)**	*G. resinaceum* (1), *Ganoderma* sp. (1)	China		100%/1.00
***G. resinaceum* (131)**	*G. resinaceum* (105), *G. lucidum* (8), *Ganoderma* sp. (8), *G. pfeifferi* (6), *G.* cf. *resinaceum* (2), Polyporales sp. (2)	Belgium, Bulgaria, China, Czech Republic, Egypt, France, Greece, India, Iran, Iraq, Italy, Netherlands, Poland, Slovakia, South Africa, South Korea, Tunisia, Turkey, UK	AD	

CLADES/Species (no. of sequences per taxon)	Sequences original labelling (no. of sequences per taxon)	Geographic origin of sequenced material	Host type	BS/BPP values
***Ganoderma* sp. A3 (12)**	*G. resinaceum* (5), *G.* cf. *resinaceum* (3), *Ganoderma* sp. (2), *G. lucidum* (1), uncultured *Ganoderma* (1)	Malaysia, Taiwan, commercial	AD	99%/1.00
***G.* aff. *sessile* (4)**	*G. lucidum* (4)	India, Turkey	AD	68%/-
***G.* aff. *polychromum* (10)**	*G. resinaceum* (5), *G. sessile* (2), *G.* cf. *sessile* (1), *G. platense* (1), *G. zonatum* (1)	Argentina, USA	AD	98%/1.00
***G. polychromum* (19)**	*G. polychromum* (11), *G. lucidum* (6), *G. sessile* (2)	China, India, USA	AD	93%/1.00
***G. sessile* (228)**	*G. sessile* (134), *G. resinaceum* (60), *Ganoderma* sp. (15), *G. lucidum* (10), *G. oregonense* (2), *G. boninense* (1), *G. lobatum* (1), *G. neojaponicum* (1), *G. polychromum* (1), *G. valesiacum* (1), *Hericium erinaceum* (1), uncultured root-associated fungus (1)	Argentina, China, India, Japan, Russia, South Korea, Taiwan, USA, commercial	AD, AM	78%/1.00
CLADE A, Cluster A.3				**76%/1.00**
***G. concinnum* (2)**	*G. chalceum* (1), *G. concinnum* (1)	Brazil		
***G. tuberculosum* (37)**	*G. tuberculosum* (28), *Ganoderma* sp. (6), *Coriolopsis caperata* (1), *G. parvulum* (1), *G. resinaceum* (1)	Brazil, Colombia, Cuba, Martinique, Mexico, Panama, USA	AD	100%/1.00
***Ganoderma* sp. A4 (2)**	*G. lucidum* (2)	Argentina		99%/1.00
***G. wiiroense* (14)**	*G. wiiroense* (9)*, *Ganoderma* sp. (3), *G. lucidum* (2)	Ghana, India, Senegal	AD	100%/1.00
***G. flexipes* (7)**	*G. flexipes* (7)	China, Laos, Vietnam	AD, GS	100%/1.00
***Ganoderma* sp. A5 (7)**	*G. multiplicatum* (7)	China, Myanmar	AD	100%/1.00
***G. philippii* (102)**	*G. pseudoferreum* (75), *G. philippii* (15), *Ganoderma* sp. (9), *G. australe* (2), uncultured soil fungus (1)	China, Indonesia, Malaysia, Thailand	AD	97%/1.00
***G. lingzhi* (615)**	*G. lingzhi* (333)*, *G. lucidum* (206), *Ganoderma* sp. (37), *G. sichuanense* (27)*, *G. tsugae* (5), *Amauroderma rugosum* (1), *G. boninense* (1), *G. calidophilum* (1), *G. cupreum* (1), *G. luteomarginatum* (1), *Haddowia longipes* (1), *Laccaria bicolor* (1)	Bangladesh, China, India, Iran, Iraq, Japan, Laos, Malaysia, Myanmar, Nepal, South Korea, Thailand, commercial	AD, AM	100%/1.00
***G. curtisii* (142)**	*G. curtisii* (124), *G. meredithae* (11)*, *G. lucidum* (3), *G. curtisii* f. sp. *meredithae* (2), *Ganoderma* sp. (2)	Mexico, USA, commercial	AD	
***G. ravenelii* (12)**	*G. ravenelii* (6), *G. curtisii* (3), *G. lucidum* (2), uncultured fungus (1)	India, USA	AD, GS	78%/1.00
***G. multiplicatum* (17)**	*G. multiplicatum* (10), *G. perzonatum* (7)	Brazil, Colombia, Mexico	AD	99%/1.00
***G. destructans – G. dunense* (43)**	*G. destructans* (39)*, *G. dunense* (3)*, uncultured soil fungus (1)	Cameroon, South Africa	AD	
***G. mizoramense* (3)**	*G. mizoramense* (2)*, *G. lucidum* (1)	India	AD	
***G. steyaertanum* (39)**	*G. steyaertanum* (34), *G.* aff. *steyaertanum* (3), *Ganoderma* sp. (2)	Australia, Indonesia	AD	89%/0.99
***G. martinicense* (49)**	*G. parvulum* (24), *G. martinicense* (18)*, *G. perzonatum* (2), *G. lucidum* (1), *G. oerstedii* (1), *G. tornatum* (1), *G. tuberculosum* (1), *Ganoderma* sp. (1)	Argentina, Brazil, Colombia, Cuba, Martinique, Mexico, USA	AD	93%/1.00
***G. multipileum* (243)**	*Ganoderma* sp. (112), *G. lucidum* (105), *G. multipileum* (22), Agaricales sp. (1), *G. leucocontextum* (1), *G. lingzhi* (1), Polyporaceae sp. (1)	China, India, Nepal, Pakistan, Philippines, Taiwan, Thailand	AD, AM, GS	74%/0.97
***Ganoderma* sp. A6 (15)**	*G. tropicum* (15)	India	AD	100%/1.00
***G. tropicum* (33)**	*G. tropicum* (15)*, *G. fornicatum* (12), *G. williamsianum* (2), *Vanderbylia fraxinea* (2), *Ganoderma* sp. (1), uncultured soil fungus (1)	China, India, Laos, Taiwan, Thailand	AD	
***Ganoderma* sp. A7 (3)**	*G. fornicatum* (3)	Malaysia		100%/1.00
CLADE B				**96%/1.00**
***Ganoderma* sp. B1 (4)**	*Ganoderma* sp. (4)	China, USA		100%/1.00
***Ganoderma* sp. B2 (3)**	*G. applanatum* (1), *G. lingzhi* (1), *G. multipileum* (1)	Nepal		100%/1.00

CLADES/Species (no. of sequences per taxon)	Sequences original labelling (no. of sequences per taxon)	Geographic origin of sequenced material	Host type	BS/BPP values
***G. applanatum* (424)**	uncultured soil fungus (230), *G. applanatum* (119), *G. lipsiense* (21), Fungi (plant leaf) (15), uncultured *Ganoderma* (15), uncultured fungus (8), *G. adspersum* (5), *G. applanatum* cplx (3), *Ganoderma* sp. (2), fungal sp. (1), *G. australe* (1), *G.* cf. *applanatum* (1), *G. lobatum* (1), *G. oregonense* (1), *Trametes* sp. (1)	Antarctica, Armenia, Austria, Bulgaria, Canada, China, Czech Republic, Estonia, France, Germany, Greece, Hungary, India, Japan, Kyrgyzstan, Latvia, Lithuania, Netherlands, Poland, Russia, Slovakia, South Korea, Thailand, UK, USA, commercial	AD, AM, GS	99%/1.00
CLADE C				**100%/1.00**
CLADE C, Cluster C.1				**99%/1.00**
***G. neojaponicum* (10)**	*G. neojaponicum* (7), *G. calidophilum* (2), *Ganoderma* sp. (1)	China, Laos, Myanmar, Taiwan	AD	99%/1.00
CLADE C, Cluster C.2				**100%/1.00**
***Ganoderma* sp. C1 (2)**	*Ganoderma* sp. (2)	Cameroon	AM	82%/1.00
***G. aridicola* (7)**	*Ganoderma* sp. (6), *G. aridicola* (1)*	Cameroon, South Africa	AD, AM, GS	
***Ganoderma* sp. C2 (3)**	*Ganoderma* sp. (3)	Cameroon	AD	100%/1.00
***G. enigmaticum* – *G. thailandicum* (10)**	*G. enigmaticum* (7)*, *G. thailandicum* (2)*, uncultured soil fungus (1)	Ghana, Ivory Coast, South Africa, Thailand	AD, GS	
***G. casuarinicola* (63)**	*Ganoderma* sp. (47), *G. casuarinicola* (6)*, *G. enigmaticum* (4), uncultured fungus (2), *G. applanatum* (1), *G. carnosum* (1), *G. lucidum* (1), uncultured *Ganoderma* (1)	China, India, Sri Lanka	AD, AM, GS	71%/-
CLADE D				
CLADE D, Cluster D.1				**98%/1.00**
***G. mbrekobenum* (36)**	*Ganoderma* sp. (21), *G. mbrekobenum* (11)*, *G. applanatum* (1), *G. carnosum* (1), *G. lucidum* (1), *G. tsugae* (1)	Ghana, India, Senegal, Sri Lanka	AD, AM, GS	98%/1.00
CLADE D, Cluster D.2				
***G. nasalanense* (17)**	*G. australe* (9), *Ganoderma* sp. (4), *G. nasalanense* (2)*, uncultured soil fungus (2)	India, Laos, Malaysia, Vietnam	AD	98%/1.00
***G. sinense* (66)**	*G. sinense* (45), *Ganoderma* sp. (8), *G. lucidum* (5), *G. japonicum* (4), *G. subresinosum* (2), *G. atrum* (1), *G. formosanum* (1)	China, Taiwan, Thailand	AD	100%/1.00
CLADE D, Cluster D.3				**75%/1.00**
***G. cupreum* (8)**	*G. cupreum* (4), *G. australe* (1), *G.* cf. *cupreum* (1), *G. chalceum* (1), uncultured fungus (1)	Cameroon, Gabon, Malaysia, South Africa, Tanzania	AD	99%/1.00
***G. orbiforme* (6)**	*G. orbiforme* (6)	Brazil		89%/0.96
***G. subfornicatum* (9)**	*G. ecuadoriense* (5)*, *Ganoderma* sp. (2), *G. subfornicatum* (1)*, uncultured fungus (1)	Brazil, Ecuador, French Guiana, India, Peru	AD	100%/0.96
***G. mastoporum* (123)**	*G. australe* (60), *G. orbiforme* (19), *G. mastoporum* (13), *Ganoderma* sp. (11), *G. cupreum* (10), uncultured soil fungus (6), *G. fornicatum* (3), *G. multicornum* (1)	Australia, China, India, Indonesia, Laos, Malaysia, Myanmar, Taiwan, Thailand, Vietnam	AD, GS	80%/1.00
CLADE D, Cluster D.4				**93%/1.00**
Group D.4.1				**87%/1.00**
***G. angustisporum* (16)**	*G. australe* (8), *Ganoderma* sp. (5), *G. angustisporum* (3)*	Australia, China, India, Indonesia, Malaysia	AD, GS	
***Ganoderma* sp. D1 (2)**	*G. applanatum* (2)	Gabon	AD	100%/1.00
Group D.4.2				**91%/1.00**
***G. zonatum* (84)**	*G. zonatum* (84)	USA	AD, AM	100%/1.00
***Ganoderma* sp. D2 (4)**	*Ganoderma* sp. (4)	Colombia	AM	100%/1.00
***G. ryvardenii* (22)**	*G. ryvardenii* (15)*, *Ganoderma* sp. (6), *G. wiiroense* (1)	Cameroon, India	AD, AM	100%/1.00
***G. boninense* (69)**	*G. boninense* (32), *Ganoderma* sp. (29), *G. miniatocinctum* (3), *G. zonatum* (3), *G. orbiforme* (2)	China, Indonesia, Japan, Malaysia, Taiwan, Thailand, Vietnam	AM	
***Ganoderma* sp. D3 (12)**	*Ganoderma* sp. (12)	Indonesia	AM	98%/1.00

CLADES/Species (no. of sequences per taxon)	Sequences original labelling (no. of sequences per taxon)	Geographic origin of sequenced material	Host type	BS/BPP values
CLADE E				**81%/1.00**
CLADE E, Cluster E.1				**99%/1.00**
***G. williamsianum* (42)**	*G. australe* (29), *G. williamsianum* (7), *G.* cf. *australe* (2), *G. australe* cplx (2), *Ganoderma* sp. (1), uncultured fungus (1)	China, Malaysia, Myanmar, Thailand	AD	99%/1.00
CLADE E, Cluster E.2				**84%/0.99**
***Ganoderma* sp. E1 (23)**	*G. applanatum* cplx (8), *G. tornatum* (7), *Ganoderma* sp. (4), *G. lobatum* (3), *G. gibbosum* (1)	Brazil, Colombia, Costa Rica, Ecuador, French Guyana, Mexico, Peru, USA	AD	87%/0.99
***Ganoderma* sp. E2 (37)**	*G. gibbosum* (12), *G. tornatum* (8), *G. lobatum* (7), *Ganoderma* sp. (6), *G. applanatum* cplx (2), *G. australe* (2)	Argentina, Brazil, Colombia, Cuba, Puerto Rico, USA	AD, AM	96%/1.00
***G.* aff. *gibbosum* (51)**	*Ganoderma* sp. (46), *G. australe* (3), *G. gibbosum* (1), *G. ryvardenii* (1)	India	AD, AM, GS	69%/1.00
***G. eickeri* (4)**	*G. eickeri* (2)*, *Ganoderma* sp. (2)	South Africa	AD	92%/1.00
***G. gibbosum* (113)**	*G. gibbosum* (61), *G. applanatum* (28), *G. australe* (10), *Ganoderma* sp. (3), *G. australe* cplx (2), *G. australe* IG1 (2), *G. lingzhi* (2), Agaricales sp. (1), *G. fulvellum* (1), *G. lucidum* (1), *Fuscoporia viticola* (1), uncultured *Ganoderma* (1)	China, Japan, Laos, Pakistan, South Korea, Taiwan, Thailand	AD, AM	
***G. ellipsoideum* (80)**	*G. gibbosum* (22), *G. australe* (10), *G. australe* cplx (10), *Ganoderma* sp. (10), *G. adspersum* (5), *G. applanatum* (5), uncultured soil fungus (5), *G. ellipsoideum* (5)*, *G. applanatum* cplx (3), *G. tornatum* (3), *G.* aff. *steyaertanum* (1), *Tomophagus* sp. (1)	Australia, Cambodia, China, India, Indonesia, Laos, Malaysia, Myanmar, Papua New Guinea, Sri Lanka, Thailand, USA, Vietnam	AD, AM, GS	-/0.99
***Ganoderma* sp. E3 (7)**	*G. australe* (6), uncultured soil fungus (1)	Australia, Indonesia		96%/1.00
***Ganoderma* sp. E4 (13)**	*G. australe* (12), *G. tornatum* (1)	Indonesia, Malaysia	AD, AM	100%/1.00
CLADE E, Cluster E.3				**71%/0.97**
***G. knysnamense* (4)**	*G. knysnamense* (4)*	South Africa	AD	100%/1.00
***G. mutabile* (2)**	*G. mutabile* (2)*	China		100%/1.00
***G. cupreolaccatum* (1)**	*G. cupreolaccatum* (1)			
***G. pfeifferi* (17)**	*G. pfeifferi* (17)	Czech Republic, Greece, Slovakia, UK	AD	93%/-
CLADE E, Cluster E.4				**-/0.99**
***G. chocoense* (1)**	*G. chocoense* (1)*	Ecuador		
***G. podocarpense* (2)**	*G. podocarpense* (1)*, uncultured soil fungus (1)	Ecuador, Panama		100%/1.00
***Ganoderma* sp. E5 (8)**	*Ganoderma* sp. (4), *G. lobatum* (2), *G. tornatum* (1), uncultured soil fungus (1)	Argentina	AD	100%/1.00
***Ganoderma* sp. E6 (35)**	*G. australe* (19), *Ganoderma* sp. (8), *G. australe* IG2 (2), *G. applanatum* (2), *G. australe* cplx (1), *G.* cf. *australe* (1), *G.* cf. *philippii* (1), uncultured *Ganoderma* (1), uncultured soil fungus (1)	China, India, Laos, New Zealand, Papua New Guinea, Taiwan, Thailand, Vietnam	AD	95%/1.00
***G. australe* (80)**	*G. australe* (27), *G. australe* cplx (14), *Ganoderma* sp. (13), uncultured soil fungus (10), *G. annulare* (2), *G. applanatum* cplx (2), *G. brownii* (2), *G. lobatum* (2), *G. tornatum* (2), fungal sp. (1), *G. adspersum* (1), *G. applanatum* (1), *G. lipsiense* (1), *G. lucidum* (1), uncultured *Ganoderma* (1)	Argentina, Australia, Brazil, Chile, Costa Rica, India, New Zealand, South Africa, UK, USA	AD, AM	
CLADE E, Cluster E.5				**97%/1.00**
***Ganoderma* sp. E7 (17)**	*Ganoderma* sp. (10), *G. applanatum* cplx (3), *G. lobatum* (3), uncultured soil fungus (1)	USA		100%/1.00
***G.* aff. *adspersum* (11)**	*G. adspersum* (4), *G. applanatum* (4), *G. australe* cplx (2), uncultured soil fungus (1)	China, Japan, Korea		72%/-
***G. adspersum* (144)**	*G. adspersum* (113), *G. australe* (13), *Ganoderma* sp. (10), *G. applanatum* (4), basidiomycetes sp. (2), uncultured *Ganoderma* (1), uncultured fungus (1)	Armenia, Belgium, Croatia, France, Georgia, Germany, Greece, India, Iran, Italy, Slovakia, Spain, Tunisia, UK, USA	AD, GS	89%/1.00

Abbreviations used for associated hosts: AD, angiosperm eudicot; AM, angiosperm monocot; GS, gymnosperm.

Table 2. Datasets of *Ganoderma* sequences constructed and details of the phylogenetic analyses conducted in the frame of this study.

Datasets constructed and analysed	No. of sequences used/total	Represented entries/total entries	Alignment length	Constant characters*	Parsimony Informative characters*	No. of Rapid Bootstraps	ML Optimisation Likelihood	Model substitution AICc TS1/5.8S/ITS2	No. of generations	Split frequency	50% credible trees	ML trees presented
DS: entire genus and individual Clades/ Clusters	440/2119	2027/3908	713	328	307	504	-10429.843785	GTR+G/GTR/TVM+G	37885000	0.004398	28415	Figs 3, 4–7
pDS1a: Cluster A.1 (expanded)	120/124	297/301	571	500	25	600	-1701.266373	JC/JC/JC	13710000	0.004400	10285	Suppl. material 3: Fig. S2a
pDS1b: Cluster A.2 (expanded)	263/274	517/528	608	436	86	600	-2929.177334	TIM2ef+G/GTR+G/ TIM3+G	63120000	0.004399	47341	Suppl. material 4: Fig. S2b
pDS1c: Cluster A.3 (expanded)	341/641	694/1385	648	376	156	552	-4501.116292	GTR+G/TVM/TVM+G	49780000	0.004400	37337	Suppl. material 5: Fig. S2c
pDS2/pDS3: Clades B & C (expanded)	26/292 67/74	224/431 88/95	607	560/459	38/89	600	-2652.570067	K80/JC/JC	7390000	0.004365	5545	Suppl. material 6: Fig. S2d
pDS4: Clade D (expanded)	292/316	449/474	631	391	149	504	-4424.884308	TPM3uf+I+G/TPM2/ TPM1uf+I+G	40320000	0.004398	30241	Suppl. material 7: Fig. S2e
pDS5: Clade E (expanded)	367/396	664/693	656	386	162	552	-5123.351039	TIM3+G/GTR/ TPM3uf+G	65585000	0.004398	49190	Suppl. material 8: Fig. S2f

through the EMBL-EBI portal. Indicative cases are illustrated by boxplot graphs depicting genetic distances and sequence similarities in the main clades, as well as within and amongst selected species of the genus *Ganoderma*.

Widely-adopted thresholds for separating amongst species in Basidiomycota are < 97% to 98% for ITS sequence similarity and > 0.010 to 0.020 for genetic distance uncorrected p-values (Smith et al. 2007; Hughes et al. 2009; Matheny et al. 2009; Schoch et al. 2012; Kondo et al. 2018; Vu et al. 2018; Zervakis et al. 2019). Although such values were generally taken into account in this study, they were not found suitable for universal application in the genus *Ganoderma*. Therefore, phylogenetic species were accepted and/or discussed after examining each case individually through the evaluation of available information (including the number and origin of sequences analysed). Apart from the thresholds quoted above, of importance was whether the terminal subclade was statistically supported and if no overlap (i.e. presence of barcoding gap) were noted between the intraspecific divergence within each taxon and the interspecific variability amongst related taxa. Especially as regards the new phylogenetic species proposed hereby, they had to fulfil all of the following criteria: (a) form a terminal clade with strong support, (b) present mean values of sequence similarity < 98% and genetic distance > 0.015 vs. the closest species terminal clade and (c) no overlap exists between intraspecific values of genetic distance and sequence similarity vs. the respective interspecific values from comparisons to the closest-related taxon. In addition, these phylospecies were linked with the corresponding DOIs of UNITE (Suppl. material 1: Table S2).

Moreover, in order to provide additional information about the variation existing in the ITS spacers for the entire genus, as well as for each major clade/cluster derived from the phylogenetic analyses, the length and GC content of ITS1 and ITS2 were calculated in Geneious Prime version 11.1.4 (https://www.geneious.com) by examining all sequences used for the construction of the main phylogenetic tree (Fig. 3). Finally, two highly-polymorphic regions, one in each spacer, are flanked by conserved oligonucleotides (from TGCAC to GAATG in ITS1 and from AATCT to TAGCT in ITS2) serving as anchor points for sequence search; consequently, these species-specific oligonucleotides could be potentially exploited for diagnostic purposes, especially in taxa/groups represented by an adequate number of entries (e.g. > 10).

Results and discussion

Analysis of *Ganoderma* ITS rDNA sequences

In total, 3970 ITS entries were retrieved from the GenBank/ENA/DDBJ and UNITE databases; 62 sequences were removed from further analysis since they were either erroneously annotated as *Ganoderma* (58) or they could not be reliably identified (Suppl. material 1: Table S3). In the meta-analysis performed, 3908 entries were employed

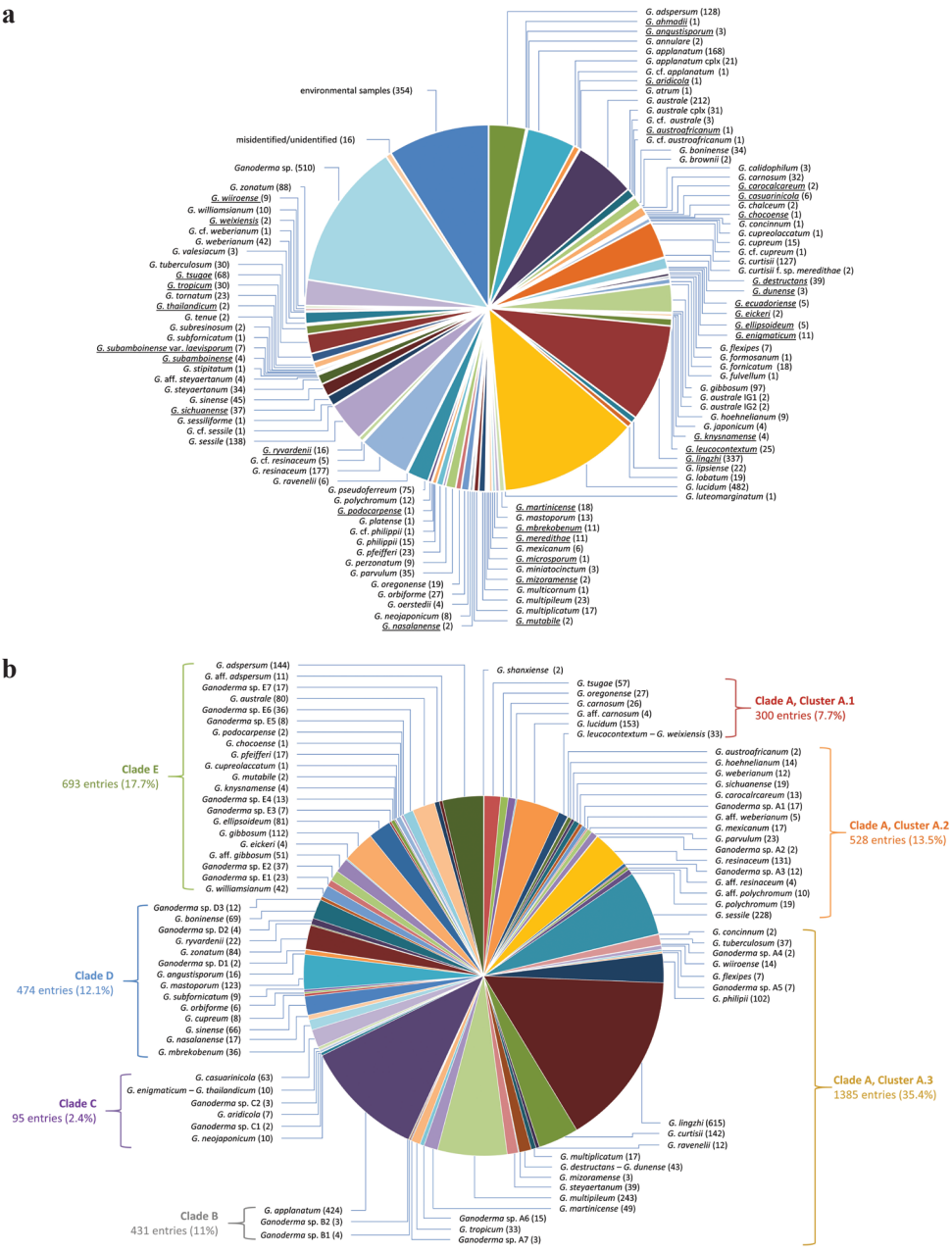

Figure 1. a Initial labelling of 3908 *Ganoderma* sequences analysed in the present study: numbers in parentheses correspond to sequences deposited under the particular name in GenBank/ENA/DDBJ and UNITE, while species names appear underlined when ITS sequences derive from type material **b** final assigment of 3908 *Ganoderma* sequences to 80 species and six distinct groups as a result of the phylogenetic analyses performed in this study: numbers in parentheses correspond to the number of sequences grouped within each taxon (data deriving from Table 1 and Suppl. material 1: Tables S2, S4).

(Fig. 1a) and these were separated into 1735 unique sequences (singletons) and 384 ASVs representing 2173 entries (Table 1, Suppl. material 1: Tables S2, S4). Amongst them, 354 (9%) corresponded to environmental samples (e.g. entries labelled as "uncultured *Ganoderma*", "uncultured fungus" or "uncultured soil fungus"), 16 were either misidentified (e.g. *Coriolopsis caperata*, *Hericium erinaceum* and *Laccaria bicolor*) or not fully identified (e.g. "Agaricales sp." and "basidiomycetes sp."), 510 (13%) were deposited as "*Ganoderma* sp.", while the rest (3028) were labelled with 91 *Ganoderma*-associated taxon names (Table 1, Fig. 1a); this number does not include material with "aff.", "cf.", "cplx", f. sp.", "IG1" and "IG2" in their labelling.

Almost half (45.3%) of all *Ganoderma* sequences deposited in GenBank/ENA/DDBJ and UNITE correspond to only eight species names, i.e. *G. lucidum* (12.3%), *G. lingzhi* (8.6%), *G. australe* (5.4%), *G. resinaceum* (4.5%), *G. applanatum* (4.3%), *G. sessile* (3.5%), *G. adspersum* (3.3%) and *G. curtisii* (3.3%) (Fig. 1a). On the other hand, 17 species names are represented by only one sequence each (seven of them derive from the type material), i.e. *G. ahmadii* (type), *G. aridicola* (type), *G. atrum*, *G. austroafricanum* (type), *G. chocoense* (type), *G. concinnum*, *G. cupreolaccatum*, *G. formosanum*, *G. fulvellum*, *G. luteomarginatum*, *G. microsporum* (type), *G. multicornum*, *G. platense*, *G. podocarpense* (type), *G. sessiliforme*, *G. stipitatum* and *G. subfornicatum* (type). Sequences from type material were available for a somewhat modest 33 taxa (Table 1, Fig. 1a). Moreover, 54 sequences from commercial strains (originally labelled as *G. lucidum* and *G. tsugae*, but turned out to be *G. lingzhi*) and European collections (*G. adspersum*, *G. applanatum*, *G. carnosum*, *G. lucidum*, *G. pfeifferi* and *G. resinaceum*) were generated for the first time and their details are given in Suppl. material 1: Table S1, while indicative photos of the collected basidiomes appear in Fig. 2.

For inferring the phylogeny of the entire genus, the main dataset (DS) included 2027 entries (i.e. ca. 52% of the total number of *Ganoderma* entries analysed) corresponding to 161 singletons and 279 ASVs (Table 1 and Suppl. material 1: Table S2). The molecular data matrix consisted of 713 aligned characters, of which 328 were constant, 78 were variable, but not parsimony informative and 307 were parsimony informative (Table 2); ITS1 aligned in 289, 5.8S in 162 and ITS2 in 262 positions. Expanded datasets (i.e. pDS1a, pDS1b, pDS1c, pDS2/ pDS3, pDS4 and pDS5) were also used for examining in greater detail phylogenetic relationships/affinities and to elucidate the identity of material within particular clades/clusters and detailed/expanded trees were then constructed (Cluster A.1, Cluster A.2, Cluster A.3, Clades B and C, Clade D and Clade E, respectively; Table 2). However, 642 singletons, which were initially included in the analysis, do not appear in the trees constructed due to overrepresentation of certain species (i.e. *G. lingzhi*, *G. multipileum* and *G. applanatum*) or to their particularly high heterogeneity causing destabilisation of the phylogenetic estimate via long-branch formation (Suppl. material 1: Table S4).

A comprehensive evaluation of all ITS sequences available permitted us to determine variation in the ITS1 and ITS2 spacers by examining their length and GC content; relevant data are presented below. In addition, the comparative assessment of ITS1 and ITS2 heterogeneity amongst *Ganoderma* species could subsequently con-

Figure 2. Basidiomes of *Ganoderma* spp. amongst those collected and analysed in this study (specimens codes appear in parantheses; Suppl. material 1: Table S1) **a** *G. lucidum* (A1180) **b** *G. carnosum* (DD1243) **c** *G. resinaceum* (2012-0077) **d** *G. adspersum* (2010-0015) **e** *G. applanatum* (DD2119) **f** *G. pfeifferi* (DD2118).

tribute to species determination since they contain information of potential diagnostic value. The multiple sequence alignment revealed two polymorphic segments which could be potentially used for the identification of *Ganoderma* specimens at species level (Table 3; Suppl. material 2: Figure S1), while they could also be exploited for the development of species-specific primers. Pertinent results are discussed for each case separately in the respective parts of the following section.

Phylogenetic relationships in the genus *Ganoderma*

The ITS analyses resulted in the formation of well-resolved/supported terminal subclades which led us to accept 80 *Ganoderma* taxa at species level in accordance with

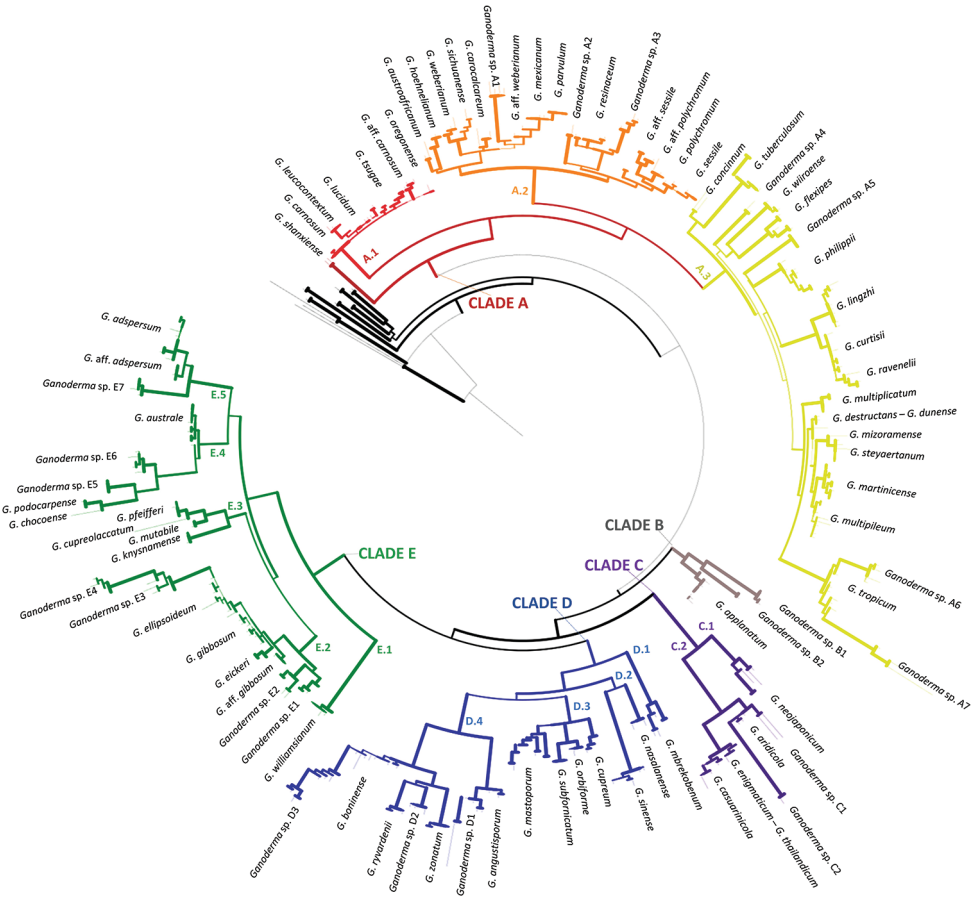

Figure 3. Summary tree of the genus *Ganoderma* inferred from ML analysis, based on ITS sequence data (main dataset, DS; Table 2). Thick lines represent ML bootstrap values (BS) ≥ 65% and Bayesian Posterior Probabilities (BPP) ≥ 0.95. Clades and Clusters within the tree appear as presented in Table 1 and Suppl. material 1: Table S2. Species names correspond to those inferred in this study. Scale bar: 0.01 nucleotide substitutions per site.

the criteria set and in conjunction with literature data available (Fig. 1b and Fig. 3). This number includes at least 21 hitherto unnamed (or not properly/fully identified) distinct phylogenetic entities for which tentative species names are hereby proposed. Six other terminal groups were phylogenetically delineated; however, since they did not fully conform to the criteria set for being recognised at the species-level, they were provisionally named in relation to their closest taxon by using the abbreviation "aff.". Furthermore, two singletons presented distinct positions in the phylogeny of the genus but their status is ambiguous as discussed below.

In all cases, ML and BI analyses provided almost identical tree topologies with minor differences and, thus, only the trees inferred from the ML analysis are presented. The genus *Ganoderma* exhibits a strongly-supported monophyly (BS: 90%, BPP: 1.00; Fig. 3). The ITS phylogeny reveals three major lineages, i.e. Clade A (72%; Figs 4, 5),

Table 3. Summary of polymorphic regions in ITS1 and ITS2 spacers assessed in *Ganoderma* species/groups represented by ≥ 10 entries in the GenBank/ENA/DDBJ and UNITE databases. For each region, the length and position between conserved oligonucleotides (i.e. TGCAC to GAATG in ITS1 and AATCT to TAGCT in ITS2) are hereby provided. Additional pertinent information is included in Suppl. material 2: Fig. S1. Grouping in Clades/Clusters, as well as names and number of sequences per name, are in accordance with Table 1 and Fig. 3.

Species/Groups	ITS1 sequence of potential diagnostic value	Length (nt)	Position in the alignment of Suppl. material 2: Fig. S1 (without gaps)	ITS2 sequence of potential diagnostic value	Length (nt)	Position in the alignment of Suppl. material 2: Fig. S1 (without gaps)
CLADE A						
Cluster A.1						
G. oregonense		13	25–37	GCCTTTGCGGGTW	26	17–42
G. tsugae	TGTGAAGCGTGCT	13	25/26–37/38	TGYRGGCTTGGAC	26	17–42
G. carnosum		13	25–37	AGCCTTGC	8	16–23
G. lucidum	TGAAGCGYNCCYY	13	27–39	nd		
G. leucocontextum – *G. weixiensis*	CGAAGCGTGC	10	27–36	nd		
Cluster A.2						
G. boehmelianum	CTTCAGTC	8	16–23	CTTGTGGGTT	10	20–29
G. weberianum	nd			nd		
G. sichuanense	nd			nd		
G. carocalcareum	AACGTCGTKAAGCGGGC	17	21–37	nd		
Ganoderma sp. A1	GGGTCTTTT	9	34–42	CGTCTTTC	8	60–67
G. mexicanum	GCTCTTTACTGAGCC	15	36–50	CGGCCGGCTCCTCT	21	65/67–85/87
G. parvulum		15	36–50	TAAATGC[1]	21	65/67–85/87
G. resinaceum	AAGCGGCG	8	55/56–62/63	nd		
Ganoderma sp. A3	GGATCGGCGT	10	55–64	ACAGATCT	8	13–20
G. polychromum	ACACCTAT	8	84–91	nd		
G. sessile	CCACAAACTCTR	12	78–89	CTTACAAA	8	10–17
Cluster A.3						
G. tuberculosum	GATTGTCG	8	21–28	CCATGCCC	8	58/59–65/66
G. wiiroense	GGCATTAT	8	21–28	TTCTCTTA	8	71/72–78/79
G. philippii	TTGCTGGG	8	39–46	CTTTTGTGGYTTT	13	18–30
G. lingzhi	CAGATTGC	8	19–26		10	54–63
G. curtisii	TGCGGAGCGCAT	12	49–60	CGGCCGTTAT	10	54–63
G. ravenelii	GAGTGCAT	8	53–60		10	54–63
G. multiplicatum	CCCTTTAT	8	35–42	nd		
G. destructans – *G. dunense*		9	22–30	nd		
G. steyaertanum	ATCVTAAAA[2]	9	22–30	CTCTTGGCC	9	61–69
G. martinicense		9	22–30	CATTCTTG	8	59–66
G. multipileum		9	22–30	G(C)AAGCTTTTG	10–11	13–22/23
Ganoderma sp. A6	TCCCAGGA	8	50–56	CTCCTCTCTT	10	72–81
G. tropicum	ACCGGGCTTTGCA	13	42–54	nd		
CLADE B						
G. applanatum	GTGCTYTT	8	32–39	TAAGCTTKTGT	11	14–24
CLADE C						
G. neojaponicum	ATGGATCGCG	10	18–27	AGGTGTTTG	9	47–55
G. enigmaticum – *G. thailandicum*	CTTCTTGTC	9	35–43	TTGCAACC	8	11–18
G. casuarinicola	GCTCTTGT	8	34–41		8	11–18
CLADE D						
G. mbrekobenum	TTWCAGASSGT	11	16–26	AGGCTATT	8	48–55
G. nasalanense	CGTTTTCA	8	70–77	TCTTTAATA	9	60/62–68/70
G. sinense	GGAGCTSGT	9	41–49	GTAAAGGC	8	24–31
G. mastoporum	nd			TTTTTARYGRKTTTGTAGG	19	19–37
G. angustisporum	GTGTAAAA	8	27–34	ATGGCTWGT	8	24/28/29–32/36/37
G. zonatum	TCGCTCGC	8	34–41	TCTCTTCA	8	3–10

Species/Groups	ITS1 sequence of potential diagnostic value	Length (nt)	Position in the alignment of Suppl. material 2: Fig. S1 (without gaps)	ITS2 sequence of potential diagnostic value	Length (nt)	Position in the alignment of Suppl. material 2: Fig. S1 (without gaps)
G. ryvardenii	TCGTGCGG	8	23–30	CTTTAACT	8	61–68
G. boninense	GTTTGACRAGTT	12	40/44–51/55	ATCTCTTTGY	10	16–25
Ganoderma sp. D3	GGCGTGGT	8	24–31		10	16–25
CLADE E						
G. williamsianum	CTTCAGGTC	9	16–24	CTTAATYGA	9	21–29
Ganoderma sp. E1	GTTTTACG	8	15–22	ATRAGCTTCT	10	13–22
Ganoderma sp. E2		8	15–22	TATGKGAG	8	23–30
G. aff. *gibbosum*		13	27–39		10	60–69
G. gibbosum	TGARRSGGGCTYG[3]	13	27–39	TCCYTTTACR[3]	10	60–69
G. ellipsoideum		13	27–39		10	60–69
Ganoderma sp. E4	RTTAAACG	8	26–33	GTCGGACTW[4]	9	59–67
G. pfeifferi	GGCCCGTTT[5]	9	34/35–42/43	GCCTTTGTC[6]	9	57–65
Ganoderma sp. E6	ACYGAGCYYGC	11	41–51	TCTTTGCGGGG	11	19–29
G. australe	CGAAACGKGCTCG	13	27–39		11	19–29
Ganoderma sp. E7	CCCCATGA	8	83/84–90/91	GTCTTTACA	9	59–67
G. aff. *adspersum*	GGGCCCGTTC	10	33–42	CTTCTTGCGG	10	18–27
G. adspersum	AGGCCCGTTC	10	33–42	AGGTTTGTAGGG	12	27/28–38/39

Clade B (95%, 1.00; Fig. 6) and the Clades C, D and E (70%, 1.00; Figs 6, 7). Further resolution of phylogenetic origins and relationships amongst and within major Clades requires the use of additional molecular markers.

Clade A

On the basis of ITS meta-analysis, Clade A is moderately supported only through ML analysis (69%; Fig. 4). It is hereby shown to represent the core of laccate species with a worldwide distribution (subgenus *Ganoderma*, sect. *Ganoderma*) and a large variation in morphological characteristics. Taxa nested in Clade A are generally characterised by laccate, usually reddish to dark-brown pilei, mostly annual (rarely biennial or even – allegedly – perennial), often stipitate or sessile to substipitate basidiomes, with elements of pileal crust possessing a regular palisade (hymenoderm) superficially covered or rarely embedded in a resinous-melanin matrix of varying thickness and a mostly pale/light-coloured context (Gilbertson and Ryvarden 1986; Moncalvo and Ryvarden 1997; Wasser et al. 2006).

Clade A includes 1927 entries distributed across 881 unique ITS sequence types of which 240 appear as ASVs representing 1414 entries in GenBank/ENA/DDBJ and UNITE. Clade A could be further divided into three well-supported Clusters (A.1, A.2 and A.3) and to the recently-introduced *G. shanxiense* L. Fan & H. Liu (Liu et al. 2019), i.e. a laccate, thin crust, dark brown context species represented by two singletons deriving from Chinese material (100%, 1.00; Fig. 4). In total, Clade A includes 28 well-supported phylogenetic species plus 14 distinct terminal clades corresponding to taxa not receiving adequate support (Figs 4, 5). Such open issues in delimiting *Ganoderma* are particularly evident in Cluster A.1, where low values of genetic distance are revealed amongst taxa and several of them are not supported – by ITS alone – as

phylogenetically distinct or in Clusters A.2 and A.3 where species complexes (i.e. evolutionary-related populations with indiscrete boundaries amongst them) exist.

Clade A – Cluster A.1

In the context of this work, Cluster A.1 corresponds to a well-supported clade (100%, 1.00; Fig. 4) and comprises 36 sequences of which 23 are ASVs with 190 entries (Suppl. material 1: Table S2), while the expanded/detailed analysis includes a total of 297 entries (Suppl. material 3: Fig. S2a). Cluster A.1 is formed by material deriving from temperate regions of the Northern Hemisphere (except of two sequences originating from Argentinian specimens) on a large range of host plants under various names (Suppl. material 1: Table S2; Fig. 4). Interspecific genetic distances within Cluster A.1 are very low (i.e. 0.008 ± 0.004) in comparison to values calculated in other *Ganoderma* groups, which, in conjunction with the high sequence similarity values noted (98.96 ± 0.62%), are indicative of low divergence amongst taxa. Therefore, the criteria set in this study for phylogenetic species are not generally met for members of Cluster A.1 since a significant overlap exists between intraspecific and interspecific variability (absence of a barcoding gap; Fig. 8). Hence, in this particular case, ITS demonstrates poor species-level resolution and delimitation of taxa seems to be supported by multigene approaches only (Zhou et al. 2015; Loyd et al. 2018; Ye et al. 2019).

The major group of Cluster A.1 corresponds to *G. lucidum* (Curtis) P. Karst. (*G. lucidum* sensu stricto), which is represented by 10 sequences (or 97 entries) in the main dataset (Fig. 4). The majority of sequences which grouped within this species were found to be accurately identified (107 out of the 153 entries; Table 1); the highest number of erroneously-labelled sequences placed in *G. lucidum* were under the name "*G. tsugae*" (12 in total, six of which derived from China). The majority of *G. lucidum* sequences derive from material originating from Eurasia, growing mainly on hardwoods with some occasional reports of occurrence on conifers, for example, *Larix* and *Pinus* spp. (Suppl. material 1: Table S2). An exception was formed by nine entries from the US (California and Utah); they most probably correspond to introduced material (Loyd et al. 2018), as well as two sequences from Argentina under the name "*G. oerstedii*" (Moncalvo et al. 1995a). On the basis of the outcome of the present study, the latter were apparently misidentified and the respective material belongs to *G. lucidum*; its existence in Argentina could probably be attributed to human-mediated transfer. A distinct subclade within *G. lucidum* consists of 18 entries corresponding to three ASVs and three singletons (75%, 0.97; Fig. 4) from East Asian collections only (Park et al. 2012; Zhou et al. 2015; Xing et al. 2018); two conserved substitutions in both ITS spacers differentiate the respective sequences from the rest of *G. lucidum* (position 225 in ITS1 and position 378 in ITS2; Table 3; Suppl. material 2: Fig. S1).

G. carnosum Pat. was first described on *Abies* in southwest France (Pyrenees Mts.) and is distributed throughout Europe (Jahn et al. 1980, 1986; Mattock 2001; Ryvarden and Melo 2017); no reports exist of its occurrence in other continents. With respect to morphology, it resembles *G. lucidum* and the most prominent discriminating characters are the preference for conifers (*Abies* and *Pinus* spp.) and the blackish shiny

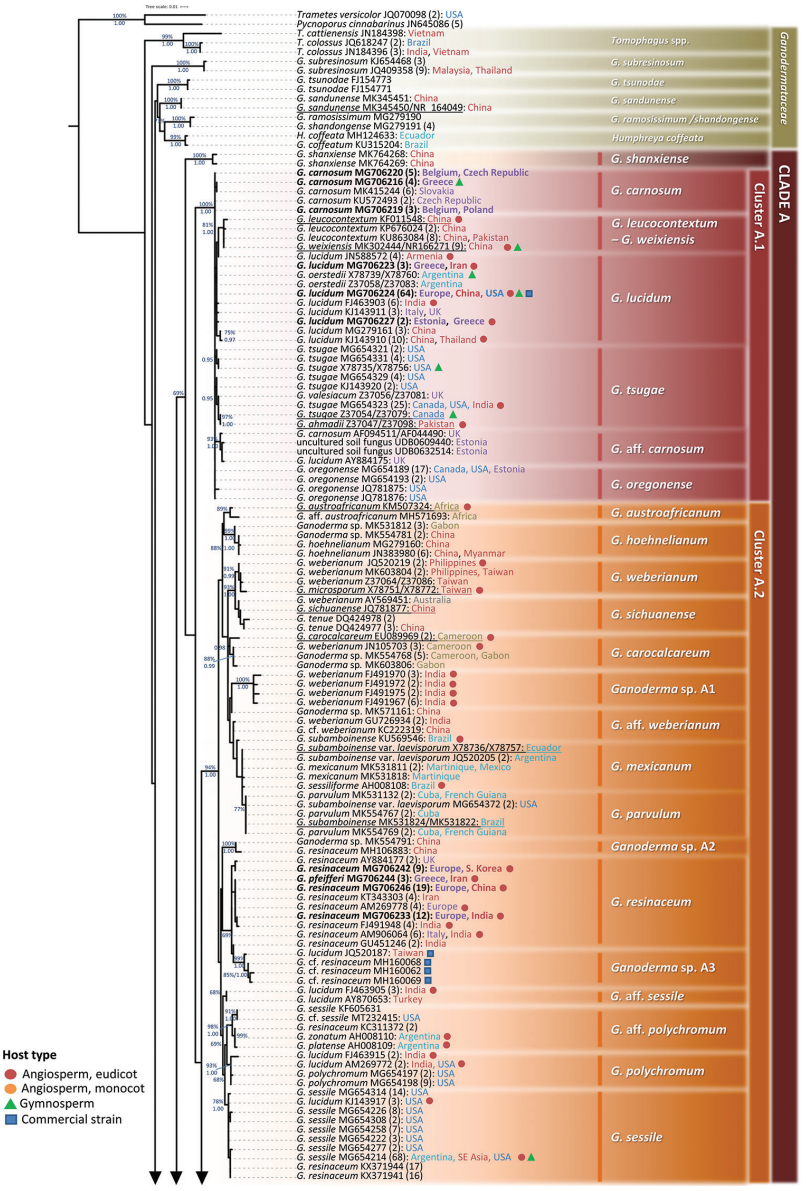

Figure 4. Detail from Fig. 3. Phylogenetic reconstruction of the genus *Ganoderma* inferred from ML analysis, based on ITS sequence data (main dataset, DS; Table 2) for Clade A, Clusters A.1 and A.2. ML bootstrap values (BS) ≥ 65% and Bayesian Posterior Probabilities (BPP) ≥ 0.95 are shown. Sequences names on the left appear as initially labelled and are followed by the respective GenBank/ENA/DDBJ or UNITE accession number, while the total number of identical entries corresponding to a particular sequence is placed in parentheses, followed by the type of host plant (legend for the coloured shapes is found at the lower left side of tree) and geographic origin of the respective material (the latter appears in different font colour depending on the continent of provenance; see also Table 1 and Suppl. material 1: Table S2). Species names on the right correspond to those inferred in this study evaluated in conjunction with literature data. Sequences generated in the present work appear in bold typeface, while underlined sequences are those originating from type material. Scale bar: 0.01 nucleotide substitutions per site.

upper surface when mature. The wider and highly-granulose (rougher) basidiospores, as well as the pore density, are also referred to as being of diagnostic value in taxonomic keys (Kotlaba and Pouzar 1993; Ryvarden and Gilbertson 1993; Ryvarden and Melo 2017). As a result of the ITS meta-analysis, 26 entries of *G. carnosum* originating from Europe (five generated in this study; Table 1 and Fig. 4) formed a group demonstrating high intraspecific sequence similarity. Most of them were accurately labelled (22 out of 32 *G. carnosum* entries available in public databases), while four were initially determined as "*G. lucidum*" (Table 1). The phylogenetically closest taxa to *G. carnosum* are *G. oregonense* and *G. lucidum* with which high values of sequence similarity were noted (99.68 ± 0.20% and 99.49 ± 0.24%, respectively).

Sequences deriving from two U.K. specimens (deposited as *G. carnosum* and *G. lucidum*) and from two environmental samples (Estonia, labelled as "uncultured soil fungus") formed a distinct group (93%, 1.00; Fig. 4). It is provisionally named "*G.* aff. *carnosum*" due to the initial sequence labelling and European distribution and presents high sequence affinity with *G. oregonense* (98.87 ± 0.22%) and *G. carnosum* (98.84 ± 0.16%).

G. oregonense Murrill and *G. tsugae* Murrill are closely-associated taxa (Adaskaveg and Gilbertson 1986, 1988; Moncalvo 2000). They are mainly distinguished on the basis of basidiospores size and geographic distribution; the former is mainly found in western USA in temperate woods dominated by *Tsuga heterophylla*, *Pseudotsuga menziesii*, *Picea* spp. and *Abies* spp. However, the inclusion of environmental samples in this study expanded the known distribution of this taxon to Europe (Estonia, UDB0287378). *G. oregonense* is represented by four sequences corresponding to 21 entries (Fig. 4) in our analysis, while six singletons are also associated with this taxon and are included in the expanded dataset (Suppl. material 1: Table S2 and Suppl. material 3: Fig. S2a). On the other hand, *G. tsugae* is mainly recorded in eastern USA in temperate hemlock forests (Loyd et al. 2018), while it is also reported to occur in Canada (Adaskaveg and Gilbertson 1986, Ryvarden and Gilbertson 1993) and in Asia (Zhao 1989; Pegler and Yao 1996; Zhao and Zang 2000). Such reports were confirmed through the outcome of the present work (Table 1). *G. tsugae* is hereby represented by nine sequences corresponding to 41 entries in the databases examined (Fig. 4), while another 13 singletons were added in the expanded analysis (Suppl. material 1: Table S2 and Suppl. material 3: Fig. S2a). Most of them were found to be correctly identified (46 entries out of 54; Table 1; a sequence from the type specimen was also included, Z37054/Z37079). The ITS sequence similarity and genetic distance between *G. tsugae* and *G. oregonense* was found to be high and low, respectively (99.19 ± 0.62% and 0.005 ± 0.003, respectively), demonstrating that their distinct phylogenetic status cannot be evidenced through the use of ITS alone. In addition, the boxplot analysis revealed the absence of a barcoding gap between the two taxa (Fig. 8). However, application of a multigene approach permitted their delimitation (Loyd et al. 2018).

In the past, *G. tsugae* was occasionally reported to be conspecific with *G. carnosum* or *G. lucidum* on the basis of morphological observations (Donk 1974; Ryvarden and Melo 2017). The analysis performed in this work separates *G. tsugae* from *G. carnosum* and *G. lucidum*, which is in agreement with recent reports (Zhou et al. 2015; Loyd

et al. 2018), although the interspecific sequence similarity values are high, i.e. 99.15 ± 0.58% and 98.91 ± 0.61%, respectively. In addition, a unique sequence, initially labelled "*G. carnosum*" (Z37057/Z37082; strain JAHN 1197-121, Germany), represents an authentic specimen of *G. atkinsonii* Jahn, Kotl. & Pouzar, which was later synonymised with *G. carnosum* (Jahn et al. 1986) and maintained as such by Moncalvo et al. (1995). The outcome of the present study shows that it forms part of *G. tsugae* (Suppl. material 1: Table S2 and Suppl. material 3: Fig. S2a).

Noteworthy cases pertain to sequences under the names of "*G. valesiacum*" and "*G. ahmadii*" which grouped within *G. tsugae* (Table 1; Fig. 4). *G. valesiacum* Boud. was described by Boudier and Fischer (1895) from a collection on *Larix* in Valais, Switzerland. The type specimen is almost destroyed; however, remains of the cutis are similar to the hymenodermiform anatomy presented by *G. lucidum*, but with smaller basidiospores possessing pronounced surface cambers and a "white, punk-like context" under a sometimes cracking-crust (Ryvarden and Gilbertson 1993; Ryvarden and Melo 2017). Three ITS sequences, labelled as "*G. valesiacum*", are found in GenBank and were included in this work: (a) Z37056/Z37081 (strain CBS 282.33; UK), also used in previous studies (Moncalvo et al. 1995a; Hong and Yung 2004), is grouped within *G. tsugae* and presents sequence similarity values higher than 97.63% to other members of this taxon; (b) MG711807 (strain LE-BIN 2350; Russia, Altai Mts.) forms a clade within *G. lucidum* presenting an identical sequence with the most common ASV of this species (i.e. MG706224); (c) JQ520218 is grouped within *G. sessile* possessing the same sequence as the most common ASV of this species (i.e. MG654214; Suppl. material 1: Table S2); this particular sequence is erroneously associated with strain CBS 428.84 (USA), which had been earlier sequenced and correctly labelled as *G. tsugae* (X78735/X78756; Moncalvo et al. 1995b). Hence, molecular evidence from sequences labelled as "*G. valesiacum*" is in accordance with the views expressed in previous studies stating that such material is conspecific with either *G. lucidum* or *G. tsugae* on the basis of morphological features alone (Steyaert 1972; Stalpers 1978; Adaskaveg and Gilbertson 1986; Nunez and Ryvarden 2000; Wasser et al. 2006). Still, in the absence of a sequence from the holotype, it is not possible to draw definite conclusions on whether this name corresponds to a valid phylogenetic species. On the other hand, the only ITS sequence representing *G. ahmadii* Steyaert derives from the type material (strain FWP14329, Pakistan; Z37047/Z37098) and presents relatively-high sequence similarity values to members of the *G. tsugae* group (98.63 ± 0.36%). Therefore, on the basis of data available, the status of *G. ahmadii* remains ambiguous and additional specimens need to be studied.

In the frame of this study, four ASVs representing 20 entries formed a well-supported group (81%, 1.00; Fig. 4) including type material of two Chinese taxa recently described, i.e. *G. leucocontextum* T.H. Li, W.Q. Deng, Sheng H. Wu, D.M. Wang & H.P. Hu and *G. weixiensis* Ye et al. (Li et al. 2014; Ye et al. 2019). The two taxa presented high intraspecific sequence similarity indicative of their close geographic origin (i.e. 99.64 ± 0.28%); all studied specimens originated from China, Tibet and Nepal. Hence, ITS data alone could not discriminate the two taxa (Fig. 4) and the use of additional markers was necessary for establishing the latter species (Ye et al. 2019).

Clade A – Cluster A.2

Cluster A.2 (94%, 1.00; Fig. 4) is represented by 73 unique sequences; 47 are ASVs deriving from 309 entries in the databases (Table 1 and Suppl. material 1: Table S2). The expanded/detailed tree is formed by 263 sequences representing 517 entries in the databases (Suppl. material 1: Table S2 and Suppl. material 4: Fig. S2b).

A major subclade is formed by specimens collected in southeast Asia and Australia growing mostly on angiosperms (93%, 1.00 and 72%, 1.00, Fig. 4 and Suppl. material 4: Fig. S2b, respectively). The sequences had been deposited under different taxonomic names, i.e. *G. weberianum* (Bres. & Henn. ex Sacc.) Steyaert, *G. sichuanense* J.D. Zhao & X.Q. Zhang, *G. tenue* J.D. Zhao, L.W. Hsu & X.Q. Zhang, *G. lucidum*, *G. microsporum* R.S. Hseu and *Ganoderma* sp. and present rather low heterogeneity as evidenced by the values of sequence similarity and genetic distance obtained (98.87 ± 0.62% and 0.010 ± 0.005, respectively). We consider that this particular subclade is related to *G. weberianum* sensu Steyaert (Moncalvo 2000) and includes at least two not adequately (by ITS alone) resolved groups. One of them corresponds to *G. sichuanense* and consists of 19 entries originally identified as *G. sichuanense* (9), *G. tenue* (2), "*G. weberianum*" (4), "*G. lucidum*" (2), *Ganoderma* sp. (1) and "uncultured soil fungus" (1), which derive from specimens collected in southeast Asia and Australia on angiosperms and gymnosperms (Table 1, Suppl. material 1: Table S2). This taxon demonstrates high sequence similarity (99.40 ± 0.22%) and low genetic distance values (0.006 ± 0.003). Two sequences assigned to *G. sichuanense* (including the holotype: HMAS 42798, JQ781877; Cao et al. 2012) group with sequences identified as *G. tenue* (Figure 3 and Suppl. material 4: Figure S2b); unfortunately, no sequence is available from the type material of *G. tenue* (Zhao et al. 1979a), which makes it difficult to comment on its relationships to associated taxa. The other group is composed of 12 sequences [originally identified as *G. weberianum* (9) and *G. microsporum* (corresponding to the type, RSH 0821; Moncalvo et al. 1995b)] which are placed together (91%, 0.99; Fig. 4) and demonstrate high intraspecific sequence similarity (99.16 ± 0.48%). On the basis of the aforementioned findings, we consider that they form part of *G. weberianum* sensu stricto (originally described from Samoa; Steyaert 1972). Moreover, although it is not possible to draw any definite conclusions about the status of *G. microsporum*, we tend to agree with the view expressed by Smith and Sivasithamparam (2000) that it is a subspecific entity within *G. weberianum*. The two groups corresponding to *G. sichuanense* and *G. weberianum* demonstrate interspecific ITS sequence similarity and genetic distance values (Fig. 8) which do not support the existence of two distinct phylospecies on the basis of the criteria hereby set.

G. hoehnelianum Bres. forms a monophyletic group in Cluster A.2 (99%, 1.00; Table 1, Fig. 4) and includes 12 entries deriving from southeast Asian (China, Myanmar) and African (Gabon) material; sequences of the two origins are separated into two subgroups (Fig. 4), but they exhibit low variability (sequence similarity: 99.63 ± 0.23%). On the other hand, *G. austroafricanum* Coetzee, M.J. Wingf., Marinc., Blanchette is also a well-supported species (87%, 0.99; Suppl. material 4: Fig. S2b) represented by two singletons, including the type specimen from South Africa. Moreover, *G. carocalcareum*

Douanla-Meli forms a subclade (67%, 0.99; Suppl. material 4: Fig. S2b) consisting of 11 sequences which originate from material collected in Africa (Table 1); two are under this name (including the type specimen), while the rest are labelled either as "*G. weberianum*" (3) or as *Ganoderma* sp. (1) and form a well-supported subgroup within the clade (88%, 0.99; Fig. 4). However, sequence similarity and genetic distance values (98.61 ± 0.36% and 0.013 ± 0.002, respectively) do not permit their dinctinction. The entry MK603806 (MUCL 49272) represents the "C2.2" clade in the study of Cabarroi-Hernández et al. (2019) which is composed of several MUCL specimens from Cameroon and Gabon. Genetic distance and sequence similarity values support the distinct status of *G. carocalcareum* from *G. weberianum* (0.022 ± 0.006 and 97.50±0.78%, respectively).

A new phylogenetic species within Cluster A.2 is hereby proposed and is provisionally named "*Ganoderma* sp. A1" (corresponding to the UNITE DOIs SH1740420.08FU, SH1740444.08FU and SH1740445.08FU); its monophyly is strongly supported in both trees (100%, 1.00; Fig. 4 and Suppl. material 4: Fig. S2b). It is represented by eight unique sequences (i.e. four ASVs and four singletons; Suppl. material 1: Table S2 and Suppl. material 4: Fig. S2b) corresponding to 17 entries. On the basis of available information, all sequences derive from specimens initially identified as "*G. weberianum*" originating from India on a large range of eudicots (Suppl. material 1: Table S2). *Ganoderma* sp. A1 presents relatively-low intraspecific genetic distances (0.010 ± 0.003) and high sequence similarity (99.01 ± 0.18%).

Other four entries of dubious identity derive from material originating from Asia (China and India) labelled as *Ganoderma* sp., "*G. weberianum*" (2) and "*Ganoderma* cf. *weberianum*", as well as from Brazil under the name "*G. subamboinense*" (Table 1 and Suppl. material 1: Table S2) and exhibit low genetic distance and high sequence similarity (0.006 ± 0.003 and 99.18 ± 0.43%, respectively). They form part of the same larger subclade together with *Ganoderma* sp. A1, *G. mexicanum* and *G. parvulum* (Fig. 4); however, they do not retain the same position in the expanded tree (Suppl. material 4: Fig. S2b). For the purposes of this work, we provisionally maintain them as *Ganoderma* aff. *weberianum* (corresponding to the UNITE DOI SH1723064.08FU) since it is not possible to determine their exact identity from the data available.

Another major subclade consisting of material originating from the Neotropics is formed by a total of 17 entries. Four of them are singletons, while the other 13 are grouped in six ASVs (Suppl. material 1: Table S2; Fig. 4); the expanded/detailed tree includes 38 entries corresponding to 31 sequences (Suppl. material 4: Fig. S2b). They were deposited under several names: *G. parvulum* Murrill (10 sequences), *G. subamboinense* var. *laevisporum* Bazzalo & J.E. Wright (7, including type material), *G. mexicanum* Pat. (6), *G. subamboinense* (Henn.) Bazzalo & J.E. Wright ex Moncalvo and Ryvarden (3, including type material), "*G. tuberculosum*" (1), "*G. weberianum*" (5), *G. sessiliforme* Murrill (1), *G. stipitatum* (Murrill) Murrill (1) and *Ganoderma* sp. (4). The outcome of this work shows that this material forms part of two terminal groups corresponding to *G. mexicanum* and *G. parvulum* (Fig. 4) in accordance with the findings of a recent study by Cabarroi-Hernández et al. (2019). Hence, the former is selected as the earliest valid name to accommodate specimens also reported as "*G. sessiliforme*" and "*G. subamboinense* var. *laevisporum*" from Argentina, Brazil, Martinique, Mexico and USA,

while the latter for material also labelled as "*G. subamboinense*", "*G. subamboinense* var. *subamboinense*" and "*G. stipitatum*" from Brazil, Colombia, Costa Rica, Cuba, French Guiana and USA (77%; Fig. 4). Such a separation is in accordance with morphological observations made by Ryvarden (2000; 2004) and Cabarroi-Hernández et al. (2019). However, the support that this group of taxa receives by ITS data is not adequate (Suppl. material 4: Fig. S2b) and the respective interspecific sequence similarity and genetic distance values (Fig. 8) do not separate them on the basis of the criteria hereby set.

Another well-supported terminal clade (100%, 1.00; Fig. 4, Suppl. material 4: Fig. S2b) is formed by two entries labelled as "*G. resinaceum*" and *Ganoderma* sp. deriving from China. It is provisionally named *Ganoderma* sp. A2 (corresponding to the UNITE DOI SH2762559.08FU) since it complies with the criteria set in this study and it is hence considered as a new phylospecies. The genetic distance and sequence similarity values versus the most closely-related species (i.e. *G. resinaceum*) are 0.028 ± 0.003 and 97.52 ± 0.23%, respectively.

G. resinaceum Boud. is represented by 10 ASVs and 65 entries (Fig. 4), while the expanded/detailed tree includes 65 sequences corresponding to 126 entries (Suppl. material 4: Fig. S2b). Intraspecific genetic distance and sequence similarity values are well within the respective ranges observed for taxa of Clade A (i.e. 0.005 ± 0.003 and 99.46 ± 0.31%, respectively). This species appears to be very common throughout Europe (type locality), but it also occurs in Asia (e.g. China, India, Iran, Iraq, South Korea and Turkey) and Africa (Egypt, South Africa and Tunisia), being reported on a wide range of angiosperms (Suppl. material 1: Table S2). On the other hand, there is great controversy regarding the existence of *G. resinaceum* in the Americas. Its occurrence was reported by several authors in the past, for example, in Mexico (Torres-Torres et al. 2015), Brazil (Loguercio-Leite et al. 2005) and Argentina (Bazzalo and Wright 1982), although it was admittedly confused with other species names (e.g. *G. oerstedii*, *G. parvulum* or *G. subincrustatum*; de Lima Júnior et al. 2014; Torres-Torres et al. 2015). In addition, it has been synonymised with Neotropical taxa, such as *G. chaffangeonii* Pat. (type locality Venezuela; Steyaert 1980; Torres-Torres et al. 2012) and *G. praelongum* Murrill (type locality Cuba). However, no report of its alleged existence in America is so far supported by DNA data. Moreover, in the frame of this study, none of the sequences examined and confirmed to be *G. resinaceum* represents material originating from this continent. Therefore and to the best of our knowledge, the presence of *G. resinaceum* in the Americas cannot be confirmed by molecular evidence and its distribution seems to be restricted to the Old World.

Another new phylogenetic species is hereby proposed, provisionally named "*Ganoderma* sp. A3" (corresponding to the UNITE DOI SH1723084.08FU). It is strongly supported in both trees (100%, 1.00 and 99%, 1.00 in Fig. 4 and Suppl. material 4: Fig. S2b, respectively) and is represented by twelve singletons under the names "*G. resinaceum*" (5), "*Ganoderma* cf. *resinaceum*" (3) *Ganoderma* sp. (2), "*G. lucidum*" (1) and "uncultured *Ganoderma*" (1), all deriving from material from east Asia (Table 1 and Suppl. material 1: Table S2). This distinct taxon (intraspecific genetic distance: 0.007

± 0.002; sequence similarity: 99.22 ± 0.37%) presents at least six different conserved positions in ITS1 and in ITS2 when compared to *G. resinaceum* (Suppl. material 3: Fig. S1), which is the closest phylogenetic relative (genetic distance: 0.024 ± 0.005; sequence similarity: 97.59 ± 0.51%).

G. sessile Murrill is a well-supported (78%, 1.00; Fig. 4) and highly-represented species in terms of deposited sequences (227; Suppl. material 1: Table S2) showing high intraspecific sequence similarity (99.73 ± 0.14%). Many of the sequences were initially labelled as "*G. resinaceum*" (60 entries) and "*G. lucidum*" (9). Most *G. sessile* sequences derived from specimens collected in the USA, while the rest originate from Asia (including the Caucasus area) and one from Argentina (JQ520199; originally labelled as *G. resinaceum*), possibly as an outcome of human-mediated transfer.

A closely-related and well-supported (93%, 1.00; Fig. 4) group is formed by sequences belonging to *G. polychromum* (Copel.) Murrill. This species is represented by 19 entries deriving from material collected in either western USA (California, Washington and Oregon; associated with hardwood) or India; some of them were deposited under the names "*G. lucidum*" (6) or "*G. sessile*" (2) (Table 1). However, pairwise comparisons of *G. polychromum* sequences with those belonging to closely-positioned taxa revealed rather low genetic distance and high sequence similarity values (for example, vs. *G. sessile*: 0.012 ± 0.004, 98.76 ± 0.32%, respectively).

A distinct phylogenetic group (98%, 1.00; Fig. 4), sister to *G. polychromum*, consists of seven sequences presenting high intraspecific similarity, i.e. 98.88 ± 0.64%; the respective material derived the Americas and it appears under the names "*G. platense*", "*G. resinaceum*", "*G. sessile*" "*G.* cf. *sessile*" and "*G. zonatum*" (Table 1). Amongst those, the only one that could possibly have been correctly identified corresponds to *G. platense* Speg. because the correct topologies of *G. resinaceum* and *G. sessile* are found elsewhere within Cluster A.2, while *G. zonatum* forms part of Clade D (Fig. 4). However, since very limited information is available concerning this particular specimen (*G. platense* isolate BAFC384, AH008109; Gottlieb et al. 2000), we prefer not to draw any conclusions concerning the name of this terminal subclade. In addition, because of the close affinity it presents with *G. polychromum* (genetic distance: 0.014 ± 0.004, sequence similarity: 98.10 ± 0.42%), it does not abide (albeit marginally) with the criteria we set in order to be characterised as a distinct phylogenetic species; therefore, it is provisionally named "*G.* aff. *polychromum*" (corresponding to the UNITE DOIs SH1723162.08FU and SH1723226.08FU).

Another terminal group, although not adequately supported in any of the trees constructed, forms a sister clade to *G. sessile*/*G. polychromum* (Fig. 4, Suppl. material 4: Fig. S2b) and includes four sequences originally identified as "*G. lucidum*" deriving from India (3) and Turkey on eudicots (i.e. *Cassia fistula* and *Tamarindus indica*). It presents low genetic distance and high sequence similarity values in pairwise comparisons to *G. sessile* (0.014 ± 0.002 and 97.34 ± 0.16%); therefore, its status is dubious and it is provisionally named "*G.* aff. *sessile*" (corresponding to the UNITE DOI SH1723202.08FU).

Clade A – Cluster A.3

Cluster A.3 (76%, 1.00; Fig. 5) includes material originating from south and east Asia, tropical Africa, Australia and America (no occurrence in Europe) growing mostly on eudicot hosts (Suppl. material 5: Fig. S2c). It is composed of a total of 1385 entries, 889 of which are grouped in 145 ASVs (Suppl. material 1: Table S2) and comprises 19 terminal groups, 14 of which are well-supported in the present analysis.

G. tuberculosum Murrill is strongly supported in the generated trees (100%, 1.00; Fig. 5 and Suppl. material 5: Fig. S2c) and is represented by 36 sequences, 23 of which are grouped in six ASVs (Suppl. material 1: Table S2 and Suppl. material 5: Fig. S2c). Most of the respective material was correctly labelled (28 entries) and collections derive entirely from the Neotropics, i.e. southeast USA, Cuba, Martinique, Panama, Colombia and Brazil (Table 1). Murrill's type material of *G. tuberculosum* from British Honduras was very similar to basidiomes from Martinique examined by Welti and Courtecuisse (2010), thus confirming the wider distribution of this species in the Caribbean as indicated by our analysis. It is worth noting that sequences from Colombia (2) and Texas (1) form a distinct strongly-supported subgroup (99%, 1.00; Suppl. material 5: Fig. S2c) presenting conserved differences in ITS sequences (three to five positions in ITS1 and three in ITS2; Table 3 and Suppl. material 3: Fig. S1); however, their similarity values to the other *G. tuberculosum* sequences are high (i.e. 99.27 ± 0.58%) and do not seem to support a distinct species status. On another issue, recent studies reported the presence of *G. oerstedii* (Fr.) Murrill in Mexico, Costa Rica and Honduras (amongst other areas in the Neotropics) and referred to diagnostic characters, such as "the color of the basidiomata, context with resinous bands, cuticle cells with protuberances and/or branches and partially anastomosed basidiospore pillars" (Mendoza et al. 2011; Torres-Torres et al. 2015). Both Ryvarden (2000) and Torres-Torres et al. (2015) considered *G. tuberculosum* as a synonym of *G. oerstedii*, but this view cannot be supported (but neither contradicted) by the findings of the present study, since sequence data from the holotype or of a correctly-designated epitype of *G. oerstedii* are missing.

Furthermore, one sequence (JX310812) labelled as "*G. chalceum*" originating from Brazilian material and one sequence under the name *G. concinnum* Ryvarden (possibly of South American origin) form a terminal subclade which nested close to *G. tuberculosum* (0.97; Fig. 5). The two sequences present relatively-low sequence similarity (98.01%) and rather high genetic distance (0.020) and their conspecificity is uncertain. Since *G. chalceum* (Cooke) Steyaert is a species described on the basis of material originating from Africa (type specimen from Sierra Leone), southeast Asia and Oceania (Steyaert 1967) and because the only other ITS sequence available under this name is grouped in Clade D of the present study (together with other entries originating from Africa), the real identity of JX310812 remains ambiguous. Therefore, we prefer to use the name *G. concinnum* for describing this particular group.

Two sister subclades (0.99, Suppl. material 5: Fig. S2c) correspond to *G. flexipes* Pat. and *G. wiiroense* E.C. Otto, Blanchette, C.W. Barnes & Held. Both are strongly supported in the generated trees (1.00%, 1.00; Fig. 5 and Suppl. material 5: Fig. S2c). The former consists of seven sequences deriving from material collected on both angio-

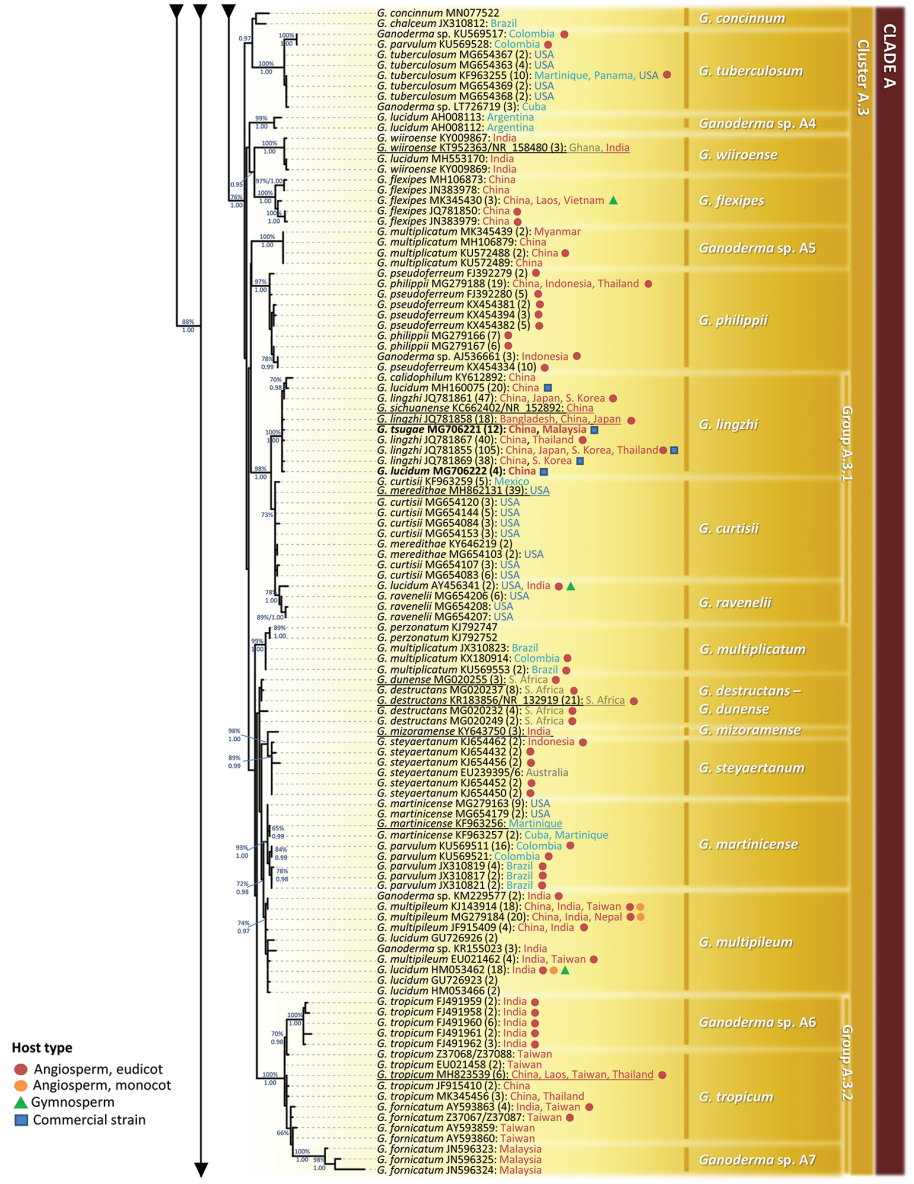

Figure 5. Detail from Fig. 3. Phylogenetic reconstruction of the genus *Ganoderma* inferred from ML analysis, based on ITS sequence data (main dataset, DS; Table 2) for Clade A, Cluster A.3. ML bootstrap values (BS) ≥ 65% and Bayesian Posterior Probabilities (BPP) ≥ 0.95 are shown. Sequences names on the left appear as initially labelled and are followed by the respective GenBank/ENA/DDBJ or UNITE accession number, while the total number of identical entries corresponding to a particular sequence is placed in parentheses, followed by the type of host plant (legend for the coloured shapes is found at the lower left side of the tree) and geographic origin of the respective material (the latter appears in different fonts colour depending on the continent of provenance; see also Table 1 and Suppl. material 1: Table S2). Species names on the right correspond to those inferred in this study evaluated in conjunction with literature data. Sequences generated in the present work appear in bold typeface, while underlined sequences are those originating from type material. Scale bar: 0.01 nucleotide substitutions per site.

sperms and gymnosperms in tropical Asia (China, Laos and Vietnam; Suppl. material 1: Table S2), presenting relatively-high intraspecies genetic distance (0.011 ± 0.005) which is in agreement with the formation of two well-supported terminal subgroups. The latter also constitutes a monophyletic species represented by 14 entries originating from Ghana (including the type specimen), Senegal and India.

Two new well-supported monophyletic species, provisionally named as "*Ganoderma* sp. A4" (no UNITE DOI available) and "*Ganoderma* sp. A5" (corresponding to the UNITE DOI SH1723120.08FU) are revealed in this study. *Ganoderma* sp. A4 is represented by two sequences deriving from Argentinian material which were originally identified as "*G. lucidum*" (100%, 1.00; Fig. 5 and Suppl. material 5: Fig. S2c). *Ganoderma* sp. A5 comprises seven sequences labelled as "*G. multiplicatum*", all originating from Asian specimens (100%, 1.00; Fig. 5 and Suppl. material 5: Fig. S2c); this name is apparently misapplied since *G. multiplicatum* occurs in the Neotropics and corresponds to another, rather distant, terminal group. Both *Ganoderma* sp. A3 and *Ganoderma* sp. A4 present high intraspecific sequence similarities (> 98.90%), whereas their respective interspecific values are indicative of their distinct status (93.64 ± 0.29% and 0.058 ± 0.03).

G. philippii (Bres. & Henn. ex Sacc.) Bres. constitutes a well-supported species (97%, 1.00; Fig. 5) represented by 102 sequences, of which 69 are grouped in 13 ASVs (Suppl. material 1: Table S2 and Suppl. material 5: Fig. S2c). The respective material originates from south and southeast Asia (China, Indonesia, Malaysia and Thailand) and is mainly deposited under the synonym *G. pseudoferreum* (Wakef.) Overeem & B.A. Steinm. Intraspecific genetic distance and sequence similarity values lie well within the ranges observed for species of Cluster A (i.e. 0.005 ± 0.003, max. 0.009; 99.44 ± 0.25%, min. 98.90%).

Three species, i.e. *G. lingzhi* S.H. Wu, Y. Cao & Y.C. Dai, *G. ravenelii* Steyaert and *G. curtisii* (Berk.) Murrill, form a strongly-supported group (A.3.1; 98%, 1.00; Fig. 5). Amongst them, *G. lingzhi* is distributed in south and east Asia on a wide range of angiosperms (Suppl. material 1: Table S2) and corresponds to a well-supported subclade (100%, 1.00; Fig. 5). It is represented by the largest number of entries for any given species in the present study (615, ca. 16% of the total generic entries; Table 1); 436 of them are grouped in 41 ASVs, while the dominant ASV is represented by 105 identical ITS entries (Suppl. material 1: Tables S2 and S4 and Suppl. material 5: Fig. S2c). Only 54% of these entries were deposited as *G. lingzhi* (including the holotype, JQ781858), while many of them were originally labelled as "*G. lucidum*" (206) since collections of the traditional medicinal fungus 'Lingzhi' were mainly identified as such for many years. Cao et al. (2012) finally proposed the name *G. lingzhi* for this fungus and thereby marked the onset of a debate concerning the real identity (correct name) of the fungus, i.e. *G. sichuanense* or *G. lingzhi*. Wang et al. (2012) and Yao et al. (2013) supported the former view by sequencing a so-called epitype (voucher HMAS252081; KC662402) of the original material. However, the epitypification of *G. sichuanense* did not comply with the International Code of Nomenclature for algae, fungi and plants (Zhou et al. 2015). Hence, this particular collection of "*G. sichuanense*" corresponds to *G. lingzhi*

as was recently explained (Dai et al. 2017). On the other hand, the holotype represents the true *G. sichuanense* which is not related to *G. lingzhi* (Cao et al. 2012; Liao et al. 2015; this work) and is positioned in Cluster A.2. It is of interest that, although a large number of *G. lingzhi* sequences were included in this meta-analysis, intraspecific genetic divergence was low (0.004 ± 0.003, 99.42 ± 0.32%).

G. curtisii (70%, 1.00; Suppl. material 5: Fig. S2c) is closely related to *G. lingzhi* in agreement with previous phylogenies (Zhou et al. 2015; Thawthong et al. 2017). It occurs in North America – being widespread in the eastern parts of the USA – primarily on angiosperms. In the context of the present study, 142 entries were grouped within this species; 89 of them correspond to 20 ASVs (Suppl. material 1: Table S2 and Suppl. material 5: Fig. S2c). The majority (124) were deposited with the correct name in databases, while nine were labelled as *G. meredithae* Adask. & Gilb. (including the type material; MH862131) and three as *G. curtisii* f. sp. *meredithae*. However, *G. meredithae* is considered to be a synonym of *G. curtisii* (Moncalvo 2000) as was later confirmed (Loyd et al. 2018). *G. curtisii* demonstrates low levels of variability evidenced by its intraspecific genetic distance and sequence similarity values (0.003 ± 0.001 and 99.49 ± 0.22%, respectively). On the other hand, *G. ravenelii* presents an overlapping geographic distribution with *G. curtisii*, for example, in south and east USA (Florida and North Carolina; Suppl. material 1: Table S2) and it forms a well-supported terminal subgroup (78%, 1.00; Fig. 5) being composed of 12 sequences from specimens isolated on both angiosperms and gymnosperms (Suppl. material 5: Fig. S2c). However, the outcome of the present work shows that these two taxa exhibit high affinity (genetic distance: 0.011 ± 0.003; sequence similarity: 98.93 ± 0.27%) and no clear ITS barcoding gap is evident between them (Fig. 8); their delineation is adequately supported only through the application of a multigene approach (Loyd et al. 2018).

Six other closely-related species are found in Cluster A.3 (i.e. *G. multiplicatum*, *G. destructans*, *G. steyaertanum*, *G. mizoramense*, *G. martinicense* and *G. multipileum*) (Fig. 5, Suppl. material 5: Fig. S2c). Amongst them, *G. multiplicatum* (Mont.) Pat. was originally described from French Guiana (Moncalvo and Ryvarden 1997) and its presence was evidenced in several other areas of South America (Ryvarden 2004; de Lima Júnior et al. 2014; Bolaños et al. 2016; Torres-Torres et al. 2012). Pertinent material, analysed in this study, formed an external subclade with strong support (99%, 1.00; Fig. 5); genetic distance and sequence similarity values (0.002 ± 0.001 and 99.54 ± 0.25%, respectively) are indicative of low intraspecific variability. All seventeen sequences derived from specimens collected in the Neotropics (Mexico, Brazil and Colombia; Table 1); seven of them were initially labelled as "*G. perzonatum*". However, the exact status of *G. perzonatum* Murrill remains ambiguous; it was originally described from Cuba and its morphological features associate it with *G. parvulum* (Cluster A.2 in this work) as reported by Moncalvo and Ryvarden (1997) and Cabarroi-Hernández et al. (2019). According to the latter study, "*G. perzonatum* could represent another closely related taxon in the vicinity of *G. mexicanum* / *G. parvulum*"; hence, examination of additional specimens is needed to arrive at robust conclusions. *G. multiplicatum* was also recorded in Asia and Africa (Steyaert 1980; Zhao 1989;

Wang and Wu 2007; Bhosle et al. 2010). To the best of our knowledge, the occurrence of this species in a region other than the Neotropics was never evidenced through the use of molecular data; the four sequences from China under this name correspond to a distinct phylospecies nested in Cluster A.3, i.e. *Ganoderma* sp. A5 (Table 1, Fig. 5) as previously explained. Therefore, the Asian material that groups in *Ganoderma* sp. A5 does not seem to be associated with the name *G. multiplicatum* in contrast to what was recently reported (Hapuarachchi et al. 2019).

In this study, *G. destructans* M.P.A. Coetzee, Marinc., M.J. Wingf. represented by 39 entries (including the type material; Table 1) is grouped together with *G. dunense* Tchotet, Rajchenb. & Jol. Roux; the latter consists of three entries (one from the type material) which are identical to *G. destructans* sequences (Table 1, Fig. 5 and Suppl. material 5: Fig. S2c). Specimens of both taxa originate from South Africa on eudicots (Coetzee et al. 2015, Tchotet Tchoumi et al. 2018). ITS sequence similarity and genetic distance values for material under these two names are indicative of the existence of a single species (0.006 ± 0.002; 99.73 ± 0.10%); hence, the distinction of these two entities cannot be supported by the use of this marker alone. However, *G. destructans* and *G. dunense* are distinguished following the outcome of a multigene analysis (Tchotet Tchoumi et al. 2018).

G. steyaertanum B.J. Smith & Sivasith. forms a well-supported group (89%, 0.99; Fig. 5) which is composed of 39 entries from specimens growing on eudicots in Indonesia and Australia (Table 1). *G. steyaertanum* was proposed as the correct name for the erroneously-labelled "*G. lucidum*" specimens reported to occur in this particular region (Smith and Sivasithamparam 2003). However, none of the sequences hereby examined was originally deposited as "*G. lucidum*"; instead, entries were labelled either as *G. steyaertanum* (34) or as *G.* aff. *steyaertanum* (3). This species forms a sister clade (98%, 1.00; Fig. 5) with *G. mizoramense* Zothanzama, Blanchette, Held, C.W. Barnes represented by only three identical sequences, all deriving from India (Suppl. material 1: Table S2 and Suppl. material 5: Fig. S2c). The two taxa appear closely related as evidenced by their genetic distance and sequence similarity values (0.016 ± 0.005 and 98.46 ± 0.31%, respectively), while the respective sequences differ at six conserved positions (Suppl. material 3: Fig. S1); furthermore, three conserved nucleotides in ITS2 are common to both and separate them from other related taxa of Cluster A.3. The very limited representation of *G. mizoramense* does not allow any definite conclusions regarding its taxonomic status.

G. martinicense Welti & Courtec. is sister to *G. multipileum* (72%, 0.98; Fig. 5), the two taxa being closely related (98.76 ± 0.36% and 0.012 ± 0.003) with no barcoding gap existing between them (Fig. 8). The former (93%, 1.00; Fig. 5) consists of 49 entries originating from specimens collected in USA, Mexico, Cuba, Martinique, Colombia, Brazil and Argentina which were deposited under various names, i.e. *G. martinicense* (18 entries, including type material), "*G. parvulum*" (24), "*G. perzonatum*" (2), "*G. tuberculosum*" (1), "*G. oerstedii*" (1) and "*G. lucidum*" (1) (Table 1, Suppl. material 5: Fig. S2c). Although at least three (not adequately supported) groups are evident in the expanded tree (which corresponds to different geographic origins, i.e. Colombia, Brazil/Argentina and Cuba/Martinique; Suppl. material 5: Fig. S2c), 'intergroup' val-

ues for ITS sequence divergence do not justify the existence of more than one phylogenetic species. Therefore and until more information becomes available, we prefer to maintain them all under *G. martinicense*. The name "*G. parvulum*" corresponds to a taxon forming part of Cluster A.2, as previously discussed.

G. multipileum Hou is phylogenetically supported (74%, 0.97; Fig. 5) and hereby represented by 243 entries; 130 entries are grouped in 29 ASVs (Suppl. material 1: Tables S2, S4). The respective collections originate from south and east Asia on a wide range of eudicot (mostly) and monocot or gymnosperm hosts, including also commercial strains (Suppl. material 5: Fig. S2c). The majority of sequences were labelled either as "*G. lucidum*" (105) or as *Ganoderma* sp. (112) and only 22 were identified as *G. multipileum*.

A second group (A.3.2; 100%, 1.00; Fig. 5) within Cluster A.3 includes sequences stemming from south and ast Asia. *G. tropicum* (Jungh.) Bres. is a species described from Indonesia (Java) and is widely distributed across subtropical and tropical Asia (Steyaert 1972; Moncalvo and Ryvarden 1997; Luangharn et al. 2019a). According to Corner (1983), this is a complex of pantropical occurrence, comprising many taxonomic varieties characterised by strongly echinulate basidiospores. However, pertinent sequenced material derives only from Asia. Hence, 15 entries, corresponding to specimens from China, Laos, Taiwan and Thailand, were originally identified as *G. tropicum* (type material included; Table 1). Moreover, 12 entries, labelled as "*G. fornicatum*" from specimens collected in India and Taiwan, presented genetic distances and sequence similarity indicative of a high affinity to *G. tropicum* sequences (i.e. 0.010 ± 0.004; 98.93 ± 0.63%, respectively). The type material of *G. fornicatum* (Fr.) Pat. originates from Brazil, but cannot be located and is most probably lost (Ryvarden 1991; Moncalvo and Ryvarden 1997). Furthermore, no recent information exists on the presence of this species in the Neotropics (Wang et al. 2014) and no sequence is available from specimens deriving from this particular region. In contrast, sequences/material under this name originates from Asia only (Imazeki 1939; Zhao and Zhang 2000; Wang and Wu 2008). Last, according to Mycobank, the current name for *G. fornicatum* is *G. orbiforme* (Fr.) Ryvarden. However, the latter is positioned in Clade D of the present analysis and is composed of entries originating solely from Brazil (Fig. 5). In view of the above, we maintain those particular entries identified as "*G. fornicatum*" under *G. tropicum*.

A strongly-supported terminal subclade in Group A.3.2 (100%, 1.00; Fig. 5) consists of 15 sequences (five ASVs) initially labelled "*G. tropicum*", originating from Indian specimens obtained from various angiosperms, for example, *Ficus benghalensis*, *Terminalia bellirica*, *Delonix regia* and *Cassia fistula* (Arulpandi and Kalaichelvan, unpublished results). It is considered as a new phylogenetic species, hereby referred to as "*Ganoderma* sp. A6" (corresponding to the UNITE DOI SH1723103.08FU) since it is clearly separated from *G. tropicum* by presenting interspecific genetic distance and sequence similarity values of 0.026 ± 0.005 and 97.24 ± 0.68%, respectively.

Furthermore, three singletons from Malaysian material (in this particular case, geographic origin is inferred from the title of the study which appears on the respective GenBank records), initially identified as "*G. fornicatum*", form another distinct well-

supported group (100%, 1.00; Fig. 5). This is also considered as a new phylogenetic species provisionally named "*Ganoderma* sp. A7" (corresponding to the UNITE DOI SH1723183.08FU) and is well distinguished from *G. tropicum* which is the closest taxon amongst those examined (sequence similarity: 94.64 ± 1.56%; genetic distance: 0.046 ± 0.015).

Clade B

Clade B (96%, 1.00; Fig. 6) includes 16 unique sequences corresponding to 431 individual entries (Table 1). It accommodates three species including the non-laccate *G. applanatum* (Pers.) Pat. (= *G. lipsiense* (Batsch) G.F. Atk.), which produces basidiomes characterised by skeleto-ligative hyphae with intercalary or terminal branching and hyphal pegs (absent in *Ganoderma* taxa of Clade A). Moreover, the pilei possess velutinous pileal surface ("trichodermatous" according to Steyaert), a pileus crust less than 0.5 mm thick, a brown context without resinous deposits and significantly smaller basidiospores than in most other non-laccate *Ganoderma* spp. (i.e. of Clade C). *G. applanatum* is the second-best represented species in the databases including 424 entries (ca. 11% of the total number of generic sequences) deriving from material collected in Europe, Asia and North America on a wide range of angiosperms/gymnosperms, as well as from environmental samples (Table 1). Amongst the latter, one sequence deriving from soil in Antarctica (KC785577, originally deposited as "uncultured *Ganoderma*") represents the only known sample of this species in the Southern Hemisphere, most possibly a human-mediated introduction by transportation of wood materials. *G. applanatum* is strongly supported (99%, 1.00; Fig. 6) and shows high intraspecific sequence similarity (99.71 ± 0.21%; min. 98.72%) and low genetic distance values (0.003 ± 0.002).

The other two species in Clade B form a well-supported sister clade (95%, 1.00; Fig. 6) and are hereby designated as "*Ganoderma* sp. B1" (corresponding to the UNITE DOI SH1723111.08FU) and "*Ganoderma* sp. B2" (corresponding to the UNITE DOI SH1723166.08FU). The former species includes four sequences from USA and China (in this particular case, geographic origins are inferred from the title of study which appears on the GenBank records), which show high similarity values (99.70 ± 0.15%) and form a terminal clade of strong support (100%, 1.00; Fig. 6). The latter species comprises three entries originating from material collected in Nepal under the names "*G. applanatum*", "*G. lingzhi*" and "*G. multipileum*" and form a well-supported subclade (100%, 1.00; Fig. 6). Pairwise comparisons of sequences belonging to *Ganoderma* sp. B1 and *Ganoderma* sp. B2 demonstrate that these are well separated on the basis of genetic distance and sequence similarity values (0.048 ± 0.002 and 95.04 ± 0.17%, respectively); both new species present clear barcoding gaps between each other and in the comparisons vs. *G. applanatum* (Fig. 8).

Clade C

Clade C is strongly supported (100%, 1.00; Fig. 6) and includes 67 unique sequences corresponding to 88 entries in total (Suppl. material 1: Table S2 and Suppl. material 6:

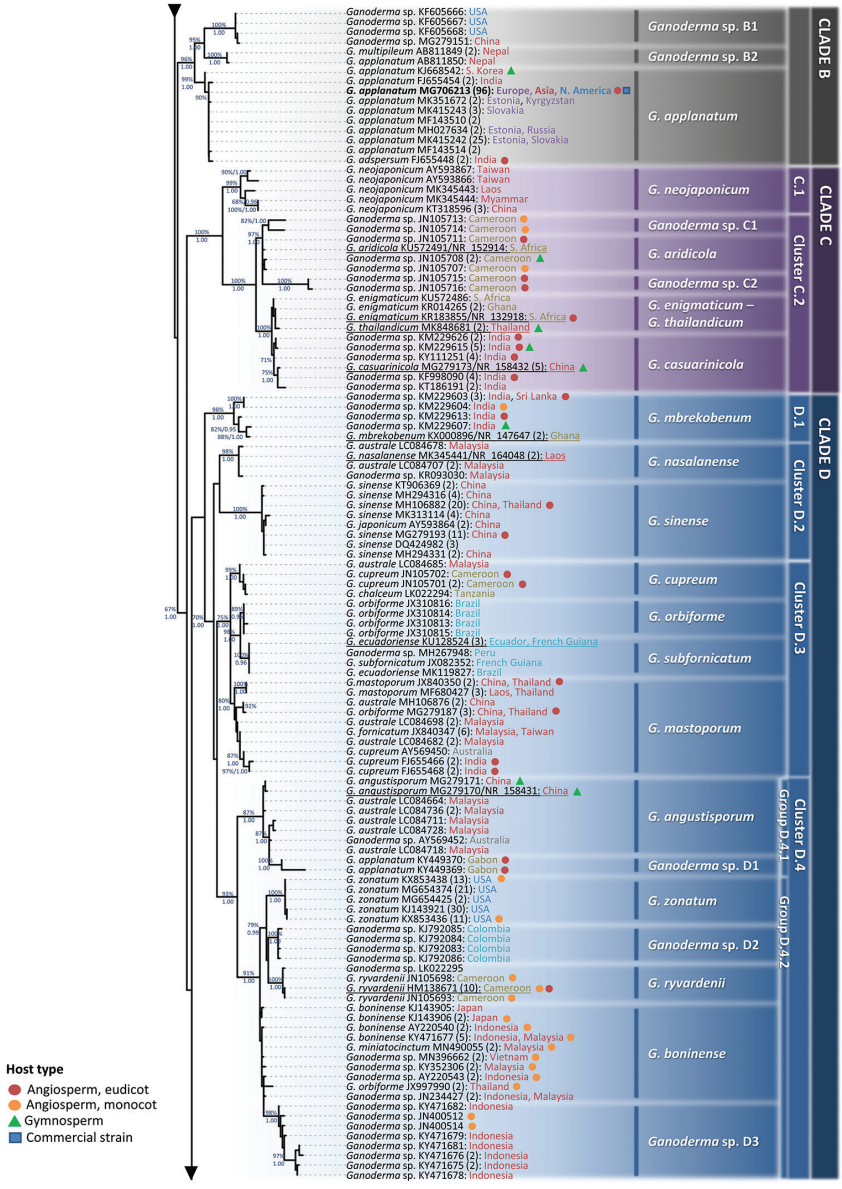

Figure 6. Detail from Fig. 3. Phylogenetic reconstruction of the genus *Ganoderma* inferred from ML analysis, based on ITS sequence data (main dataset, DS; Table 2) for Clades B, C and D. ML bootstrap values (BS) ≥ 65% and Bayesian Posterior Probabilities (BPP) ≥ 0.95 are shown. Sequences names on the left appear as initially labelled and are followed by the respective GenBank/ENA/DDBJ or UNITE accession number, while the total number of identical entries corresponding to a particular sequence is placed in parentheses, followed by the type of host plant (legend for the coloured shapes is found at the lower left side of the tree) and geographic origin of the respective material (the latter appears in different fonts colour depending on the continent of provenance; see also Table 1 and Suppl. material 1: Table S2). Species names on the right correspond to those inferred in this study evaluated in conjunction with literature data. Sequences generated in the present work appear in bold typeface, while underlined sequences are those originating from type material. Scale bar: 0.01 nucleotide substitutions per site.

Fig. S2d). The respective material presents a paleotropic distribution and originates from angiosperm and gymnosperm hosts. This clade is further divided into two clusters, including six species. Cluster C.1 (99%, 1.00; Fig. 6) corresponds to *G. neojaponicum* Imazeki and comprises eight sequences representing 10 entries from material originating from China, Laos, Myanmar and Taiwan. The taxon is characterised by a rather high sequence heterogeneity as evidenced by the respective intraspecific similarity (97.51 ± 1.44%) and genetic distance values (0.019 ± 0.009); variability in their ITS sequences is expressed by at least four to seven different positions in ITS1 and one to eight in ITS2 (Suppl. material 3: Fig. S1).

Cluster C.2 is strongly supported (100%, 1.00; Fig. 6) and it is composed of 23 sequences corresponding to 42 entries. It is further divided into two sister groups. One of them represents *G. aridicola* J.H. Xing & B.K. Cui and consists of sequences from specimens collected in Cameroon and South Africa growing on a large range of gymnosperms and angiosperms (Table 1; Fig. 6). The *G. aridicola* type material of South African origin grouped together with sequences provisionally labelled "Group 3" and "Group 4" by Kinge et al. (2012) by showing high intraspecific similarity (99.52 ± 0.19%). In addition, four GenBank entries, corresponding to what Kinge et al. (2012) named "Group 5" (JN105713 and JN105714) and "Group 6" (JN105715 and JN105716), formed two distinct well-supported subclades (82%, 1.00 and 100%, 1.00, respectively; Fig. 6). The former ("Group 5") derives from material isolated on oil palm trees in Lobe (Cameroon) and is well separated from *G. aridicola* on the basis of both genetic distance and sequence similarity values (0.024 ± 0.002 and 96.29 ± 0.48%, respectively); therefore, it is considered as a distinct phylospecies and is hereby designated as "*Ganoderma* sp. C1" (corresponding to the UNITE DOI SH1723198.08FU). Similarly, sequences of "Group 6" originating from Cameroon as well, are also distantly placed from *G. aridicola* (genetic distance and sequence similarity values are 0.042 ± 0.002 and 94.48 ± 0.23%, respectively). Therefore, they are considered to represent a new phylogenetic species provisionally named "*Ganoderma* sp. C2" (corresponding to the UNITE DOIs SH1843092.08FU and SH1843096.08FU). The three taxa compose a well-supported subgroup (97%, 1.00; Fig. 6).

The other group (100%, 1.00; Fig. 6) within Cluster C.2 is formed by *G. enigmaticum*, M.P.A. Coetzee, Marinc., M.J. Wingf., *G. thailandicum* Luangharn, P.E. Mortimer, Karun. & J.C. Xu and *G. casuarinicola* J.H. Xing, B.K. Cui & Y.C. Dai. The former two are represented by six sequences from South Africa, Ghana and the Ivory Coast (including the type material of *G. enigmaticum*), as well as by two identical sequences from Thailand (type material of *G. thailandicum*) showing high sequence similarity (i.e. 99.55 ± 0.37%), which indicates that the Asian and African specimens do not correspond to two phylospecies on the basis of ITS data alone. However, the two taxa are maintained as distinct on the basis of the outcome of a multigene analysis of pertinent material (Luangharn et al. 2019b). On the other hand, *G. casuarinicola* is adequately supported (71%; Fig. 6) and here represented by 63 entries deriving from material (including the type specimen) originating mainly from India, Sri Lanka and China isolated from a large diversity of host plants; only four sequences were identified under this name, whereas the majority (47) were deposited as *Ganoderma* sp.

(Table 1). In addition, sequence similarity values of *G. enigmaticum – G. thailandicum* vs. *G. casuarinicola* (98.97 ± 0.36) are indicative of their high affinity since overlapping intra- (e.g. 99.16 ± 0.42% within *G. casuarinicola*) and interspecific values are obtained; hence, a barcoding gap is absent between them (Fig. 8).

Clade D

Clade D includes 291 sequences representing 449 individual entries separated into four clusters (Suppl. material 7: Fig. S2e); Cluster D.1 is evolutionary distant from Clusters D.2 to D.4 which jointly form a well-supported subclade (70%, 1.00; Fig. 6). Specimens present a tropical/subtropical distribution and originate from both Hemispheres excluding Europe, on angiosperm and gymnosperm hosts (Table 1, Suppl. material 7: Fig. S2e). Clade D is composed of laccate and partly laccate to dull taxa, which are morphologically distinguished from species grouped in Clade A by differences in spore shape (oblong-ellipsoid to ellipsoid, finely echinulate) and/or shape of cuticle cell (often irregular, clavate or cylindrical, with blunt outgrowths or protuberances or slight branches) and by darker pilei and/or context colour. Moreover, taxa placed in Clade D do not produce chlamydospores.

Clade D – Cluster D.1

Cluster D.1 is placed at the base of Clade D and it is strongly supported (98%, 1.00; Fig. 6). It consists of five sequences corresponding to eight entries; two entries are under the name *G. mbrekobenum* E.C. Otto, Blanchette, Held, C.W. Barnes & Obodai from Ghana (including the type material representing a laccate stipitate taxon; Otto et al. 2016), while the rest originated from Asia (India and Sri Lanka; Fig. 6) on a broad range of plant hosts and were deposited as *Ganoderma* sp. Similarly, good support for Cluster D.1 was obtained when additional (23) singletons/sequences were included in the analysis (99%, 1.00; Suppl. material 7: Fig. S2e, Suppl. material 1: Table S2); this larger sample-set presented intraspecies sequence similarity of 98.65 ± 0.70%. Although two or more subgroups are formed within this species (Fig. 6 and Suppl. material 7: Fig. S2e), ITS similarity and genetic distance values do not adequately support their distinct status; therefore and in the absence of additional data, we prefer to maintain a single species (i.e. *G. mbrekobenum*) in Cluster D.1.

Clade D – Cluster D.2

Cluster D.2 comprises two distantly-related species, i.e. *G. sinense* Zhao, Hsu & Zhang (Zhao et al. 1979b) and *G. nasalanense* Hapuar., Pheng. & K.D. Hyde (Hapuarachchi et al. 2019). The monophyletic *G. sinense* (100%, 1.00; Fig. 6) includes 26 sequences representing 66 entries deriving from Chinese material plus four collections from Thailand and a single collection from Taiwan (Suppl. material 1: Table S2). Most of them were labelled as *G. sinense* (45), while six were deposited under the names "*G. japonicum*", "*G. formosanum*" and "*G. atrum*". This finding is in accordance with reports

advocating synonymy of *G. sinense* and *G. japonicum* (Fr.) Sawada (Liao et al. 2015; Wang and Yao 2005), whose authors examined specimens from China only. Therefore, in the absence of material from the type locality (Japan), a definite conclusion cannot be drawn regarding the status of *G. japonicum*. In addition, the sole sequence available under the name *G. atrum* Zhao, Hsu & Zhang (JQ886403; China, Hainan Island) grouped together with *G. sinense* in the present phylogeny. Similarly, a sequence (the joinder of X78752 and X78773) from a specimen originally identified as *G. formosanum* T.T. Chang & T. Chen was also positioned within *G. sinense*. On the other hand, *G. nasalanense* is strongly supported (98%, 1.00; Fig. 6) and includes two identical sequences (one from the type material) from Laos plus 13 entries from specimens collected in India, Malaysia and Vietnam, initially labelled as "*G. australe*", *Ganoderma* sp. and "uncultured soil fungus" (Table 1, Suppl. material 7: Fig. S2e). Sequence similarity and genetic distance values support the distinct phylogenetic status of *G. nasalanense* with respect to *G. sinense* as evidenced by the clear barcoding gap they exhibit (94.17 ± 0.55% and 0.051 ± 0.002, respectively; Fig. 8).

Clade D – Cluster D.3

Cluster D.3 is well supported (75%, 1.00; Fig. 6) and includes four species. One corresponds to *G. cupreum* (Cooke) Bres. described on the basis of material collected in Africa and is represented by eight entries; three of them originate from Cameroon, one (deposited as "*G.* cf. *cupreum*") from South Africa, one as "*G. chalceum*" (originating from Tanzania on the basis of the respective submission's title), one environmental sample from Gabon and one of unknown origin, while a "*G. australe*" entry from Malaysia was placed at the base of the subclade. We maintain the name *G. cupreum* (since it has priority over *G. chalceum*) for the respective phylogenetic species, which forms a well-supported clade (99%, 1.00; Fig. 6) presenting high intraspecific values for sequence similarity (99.61 ± 0.21%) and low for genetic distance (0.004 ± 0.002).

Another terminal subclade is composed of nine entries (98%, 1.00; Fig. 6); five of them were originally deposited as *G. ecuadoriense* W.A. Salazar, C.W. Barnes & Ordóñez (three from Ecuador, including the type specimen and two from Brazil), one as *G. subfornicatum* Murrill, two as *Ganoderma* sp. (Brazil and Peru) and one labelled as "uncultured fungus" (Suppl. material 1: Table S2). The latter is the only one not originating from the Neotropics and derives from soil sampled in India (KJ411557). Material labelled as *G. subfornicatum* was identified as *G. orbiforme* (Fr.) Ryvarden (Ryvarden and de Meijer 2002) and, hence, the former was not included in a subsequent study of Ryvarden (2004) on neotropical polypores. On the other hand, Torres-Torres et al. (2012) treated *G. subfornicatum* and *G. orbiforme* as distinct taxa despite their being very similar in morphology. In addition and in the context of the present study, it was evidenced that the sole sequence available under the name *G. subfornicatum* (JX082352, French Guiana) was placed within the same terminal clade as sequence KU128524 representing the holotype of *G. ecuadoriense*. The latter is a recently-described species from Ecuador (Salazar et al. 2016); however, although those authors

conducted a morphological and molecular study on their material, they did not include specimens of *G. subfornicatum*, which commonly occurs in the same larger area (type material from Belize) (Welti and Courtecuisse 2010; Torres-Torres et al. 2012). On the basis of the previously-presented information, *G. subfornicatum* is maintained to describe this terminal subclade (although only one sequence is available under this name in GenBank) and "*G. ecuadoriense*" is abandoned as nom. illeg.

Five sequences, representing *G. orbiforme*, form a well-supported terminal group (89%, 0.96; Fig. 6) which, however, presents high affinity to the sister clade of *G. subfornicatum* (100%, 0.96; Fig. 6), as is evidenced by the absence of a barcoding gap in the pairwise comparison of the two taxa (genetic distance and sequence similarity: 0.011 ± 0.002 and 98.69 ± 0.23%, respectively). *G. orbiforme* was originally described from Guinea, but was also reported from South America (Ryvarden 2000; Baltazar and Gibertoni 2009; Gomes-Silva et al. 2011; Torres-Torres et al. 2012). Although none of these studies included molecular data, in some of them (e.g. Ryvarden 2000; Torres-Torres et al. 2012), the type specimen of *G. orbiforme* was examined alongside *Ganoderma* basidiomes from the Neotropics to assess the identity of the latter. Moreover, four sequences from Brazilian specimens identified as *G. orbiforme* (de Lima Júnior et al. 2014) were grouped within this particular subclade. Therefore, we believe that *G. orbiforme* is the correct name for this phylogenetic species which occurs in the Neotropics. The use of this name for material originating from Asia and Australia (Wang et al. 2014; Hapuarachchi et al. 2019) is not supported by molecular evidence and erroneous conclusions could be attributed to the high morphological variability of specimens belonging to closely-related taxa of Cluster D.3, for example, *G. mastoporum* and *G. orbiforme* (Fig. 6).

Finally, a well-represented and supported terminal subclade of Cluster D.3 (80%, 1.00; Fig. 6) includes 122 entries (95 of them are singletons; Suppl. material 1: Table S2) deriving from specimens collected in southeast Asia and Australia mainly on eudicot angiosperms. It consists of sequences deposited under the names *G. mastoporum* (12), "*G. orbiforme*" (19), "*G. cupreum*" (10), "*G. fornicatum*" (3), "*G. multicornum*" (1) and *Ganoderma* sp. (11), as well as under "*G. australe*" (60, resulting from a single study conducted on material originating from Borneo). On the basis of what was previously mentioned about the correct phylogenetic position of *G. orbiforme* and although sequences labelled as "*G. orbiforme*" deriving from China were included under this name in previous studies (Wang et al. 2014; Hapuarachchi et al. 2018b; Xing et al. 2018), we believe that relevant material originating from southeast Asia and Oceania corresponds to *G. mastoporum* (Lév.) Pat. (initially described on the basis of material collected in Singapore) and that the 12 *G. mastoporum* entries in this particular subclade of Cluster D.3 were correctly identified. Therefore, *G. mastoporum* cannot be considered as a synomym of *G. orbiforme* (as stated in MycoBank and Index Fungorum) since the latter name corresponds to a related – yet distinct – phylogenetic species (interspecific sequence similarity and genetic distance values: 97.34 ± 0.49% and 0.025 ± 0.005, respectively). Similarly, *G. mastoporum* and *G. cupreum* could be separated on the basis of the outcome of the present study because they form distinct well-supported terminal

groups (Fig. 6, Suppl. material 7: Fig. S2e) presenting interspecific sequence similarity of 97.20 ± 0.45%. One entry, labelled as *G. multicornum* (MT772000, Suppl. material 1: Table S2; Suppl. material 7: Fig. S2e), shows relatively high affinity (genetic distance: 0.012 ± 0.008, sequence similarity: 98.65 ± 0.70%) with the rest of the entries within the *G. mastoporum* clade (Fig. 6, Suppl. material 7: Fig. S2e).

Clade D – Cluster D.4

Cluster D.4 is strongly supported (93%, 1.00; Fig. 6) and is further divided into two sister groups, i.e. Group D.4.1 and D.4.2; the former includes species collected on angiosperms and gymnosperms, while the latter, the so-called "palm group", comprises sequences from material mostly associated with monocotyledons.

Group D.4.1 (87%, 1.00; Fig. 6) includes the recently-introduced sessile and laccate *G. angustisporum* J.H. Xing, B.K. Cui & Y.C. Dai reported from China on *Casuarina equisetifolia* (Xing et al. 2018). Moreover, sequences from specimens of different origin (India, Malaysia and Australia, labelled as "*G. australe*" and *Ganoderma* sp.; Table 1) growing on other eudicots also nested together with *G. angustisporum* and present high intraspecific similarity values (99.07 ± 0.43%), thus largely expanding the known distribution of this species and the number of host plant taxa it is associated with (Table 1, Suppl. material 7: Fig. S2e). A closely-related entity to *G. angustisporum* is found as a terminal subgroup (100%, 1.00; Fig. 6) and it includes two singletons initially labelled as "*G. applanatum*" from material collected in Africa (Gabon) on eudicots. It presents genetic distances and sequence similarity values of 96.87 ± 1.21% and 0.027 ± 0.004, respectively, vs. *G. angustisporum*. It is therefore considered as a new phylogenetic species and is provisionally labelled as "*Ganoderma* sp. D1" (corresponding to the UNITE DOIs SH1740449.08FU and SH1740450.08FU).

Group D.4.2 (91%, 1.00; Fig. 6) is composed of five species comprising material originating mainly from monocot angiosperms. Three of them are distinguished by a clear barcoding gap (Fig. 8) and form a well-supported terminal subclade (79%, 0.99, Fig. 6). *G. zonatum* Murill (100%, 1.00; Fig. 6 and Suppl. material 7: Fig. S2e) consists of 84 correctly-labelled entries with high similarity values (99.86 ± 0.08%), originating from specimens growing on palms in southeast USA. *G. ryvardenii* Tonjock & Mih (100%, 1.00; Fig. 6) is represented by 22 entries mainly deriving from Cameroon (including the sequence from the type material, Table 1). Moreover, four entries, labelled as *Ganoderma* sp. from Colombia, form a distinct strongly-supported clade (100%, 1.00; Suppl. material 7: Fig. S2e) representing, thus, a new phylogenetic species provisionaly named *Ganoderma* sp. D2 (corresponding to the UNITE DOI SH1723113.08FU).

The other two species comprise material from Asia only; the 'core' part corresponds to *G. boninense* Pat. and it is represented by 69 entries deposited as *G. boninense* (32), "*G. miniatocinctum*" (3), "*G. orbiforme*" (2), "*G. zonatum*" (3) and *Ganoderma* sp. (29) (Table 1; Fig. 6). The rest of the entries form a terminal subgroup with strong support (98%, 1.00; Fig. 6) and includes material originating from Indonesia. This material

was originally identified to genus level only (12 entries, labelled as *Ganoderma* sp.; Table 1). Sequence similarity and genetic distance values vs. *G. boninense* (97.30 ± 0.67% and 0.029 ± 0.006, respectively) are indicative of the presence of a new phylogenetic species, provisionally named *Ganoderma* sp. D3 (corresponding to the UNITE DOIs SH1723050.08FU and SH1723098.08FU).

On the basis of the results presented above, it is apparent that *G. zonatum* is not related to *G. sessile* (the latter forms part of Cluster A.2), as previously reported by Gottlieb et al. (2000); the former name was misapplied to a specimen originating from Argentina. Neither *G. zonatum* nor *G. boninense* forms part of the *G. lucidum* complex (Zhou et al. 2015) since they are distinctly positioned into Clade D (Fig. 4). In addition, three sequences available under the name *G. miniatocinctum* Steyaert are grouped together with *G. boninense* material.

Clade E

Clade E is strongly supported (81%, 1.00; Fig. 7). It includes 98 unique sequences representing 393 individual entries (or 367 sequences representing 664 individual entries; Suppl. material 8: Fig. S2f) and comprises 15 well-supported phylospecies (Table 1). The respective material presents a worldwide distribution and originates from angiosperm and gymnosperm hosts (Table 1 and Suppl. material 1: Table S2 and Suppl. material 8: Fig. S2f). Clade E is further subdivided into five Clusters (E.1 to E.5) and includes sequences from specimens that are characterised by sessile and perennial basidiomes, mostly dull and less often laccate (e.g. Cluster E.3). In addition, their pileal crust does not appear as a regular palisade, often consisting of a mixture of randomly orientated, branched arboriform skeletal hyphae and a degenerated palisade of irregular generative hyphal ends. The latter are usually embedded in a resinous matrix which may become very thick in aged basidiomes, making the examination of crust anatomy practically impossible. The presence of species producing either laccate or non-laccate pilei evidences that this particular morphological trait, widely used for grouping *Ganoderma* taxa at the subgeneric level, is not in congruence with phylogenetic data.

Clade E – Cluster E.1

Cluster E.1 corresponds to a single strongly-supported phylospecies (99%, 1.00; Fig. 7) distinctly placed at the base of Clade E. It includes material from tropical/subtropical Asia which is mainly associated with the name "*G. australe*" (29 entries) (Table 1); however, *G. williamsianum* Murrill. (7) is the correct name to assign to this terminal group since relevant descriptions and reported occurrence (Steyaert 1972; Corner 1983; Wang and Wu 2010; Xing et al. 2018) are in agreement with the phylogenetic position presented here. In addition, *G. williamsianum* presents high intraspecific similarity values (99.47 ± 0.22%) despite the large number of entries examined and their rather wide geographic origin. Cluster E.1 corresponds to 'clade 8' of the phylogeny presented by Moncalvo and Buchanan (2008).

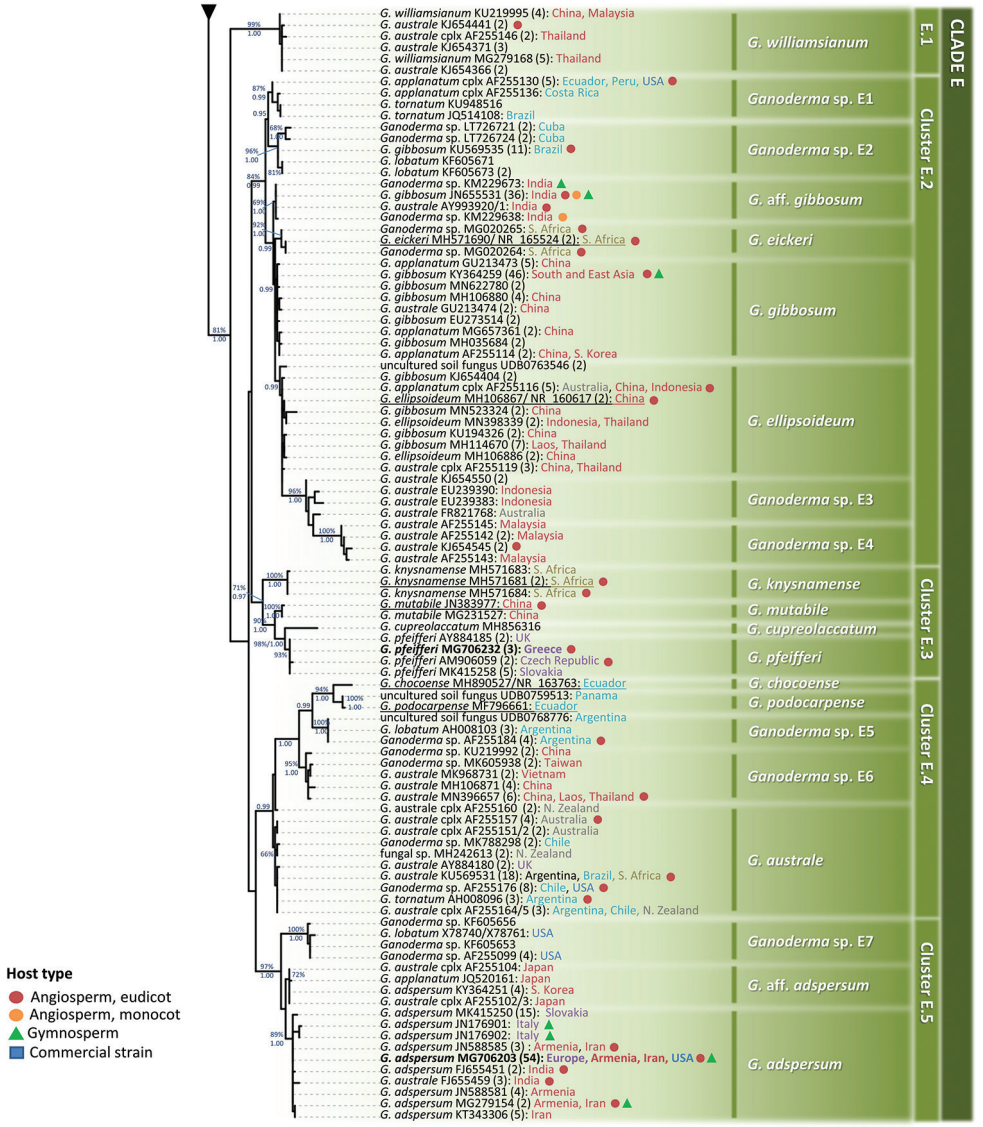

Figure 7. Detail from Fig. 3. Phylogenetic reconstruction of the genus *Ganoderma* inferred from ML analysis, based on ITS sequence data (main dataset, DS; Table 2) for Clade E. ML bootstrap values (BS) ≥ 65% and Bayesian Posterior Probabilities (BPP) ≥ 0.95 are shown. Sequences names on the left appear as initially labelled and are followed by the respective GenBank/ENA/DDBJ or UNITE accession number, while the total number of identical entries corresponding to a particular sequence is placed in parentheses, followed by the type of host plant (legend for the coloured shapes is found at the lower left side of tree) and geographic origin of the respective material (the latter appears in different fonts colour depending on the continent of provenance; see also Table 1 and Suppl. material 1: Table S2). Species names on the right correspond to those inferred in this study evaluated in conjunction with literature data. Sequences generated in the present work appear in bold typeface, while underlined sequences are those originating from type material. Scale bar: 0.01 nucleotide substitutions per site.

Clade E – Cluster E.2

Cluster E.2 (84%, 0.99; Fig. 7) includes 43 sequences representing 176 entries (or 177 sequences deriving from 310 entries in the expanded dataset; Suppl. material 8: Fig. S2f). It consists of seven phylogenetic species, two of which have a neotropical distribution (including USA) while the rest occur in Asia, Africa and Oceania (Table 1).

A well-supported terminal subclade (87%, 0.99; Fig. 7) is formed by 23 entries with high intraspecific sequence similarity (99.64 ± 0.23%, min. 99.11%) deriving from material originating from the Neotropics on eudicots under various names, i.e. "*G. tornatum*" (6), "*G. lobatum*" (3), "*G. parvulum*" (1), "*G. gibbosum*" (1), "*G. applanatum* complex" (8) and *Ganoderma* sp. (4) (Table 1 and Suppl. material 1: Table S2). Since some of these names are in use for other sequences examined in this study (positioned in other Clades/Clusters, for example, as is the case for *G. parvulum* and *G. lobatum*), while for others there is not adequate evidence to support their correct use in this particular case (e.g. *G. tornatum*), we prefer to label this distinct phylogenetic entity as *Ganoderma* sp. E1 (corresponding to the UNITE DOI SH1723047.08FU). This species corresponds to 'clade 7' in the study of Moncalvo and Buchanan (2008). As is the case elsewhere in the present study, properly/accurately identified type material (representing one or more of the taxa whose names appear in this subclade) needs to be sequenced in order to arrive at robust conclusions regarding the real identity of this particular phylospecies.

A strongly-supported (96%, 1.00; Fig. 7) sister group to the previous phylospecies consists of 37 sequences deriving from specimens collected in South and Central America, as well as in the USA (Florida) on a wide range of host-plants, for example, *Cenostigma pluviosum* var. *peltophoroides*, *Inga vera*, *Jacaranda mimosifolia*, *Leucaena leucocephala* and *Elaeis guineensis*. These sequences, initially deposited under various names (i.e. "*G. gibbosum*" (12), "*G. tornatum*" (8), "*G. lobatum*" (7), "*G. australe*" (2) and "*G. applanatum* complex" (2)), are hereby placed under the name *Ganoderma* sp. E2 (corresponding to the UNITE DOI SH1723047.08FU). We believe that accurate association of this species to any established *Ganoderma* taxon name is not possible until additional information – through the study of relevant type material – becomes available. Although *Ganoderma* sp. E1 and *Ganoderma* sp. E2 demonstrate relatively-high sequence similarity and rather low genetic distances in pairwise comparisons (97.73 ± 0.54% and 0.017 ± 0.005, respectively), there is no overlap between the respective intra- and interspecies values; their distinct species status is therefore proposed.

Cluster E.2 also includes a large terminal subclade (65%, 1.00; Suppl. material 8: Fig. S2f) comprising material from Asia, Africa and Oceania. Clade E.2 corresponds to the *G. gibbosum* complex and consists of (at least) five species, i.e. *G. gibbosum* (Blume & T. Nees) Pat., the recently introduced *G. eickeri* Tchotet, M.P.A. Coetzee, Rajchenb. & Jol. Roux, *G. ellipsoideum* Hapuar., T.C. Wen & K.D. Hyde, as well as two new phylospecies (*Ganoderma* sp. E3 and *Ganoderma* sp. E4). *G. gibbosum* is composed of 107 entries (40 of which are singletons) labelled mainly under the names *G. gibbosum* (59), "*G. applanatum*" (27) and "*G. australe*" (8) (Suppl. material 1: Table S2 and Sup-

pl. material 8: Fig. S2f). It shows low intraspecific sequence variability (sequence similarity: 99.58 ± 0.17%; genetic distance: 0.004 ± 0.002). A distinct entity, here called *G.* aff. *gibbosum*, is exclusively composed of sequences of Indian origin (51 entries including 10 singletons; 69%, 1.00; Fig. 7) which are mainly deposited as *Ganoderma* sp. However, the relatively-high affinity exhibited by sequences of *G.* aff. *gibbosum* vs. other *G. gibbosum* sequences from Asia (sequence similarity and genetic distance values: 99.04 ± 0.27% and 0.009 ± 0.002, respectively) prevents us from considering it as a distinct phylospecies, at least until further evidence becomes available.

The other terminal clade (92%, 1.00; Fig. 7) represents the recently-introduced *G. eickeri* consisting of four entries, including the type material, which originate from South Africa on angiosperms (Tchotet Tchoumi et al. 2019). However, on the basis of the ITS data evaluated in this study, *G. eickeri* appears closely related to *G. gibbosum* (interspecific sequence similarity and genetic distance values: 98.90 ± 0.25% and 0.011 ± 0.003, respectively).

G. ellipsoideum is a recently-described species from Hainan Island, China (Hapuarachchi et al. 2018b). It is here represented by 81 entries corresponding to 10 ASVs and 44 singletons (0.99; Fig. 7). Sequences within the *G. ellipsoideum* subclade (including the one from the type material) were mainly labelled as "*G. gibbosum*" (22), "*G. australe*" (10), "*G. australe* cplx" (10), "*G. applanatum*" (5) and *Ganoderma* sp. (10); they originate from material of broad geographic distribution (south and east Asia, Oceania) on eudicots. In addition, this study revealed that two environmental samples deriving from the USA (UDB0769802 and UDB0763546) formed part of this terminal subclade. As in the case of *G. eickeri*, *G. ellipsoideum* is closely related to *G. gibbosum* (sequence similarity and genetic distance values: 98.84 ± 0.19% and 0.012 ± 0.002, respectively) and no barcoding gaps were detected with respect to the closest related species (i.e. *G. gibbosum* and *G. eickeri*; Fig. 8); therefore, its distinct phylogenetic status is questionable on the basis of ITS data. *G. gibbosum* and *G. ellipsoideum* correspond to 'clade 5' of the phylogeny presented by Moncalvo and Buchanan (2008).

The other two phylogenetic species appearing on the terminal subclade of Cluster E.2 (96%, 1.00; Fig. 7) are hereby designated as *Ganoderma* sp. E3 (corresponding to the UNITE DOIs SH1723116.08FU and SH1723270.08FU) and *Ganoderma* sp. E4 (corresponding to the UNITE DOI SH1677211.08FU); both demonstrate high intraspecific sequence similarity values (> 99.31%). The former consists of six sequences deposited as "*G. australe*" deriving from Indonesian and Australian material. The latter species (100%, 1.00; Fig. 7) corresponds to 'clade 6' in the study of Moncalvo and Buchanan (2008) and includes 13 entries from specimens originating from Malaysia and Indonesia on eudicots, which were also labelled "*G. australe*" (Table 1). Both species are well separated from each other (*Ganoderma* sp. E3 vs. *Ganoderma* sp. E4: 94.67 ± 1.02% and 0.030 ± 0.006 for sequence similarity and genetic distance values, respectively), as well as from the rest of the species within Cluster E.2, for example, *Ganoderma* sp. E3 vs. *G. ellipsoideum*: 96.84 ± 1.01% and 0.025 ± 0.006, respectively.

Clade E – Cluster E.3

Cluster E.3 consists of material corresponding to the laccate taxa *G. pfeifferi* Bres. (17 sequences from Europe only; Table 1), *G. cupreolaccatum* Kalchbr. ex Z. Igmándy (invalid name, type locality: Hungary), *G. mutabile* Cao & Yuan (two sequences from China, including one from the type specimen) and the recently-introduced *G. knysnamense* Tchotet, M.P.A. Coetzee, Rajchenb. & Jol. Roux (four entries from South Africa, including the type; Tchotet Tchoumi et al. 2019), which were adequately supported (71%, 0.97; Fig. 7). Amongst them, *G. knysnamense* is placed at the base of this cluster (100%, 1.00; Fig. 7) and is well separated from the closest species (i.e. *G. mutabile*: 0.036 ± 0.001 and 96.43 ± 0.13%). Furthermore, *G. pfeifferi* and *G. mutabile* are placed on well-supported terminal subclades (90%, 1.00; Fig. 7) and they both present high intraspecific similarity (> 99.84%); however, the respective interspecific values in pairwise comparisons are indicative of their affinity (98.14 ± 0.19%, 0.019 ± 0.005; Fig. 8). *G. mutabile* was introduced as a distinct species after examining only one collection which, according to its authors (Cao and Yuan 2013), resembles *G. pfeifferi* with respect to the dark brown context and the similar spore size; however, it differs by its laccate crust and non-stratified tubes. The other noteworthy sequence within Cluster E.3 derives from a specimen identified as *G. cupreolaccatum*, which was previously considered as a facultative (heterotypic) synonym of *G. pfeifferi* (Mycobank). However, both similarity and genetic distance values of this particular sequence vs. *G. pfeifferi* are indicative of a distinct species (i.e. 94.97 ± 0.17% and 0.030 ± 0.007, respectively). Still, the variability of this unique sequence is located exclusively at the beginning of ITS1, a region generally conserved between closely-related taxa of the genus (Nilsson et al. 2017), while the rest is identical to those of *G. pfeifferi*. Therefore, questions are raised about the quality of this particular sequence and no definite conclusions could be drawn concerning the exact status of *G. cupreolaccatum*.

The close phylogenetic position of *G. pfeifferi* and *G. adspersum* (Schulzer) Donk (Cluster E.5) is congruent with their similar pileus dark-brown context and the complex structure of the crust in contrast to the normal palisade appearance in laccate species of Clade A (Hansen 1958; our observations); still, *G. pfeifferi* clearly differs by the laccate pileus and the width and quotient of spores (Ryvarden and Gilbertson 1993; Niemelä and Miettinen 2008; Ryvarden and Melo 2017). In addition, these characteristics, in conjunction with the cracked/wrinkled resinous layer on the pileus, distinguish *G. pfeifferi* from specimens of *G. lucidum* and *G. resinaceum* (Ryvarden and Gilbertson 1993). Furthermore, the outcome of the present study evidences the grouping of *G. pfeifferi* within Clade E and contrasts previous reports by Hseu et al. (1996) and Cao and Yuan (2013), which linked this taxon with the *G. lucidum* complex and *G. resinaceum*, respectively. This discrepancy is apparently due to an initial misidentification of strain CBS 747.84 (sequences X78738/ X78759) which was labelled as "*G. pfeifferi*" instead of *G. resinaceum* (Moncalvo et al. 1995a).

Clade E – Cluster E.4

Cluster E.4 (0.99; Fig. 7, and 82%, 1.00; Suppl. material 8: Fig. S2f) includes five species represented by sequences from material with a world-wide distribution (apart from Europe) occurring on angiosperms. A well-supported subgroup within this cluster is formed by the recently-introduced *G. chocoense* J.A. Flores, C.W. Barnes & Ordoñez, including only the sequence from the type material (Ecuador; Flores et al. 2018) and *G. podocarpense* J.A. Flores, C.W. Barnes & Ordoñez (Flores et al. 2017), consisting of two sequences from Ecuador and Panama. Despite their overlapping distribution range, the values of sequence similarity (97.57 ± 0.13%) and genetic distance (0.025 ± 0.003) are indicative of their distinct status at species level.

A sister group to the former (1.00; Fig. 7 and 95%, 1.00; Suppl. material 8: Fig. S2f) is composed of eight sequences originating from Argentinian material under the names "*G. lobatum*", "*G. tornatum*" and *Ganoderma* sp. (Table 1). On the basis of the information available, it is not possible to assign a particular taxonomic name to these sequences. Therefore, we prefer to designate this phylogenetic species as *Ganoderma* sp. E5 (corresponding to the UNITE DOI SH1678465.08FU) (100%, 1.00; Fig. 7). The latter entity is well separated from *G. podocarpense*, i.e. sequence similarity: 95.58 ± 0.59% and genetic distance: 0.044 ± 0.006.

A sister terminal subclade to the previous group (*G. chocoense*, *G. podocarpense* and *Ganoderma* sp. E5) consists of sequences originating from material collected in south and southeast Asia, while a single sequence indicates its presence also in Papua New Guinea (95%, 1.00; Fig. 7). They are labelled mainly as "*G. australe*" (19), "*G. applanatum*" (2) and *Ganoderma* sp. (8) (Table 1). Again, none of the initially-assigned names could be maintained; therefore, we refer to this distinct phylogenetic species as *Ganoderma* sp. E6 (corresponding to the UNITE DOI SH1723070.08FU) presenting low interspecific sequence similarity and high genetic distance vs. *Ganoderma* sp. E5 (i.e. 95.59 ± 0.70% and 0.040 ± 0.006, respectively). *Ganoderma* sp. E5 and *Ganoderma* sp. E6 appear as sister subclades in 'clade 4' of the phylogeny presented by Moncalvo and Buchanan (2008). Moreover, a single sequence (AF255183; Suppl. material 1: Table S2 and Suppl. material 8: Fig. S2f), originating from New Zealand, seems to correspond to a distinct entity, which however does not fulfil the criteria set in this study to merit recognition as a *Ganoderma* phylospecies (genetic distance and sequence similarity values vs. *Ganoderma* sp. E6: 0.017 ± 0.002 and 98.27 ± 0.18, respectively).

Finally, a distinct group included 80 entries deriving from specimens mainly from southeast Asia, South America and Oceania, as well as from central/north America and South Africa. That said, one sequence originated in the vicinity of the Kew Botanical Gardens, UK, such that we suspect it to have been imported with plant material. These sequences were mostly deposited as "*G. australe*" (27), "*G. australe* complex" (14) and *Ganoderma* sp. (13). Despite the widespread use of the "australe" epithet to describe several entities (14) placed in other terminal clades of the present study, we believe that this particular terminal group coincides with *G. australe* (Fr.) Pat. after evaluating all available ITS sequence data, the geographic distribution of specimens analysed

and pertinent publications (Ryvarden and Gilbertson 1993; Moncalvo and Ryvarden 1997; Moncalvo and Buchanan 2008). As regards sequence similarity, intraspecific values are notably high (99.56 ± 0.25%) considering the diverse geographic origin of the respective material, whereas interspecific values to the closest taxon is low (i.e. *Ganoderma* sp. E6; 95.04 ± 0.66%). Although ambiguities exist about the exact distribution range of *G. australe* (Yeh and Chen 1990; Buchanan and Wilkie 1995; Moncalvo and Ryvarden 1997; Smith and Sivasithamparam 2000) and the type specimen originating from the Pacific area is lost, this appears to be the most common *Ganoderma* species throughout the tropics and subtropics and corresponds to 'clade 3' in the study of Moncalvo and Buchanan (2008).

Clade E – Cluster E.5

Cluster E.5 (97%, 1.00; Fig. 7) comprises sequences from specimens originating from the Northern Hemisphere and it is further divided into two well-supported subclades. One corresponds to a new phylogenetic species hereby designated as *Ganoderma* sp. E7 (corresponding to the UNITE DOI SH1723077.08FU), which is composed of 17 entries (100%, 1.00; Fig. 7) deposited under the name "*Ganoderma* sp.", "*G. lobatum*" and "*G. applanatum* cplx" deriving from US material only (intraspecific sequence similarity: 98.83 ± 0.90%; interspecific sequence similarity vs. *G. adspersum*: 95.29 ± 0.51%). "*Ganoderma* sp. E7" forms part of 'clade 2' in the phylogeny presented by Moncalvo and Buchanan (2008).

A sister subclade to the aforementioned clade corresponds to *G. adspersum* sensu lato and is represented by 155 entries deriving from Europe, south and west Asia and North Africa (1.00; Suppl. material 8: Fig. S2f). *G. adspersum* (Schulzer) Donk is a common species in the Palearctic realm; in Europe, it is usually reported on a wide range of angiosperms (Ryvarden and Gilbertson 1993), but it also appears on gymnosperms (i.e. *Abies cephalonica*; Zervakis et al. 1998; this study). Most of the sequences (117) examined in this study were properly identified as *G. adspersum*. However, several misidentifications were noted, mainly for Asian material labelled as "*G. applanatum*", "*G. australe*" and "*G. australe* complex" (Suppl. material 1: Table S2). In fact, *G. adspersum* was considered as a synonym of *G. australe* (Ryvarden 1976; Ryvarden and Gilbertson 1993; Ryvarden and Melo 2017), but ITS sequence data clearly separated it from *G. australe*. The outcome of this study reveals that *G. adspersum* includes specimens with a distribution ranging from Europe to India (89%, 1.00; Fig. 7). Moreover, nine entries from samples, originally identified as *G. adspersum*, "*G. australe* complex", "*G. applanatum*" and "uncultured fungus" (China, Japan and South Korea; Suppl. material 1: Table S2), form a distinct terminal subgroup (72%; Fig. 7), which is hereby named *G.* aff. *adspersum* on the basis of its close affinity to *G. adspersum* (i.e. sequence similarity and genetic distance values: 98.47 ± 0.33% and 0.013 ± 0.004, respectively).

In conclusion, the plasticity of morphological characters and substantial overlap of alleged diagnostic features is prevalent in the 'dull' taxa of this group; consequently, their taxonomic significance is dubious. Moreover, the massive, heavily-agglutinated

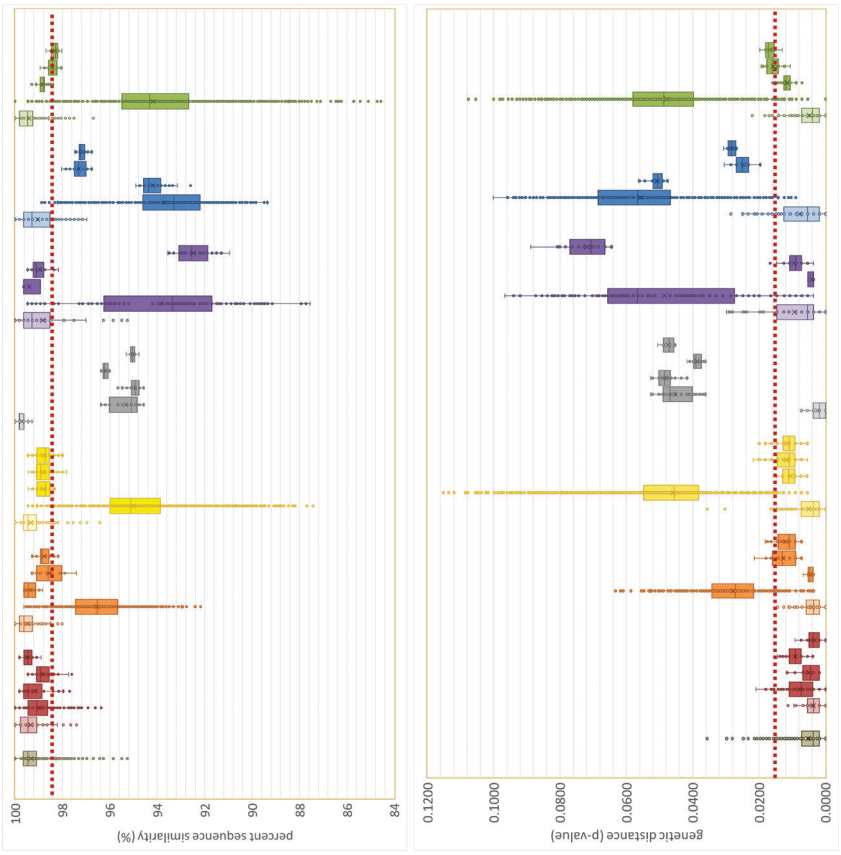

Figure 8. Box plots of **a** ITS sequence similarity (%) and **b** genetic distances (p-values) within (intra) and between (inter) *Ganoderma* species for each one of the main lineages (Clades/Clusters) of the genus, as well as pairwise comparisons between selected species. The size of each box represents 50% of the values, the black horizontal line within each box indicates the median, the 'x' represents the average value, the error bars represent interquartile ranges and circles indicate outliers. The red-dotted horizontal line, transversing the plots, represents the value levels accepted in this study for proposing new phylogenetic species.

matrix of the pileal crust in such non-laccate species often obstructs observation of discriminating features in pileal elements. The situation is further aggravated by the loss of type material of widely and commonly used species names (e.g. *G. australe* and *G. gibbosum*), the absence of (correct) neo-typification (as there are ambiguous synonymies regarding several taxa) and unclear species descriptions (e.g. *G. tornatum* and *G. lobatum*). All of the above could explain the obstacles which prevented the establishment of a stable classification system for species of Clade E. Still, the highly variable morphology of basidiomes and the ITS divergence are indicative of underestimated diversity and the presence of cryptic species is quite certain as is also indicated by the outcome of the present study.

Variation in ITS spacers of *Ganoderma* sequences

As determined from the analysis performed in this study, the combined length of the two spacers (excluding the intercalary 5.8S gene) ranged from 378 (*Ganoderma* sp. D1) to 429 bases (*Ganoderma* sp. E4) with an average value of 400 (± 6.8) bases (Fig. 9). In addition, the ITS1/ITS2 lengths in Clades C (404.3 ± 4.4 bases), D (402.4 ± 7.9) and E (405.70 ± 6.3) are greater than those in Clade A (396.5 ± 4.2) and B (396.7 ± 1.1). The length of ITS1 ranged from 182 (*Ganoderma* sp. D1) to 219 bases (*Ganoderma* sp. E4) with an average value of 204.4 (± 4.1) bases, while the respective values for ITS2 were from 183 (*G. shanxiense*) to 210 bases (*Ganoderma* sp. E4) and average values of 195.6 ± 4.9 bases (Fig. 9). The vast majority of *Ganoderma* species (ca. 95%) exhibit longer ITS1 than ITS2 sequences; the greatest difference was recorded in *G. wiiroense* (average size difference 21.5 bases) and *G. shanxiense* (18.0). In addition, a clear delimitation in this respect was observed amongst various clades since the difference in length between ITS1 and ITS2 was higher in Clades A (11.6 bases in average) and B (11.3) than in E (7.2), D (4.0) and C (2.5). These results are in agreement with those previously reported on the ITS1/ITS2 spacers length in Basidiomycota and Ascomycota; in both cases, ITS1 was longer that ITS2 (Wang et al. 2015). In contrast, data originating from various fungal phyla (including Basidiomycota) showed that ITS2 is generally longer than ITS1 (Yang et al. 2018).

In the ITS1 region (289 sites), 195 (67%) were variable and 159 (55%) were parsimony informative; the ITS2 region (262 sites) included 169 (65%) variable and 137 (52%) parsimony informative sites. This is in accordance with the outcome of previous reports indicating a larger variability for ITS1 in comparison to ITS2 in Fungi (Nilsson et al. 2008). The largest intraspecies variability in ITS1 size was found in *Ganoderma* sp. C1 (203.0 ± 4.2 bases), *G. wiiroense* (209.0 ± 3.6), *G. martinicense* (204.3 ± 2.3), *G. aridicola* (206.0 ± 2.2), *Ganoderma* sp. D1 (183.5 ± 2.1) and *G. subfornicatum* (206.0 ± 2.0), while the greatest intraspecies variability in ITS2 length was observed in *Ganoderma* sp. E3 (206.3 ± 2.5 bases), *Ganoderma* sp. D3 (200.1 ± 2.0), *Ganoderma* sp. E7 (195.0 ± 2.0), *G. angustisporum* (199.0 ± 1.9) and *G. wiiroense* (187.5 ± 1.9). In general, for the entire genus and for individual Clades/Clusters, ITS2 showed a greater variability in length (with the notable exception of Clade D).

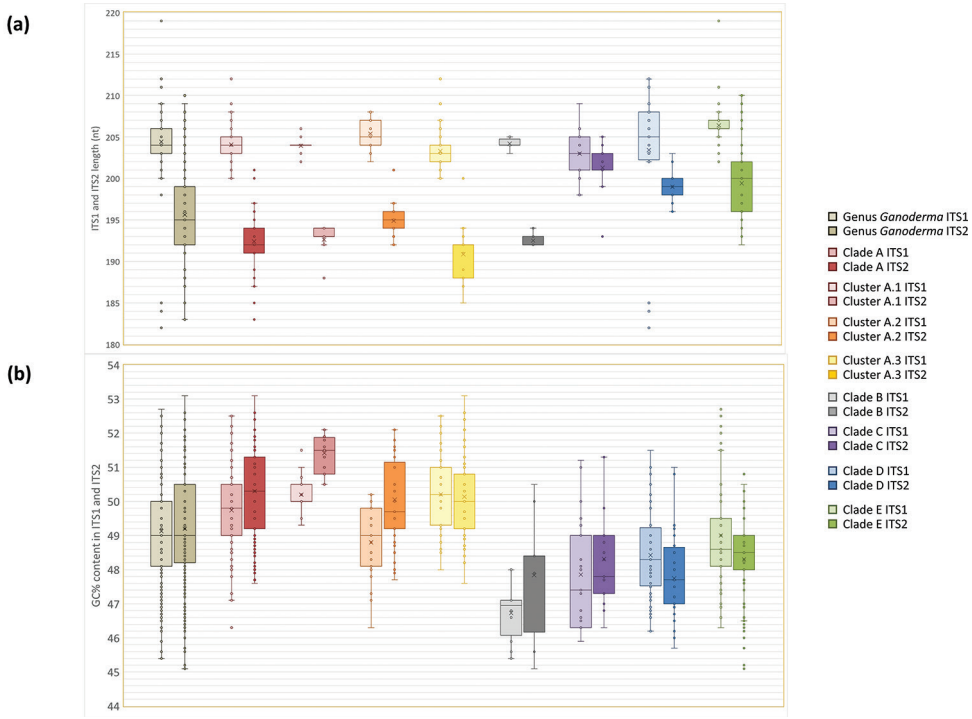

Figure 9. Box plots of **a** length (bases) and **b** GC (%) content of ITS1 and ITS2 sequences for each one of the main lineages (Clades/Clusters) of the genus *Ganoderma*. The size of each box represents 50% of the values, the black horizontal line within each box indicates the median, the 'x' represents the average value, the error bars represent interquartile ranges and circles indicate outliers.

The GC content was almost identical in ITS1 and ITS2 spacers when calculated for the entire genus (49.1 ± 1.5% and 49.2 ± 1.7%, respectively) (Fig. 9); however, species of Clade A showed distinctly higher GC content for the two spacers (49.7 ± 1.2% and 50.3 ± 1.2%, respectively) in comparison to the rest of the *Ganoderma* spp., whereas the lowest values were recorded in Clade B (46.7 ± 0.8% and 47.8 ± 1.6%, respectively). Relevant literature data on Basidiomycota refer to slightly higher values of GC content in ITS2 compared to ITS1, i.e. median values of 45% vs. 44% (Wang et al. 2015) or average values of 46.06% vs. 43.49% (Yang et al. 2018), respectively.

Phylospecies in *Ganoderma*

The application of criteria of wide applicability/suitability for delineating taxa in the genus *Ganoderma* is a particularly challenging task because species exhibit complex evolutionary backgrounds, widespread occurrence and/or problematic taxonomy as previously mentioned. Since this study was principally based on the analysis of ITS metadata, difficulties related to erroneous, fragmentary and/or incomplete information on the origin and the true identity of the sequenced material had to be addressed,

together with labelling referring to the genus only (i.e. "*Ganoderma* sp.") or with unidentified sequences (e.g. "Agaricales sp.", "uncultured fungus" and "unidentified soil fungus"). The outcome demonstrated that the use of ITS rDNA could confer valuable data on the establishment of phylogenetic species within the genus since the majority of terminal clades were strongly supported and species boundaries were – in the majority of cases – elucidated, although relationships/affinities amongst particular sections or within certain species complexes were not adequately resolved.

Intraspecific ITS sequence similarity values were relatively high (i.e. overall average: 99.32 ± 0.59%) for the *Ganoderma* species examined. Moreover, genetic distance, based on uncorrected p-values, provided an additional effective tool for species delineation which was found to be congruent with ITS sequence similarities (overall average of intraspecies genetic distance within the genus: 0.005 ± 0.004). Hence, in the context of the criteria adopted, these parameters contributed significantly to delineating *Ganoderma* species and were generally in accordance with the concepts of already accepted morpho- and/or phylospecies. In addition, a species hypothesis using a threshold of interspecific values for ITS similarity (≤ 98%) and genetic distance (≥ 0.015) was effectively applied for the 21 putatively new phylospecies hereby proposed, while several other distinct entities of dubious status are revealed in the trees inferred. Finally, 59 terminal groups correspond to already established species of the genus which demonstrate a large variability in genetic distance and sequence similarity when selected pairs of phylogenetically-related taxa are compared within different clades (Fig. 8). This was particularly evident in lineages where the barcoding gap amongst taxa is often minimal (i.e. Cluster A.2) or even non-existent (i.e. Cluster A.1). In such cases, species discrimination on the basis of ITS sequence variability is problematic.

Especially as regards taxa of Cluster A.1, average interspecific distances (0.008 ± 0.004) are close to the respective intraspecific values (0.004 ± 0.003); similarly, sequence similarity in interspecific comparisons is high (99.0 ± 0.6; Fig. 8). In this particular case, only the formation of well-supported terminal clades in ITS phylogenies could help to address taxonomic issues (in conjunction with other criteria, for example, distribution, ecology and distinct morphoanatomical characters where available), as is the case with *G. leucocontextum* – *G. weixiensis*. No other taxon of A.1 is adequately resolved through ITS and multigene data are needed in order to delineate them (Zhou et al. 2015; Loyd et al. 2018; Ye et al. 2019). As regards the rest of Clade A, a barcoding gap – albeit narrow – is present for several species of Clusters A.2 and A.3 (Fig. 8), while the difference between genetic distance values within and amongst species is generally higher than in the case of Cluster A.1 (interspecies: 0.028 ± 0.010 and 96.5 ± 1.2% in A.2 and 0.046 ± 0.016 and 95.0 ± 1.4% in A.3). Still, comparisons between several taxa (e.g. *G. parvulum* and *G. mexicanum*, *G. sichuanense* and *G. weberianum*, *G. sessile* and *G. polychromum*, *G. ravenelii* and *G. curtisii* and *G. multipileum* and *G. martinicense*) produce values of genetic distance and sequence similarity which are lower than 0.015 and/or higher than 98%, respectively. Therefore, a 'clear-cut' threshold, based on such parameters, cannot be easily applied to separate them. ITS alone is not effective here and a combination of

criteria (or the outcome of multigene phylogenies) is needed to elucidate the status of these taxa.

On the other hand, species in Clade B present a clear barcoding gap and distinct 'sequence diameters' (as defined by Schoch et al. 2012) corresponding to high interspecific distance and low sequence similarity values (> 0.045 and < 95.33%, respectively). Despite the large interspecies divergence between taxa of Clade B, the respective intraspecies values (0.003 ± 0.002 and 99.71 ± 0.20%) are similar to the total average of the genus. Hence, all three phylospecies comprising this clade (two of them proposed in this study) are well separated by using ITS only.

As regards Clades C, D and E, barcoding gaps are quite pronounced and delimitation of many species could be made on the basis of the 98% sequence similarity and the 0.015 genetic distance values previously mentioned and used for the establishment of the phylospecies proposed herein (Fig. 8). In particular, Clade C presents interspecific distance and sequence similarity values with considerable variability (0.049 ± 0.022 and 93.83 ± 1.26%, respectively); *G. casuarinicola* and *G. enigmaticum* – *G. thailandicum* are the only taxa demonstrating high phylogenetic affinity (on the basis of ITS data) which questions their distinct taxonomic position. Clade D includes well-separated species with pronounced differences when interspecific values of genetic distance and sequence similarity are considered (0.056 ± 0.017 and 93.68 ± 1.64%, respectively), whereas Clade E presents a rather high variability in the respective values amongst species (0.048 ± 0.016 and 94.19 ± 2.27%, respectively). Most taxa presented a clear barcoding gap between inter- and intraspecific values calculated, with the distinct exception of *G. gibbosum*, *G. eickeri*, *G.* aff. *gibbosum* and *G. ellipsoideum* which are closely related.

In conclusion, ITS phylogeny, in conjunction with sequence similarity and genetic distance measurements, do not fully support the delineation of some well-established *Ganoderma* taxa; instead, they advocate their inclusion in monophyletic units representing species complexes. On the other hand, *G. neojaponicum* (intraspecific values: 0.019 ± 0.009; 97.51 ± 1.44%), *Ganoderma* sp. A6 (0.028 ± 0.005; 97.24 ± 1.02), *Ganoderma* sp. C1 (0.029, 95.50%) and *Ganoderma* sp. D1 (0.020, 97.76%) seem to harbour cryptic variation and might correspond to more than one phylospecies. Relatively high intraspecies genetic distance values were also detected in *G. flexipes*, *G. mastoporum*, *G. mbrekobenum* and *Ganoderma* sp. D3 (Fig. 8), where terminal (often well-supported) subgroups were formed according to the ITS phylogeny (Fig. 4).

Notes on *Ganoderma* biogeography and host range

Members of the genus *Ganoderma* exhibit relatively-complex microanatomy (Ryvarden 1991) and low levels of sequence divergence as evidenced in early studies on ribosomal DNA phylogeny (Moncalvo et al. 1995a). In addition, Moncalvo and Buchanan (2008) showed that neither the Northern Hemisphere nor the Southern Hemisphere *Ganoderma* taxa formed monophyletic groups. This is in conflict with a strict vicariant scenario and shows that global-scale vicariance models (Rosen 1978) are too

simplistic to provide the sole explanation for the population structure and evolution of species like those of the genus *Ganoderma*. In this particular case, long-distance (inter-continental) dispersal seems to be more likely since it better explains the broad distribution of *Ganoderma* species evidenced from phylogenetic analyses, indicating strong geographic structure associated with allopatric divergence. On the other hand, little correlation was evident between phylogeny and host relationships (monocot and angiosperms, as well as gymnosperms) in *Ganoderma*, showing that host-based distribution cannot adequately explain the observed geographic pattern with some exceptions (e.g. the 'palm-clade', Cluster D.4).

Three main lineages of the genus were identified: Clade A, Clade B and Clades C through E. Clades A and E include taxa with a cosmopolitan distribution, while species of Clade B are distributed across the Holarctic region; species of Clades C occur in the Paleotropics and taxa of Clade D exhibit a pantropical distribution. Their subsequent analysis results are consistent with the hypothesis of a Northern Hemisphere origin (tropical Asia) for *Ganoderma* species with subsequent range expansions to the Southern Hemisphere and by colonisation of the Neotropics through long distance dispersal (Moncalvo and Buchanan 2008). Consequently, a large diversity of *Ganoderma* taxa is found in Asia; amongst the 80 *Ganoderma* species of the present study, the following occur in east – southeast Asia only: *G. leucocontextum* – *G. weixiensis*, *Ganoderma* sp. A1, *G. weberianum*, *Ganoderma* sp. A2, *Ganoderma* sp. A3, *Ganoderma* sp. A5, *G. flexipes*, *G. philippii*, *G. lingzhi*, *Ganoderma* sp. A6, *G. tropicum*, *Ganoderma* sp. A7, *G. mizoramense*, *G. multipileum*, *G. shanxiense*, *Ganoderma* sp. B2, *G. neojaponicum*, *G. casuarinicola*, *G. nasalanense*, *G. sinense*, *G. boninense*, *Ganoderma* sp. D3, *G. williamsianum*, *G. gibbosum*, *Ganoderma* sp. E4 and *G. mutabile*.

Indicative cases of *Ganoderma* species distribution include:

a Palearctic – Eurasian, Old World: *G. lucidum*, *G. resinaceum* and *G. adspersum* occur across Eurasia and share several common host plants, for example, the genera *Quercus*, *Salix*, *Populus*, *Abies* and *Larix*. A strictly European distribution is exhibited by *G. carnosum*, *G.* aff. *carnosum* and *G. pfeifferi*. Allopatric speciation seems to be under way between Eurasian *G. resinaceum* and Taiwanese collections corresponding to *Ganoderma* sp. A3. An Old Word distribution is also presented by species of the Cluster E.3, since each one of them has been reported exclusively from Africa (*G. knysnamense*), from Asia (*G. mutabile*) or from Europe (*G. pfeifferi*).

b East Asia – Malay Archipelago – Oceania: *G. weberianum* complex (*G. sichuanense* – *G. weberianum*) and *G. steyaertanum* (Clade A), *G. angustisporum* and *G. mastoporum* (Clade D) and *Ganoderma* sp. E3 and *Ganoderma* sp. E6 (Clade E). Particularly as regards *G. ellipsoideum*, its distribution extends to USA on the basis of sequences deriving from environmental samples.

c East Asia and South Africa (Paleotropic): All taxa of Clade C, as well as *G. hoehnelianum* (Cluster A.2), *G. wiiroense* (Cluster A.3), *G. angustisporum* and *Ganoderma* sp. D1 (Clade D). Moreover, *G. carocalcareum* and *G. austroafricanum* (Cluster

A.2), *G. destructans* – *G. dunense* (Cluster A.3), *G. aridicola*, *G. enigmaticum* – *G. thailandicum*, *Ganoderma* sp. C1 and *Ganoderma* sp. C2 (Clade C), *G. cupreum*, *Ganoderma* sp. D1 and *G. ryvardenii* (Clade D), as well as *G. eickeri* (Clade E) have so far only been recorded in Africa.

d Holoarctic/Nearctic – Palearctic: Within Clade B, *G. applanatum* presents an inter-continental distribution indicating gene exchange between the Palearctic and the Nearctic regions through land bridges which were widely accepted as corridors for such transfers (Hibbett 2001; James et al. 2001; Zervakis et al. 2004; Geml et al. 2006; Geml et al. 2008; Matheny et al. 2009; Feng et al. 2012). The same pattern is presented by members of Cluster A.1. None of the Holarctic groups (Cluster A.1 and Clade B) shows any significant molecular divergence between collections from Europe and North America. Especially, the biogeographic pattern of Clade B evidences a recent common ancestral distribution in the Holoarctic region which explains the inter-continental distribution pattern of *G. applanatum*. In addition, allopatric speciation is evident at the terminal clades of the Cluster E.5, where Eurasian and east Asian collections of *G. adspersum* and *G.* aff. *adspersum*, respectively, are well-separated from their sister Nearctic *Ganoderma* sp. E7. A Nearctic distribution is also presented by *G. curtisii* (Cluster A.3).

e East Asian – North American: Several biogeographic studies evidenced migration of fungi from east Asia to North America via the Bering Land Bridge route (Wu and Mueller 1997; Wu et al. 2000; Chapela and Garbelotto 2004; Geml et al. 2006). *Ganoderma* species exhibiting an east Asian – northeast American disjunction are grouped within the *G. lingzhi* and *G. curtisii* – *G. ravenelii* complex (Cluster A.3). The same pattern is present in several sister clades within Cluster A.2, for example, the *G. sessile* – *G. polychromum* complex, since *G. sessile* shows a broad distribution in southeast Asia and America.

f Neotropical: *G. mexicanum* – *G. parvulum* complex, *G.* aff. *polychromum* (Cluster A.2), *G. tuberculosum* and *G. martinicense* (Cluster A.3), *Ganoderma* sp. D2 (Clade D) and *Ganoderma* sp. E1 and sp. E2 (Clade E). As regards other species occurring in the Americas only, *G. curtisii* (Cluster A.3), *G. zonatum* (Clade D) and *Ganoderma* sp. E7 (Clade E) are confined to North America. The closely-related *G. podocarpense* and *G. chocoense* (Clade E) were reported only in Central America, whereas *Ganoderma* sp. A4, *G. concinnum* and *G. multiplicatum* (Cluster A.3), *G. orbiforme* (Clade D) and *Ganoderma* sp. E5 (Clade E) were recorded in South America.

g Southern Hemisphere: The phylogenetic analysis of Southern Hemisphere species and complexes (species in Clusters A.2 and A.3, Clusters D.3 and D.4 and E.2 and E.4) indicated a restricted gene flow apparently due to geographic isolation, although episodic long-distance dispersal still occurs (Moncalvo and Buchanan 2008). The sister group relationships amongst the tropical southeast Asian species, South American and African species are not surprising since the two continents were connected after the collision of the African, Australian and Asian plates (McElhinny and Embleton 1974; Hall 2002). In all clades deriving from this analysis, several groups of closely-related taxa were identified, for example, the

G. mexicanum – *G. parvulum* complex and the group of *G. hoehnelianum*, *G. austroafricanum* and *G. carocalcareum*.

The majority of *Ganoderma* species were collected on angiosperm hosts, 41 species on eudicots and 19 species on monocots, while another 18 species were reported on gymnosperms (Table 1 and Suppl. material 1: Table S2). Seven species were collected on both eudicot and monocots (but not on gymonsperms), i.e. *G. sessile*, *G. zonatum*, *G. ryvardenii*, *Ganoderma* sp. E2, *G. gibbosum*, *Ganoderma* sp. E4 and *G. australe*. On the other hand, *G. lucidum*, *G. leucocontextum* – *G. weixiensis*, *G. ravenelii*, *G. enigmaticum* – *G. thailandicum*, *G. mastoporum*, *G. angustisporum*, and *G. adspersum* were noted on both eudicots and gymnosperms, while *G. multipileum*, *G. applanatum*, *G. aridicola*, *G. casuarinicola*, *G. mbrekobenum*, *G.* aff. *gibbosum* and *G. ellipsoideum* were recorded on all three type of hosts. Cluster A.1 comprises species collected on eudicots and gymnosperms; two of them (*G. carnosum* and *G. oregonense*) were recorded on gymnosperm hosts only. Species of Clusters A.2 and A.3 present a marked preference for eudicots; only *G. sessile* (one record), *G. lingzhi* and *G. multipileum* are also reported from monocots, whereas *G. flexipes*, *G. ravenelii* and *G. multipileum* are reported on gymnosperms as well. In Clade B, host data are available only for *G. applanatum*; the respective specimens were collected on a broad range of hosts. In addition, this is the only species for which the host range is expanded to include also monocots (i.e. *Phoenix canariensis* and *Tradescantia zanonia*) as an outcome of including environmental samples in this study. However, these data should be treated with caution since the respective material was obtained from plant leaves. Clades C and D comprise species collected on a broad range of eudicots, monocots and gymnosperms. Cluster D.4 includes five species with a preference for monocots, three of them growing strictly on this particular host type (i.e. *G. boninense*, *Ganoderma* sp. D2 and *Ganoderma* sp. D3). Regarding Clade E, the majority of species were recorded on eudicots and only three on gymnosperms (i.e. *G. adspersum*, *G. aff. gibbosum* and *G. ellipsoideum*).

Erroneous *Ganoderma* sequences labelling in public depositories

As previously stated, one of the major obstacles for exploiting sequences present in public depositories is that many of them are inaccurate; errors in labelling of metadata were estimated to correspond to as much as 20% – or even 30% according to a recent report – of GenBank accessions including also recent deposits (Vilgalys 2003; Nilsson et al. 2006; Schoch et al. 2014; Hofstetter et al. 2019). The outcome of our study shows that the extent of the problem is even more pronounced in the case of *Ganoderma* entries and it could be clearly exemplified when pertinent data are presented either (a) by the most commonly-used names under which *Ganoderma* sequences were deposited or (b) by the names used much less than they ought. As regards the former, the most widely-used names were *G. lucidum* [482 entries; 375 (78%) were subsequently grouped in 24 species other than *G. lucidum*)], *G. australe* [(212 entries; 185 (87%) of them were

found to correspond to 15 species other than *G. australe*)] and *G. resinaceum* [(177 entries; 72 (41%) of them were found to represent five species other than *G. resinaceum*)]. On the basis of the metadata analysis performed, *G. lucidum* is actually represented by 107 entries under this name (meaning that only 22% of the initial identifications were correct), *G. australe* by 27 entries (13% correct) and *G. resinaceum* by 105 entries (59% correct while 34% are erroneously labelled as "*G. sessile*"). On the other hand, 22 out of 23 sequences initially deposited as *G. multipileum* were correct; however, the end result revealed that 243 entries belong to this species (the extra entries were originally labelled either as *Ganoderma* sp. or as "*G. lucidum*"). A similar case is demonstrated by *G. lingzhi*; 333 out of 337 sequences deposited under this name were correct, but the final number of entries which correspond to this species is 615 (the additional sequences were mainly labelled as "*G. lucidum*", *Ganoderma* sp. or as "*G. sichuanense*"). Moreover, *G. applanatum* species consists of 424 entries; the majority of them (269, 63%) derive from environmental samples (Table 1, Suppl. material 1: Tables S2, S5). In general, sequences originating from environmental samples correspond to ca. 9% of the total *Ganoderma* dataset examined and represent 32 species identified in the frame of the present study (Suppl. material 1: Table S5). In three notable cases, the known distribution of *Ganoderma* species appears to be expanded to other continents thanks to the information provided by such type of data, i.e. the Nearctic *G. oregonense* in Europe (Estonia), the neotropical *G. cupreum* in India and the Australasian *G. ellipsoideum* in USA. All relevant data concerning the identity of environmental samples, as well as the correct names of mis-annotated sequences, are included in Suppl. material 1: Tables S5, S6.

Conclusions

The study of a large dataset comprising almost four thousand ITS entries proved to be valuable in obtaining a significant amount of phylogenetic information which contributed to elucidating the status of *Ganoderma* species. In addition, it contributed to establishing robust relationships amongst the majority of them, while it also revealed limitations in the use of ITS (alone) to assess certain taxa which have to be addressed through a multigene approach. However, it is interesting that the outcome of recent publications employing more than one marker (by focusing on particular groups in the genus, for example, Loyd et al. 2018; Cabarroi-Hernández et al. 2019; Tchotet Tchoumi et al. 2019) is congruent with the phylogeny obtained from the present meta-analysis. Furthermore, the results of this work demonstrated that even recent sequence deposits in public databases are associated with a remarkably high number of misidentifications or errors. The very high variability/plasticity in morphological characters, the improper use of terms describing anatomical features, the existence of ambiguous synonyms or misapplied names, the non-uniformity of taxonomic criteria adopted by researchers and the expanding number of non-experts working on (and sequencing) *Ganoderma* material are some of the reasons behind the unreliability of such information. Consequently, interpretation of specimen identity vis-à-vis BLAST results often leads to mistaken conclusions. Therefore, a phylogenetic framework is

preferable to identify new material since taxonomic determinations, based solely on BLAST results, are often erroneous and should be performed with great care. The effectiveness of DNA barcoding greatly depends on establishing reference sequences from validated (authentic) type specimens after careful evaluation of phylogenetic data. Especially in the case of the genus *Ganoderma*, the holotype of many species is either missing or destroyed, thus the need for epitypification is apparent. In addition, as the present study assessed, annotations of submitted sequences are frequently fragmentary and important information is lacking (e.g. geographic origin, even for those corresponding to newly-described taxa), which is unfortunately widespread in GenBank submissions pertaining to fungal specimens (Schoch et al. 2014; Durkin et al. 2020). A special mention should also be made to the usefulness of morphological characters in *Ganoderma* specimens, which (for the reasons previously explained) must be evaluated with caution and preferably in conjunction with other approaches (including DNA sequencing) to provide data suitable for resolving taxonomic issues and at inferring robust conclusions on species concepts.

At a more general level, this study evidences that significant – yet largely untapped – mycological explanatory power resides in the public DNA sequence corpus and we hope that other mycologists will start scrutinising the sequence data available for their fungal groups of expertise. Our results also demonstrated that the so-called environmental sequences – usually ignored in a taxonomic/phylogenetic context – should be included in such pursuits (cf. Ryberg et al. 2008) since they were found to confer valuable information.

Acknowledgements

We are indebted to the curators of the fungaria of the Bulgarian Academy of Sciences (FBE), the Catholic University of Louvain (MUCL) and the University of Palermo (PAL) for providing specimens to be examined. In particular, we thank our long-standing collaborator D. Dimou for collecting part of the material (basidiomes) examined in this study and for kindly sharing photos of some specimens. We would also like to thank Dr. R.H. Nilsson (University of Gothenburg, Sweden) for reviewing the manuscript and for contributing to its improvement through helpful comments/suggestions.

This research was performed in the frame of a project (THALIS – UOA – MIS 377062) cofinanced by the European Union (European Social Fund – ESF) and Greek National Funds through the Operational Programme 'Education and Lifelong Learning' of the National Strategic Reference Framework (NSRF).

References

Adaskaveg JE, Gilbertson RL (1986) Cultural studies and genetics of sexuality of *Ganoderma lucidum* and *G. tsugae* in relation to the taxonomy of the *G. lucidum* complex. Mycologia 78(5): 694–705. https://doi.org/10.1080/00275514.1986.12025312

Adaskaveg JE, Gilbertson RL (1988) Basidiospores, pilocystidia, and other basidiocarp characters in several species of the *G. lucidum* complex. Mycologia 80(4): 493–507. https://doi.org/10.1080/00275514.1988.12025571

Altschul SF, Madden TL, Schäffer AA, Zhang J, Zhang Z, Miller W, Lipman DJ (1997) Gapped BLAST and PSI-BLAST: a new generation of protein database search programs. Nucleic Acids Research 25(17): 3389–3402. https://doi.org/10.1093/nar/25.17.3389

Ankenbrand MJ, Keller A, Wolf M, Schultz J, Förster F (2015) ITS2 database V: Twice as much. Molecular Biology and Evolution 32(11): 3030–3032. https://doi.org/10.1093/molbev/msv174

Badotti F, de Oliveira FS, Garcia CF, Vaz AB, Fonseca PL, Nahum LA, Oliveira G, Góes-Neto A (2017) Effectiveness of ITS and sub-regions as DNA barcode markers for the identification of Basidiomycota (Fungi). BMC Microbiology 17(1): 1–42. https://doi.org/10.1186/s12866-017-0958-x

Baltazar JM, Gibertoni TB (2009) A checklist of aphyllophoroid fungi (Basidiomycota) recorded from the Brazilian Atlantic rain forest. Mycotaxon 109(1): 439–442. https://doi.org/10.5248/109.439

Bazzalo ME, Wright JE (1982) Survey of the Argentine species of the *Ganoderma lucidum* complex. Mycotaxon 16(1): 293–325.

Bhosle S, Ranadive K, Bapat G, Garad S, Deshpande G, Vaidya J (2010) Taxonomy and Diversity of *Ganoderma* from the Western parts of Maharashtra (India). Mycosphere 1(3): 249–262.

Bidartondo MI (2008) Preserving accuracy in GenBank. Science 319 (5870): e1616. https://doi.org/10.1126/science.319.5870.1616a

Boh B, Berovic M, Zhang J, Zhi-Bin L (2007) *Ganoderma lucidum* and its pharmaceutically active compounds. Biotechnology Annual Review 13: 265–301. https://doi.org/10.1016/S1387-2656(07)13010-6

Bolaños AC, Bononi VLR, de Mello Gugliotta A (2016) New records of *Ganoderma multiplicatum* (Mont.) Pat. (Polyporales, Basidiomycota) from Colombia and its geographic distribution in South America. Check List 12(4): 1–7. https://doi.org/10.15560/12.4.1948

Bonito GM, Gryganskyi AP, Trappe JM, Vilgalys R (2010) A global meta-analysis of *Tuber* ITS rDNA sequences: species diversity, host associations and long-distance dispersal. Molecular Ecology 19(22): 4994–5008. https://doi.org/10.1111/j.1365-294X.2010.04855.x

Cabarroi-Hernández M, Villalobos-Arámbula AR, Torres-Torres MG, Decock C, Guzmán-Dávalos L (2019) The *Ganoderma weberianum-resinaceum* lineage: multilocus phylogenetic analysis and morphology confirm *G. mexicanum* and *G. parvulum* in the Neotropics. MycoKeys 59: 95–131. https://doi.org/10.3897/mycokeys.59.33182

Callahan B, McMurdie P, Holmes S (2017) Exact sequence variants should replace operational taxonomic units in marker-gene data analysis. ISME Journal 11: 2639–2643. https://doi.org/10.1038/ismej.2017.119

Cao Y, Wu SH, Dai YC (2012) Species clarification of the prize medicinal *Ganoderma* mushroom "Lingzhi". Fungal Diversity 56: 49–62. https://doi.org/10.1007/s13225-012-0178-5

Cao Y, Yuan HS (2013) *Ganoderma mutabile* sp. nov. from south-western China based on morphological and molecular data. Mycological Progress 12: 121–126. https://doi.org/10.1007/s11557-012-0819-9

Chapela IH, Garbelotto M (2004) Phylogeography and evolution in matsutake and close allies inferred by analyses of ITS sequences and AFLPs. Mycologia 96(4): 730–741. https://doi.org/10.1080/15572536.2005.11832921

Coelho-Moreira JDS, Brugnari T, Sá-Nakanishi AB, Castoldi R, de Souza CGM, Bracht A, Peralta RM (2018) Evaluation of diuron tolerance and biotransformation by the white-rot fungus *Ganoderma lucidum*. Fungal Biology 122(6): 471–478. https://doi.org/10.1016/j.funbio.2017.10.008

Coetzee MP, Marincowitz S, Muthelo VG, Wingfield MG (2015) *Ganoderma* species, including new taxa associated with root rot of the iconic *Jacaranda mimosifolia* in Pretoria, South Africa. IMA Fungus 6(1): 249–256. https://doi.org/10.5598/imafungus.2015.06.01.16

Corner EJH (1983) Ad Polyporaceas I. *Amauroderma* and *Ganoderma*. Beihefte zur Nova Hedwigia 75: 1–183.

Costa-Rezende DH, Robledo GL, Góes-Neto A, Reck MA, Crespo E, Drechsler-Santos ER (2017) Morphological reassessment and molecular phylogenetic analyses of *Amauroderma* s. lat. raised new perspectives in the generic classification of the Ganodermataceae family. Persoonia 39: 254–269. https://doi.org/10.3767/persoonia.2017.39.10

Dai YC, Zhou LW, Hattori T, Cao Y, Stalpers JA, Ryvarden L, Buchanan P, Oberwinkler F, Hallenberg N, Liu P-G, Wu S-H (2017) *Ganoderma lingzhi* (Polyporales, Basidiomycota): the scientific binomial for the widely cultivated medicinal fungus Lingzhi. Mycological Progress 16: 1051–1055. https://doi.org/10.1007/s11557-017-1347-4

Darriba D, Taboada GL, Doallo R, Posada D (2012) jModelTest 2: more models, new heuristics and parallel computing. Nature Methods 9(8): e772. https://doi.org/10.1038/nmeth.2109

de Lima Júnior NC, Gibertoni TB, Malosso E (2014) Delimitation of some neotropical laccate *Ganoderma* (Ganodermataceae): molecular phylogeny and morphology. Revista de Biología Tropical 62(3): 1197–1208. https://doi.org/10.15517/rbt.v62i3.12380

Donk MA (1948) Notes on Malesian fungi, I. Bulletin du Jardin Botanique de Buitenzorg Série 3 17: 473–482.

Donk MA (1974) Check List of European Polypores. North-Holland Publishing Company (eds), Amsterdam-London, 469 pp.

Donoghue MJ, Cracraft J (2004) Charting the Tree of Life. In: Cracraft J, Donoghue MJ (Eds) Assembling the Tree of Life. Oxford University Press, New York, 592 pp.

Douanla-Meli C, Langer E (2009) *Ganoderma carocalcareum* sp. nov., with crumbly-friable context parasite to saprobe on *Anthocleista nobilis* and its phylogenetic relationship in *G. resinaceum* group. Mycological Progress 8: 145–155. https://doi.org/10.1007/s11557-009-0586-4

Durkin L, Jansson T, Sanchez M, Khomich M, Ryberg M, Kristiansson E, Nilsson RH (2020) When mycologists describe new species, not all relevant information is provided (clearly enough). MycoKeys 72: 109–128. https://doi.org/10.3897/mycokeys.72.56691

Elliott M, Broschat T (2001) Observations and pathogenicity experiments on *Ganoderma zonatum* in Florida. Palms 45: 62–73.

Feng B, Xu J, Wu G, Hosen MI, Zeng NK, Li YC, Tolgor B, Kost GW, Yang ZL (2012) DNA sequence analyses reveal abundant diversity, endemism and evidence for Asian origin of the porcini mushrooms. PloS ONE 7(5): e37567. https://doi.org/10.1371/journal.pone.0037567

Flores JA, Barnes CW, Ordoñez ME (2017) *Ganoderma podocarpense* sp. nov. Persoonia 39: : 270–467. https://doi.org/10.3767/persoonia.2017.39.11

Flores JA, Barnes CW, Ordoñez ME (2018) *Ganoderma chocoense* J.A. Flores, C.W. Barnes, & Ordoñez, sp. nov. Persoonia 41: 238–417. https://doi.org/10.3767/persoonia.2018.41.12

Gardes M, Bruns TD (1993) ITS primers with enhanced specificity for basidiomycetes – application to the identification of mycorrhizae and rusts. Molecular Ecology 2(2): 113–118. https://doi.org/10.1111/j.1365-294X.1993.tb00005.x

Gargano ML, van Griensven LJLD, Isikhuemhen OS, Lindequist U, Venturella G, Wasser SP, Zervakis GI (2017) Medicinal mushrooms: Valuable biological resources of high exploitation potential. Plant Biosystems 151(3): 548–565. https://doi.org/10.1080/11263504.2017.1301590

Geml J, Gravendeel B, van der Gaag KJ, Neilen M, Lammers Y, Raes N, Semenova TA, de Knijff P, Noordeloos ME (2014) The contribution of DNA metabarcoding to fungal conservation: diversity assessment, habitat partitioning and mapping red-listed fungi in protected coastal *Salix repens* communities in the Netherlands. PLoS ONE 9(6): e99852. https://doi.org/10.1371/journal.pone.0099852

Geml J, Laursen GA, O'Neill K, Nusbaum C, Taylor DL (2006) Beringian origins and cryptic speciation events in the fly agaric (*Amanita muscaria*). Molecular Ecology 15(1): 225–239. https://doi.org/10.1111/j.1365-294X.2005.02799.x

Geml J, Tulloss RE, Laursen GA, Sazanova NA, Taylor DL (2008) Evidence for strong inter- and intracontinental phylogeographic structure in *Amanita muscaria*, a wind-dispersed ectomycorrhizal basidiomycete. Molecular Phylogenetics and Evolution 48(2): 694–701. https://doi.org/10.1016/j.ympev.2008.04.029

Gilbertson RL, Ryvarden L (1986) North American polypores (Vol. I). Abortiporus-Lindtneria. Fungiflora, Oslo, 433 pp.

Gomes-Silva AC, Ryvarden L, Gibertoni TB (2011) New records of Ganodermataceae (Basidiomycota) from Brazil. Nova Hedwigia 92(1–2): 83–94. https://doi.org/10.1127/0029-5035/2011/0092-0083

Gottlieb AM, Ferrer E, Wright JE (2000) rDNA analyses as an aid to the taxonomy of species of *Ganoderma*. Mycological Research 104(9): 1033–1045. https://doi.org/10.1017/S095375620000304X

Gweon HS, Oliver A, Taylor J, Booth T, Gibbs M (2015) PIPITS: an automated pipeline for analyses of fungal internal transcribed spacer sequences from the Illumina sequencing platform. Methods in Ecology and Evolution 6(8): 973–980. https://doi.org/10.1111/2041-210X.12399

Hall R (2002) Cenozoic geological and plate tectonic evolution of SE Asia and the SW Pacific: computer-based reconstructions, model and animations. Journal of Asian Earth Sciences 20(4): 353–431. https://doi.org/10.1016/S1367-9120(01)00069-4

Hansen L (1958) On the anatomy of the Danish species of *Ganoderma*. Botanisk Tidskrift 54: 333–352.

Hapuarachchi KK, Elkhateeb WA, Karunarathna SC, Cheng CR, Bandara AR, Kakumyan P, Hyde KD, Daba GM, Wen TC (2018a) Current status of global *Ganoderma* cultivation, products, industry and market. Mycosphere 9(5): 1025–1052. https://doi.org/10.5943/mycosphere/9/5/6

Hapuarachchi KK, Karunarathna SC, Phengsintham P, Yang HD, Kakumyan P, Hyde KD, Wen TC (2019) Ganodermataceae (Polyporales): Diversity in Greater Mekong Subregion countries (China, Laos, Myanmar, Thailand and Vietnam). Mycosphere 10(1): 221–309. https://doi.org/10.5943/mycosphere/10/1/6

Hapuarachchi, KK, Karunarathna SC, Raspé O, De Silva KHWL, Thawthong A, Wu XL, Kakumyan P, Hyde KD, Wen TC (2018b) High diversity of *Ganoderma* and *Amauroderma* (Ganodermataceae, Polyporales) in Hainan Island, China. Mycosphere 9(5): 931–982. https://doi.org/10.5943/mycosphere/9/5/1

Hennicke F, Cheikh-Ali Z, Liebisch T, Maciá-Vicentea JG, Bode HB, Piepenbring M (2016) Distinguishing commercially grown *Ganoderma lucidum* from *Ganoderma lingzhi* from Europe and East Asia on the basis of morphology, molecular phylogeny, and triterpenic acid profiles. Phytochemistry 127: 29–37. https://doi.org/10.1016/j.phytochem.2016.03.012

Hibbett DS (2001) Shiitake mushrooms and molecular clocks: historical biogeography of *Lentinula*. Journal of Biogeography 28(2): 231–241. https://doi.org/10.1046/j.1365-2699.2001.00528.x

Hofstetter V, Buyck B, Eyssartier G, Schnee S, Gindro K (2019) The unbearable lightness of sequenced-based identification. Fungal Diversity 96: 243–284. https://doi.org/10.1007/s13225-019-00428-3

Hong SG, Jung HS (2004) Phylogenetic analysis of *Ganoderma* based on nearly complete mitochondrial small-subunit ribosomal DNA sequences. Mycologia 96(4): 742–755. https://doi.org/10.1080/15572536.2005.11832922

Hseu RS, Wang HH, Wang HF, Moncalvo JM (1996) Differentiation and grouping of isolates of the *Ganoderma lucidum* complex by random amplified polymorphic DNA–PCR compared with grouping on the basis of internal transcribed spacer sequences. Applied and Environmental Microbiology 62(4): 1354–1363. https://doi.org/10.1128/AEM.62.4.1354-1363.1996

Hsu KD, Cheng KC (2018) From nutraceutical to clinical trial: frontiers in *Ganoderma* development. Applied Microbial and Biotechnology 102: 9037–9051. https://doi.org/10.1007/s00253-018-9326-5

Hughes KW, Petersen RH, Lickey EB (2009) Using heterozygosity to estimate a percentage DNA sequence similarity for environmental species' delimitation across basidiomycete fungi. New Phytologist 182(4): 795–798. https://doi.org/10.1111/j.1469-8137.2009.02802.x

Hurvich CM, Tsai CL (1989) Regression and time series model selection in small samples. Biometrika 76: 297–307. https://doi.org/10.1093/biomet/76.2.297

Imazeki R (1939) Studies on *Ganoderma* of Nippon. Bulletin of the Tokyo Science Museum 1: 29–52.

Imazeki R (1952) A contribution to the fungus flora of Dutch New Guinea. Bulletin of the Government Forest Experimental Station Meguro 57: 87–128.

Jahn H, Kotlaba F, Pouzar Z (1980) *Ganoderma atkinsonii* Jahn, Kotl. & Pouz., spec. nova, a parallel species to *Ganoderma lucidum*. Westfälische Pilzbriefe 11(6): 97–121.

Jahn H, Kotlaba F, Pouzar Z (1986) Notes on *Ganoderma carnosum* Pat. (*G. atkinsonii* Jahn, Kotl. & Pouz.). Westfälische Pilzbriefe 10–11: 378–382.

James TY, Moncalvo JM, Li S, Vilgalys R (2001) Polymorphism at the ribosomal DNA spacers and its relation to breeding structure of the widespread mushroom *Schizophyllum commune*. Genetics 157(1): 149–161.

Karsch-Mizrachi I, Nakamura Y, Cochrane G (2012) The International Nucleotide Sequence Database Collaboration. Nucleic Acids Research 40(D1): D33–D37. https://doi.org/10.1093/nar/gkr1006

Karsten P (1881) Enumeratio Boletinarum et Polyporarum Fennicarum systemate novo dispositorum. Revue de Mycologie 3: 16–18.

Katoh K, Standley DM (2013) MAFFT multiple sequence alignment software version 7: improvements in performance and usability. Molecular Biology and Evolution 30(4): 772–780. https://doi.org/10.1093/molbev/mst010

Kearse M, Moir R, Wilson A, Stones-Havas S, Cheung M, Sturrock S, Buxton S, Cooper A, Markowitz S, Duran C, Thierer T, Ashton B, Meintjes P, Drummond A (2012) Geneious Basic: an integrated and extendable desktop software platform for the organization and analysis of sequence data. Bioinformatics 28(12): 1647–1649. hhttps://doi.org/10.1093/bioinformatics/bts199

Khan I, Huang G, Li X, Leong W, Xia W, Hsiao WLW (2018) Mushroom polysaccharides from *Ganoderma lucidum* and *Poria cocos* reveal prebiotic functions. Journal of Functional Foods 41: 191–201. https://doi.org/10.1016/j.jff.2017.12.046

Kinge TR, Mih AM (2011) *Ganoderma ryvardense* sp. nov. associated with basal stem rot (BSR) disease of oil palm in Cameroon. Mycosphere 2(2): 179–188.

Kinge TR, Mih AM, Coetzee MPA (2012) Phylogenetic relationships among species of *Ganoderma* (Ganodermataceae, Basidiomycota) from Cameroon. Australian Journal of Botany 60: 526–538. https://doi.org/10.1071/BT12011

Kirk PM, Cannon PF, David JC, Stalpers J (2008) Ainsworth and Bisby's Dictionary of the Fungi (10th edn.). CABI Publishing, Oxfordshire, 771 pp. https://doi.org/10.1079/9780851998268.0000

Kõljalg U, Nilsson RH, Abarenkov K, Tedersoo L, Taylor AF, Bahram M, Bates ST, Bruns TD, Bengtsson-Palme J, Callaghan TM, Douglas B, Drenkhan T, Eberhardt U, Dueñas M, Grebenc T, Griffith GW, Hartmann M, Kirk PM, Kohout P, Larsson E, Lindahl BD, Lücking R, Martín MP, Matheny PB, Nguyen NH, Niskanen T, Oja J, Peay KG, Peintner U, Peterson M, Põldmaa K, Saag L, Saar I, Schüßler A, Scott JA, Senés C, Smith ME, Suija A, Taylor DL, Telleria MT, Weiss M, Larsson KH (2013) Towards a unified paradigm for sequence-based identification of fungi. Molecular Ecology 22(21): 5271–5277. https://doi.org/10.1111/mec.12481

Kondo K, Nakamura K, Ishigaki T, Sakata K, Obitsu S, Noguchi A, Fukuda N, Nagasawa E, Teshima R, Nishimaki-Mogami T (2017) Molecular phylogenetic analysis of new *Entoloma rhodopolium*-related species in Japan and its identification method using PCR-RFLP. Scientific Reports 7(1): e14942. https://doi.org/10.1038/s41598-017-14466-x

Kotlaba F, Pouzar Z (1993) Taxonomic and nomenclatural notes on *Trametes cervina* and *Ganoderma atkinsonii*. Ceska Mykologie 37(1): 49–51.

Koutrotsios G, Patsou M, Mitsou EK, Bekiaris G, Kotsou M, Tarantilis PA, Pletsa V, Kyriacou A, Zervakis GI (2019) Valorization of olive by-products as substrates for the cultivation of *Ganoderma lucidum* and *Pleurotus ostreatus* mushrooms with enhanced functional and prebiotic properties. Catalysts 9(6): e537. https://doi.org/10.3390/catal9060537

Kumar S, Stecher G, Li M, Knyaz C, Tamura K (2018) MEGA X: molecular evolutionary genetics analysis across computing platforms. Molecular Biology and Evolution 35(6): 1547–1549. https://doi.org/10.1093/molbev/msy096

Lai T, Gao Y, Zhou S (2004) Global marketing of medicinal Lingzhi mushroom *Ganoderma lucidum* (W. Curt.: Fr.) Lloyd (Aphyllophoromycetideae) products and safety concerns.

International Journal of Medicinal Mushrooms 6(2): 189–194. https://doi.org/10.1615/IntJMedMushr.v6.i2.100

Letunic I, Bork P (2019) Interactive Tree Of Life (iTOL) v4: recent updates and new developments. Nucleic Acids Research 47(W1): W256–W259. https://doi.org/10.1093/nar/gkz239

Li S, Dong C, Wen H, Liu X (2016) Development of Ling-zhi industry in China – emanated from the artificial cultivation in the Institute of Microbiology, Chinese Academy of Sciences (IMCAS). Mycology 7(2): 74–80. https://doi.org/10.1080/21501203.2016.1171805

Li TH, Hu HP, Deng WQ, Wub SH, Wang DM, Tsering T (2015). *Ganoderma leucocontextum*, a new member of the *G. lucidum* complex from southwestern China. Mycoscience 56(1): 81–85. https://doi.org/10.1016/j.myc.2014.03.005

Liao B, Chen X, Han J, Dan Y, Wang L, Jiao W, Song J, Chen S (2015) Identification of commercial *Ganoderma* (Lingzhi) species by ITS2 sequences. Chinese Medicine 10: 1–22. https://doi.org/10.1186/s13020-015-0056-7

Liu H, Guo L-J, Li S-L, Fan L (2019) *Ganoderma shanxiense*, a new species from northern China based on morphological and molecular evidence. Phytotaxa 406(2): 129–136. https://doi.org/10.11646/phytotaxa.406.2.4

Loguercio-Leite C, Groposo C, Halmenschlager MA (2005) Species of *Ganoderma* Karsten in a subtropical area (Santa Catarina State, Southern Brazil). Iheringia, Série Botânica 60(2): 135–139.

Loyd AL, Barnes CW, Held BW, Schink MJ, Smith ME, Smith JA, Blanchette RA (2018) Elucidating "lucidum": Distinguishing the diverse laccate *Ganoderma* species of the United States. PLoS ONE 13(7): e0199738. https://doi.org/10.1371/journal.pone.0199738

Luangharn T, Karunarathna SC, Mortimer PE, Hyde KD, Thongklang N, Xu J (2019a) A new record of *Ganoderma tropicum* (Basidiomycota, Polyporales) for Thailand and first assessment of optimum conditions for mycelia production. MycoKeys 51: 65–83. https://doi.org/10.3897/mycokeys.51.33513

Luangharn T, Karunarathna SC, Mortimer PE, Hyde KD, Xu J (2019b) Additions to the knowledge of *Ganoderma* in Thailand: *Ganoderma casuarinicola*, a new record; and *Ganoderma thailandicum* sp. nov. MycoKeys 59: 47–65. https://doi.org/10.3897/mycokeys.59.36823

Matheny PB, Aime MC, Bougher NL, Buyck B, Desjardin DE, Horak E, Kropp BR, Lodge DJ, Soytong K, Trappe JM, Hibbett DS (2009) Out of the Palaeotropics? Historical biogeography and diversification of the cosmopolitan ectomycorrhizal mushroom family Inocybaceae. Journal of Biogeography 36(4): 577–592. https://doi.org/10.1111/j.1365-2699.2008.02055.x

Mattock G (2001) Notes on British *Ganoderma* species: Emphasizing the annual species and *G. carnosum*. Field Mycology 2(2): 60–64. https://doi.org/10.1016/S1468-1641(10)60517-8

McElhinny MW, Embleton BJJ (1974) Australian palaeomagnetism and the Phanerozoic plate tectonics of eastern Gondwanaland. Tectonophysics 22(1–2): 1–29. https://doi.org/10.1016/0040-1951(74)90032-8

Mendoza G, Guzmán G, Ramírez-Guillén F, Luna M, Trigos A (2011) *Ganoderma oerstedii* (Fr.) Murrill (Higher Basidiomycetes), a tree parasite species in Mexico: taxonomic description, rDNA study, and review of its medical applications. International Journal of Medicinal Mushrooms 13(6): 545–552. https://doi.org/10.1615/IntJMedMushr.v13.i6.60

Miller MA, Pfeiffer W, Schwartz T (2010) Creating the CIPRES Science Gateway for inference of large phylogenetic trees. Proceedings of the Gateway Computing Environments Workshop (GCE), New Orleans, 8 pp. https://doi.org/10.1109/GCE.2010.5676129

Mohanty PS, Harsh NSK, Pandey A (2011) First report of *Ganoderma resinaceum* and *G. weberianum* from north India based on ITS sequence analysis and micromorphology. Mycosphere 2(4): 469–474.

Moncalvo JM (2000) Systematics of *Ganoderma*. In: Flood J, Bridge PD, Holderness M (Ed.) *Ganoderma* diseases of perennial crops. CABI Publishing , New York, 23–45. https://doi.org/10.1079/9780851993881.0023

Moncalvo JM, Buchanan PK (2008) Molecular evidence for long distance dispersal across the Southern Hemisphere in the *Ganoderma applanatum-australe* species complex (Basidiomycota). Mycological Research 112(4): 425–436. https://doi.org/10.1016/j.mycres.2007.12.001

Moncalvo JM, Ryvarden L (1997) A nomenclatural study of the Ganodermataceae Donk. Synopsis Fungorum 11: 1–114.

Moncalvo JM, Wang HF, Hseu RS (1995a) Gene phylogeny of the *Ganoderma lucidum* complex based on ribosomal DNA sequences. Comparison with traditional taxonomic characters. Mycological Research 99(12): 1489–1499. https://doi.org/10.1016/S0953-7562(09)80798-3

Moncalvo JM, Wang HH, Hseu RS (1995b) Phylogenetic relationships in *Ganoderma* inferred from the internal transcribed spacers and 25S ribosomal DNA sequences. Mycologia 87(2): 223–238. https://doi.org/10.1080/00275514.1995.12026524

Murrill WA (1908) Agaricales (Polyporaceae). North American Flora 9: 73–131.

Nilsson RH, Kristiansson E, Ryberg M, Hallenberg N, Larsson KH (2008) Intraspecific ITS variability in the kingdom fungi as expressed in the international sequence databases and its implications for molecular species identification. Evolutionary Bioinformatics Online 4: 193–201. https://doi.org/10.4137/EBO.S653

Nilsson RH, Larsson KH, Taylor AFS, Bengtsson-Palme J, Jeppesen TS, Schigel D, Kennedy P, Picard K, Glöckner FO, Tedersoo L, Saar I, Kõljalg U, Abarenkov K (2019) The UNITE database for molecular identification of fungi: handling dark taxa and parallel taxonomic classifications. Nucleic Acids Research 47(D1): D259–D264. https://doi.org/10.1093/nar/gky1022

Nilsson RH, Ryberg M, Kristiansson E, Abarenkov K, Larsson K-H, Kõljalg U (2006) Taxonomic reliability of DNA sequences in public sequence databases: a fungal perspective. PLoS ONE 1(1): e59. https://doi.org/10.1371/journal.pone.0000059

Nilsson RH, Sánchez-García M, Ryberg M, Abarenkov K, Wurzbacher C, Kristiansson E (2017) Read quality-based trimming of the distal ends of public fungal DNA sequences is nowhere near satisfactory. MycoKeys 26: 13–24. https://doi.org/10.3897/mycokeys.26.14591

Nilsson R, Tedersoo L, Abarenkov K, Ryberg M, Kristiansson E, Hartmann M, Schoch C, Nylander J, Bergsten J, Porter T, Jumpponen A, Vaishampayan P, Ovaskainen O, Hallenberg N, Bengtsson-Palme J, Eriksson K, Larsson K, Larsson E, Kõljalg U (2012) Five simple guidelines for establishing basic authenticity and reliability of newly generated fungal ITS sequences. MycoKeys 4: 37–63. https://doi.org/10.3897/mycokeys.4.3606

Ntougias S, Baldrian P, Ehaliotis C, Nerud F, Antoniou T, Merhautová V, Zervakis GI (2012) Biodegradation and detoxification of olive mill wastewater by selected strains of the mushroom genera *Ganoderma* and *Pleurotus*. Chemosphere 88(5): 620–626. https://doi.org/10.1016/j.chemosphere.2012.03.042

Nunez M, Ryvarden L (2000) East Asian polypores 1. Ganodermataceae and Hymenochaetaceae. Synopsis Fungorum 13: 1–168.

Okonechnikov K, Golosova O, Fursov M (2012) Unipro UGENE: a unified bioinformatics toolkit. Bioinformatics 28(8): 1166–1167. https://doi.org/10.1093/bioinformatics/bts091

Otto EC, Blanchette RA, Held BW, Barnes CW, Obodai M (2016) *Ganoderma mbrekobenum*. Persoonia 36: 316–458. https://doi.org/10.3767/003158516X692185

Papp V, Dima B, Wasser SP (2017) What is *Ganoderma lucidum* in the Molecular Era? International Journal of Medicinal Mushrooms 19(7): 575–593. https://doi.org/10.1615/IntJMedMushrooms.2017021195

Park YJ, Kwon OC, Son ES, Yoon DE, Han W, Yoo Y-B, Lee C-S (2012) Taxonomy of *Ganoderma lucidum* from Korea based on rDNA and partial beta-tubulin gene sequence analysis. Mycobiology 40(1): 71–75. https://doi.org/10.5941/MYCO.2012.40.1.071

Paterson RR (2006) *Ganoderma* – a therapeutic fungal biofactory. Phytochemistry 67(18): 1985–2001. https://doi.org/10.1016/j.phytochem.2006.07.004

Patouillard N (1889) Le genre *Ganoderma*. Bulletin Trimestriel de la Société Mycologique de France 5: 64–80.

Pegler DN, Yao YJ (1996) Oriental species of *Ganoderma* section *Ganoderma*. In: Wasser SP (Ed.) Botany and Mycology for the Next Millennium: Collection of Scientific Articles Devoted to the 70th Anniversary of Academician Sytnik KM. Kholodny NG Institute of Botany. National Academy of Sciences of Ukraine, Kyiv, 336–347.

Richter C, Wittstein K, Kirk PM, Stadler M (2015) An assessment of the taxonomy and chemotaxonomy of *Ganoderma*. Fungal Diversity 71: 1–15. https://doi.org/10.1007/s13225-014-0313-6

Ronquist F, Teslenko M, van der Mark P, Ayres DL, Darling A, Höhna S, Larget B, Liu L, Suchard MA, Huelsenbeck JP (2012) MrBayes 3.2: efficient Bayesian phylogenetic inference and model choice across a large model space. Systematic Biology 61(3): 539–542. https://doi.org/10.1093/sysbio/sys029

Ryberg M, Nilsson RH, Kristiansson E, Töpel M, Jacobsson S, Larsson E (2008) Mining metadata from unidentified ITS sequences in GenBank: A case study in *Inocybe* (Basidiomycota). BMC Evolutionary Biology 8: 1–50. https://doi.org/10.1186/1471-2148-8-50

Ryvarden L (1976) The Polyporaceae of North Europe. Fungiflora, Oslo, 214 pp.

Ryvarden L (1991) Genera of Polypores; nomenclature and taxonomy. Synopsis Fungorum 5: 1–373.

Ryvarden L (2000) Studies in Neotropical polypores 2: a preliminary key to Neotropical species of *Ganoderma* with a laccate pileus. Mycologia 92(1): 180–191. https://doi.org/10.1080/00275514.2000.12061142

Ryvarden L (2004) Neotropical polypores: Part 1. Introduction, Ganodermataceae & Hymenochataceae. Fungiflora, Oslo, 227 pp.

Ryvarden L, Gilbertson RL (1993) European polypores (Vol. 1). (Abortiporus-Lindtneria). Synopsis Fungorum 6, Fungiflora, Oslo, 387 pp.

Ryvarden L, Meijer AAR de (2002) Studies in neotropical polypores 14. New species from the state of Paraná, Brazil. Synopsis Fungorum 15: 34–69.

Ryvarden L, Melo I (2017) Poroid fungi of Europe, 2nd Edition. Synopsis Fungorum 37: 1–431.

Sahebi M, Hanafi MM, van Wijnen AJ, Akmar ASN, Azizi P, Idris AS, Taheri S, Foroughi M (2017) Profiling secondary metabolites of plant defence mechanisms and oil palm in response to *Ganoderma boninense* attack. International Biodeterioration and Biodegradation 122: 151–164. https://doi.org/10.1016/j.ibiod.2017.04.016

Salazar WA, Barnes CW, Ordoñez ME (2016) *Ganoderma ecuadoriense*. Persoonia 36: 316–458. https://doi.org/10.3767/003158516X692185

Santamaria M, Fosso B, Licciulli F, Balech B, Larini I, Grillo G, De Caro G, Liuni S, Pesole G (2018) ITSoneDB: a comprehensive collection of eukaryotic ribosomal RNA Internal Transcribed Spacer 1 (ITS1) sequences. Nucleic Acids Research 46(D1): D127–D132. https://doi.org/10.1093/nar/gkx855

Schoch CL, Robbertse B, Robert V, Vu D, Cardinali G, Irinyi L, Meyer W, Nilsson RH, Hughes K, Miller AN, Kirk PM, Abarenkov K, Aime MC, Ariyawansa HA, Bidartondo M, Boekhout T, Buyck B, Cai Q, Chen J, Crespo A, Crous PW, Damm U, De Beer ZW, Dentinger BTM, Divakar PK, Dueñas M, Feau N, Fliegerova K, García MA, Ge Z-W, Griffith GW, Groenewald JZ, Groenewald M, Grube M, Gryzenhout M, Gueidan C, Guo L, Hambleton S, Hamelin R, Hansen K, Hofstetter V, Hong S-B, Houbraken J, Hyde KD, Inderbitzin P, Johnston PR, Karunarathna SC, Kõljalg U, Kovács GM, Kraichak E, Krizsan K, Kurtzman CP, Larsson K-H, Leavitt S, Letcher PM, Liimatainen K, Liu J-K, Lodge DJ, Luangsa-ard JJ, Lumbsch HT, Maharachchikumbura SSN, Manamgoda D, Martín MP, Minnis AM, Moncalvo J-M, Mulè G, Nakasone KK, Niskanen T, Olariaga I, Papp T, Petkovits T, Pino-Bodas R, Powell MJ, Raja HA, Redecker D, Sarmiento-Ramirez JM, Seifert KA, Shrestha B, Stenroos S, Stielow B, Suh S-O, Tanaka K, Tedersoo L, Telleria MT, Udayanga D, Untereiner WA, Uribeondo JD, Subbarao KV, Vágvölgyi C, Visagie C, Voigt K, Walker DM, Weir BS, Weiß M, Wijayawardene NN, Wingfield MJ, Xu JP, Yang ZL, Zhang N, Zhuang W-Y, Federhen S (2014) Finding needles in haystacks: linking scientific names, reference specimens and molecular data for Fungi. Database (Oxford), Article ID bau061, 21 pp. https://doi.org/10.1093/database/bau061

Schoch CL, Seifert KA, Huhndorf S, Robert V, Spouge JL, Levesque CA, Chen W, Fungal Barcoding Consortium (2012) Nuclear ribosomal internal transcribed spacer (ITS) region as a universal DNA barcode marker for fungi. Proceedings of the National Academy of Sciences of USA 109(16): 6241–6246. https://doi.org/10.1073/pnas.1117018109

Smith BJ, Sivasithamparam K (2000) Internal transcribed spacer ribosomal DNA sequence of five species of *Ganoderma* from Australia. Mycological Research 104(8): 943–951. https://doi.org/10.1017/S0953756200002458

Smith ME, Douhan GW, Rizzo DM (2007) Intra-specific and intra-sporocarp ITS variation of ectomycorrhizal fungi as assessed by rDNA sequencing of sporocarps and pooled ectomycorrhizal roots from a *Quercus* woodland. Mycorrhiza 18(1): 15–22. https://doi.org/10.1007/s00572-007-0148-z

Stalpers JA (1978) Identification of wood-inhabiting fungi in pure culture. Studies in Mycology 16: 1–248.

Stamatakis A (2014) RAxML version 8: a tool for phylogenetic analysis and post-analysis of large phylogenies. Bioinformatics 30(9): 1312–1313. https://doi.org/10.1093/bioinformatics/btu033

Steyaert RL (1967) Les Ganoderma palmicoles. Bulletin du Jardin Botanique National de Belgique 37(4): 465–492. https://doi.org/10.2307/3667472

Steyaert RL (1972) Species of *Ganoderma* and related genera mainly of the Bogor and Leiden Herbaria. Persoonia 7(1): 55–118.

Steyaert RL (1980) Study of some *Ganoderma* species. Bulletin du Jardin Botanique National de Belgique 50(1/2): 135–186. https://doi.org/10.2307/3667780

Swofford DL (2003) PAUP* Phylogenetic Analysis Using Parsimony (*and Other Methods). Sinauer Associates, Sunderland, Massachusetts.

Tchotet Tchoumi JM, Coetzee MPA, Rajchenberg M, Wingfield MJ, Roux J (2018) Three *Ganoderma* species, including *Ganoderma dunense* sp. nov., associated with dying *Acacia cyclops* trees in South Africa. Australasian Plant Pathology 47: 431–447. https://doi.org/10.1007/s13313-018-0575-7

Tchotet Tchoumi JM, Coetzee MPA, Rajchenberg M, Roux J (2019) Taxonomy and species diversity of *Ganoderma* species in the Garden Route National Park of South Africa inferred from morphology and multilocus phylogenies. Mycologia 111(5): 730–747. https://doi.org/10.1080/00275514.2019.1635387

Thawthong A, Hapuarachchi KK, Wen TC, Raspé O, Thongklang N, Kang J-C, Hyde KD (2017) *Ganoderma sichuanense* (Ganodermataceae, Polyporales) new to Thailand. MycoKeys 22: 27–43. https://doi.org/10.3897/mycokeys.22.13083

Torres-Torres MG, Guzmán-Dávalos L, de Mello Gugliotta A (2012) *Ganoderma* in Brazil: known species and new records. Mycotaxon 121: 93–132. https://doi.org/10.5248/121.93

Torres-Torres MG, Ryvarden L, Guzmán-Dávalos L (2015) *Ganoderma* subgenus *Ganoderma* in Mexico. Revista Mexicana de Micologıa 41: 27–45.

Vilgalys R (2003) Taxonomic misidentification in public DNA databases. New Phytologist 160(1): 4–5. https://doi.org/10.1046/j.1469-8137.2003.00894.x

Vu D, Groenewald M, de Vries M, Gehrmann T, Stielow B, Eberhardt U, Al-Hatmi A, Groenewald JZ, Cardinali G, Houbraken J, Boekhout T, Crous PW, Robert V, Verkley GJM (2018) Large-scale generation and analysis of filamentous fungal DNA barcodes boosts coverage for kingdom fungi and reveals thresholds for fungal species and higher taxon delimitation. Studies in Mycology 92: 135–154. https://doi.org/10.1016/j.simyco.2018.05.001

Wang DM, Wu SH (2007) Two species of *Ganoderma* new to Taiwan. Mycotaxon 102: 373–378.

Wang DM, Wu SH (2008) A taxonomic revision of the Ganodermataceae reported from Taiwan. Mycotaxon 104: 297–308.

Wang DM, Wu SH (2010) *Ganoderma hoehnelianum* has priority over *G. shangsiense*, and *G. williamsianum* over *G. meijiangense*. Mycotaxon 113: 343–349. https://doi.org/10.5248/113.343

Wang DM, Wu SH, Yao Y-J (2014) Clarification of the concept of *Ganoderma orbiforme* with high morphological plasticity. PLoS ONE 9(5): e98733. https://doi.org/10.1371/journal.pone.0098733

Wang DM, Yao Y-J (2005) Intrastrain internal transcribed spacer heterogeneity in *Ganoderma* species. Canadian Journal of Microbiology 51(2): 113–121. https://doi.org/10.1139/w04-118

Wang X-C, Liu C, Huang L, Bengtsson-Palme J, Chen H, Zhang, J-H, Cai D, Li J-Q (2015) ITS1: A DNA barcode better than ITS2 in eukaryotes? Molecular Ecology Resources 15(3): 573–586. https://doi.org/10.1111/1755-0998.12325

Wang XC, Xi RJ, Li Y, Wang D-M, Yao Y-J (2012) The species identity of the widely cultivated *Ganoderma*, 'G. lucidum' (Ling-zhi), in China. PLoS ONE 7(7): e40857. https://doi.org/10.1371/journal.pone.0040857

Wasser SP, Zmitrovich IV, Didukh MY, Didukh MY, Spirin WA, Malysheva VF (2006) Morphological Traits of *Ganoderma lucidum* Complex Highlighting *G. tsugae* var. *jannieae*: the Current Generalization. Ruggel: A.R.A. Gantner Verlag K.-G, Germany, 187 pp.

Welti S, Courtecuisse R (2010) The Ganodermataceae in the French West Indies (Guadeloupe and Martinique). Fungal Diversity 43: 103–126. https://doi.org/10.1007/s13225-010-0036-2

White TJ, Burns T, Lee S, Taylor J (1990) Amplification and direct sequencing of fungal ribosomal RNA genes for phylogenetics. In: Innis M, Gelfand D, Sninsky J, White T (Eds) PCR protocols: a guide to methods and applications. San Diego: Academic Press, 315–322. https://doi.org/10.1016/B978-0-12-372180-8.50042-1

Wu Q-X, Mueller GM, Lutzoni FM, Huang YQ, Guo SY (2000) Phylogenetic and biogeographic relationships of eastern Asian and eastern North American disjunct *Suillus* species (Fungi) as inferred from nuclear ribosomal RNA ITS sequences. Molecular Phylogenetics and Evolution 17(1): 37–47. https://doi.org/10.1006/mpev.2000.0812

Xing J-H, Song J, Decock C, Cui BK (2016) Morphological characters and phylogenetic analysis reveal a new species within the *Ganoderma lucidum* complex from South Africa. Phytotaxa 266(2): 115–124. https://doi.org/10.11646/phytotaxa.266.2.5

Xing J-H, Sun YF, Han YL, Cui BK, Dai YC (2018) Morphological and molecular identification of two new *Ganoderma* species on *Casuarina equisetifolia* from China. MycoKeys 34: 93–108. https://doi.org/10.3897/mycokeys.34.22593

Yang RH, Su JH, Shang JJ, Wu YY, Li Y, Bao DP, Yao YJ (2018) Evaluation of the ribosomal DNA internal transcribed spacer (ITS), specifically ITS1 and ITS2, for the analysis of fungal diversity by deep sequencing. PLoS ONE 13(10): e0206428. https://doi.org/10.1371/journal.pone.0206428

Yao Y-J, Wang X-C, Wang B (2013) Epitypification of *Ganoderma sichuanense* J.D. Zhao & X.Q. Zhang (Ganodermataceae). Taxon 62(5): 1025–1031. https://doi.org/10.12705/625.10

Ye L, Karunarathna SC, Mortimer PE, Li H, Qiu MH, Peng XR, Luangharn T, Li YJ, Promputtha I, Hyde KD, Xu JC (2019) *Ganoderma weixiensis* (Polyporaceae, Basidiomycota), a new member of the *G. lucidum* complex from Yunnan Province, China. Phytotaxa 423(2): 75–86. https://doi.org/10.11646/phytotaxa.423.2.3

Zervakis G, Dimou D, Balis C (1998) A check-list of the Greek macrofungi, including hosts and biogeographic distribution: I. Basidiomycotina. Mycotaxon 66: 273–336.

Zervakis GI, Moncalvo JM, Vilgalys R (2004) Molecular phylogeny, biogeography and speciation of the mushroom species *Pleurotus cystidiosus* and allied taxa. Microbiology 150(3): 715–726. https://doi.org/10.1099/mic.0.26673-0

Zervakis GI, Ntougias S, Gargano ML, Besi MI, Polemis E, Typas MA, Venturella G (2014) A reappraisal of the *Pleurotus eryngii* complex – New species and taxonomic combinations based on the application of a polyphasic approach, and an identification key to *Pleurotus* taxa associated with Apiaceae plants. Fungal Biology 118(9–10): 814–834. https://doi.org/10.1016/j.funbio.2014.07.001

Zervakis GI, Venturella G, Fryssouli V, Inglese P, Polemis E, Gargano ML (2019) *Pleurotus opuntiae* revisited – An insight to the phylogeny of dimitic *Pleurotus* species with emphasis on the *P. djamor* complex. Fungal Biology 123(3): 188–199. https://doi.org/10.1016/j.funbio.2018.12.005

Zhao JD (1989) The Ganodermataceae in China. Bibliotheca Mycologica, Band 132. J. Cramer, Berlin – Stuttgart, 176 pp.

Zhao JD, Hsu LW, Zhang XQ (1979a) *Ganoderma tenue*. Acta Microbiologica Sinica 271.

Zhao JD, Xu LW, Zhang XQ (1979b) Taxonomic studies on the subfamily Ganodermiodeae of China. Acta Microbiologica Sinica 19: 265–279.

Zhao JD, Zhang XQ (2000) Flora fungorum sinicorum vol.18, Ganodermataceae. Science Press, Beijing, 178 pp.

Zhou LW, Cao Y, Wu SH, Vlasák J, Li DW, Li MJ, Dai YC (2015) Global diversity of the *Ganoderma lucidum* complex (Ganodermataceae, Polyporales) inferred from morphology and multilocus phylogeny. Phytochemistry 114: 7–15. https://doi.org/10.1016/j.phytochem.2014.09.023

Zhou XW, Cong WR, Su KQ, Zhang YM (2013) Ligninolytic enzymes from *Ganoderma* spp: current status and potential applications. Critical Reviews in Microbiology 39(4): 416–426. https://doi.org/10.3109/1040841X.2012.722606

Supplementary material 1

Tables S1–S6

Authors: Vassiliki Fryssouli, Georgios I. Zervakis, Elias Polemis, Milton A. Typas

Data type: species data

Explanation note: **Table S1.** Information about the *Ganoderma* material/specimens analyzed for the first time in the frame of this work: species name (the initial name appears in parenthesis when different from the one determined in the present study), specimens code, plant host, geographic origin, collector and date of collection, type of material examined (H: herbarium specimen, C: pure culture) and GenBank accession number of the generated ITS sequences. **Table S2.** Detailed information on the *Ganoderma* ITS sequences used in this study. **Table S3.** *Ganoderma* sequences excluded from the analysis since they were either erroneously labelled as *Ganoderma* or whose identity could not be reliably resolved. **Table S4.** *Ganoderma* sequences (642) included in the data analysis but excluded from the trees inferred (Figs. 4 to 7, and Figs. S2a to Fig. S2f) due to overrepresentation of certain species (i.e., > 100 singletons for *G. lingzhi*, *G. multipileum* and *G. applanatum*) or to their particularly high heterogeneity. **Table S5.** Information about the 354 environmental samples analyzed and their identity on the basis of the outcome of the present study. **Table S6.** *Ganoderma* entries (3908) analyzed: initial identification (as labelled in GenBank/ENA/DDBJ and UNITE databases), accession number, corresponding UNITE DOI and taxon name on the basis of the outcome of this study.

Link: https://doi.org/10.3897/mycokeys.75.59872.suppl1

Supplementary material 2

Figure S1

Authors: Vassiliki Fryssouli, Georgios I. Zervakis, Elias Polemis, Milton A. Typas

Data type: molecular data

Explanation note: Hypervariable regions of potential diagnostic value in ITS1 and ITS2 spacers for the *Ganoderma* taxa appearing in Table 1, Supplementary Table S2 and Fig. 3.

Link: https://doi.org/10.3897/mycokeys.75.59872.suppl2

Supplementary material 3

Figure S2a

Authors: Vassiliki Fryssouli, Georgios I. Zervakis, Elias Polemis, Milton A. Typas

Data type: molecular data

Explanation note: Phylogenetic reconstruction of the genus *Ganoderma* inferred from ML analysis based on ITS sequence data (pDS1a; Table 2) for Clade A, Cluster A.1. ML bootstrap values (BS) ≥ 65% and Bayesian posterior probabilities (BPP) ≥ 0.95 are shown.

Link: https://doi.org/10.3897/mycokeys.75.59872.suppl3

Supplementary material 4

Figure S2b

Authors: Vassiliki Fryssouli, Georgios I. Zervakis, Elias Polemis, Milton A. Typas

Data type: molecular data

Explanation note: Phylogenetic reconstruction of the genus *Ganoderma* inferred from ML analysis based on ITS sequence data (pDS1b; Table 2) for Clade A, Cluster A.2. ML bootstrap values (BS) ≥ 65% and Bayesian posterior probabilities (BPP) ≥ 0.95 are shown.

Link: https://doi.org/10.3897/mycokeys.75.59872.suppl4

Supplementary material 5

Figure S2c

Authors: Vassiliki Fryssouli, Georgios I. Zervakis, Elias Polemis, Milton A. Typas

Data type: molecular data

Explanation note: Phylogenetic reconstruction of the genus *Ganoderma* inferred from ML analysis based on ITS sequence data (pDS1c; Table 2) for Clade A, Cluster A.3. ML bootstrap values (BS) ≥ 65% and Bayesian posterior probabilities (BPP) ≥ 0.95 are shown.

Link: https://doi.org/10.3897/mycokeys.75.59872.suppl5

Supplementary material 6

Figure S2d

Authors: Vassiliki Fryssouli, Georgios I. Zervakis, Elias Polemis, Milton A. Typas

Data type: molecular data

Explanation note: Phylogenetic reconstruction of the genus *Ganoderma* inferred from ML analysis based on ITS sequence data (pDS2 & pDS3; Table 2) for Clades B & C. ML bootstrap values (BS) ≥ 65% and Bayesian posterior probabilities (BPP) ≥ 0.95 are shown.

Link: https://doi.org/10.3897/mycokeys.75.59872.suppl6

Supplementary material 7

Figure S2e

Authors: Vassiliki Fryssouli, Georgios I. Zervakis, Elias Polemis, Milton A. Typas

Data type: molecular data

Explanation note: Phylogenetic reconstruction of the genus *Ganoderma* inferred from ML analysis based on ITS sequence data (pDS4; Table 2) for Clade D. ML bootstrap values (BS) ≥ 65% and Bayesian posterior probabilities (BPP) ≥ 0.95 are shown.

Link: https://doi.org/10.3897/mycokeys.75.59872.suppl7

Supplementary material 8

Figure S2f

Authors: Vassiliki Fryssouli, Georgios I. Zervakis, Elias Polemis, Milton A. Typas

Data type: molecular data

Explanation note: Phylogenetic reconstruction of the genus *Ganoderma* inferred from ML analysis based on ITS sequence data (pDS5; Table 2) for Clade E. ML bootstrap values (BS) ≥ 65% and Bayesian posterior probabilities (BPP) ≥ 0.95 are shown.

Link: https://doi.org/10.3897/mycokeys.75.59872.suppl8

MycoKeys 75: 145–161 (2020)
doi: 10.3897/mycokeys.75.59600
https://mycokeys.pensoft.net

RESEARCH ARTICLE

A peer-reviewed open-access journal
MycoKeys
Launched to accelerate biodiversity research

Three new species from Guangdong Province of China, and a molecular assessment of *Hygrocybe* subsection *Hygrocybe*

Chao-Qun Wang[1], Ming Zhang[1], Tai-Hui Li[1]

1 *Guangdong Provincial Key Laboratory of Microbial Culture Collection and Application, State Key Laboratory of Applied Microbiology Southern China, Guangdong Institute of Microbiology, Guangdong Academy of Sciences, Guangzhou 510070, Guangdong, China*

Corresponding author: Tai-Hui Li (mycolab@263.net)

Academic editor: M. P. Martín | Received 13 October 2020 | Accepted 11 November 2020 | Published 9 December 2020

Citation: Wang C-Q, Zhang M, Li T-H (2020) Three new species from Guangdong Province of China, and a molecular assessment of *Hygrocybe* subsection *Hygrocybe*. MycoKeys 75: 145–161. https://doi.org/10.3897/mycokeys.75.59600

Abstract

Blackening waxcaps (*Hygrocybe* subsect. *Hygrocybe*) are a group of colorful and attractive mushrooms. However, the species diversity of subsect. *Hygrocybe* in China is still poorly known due to the limited sampling. In this study, three new species of this group from Guangdong Province, China are described and illustrated based on their morphological characteristics and molecular analyses of the internal transcribed spacer and large subunit ribosomal DNA regions. *Hygrocybe debilipes* from grasslands of South China Sea islands is mainly characterized by its orange red to vivid red pileus, fragile stipe, and ellipsoid to oblong basidiospores; *H. griseonigricans* from woodlands is characterized by its whitish to dull yellow pileus, quick black discoloration and the globose, subglobose to broadly ovoid basidiospores; *H. rubroconica* from woodlands is characterized by the hemispheric to plano-convex pileus when mature, semitranslucent fibrose stipe, and globose to ellipsoid basidiospores.

Keywords

Asia, black discoloration, new taxa, phylogeny, waxcaps

Introduction

The type species of genus *Hygrocybe* (Fr.) P. Kumm., *H. conica* (Schaeff.) P. Kumm., belongs to subgen. *Hygrocybe* (Fr.) P. Kumm., sect. *Hygrocybe* (Fr.) P. Kumm., subsect. *Hygrocybe* (Fr.) P. Kumm. (Lodge et al. 2014). Taxa of subsect. *Hygrocybe* (*H. conica*-complex) are widely distributed, common and attractive. Morphologically, the group is mainly characterized by the blackening basidiomata, conical and usually fibrillose pileus, free to slightly attached lamellae, parallel and long hymenophoral trama hyphae usually over 200 μm long, and length ratio of basidium to basidiospore usually less than 5 (Lodge et al. 2014). Phylogenetically, members of subsect. *Hygrocybe* are clustered as a monophyletic group using the internal transcribed spacer (ITS) and/or the nuclear large subunit ribosomal DNA (LSU) as gene markers (Babos et al. 2011; Lodge et al. 2014; Vizzini et al. 2015; Deepnalatha and Manimohan 2018; Wang et al. 2019). Ecologically, they are positive environmental indicators in ecosystems since they typically grow in less polluted grasslands or woodlands (Griffith et al. 2002; Wood and Dunkelman 2017).

To date, there are 25 taxa in the world that fit the morphological characteristics of subsect. *Hygrocybe*. Ten taxa under the group have been originally described from Europe: *H. cinereifolia* Courtec. & Priou and *H. nigrescens* (Quél.) Kühner from France, *H. conica* from Germany, *H. conica* var. *aurantiolutea* T. Borgen & Arnolds from Greenland, *H. conica* var. *conicopalustris* (Bon) Arnolds and *H. conica* var. *minor* Monthoux & Röllin from Switzerland, *H. conicoides* (P.D. Orton) P.D. Orton & Watling and *H. olivaceonigra* (P.D. Orton) M.M. Moser from the UK (England), *H. pseudoconica* J.E. Lange from Denmark, and *H. veselskyi* Singer & Kuthan from Czech Republic (Kummer 1871; Lange 1923; Kühner 1926; Moser 1967; Orton and Watling 1969; Singer and Kuthan 1976; Arnolds 1986; Courtecuisse 1992; Monthoux and Röllin 1993; Borgen and Arnolds 2004). Five taxa were originally described from Africa; they are *H. astatogala* (R. Heim) Heinem. from Madagascar, *H. astatogala* var. *laeticolor* Heinem., *H. conica* var. *pallidipes* Heinem. and *H. cortinata* Heinem. from Zaire, and *H. chloroides* (Malançon) Kovalenko from Marocco (Heinemann 1963; Kovalenko 1989). Five taxa have been originally described from North America, including *H. albifolia* (Hesler & A.H. Sm.) R. Valenz., Guzmán & J. Castillo, *H. foliirubens* Murrill, *H. singeri* (A.H. Sm. & Hesler) Singer and *H. cuspidata* (Peck) Murrill from the USA, and *H. conica* var. *atrosanguinea* (Grund & K.A. Harrison) Malloch from Canada (Nova Scotia) (Murrill 1941; Singer 1958; Valenzuela et al. 1981; Malloch 2010). Two taxa have been originally described from Asia, *H. conica* var. *peradenyca* (Sacc.) Pegler from Sri Lanka and *H. erinacea* (Pat.) Singer from Vietnam (Singer 1958; Pegler 1986). Two taxa were described from the Caribbean Region, *H. atrosquamosa* Pegler from Martinique and *H. conica* var. *brevispora* (Dennis) S.A. Cantrell & Lodge from Venezuela (Pegler 1983; Cantrell and Lodge 2000). In addition, *H. conica* var. *tierneyi* A.M. Young was originally described from Australia (Young and Wood 1997).

The existing knowledge about blackening *Hygrocybe* in China is still rather limited. There have been no phylogenetic studies based on Chinese specimens until now. No new species of subsect. *Hygrocybe* has been described from China, while the Chinese

samples of this group are commonly treated as European species, such as *H. conica* and *H. nigrescens* (Chen and Li 2013).

Guangdong Province, which is located in South China, belongs to the East Asian monsoon region. The climate can be divided into the middle subtropical, the southern subtropical, and the tropical climate zones, from north to south. The annual average temperature is 19–24 °C and the average annual precipitation is 1300–2500 mm. During the authors' field trips over the past ten years, numerous samples of blackening waxcaps with diverse morphological characteristics have been found. Obviously, the species diversity of subsect. *Hygrocybe* in Guangdong Province has been underestimated in the past.

In this study, a new worldwide phylogenetic framework of subsect. *Hygrocybe* is reconstructed using the ITS and LSU regions. Three new species from Guangdong Province are described based on the morphological characteristics, molecular phylogenetic evidence, and ecological data.

Materials and methods

Sampling and morphological studies

For each collection, fresh specimens were observed, photographed, and collected in situ; the date, location, collector, elevation, habitat and macroscopic characteristics were documented, and then, the specimens were dried below 50 °C overnight in an electric dryer. Macroscopic descriptions were based on the field records and colored photos. Color descriptions and codes refer to Kornerup and Wanscher (1978). Sizes and shapes of basidiospores, basidia, pileipellis, stipitipellis, and hymenophoral trama were observed using handmade tissues stained with 5% potassium hydroxide solution and/or 1% Congo red solution under an AX10 light microscope and photographed using ZEN 2 lite software (Zeiss, Oberkochen, Germany). The detailed measurement method has been described by Wang et al. (2020). Specimens are deposited in the Fungarium of Guangdong Institute of Microbiology, Guangzhou, China (GDGM).

DNA extraction, PCR amplification and sequencing

Genomic DNAs were extracted from a small amount of dry lamellar tissue using the HiPure Fungus DNA Mini kit (Magen Biotech, Guangzhou, China). ITS and LSU gene regions were amplified using Polymerase chain reactions (PCR) with primers ITS1/ITS1F/ITS5 and ITS4 (White et al. 1990; Gardes and Bruns 1993), LR0R and LR5/LR7 (https://sites.duke.edu/vilgalyslab/rdna_primers_for_fungi/), respectively. Bidirectional PCR product sequencing was carried out using the same primers that were used in the PCR reactions. The forward and reverse raw sequences were assembled and trimmed using SeqMan version 7.1.0 (DNAStar, Inc.). The consensus sequences were blasted in the National Center for Biotechnology Information (NCBI) to rule out the possibility of contamination, and then the correct consensus sequences were

deposited in the International Nucleotide Database [accession numbers: MW001782–MW001792 (ITS), MW007875–MW007884 (LSU)].

Phylogenetic analyses

To elucidate the phylogenetic position of the fungal samples with new sequences within the genus *Hygrocybe*, the newly obtained and all the available *Hygrocybe* LSU sequences in NCBI were included. In addition, the sequences of *Hygroaster albellus* Singer (EF551314), *Ha. nodulisporus* (Dennis) Singer (EF561625), and "*H. andersonii* Cibula & N.S. Weber" (KF291171) were selected as the outgroup, according to Vizzini et al. (2015). To clarify the phylogenetic position of the new sequences within subsect. *Hygrocybe*, the newly gained and all usable ITS sequences of sect. *Hygrocybe* were included, and members of subsect. *Macrosporae* were treated as the outgroup, according to Lodge et al. (2014) and Wang et al. (2019). To make LSU and ITS matrixes, the new sequences and the downloaded reference sequences were first combined, aligned using MAFFT online service (Katoh et al. 2017) by applying the auto strategy, and then viewed and trimmed (the front and back parts) using MEGA-X software (Kumar et al. 2018). The data alignments have been submitted to TreeBASE, submission ID 27252 (LSU) and 27253 (ITS). The substitution models were selected using the Bayesian information criterion with ModelFinder (Kalyaanamoorthy et al. 2017) in PhyloSuite (Zhang et al. 2020). Phylogenetic analysis for each dataset was performed using the maximum likelihood (ML) in IQ-TREE (Nguyen et al. 2015); and the node bootstrap support values (BS) were estimated using an ultrafast bootstrap with 5000 replicates (Minh et al. 2013). Phylograms were viewed and annotated with iTOL version 5.5 (Letunic and Bork 2016).

Results

Phylogenetic analyses

The LSU alignment contains 138 sequences with 1067 columns, of which 611 are constant sites and 333 are parsimony informative sites. The model of substitution is TIM3e+R4 according to Bayesian Information Criterion using ModelFinder. The ITS alignment has 103 sequences with 772 columns, of which 380 are constant sites and 294 are parsimony informative sites. K3Pu+F+G4 is selected as the best-fit model for the ITS dataset.

In the LSU phylogram (Fig. 1), genus *Hygrocybe* [except for "*H. andersonii*" (KF291171)] forms a strongly supported monophyletic clade with 97% BS; *Hygroaster nodulisporus* (EF561625) and "*H. andersonii*" (KF291171) are clustered (100% BS), in accordance with the LSU analysis of Vizzini et al. (2015). The division of *Hygrocybe* into two subgenera is strongly supported (97% BS). Ten newly generated sequences are present as members of subsect. *Hygrocybe*: three sequences of *H. debilipes* are located at the most distal part of subsect. *Hygrocybe* with 100% BS; three sequences of *H. griseonigricans* appear as a sister clade to an undescribed species (KY090808 and KY090827)

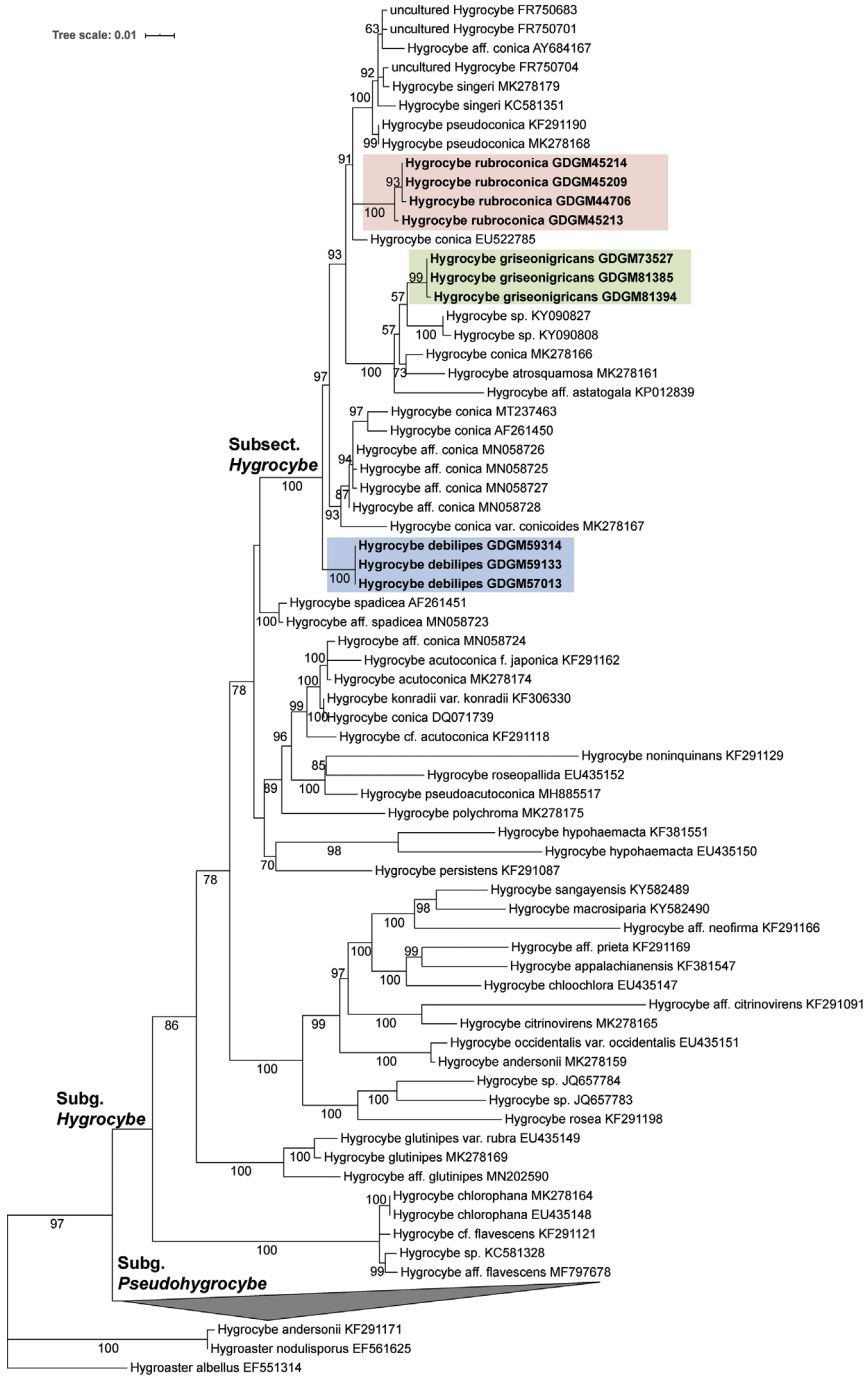

Figure 1. Maximum Likelihood phylogram of genus *Hygrocybe* based on LSU matrix, rooted with *Hygroaster albellus* (EF551314), *H. nodulisporus* (EF561625) and *H. andersonii* (KF291171). The newly generated sequences in this study are showed in bold. GenBank accession numbers of downloaded sequences or voucher numbers of new sequences are given after the species names. Bootstrap values more than 50% are shown around the branches.

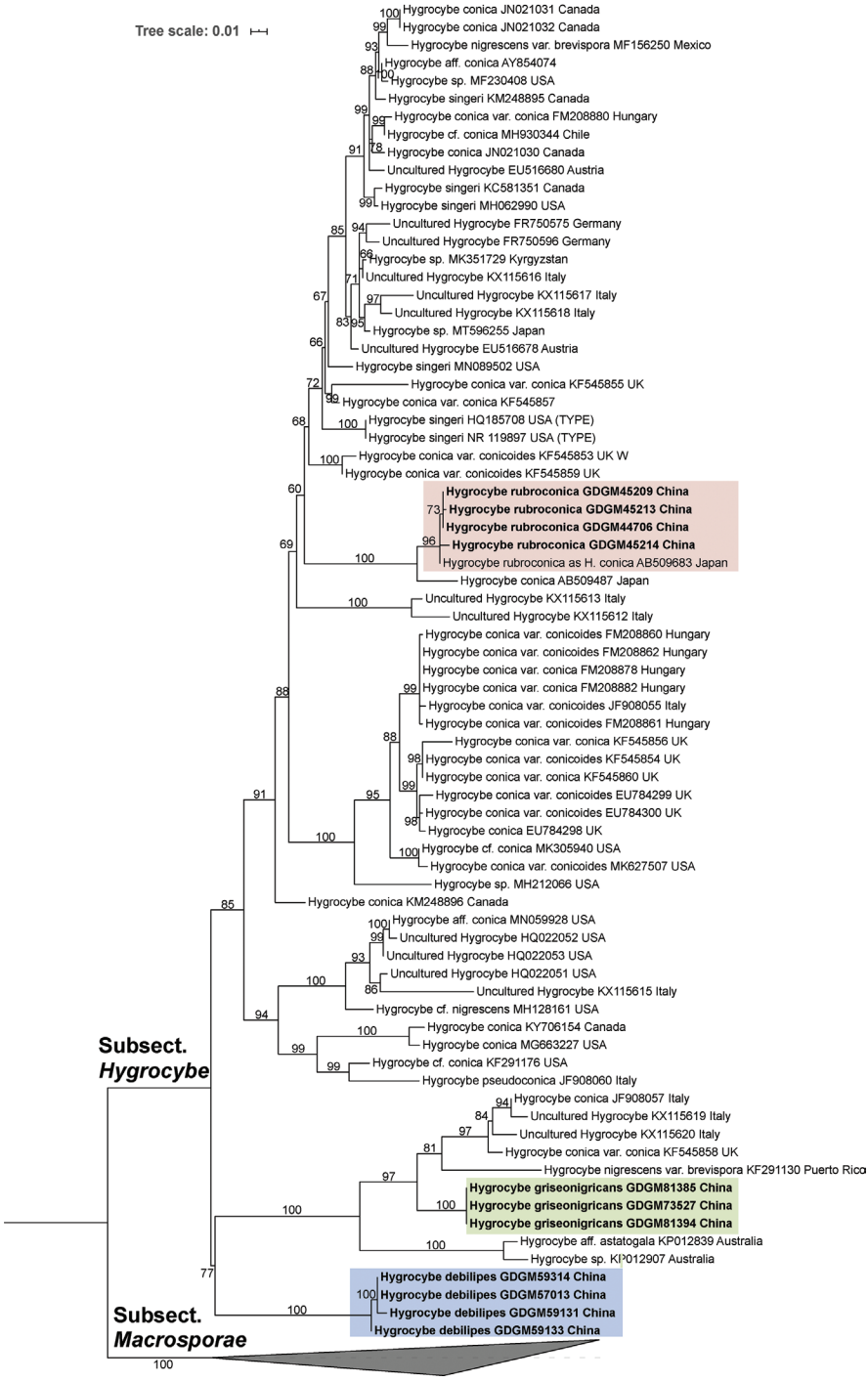

Figure 2. Maximum-likelihood tree of sect. *Hygrocybe* based on ITS matrix, rooted with members of subsect. *Macrosporae*. The newly generated sequences in this study are indicated in bold face. GenBank accession number of downloaded sequence or voucher number of newly generated sequence and place of origin are given after the species name of each sequence. Bootstrap values more than 50% are shown around the branches.

Table 1. Taxa, vouchers, geographic origins and sequence accession numbers of newly generated sequences.

Taxon	Voucher	Geographic origin	ITS	LSU
H. debilipes	GDGM59314	China: Guangdong	MW001783	MW007877
	GDGM57013	China: Guangdong	MW001782	MW007875
	GDGM59131	China: Guangdong	MW001785	–
	GDGM59133	China: Guangdong	MW001784	MW007876
H. griseonigricans	GDGM73527	China: Guangdong	MW001790	MW007883
	GDGM81385	China: Guangdong	MW001791	MW007882
	GDGM81394	China: Guangdong	MW001792	MW007884
H. rubroconica	GDGM45213	China: Guangdong	MW001786	MW007881
	GDGM44706	China: Hunan	MW001788	MW007878
	GDGM45209	China: Guangdong	MW001787	MW007879
	GDGM45214	China: Guangdong	MW001789	MW007880

with limited support (57% BS) within a larger clade containing *H.* aff. *astatogala* (KP012839) and *H. atrosquamosa* (MK278161); four sequences of *H. rubroconica* form an independent clade with high support (100% BS).

In the ITS phylogram (Fig. 2), members of subsect. *Hygrocybe* and subsect. *Macrosporae* are treated as the ingroups and outgroups, respectively. Although all new species are present in subsect. *Hygrocybe*, the ITS analysis produces partially different typologies from the LSU analysis regarding the relationships of taxa under subsect. *Hygrocybe*. In the ITS analysis, four new sequences of *H. debilipes*, three new sequences of *H. griseonigricans*, and five sequences [four newly from China and one from Japan labeled as "*H. conica*" (AB509683)] of *H. rubroconica* form three independent clades, respectively.

Taxonomy

Hygrocybe debilipes **C.Q. Wang & T.H. Li, sp. nov.**
MycoBank No:836234
Figures 3A, B, 4

Typification. China. Guangdong Province, Taishan City, Chuandao Town, Xiachuan Island, on a grassland, elev. ca. 50 m, 21°37'36"N, 112°34'30"E, 17 July 2017, H. Huang, Q.J. Huang & X.R. Zhong (GDGM59314, holotype!).

Sequences ex holotype. MW001783 (ITS), MW007877 (LSU).

Etymology. "*debili-*": not strong, "*-pes*": stipe. The species epithet "*debilipes*" (Lat.) refers to the fragile stipe of the new species.

Diagnosis. *Hygrocybe debilipes* differs from *H. singeri* in having a smaller pileus, orange red to vivid red pileus before discoloration, pale yellow to light orange lamellae, a fragile and less sticky stipe, ellipsoid to oblong basidiospores, and the distribution in South China Sea islands.

Description. Pileus 5–12 mm diam., conical with an acute umbo when young, convex to hemispherical in age, inrolled at margin, orange red (8A7–8), red to vivid red (9A7–8, 9B7–8), blackening with injury or aging, sticky when moist, hygrophanous. Lamellae free, pale yellow (4A3) to light orange (5A4) when mature, blackening

Figure 3. Basidiomes of *Hygrocybe* species **A** *Hygrocybe debilipes* (GDGM59314) **B** *Hygrocybe debilipes* (GDGM57013) **C** *Hygrocybe griseonigricans* (GDGM73527) **D** *Hygrocybe griseonigricans* (GDGM81394) **E** *Hygrocybe rubroconica* (GDGM45213) **F** *Hygrocybe rubroconica* (GDGM45214).

with injury or aging, up to 4 mm broad, distant, waxy, with 1–3 unequal lamellulae between two entire lamellae, with lighter color at lamellar edge. Stipe 22–45 × 2–5 mm, central, cylindrical, equal or slightly tapered at apex, fistulous, semitranslucent, usually too fragile to obtain a complete stipe base, pale yellow (4A3) to light orange (5A4) with white base, blackening with injury or aging, glabrous to fibrillose, moist.

Basidiospores (7.5)8–11.5(12) × (4.5)5–7(7.5) µm [mean length = 9.4 µm, mean width = 6 µm], Q = 1.3–1.8, Q_m = 1.6, ellipsoid to oblong, smooth, thin-walled,

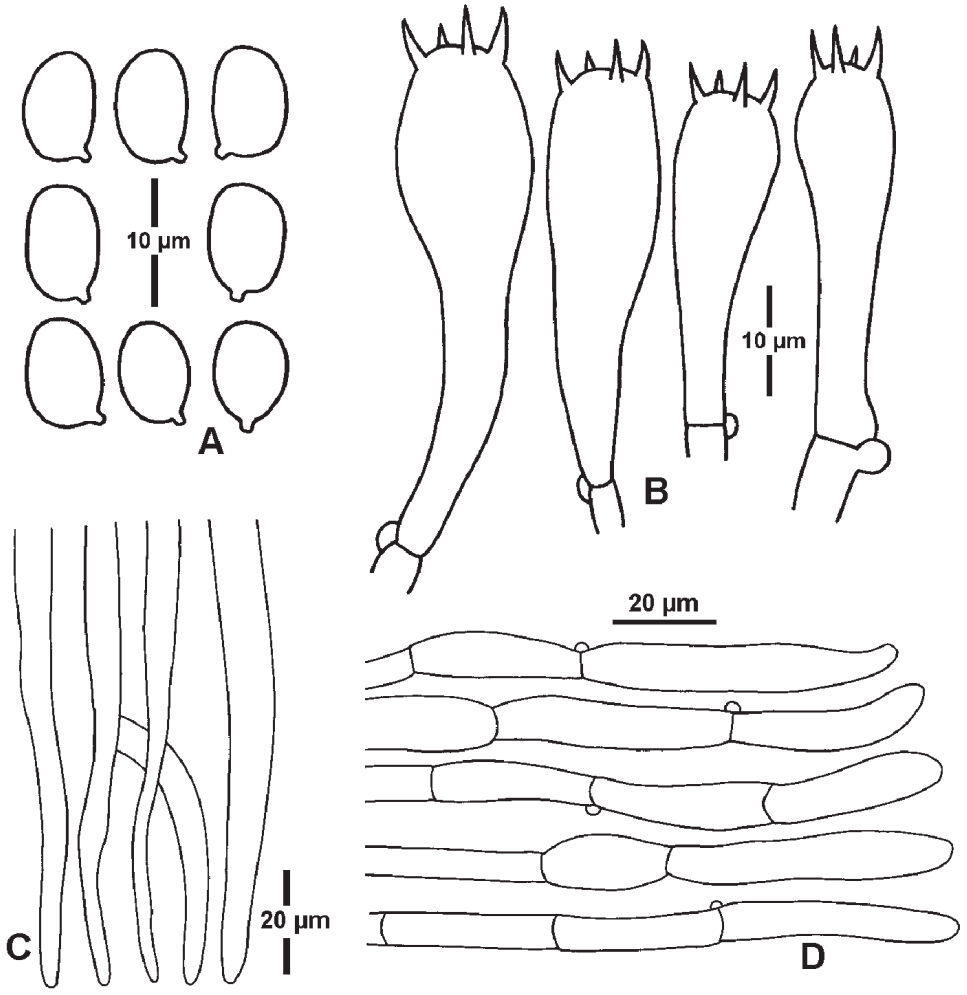

Figure 4. Microscopic features *Hygrocybe debilipes* (GDGM59314) **A** basidiospores **B** basidia **C** terminal cells of hymenophoral trama **D** terminal cells of pileipellis.

hyaline. Basidia 32–53 × 8–13 µm, 4-spored, clavate, with sterigmata up to 7 µm long. Pileipellis a cutis of cylindrical hyphae 2–11 µm diam., thin-walled, hyaline. Stipitipellis a cutis or ixocutis of repent, thin-walled, clamped hyphae 2.5–16 µm diam. Hymenophoral trama regular to subregular, consisting of parallel hyphal cells 4–17 µm diam., thin-walled, hyaline.

Habit, habitat and distribution. Scattered on grasslands in summer. Known from South China Sea islands.

Additional specimens examined. China. Guangdong Province, Taishan City, Chuandao Town, Xiachuan Island, elev. ca. 50 m, 17 July 2017, Q.J. Huang, H. Huang & X.R. Zhong (GDGM59131, GDGM59133); Zhuhai City, Dawanshan Island, 28 July 2013, T.H. Li, H. Huang & Y.W. Xia (GDGM57013).

Remarks. *Hygrocybe debilipes* is morphologically and genetically a distinct species. *Hygrocybe debilipes* is characterized by its tiny basidioma, orange red to vivid red pileus, pale yellow to light orange lamellae when mature, fragile and semitranslucent stipe, and ellipsoid to oblong basidiospores measuring (7.5)8–11.5(12) × (4.5)5–7(7.5) µm. *Hygrocybe debilipes* forms a strongly supported independent clade in both ITS and LSU phylogeny trees (Figs 1–2).

Hygrocybe cinereifolia, originally described from France, is morphologically similar to *H. debilipes* in its general appearance. However, *H. cinereifolia* has larger basidiomata and grayish to gray lamellae (Courtecuisse 1992, http://www.pharmanatur.com/Mycologie/Hygrocybe%20cinereifolia.htm). *Hygrocybe singeri*, originally described from northwestern USA, is also morphologically similar to *H. debilipes*. However, *H. singeri* is larger (10–50 mm diam.), and possesses a yellow to orange pileus and greenish yellow lamellae (Hesler and Smith 1963).

Hygrocybe griseonigricans **C.Q. Wang & T.H. Li, sp. nov.**
MycoBank No:836235
Figures 3C, D, 5

Typification. China. Guangdong Province, Nanxiong City, Qingzhang Mountain, elev. ca. 340 m, 15 May 2018, M. Zhang & X.N. Chen (GDGM73527, holotype!).

Sequences ex holotype. MW001790 (ITS), MW007883 (LSU).

Etymology. "*griseo-*": gray, "*-nigricans*": black. The species epithet "*griseonigricans*" refers to its gray pileus with obvious blackening reaction.

Diagnosis. *Hygrocybe griseonigricans* differs from *H. astatogala* by having a duller pilus color, variable (subglobose to elongate) basidiopore shapes, 1-, 2- and 4-spored basidia and differences in molecular sequences.

Description. Pileus 25–70 mm diam., broad conical to umbonate disc when young, expanded to umbonate, convex, even to almost plane when mature, white, pale yellow (3A3) to dull yellow (3B3), densely covered with radially arranged black hairy fibrils with appressed or uplifted ends on surface, nigrescent when bruised or mature; margin incurved when young, expanded to straight when mature. Lamellae free, white at first, turning black when bruised or mature, up to 7 mm wide, waxy, fragile, with 1–3 lamelluate between two entire lamellae, edge usually eroded. Stipe 50–150 × 5–12 mm, central, cylindrical, sometimes slightly curve, usually wider at base, hollow, white to yellow at the upper part, usually white at the base, changing to black with age or when bruised, covered with clustered black longitudinal fibrils.

Basidiospores 9–10.5 × (6)6.5–9.5(10) µm [mean length = 9.7 µm, mean width = 8 µm], Q = (0.95)1.1–1.6, Q_m = 1.23, globose, subglobose to broadly ovoid, smooth, thin-walled. Basidia 32–44.5 × 8–11.5 µm, 1-, 2- or 4-spored, clavate, with sterigmata up to 10 µm long, sterigmata of 2-spored basidia usually longer than those of 4-spored basidia. Pileipellis a cutis or trichoderm, hyphae 2–15 µm in diam. Hymenophoral trama regular, hyphae 2.5–21 µm broad, translucent, mainly thin-walled rarely thick-walled.

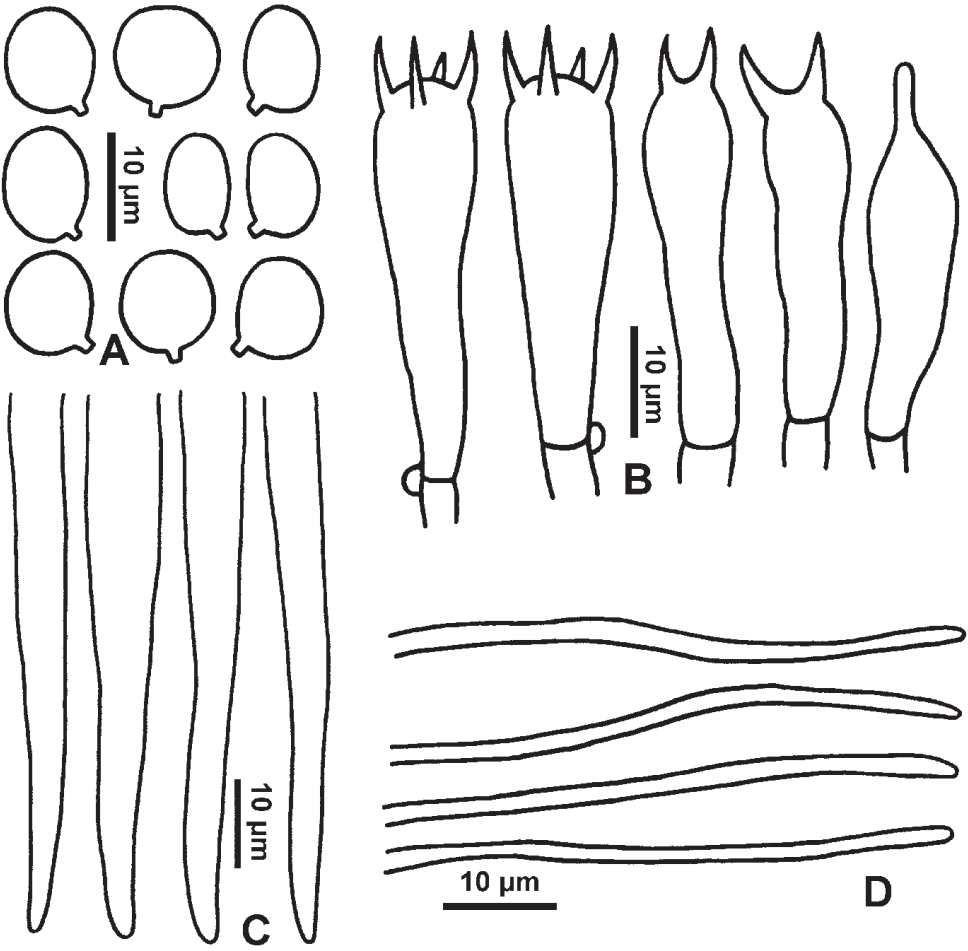

Figure 5. Microscopic features *Hygrocybe griseonigricans* (GDGM73527) **A** basidiospores **B** basidia **C** terminal cells of hymenophoral trama **D** terminal cells of pileipellis.

Habit, habitat and distribution. Solitary to scattered on soil; basidiomata occurring from April to September. So far known from Southern China.

Additional specimens examined. China. Guangdong Province, Nanxiong City, Qingzhang Mountain, elev. ca. 340 m, 15 May 2018, M. Zhang & X.N. Chen (GDGM73528); Renhua County, Danxia Mountain, elev. ca. 100 m, 12 June 2020, M. Zhang & L.Q. Wu (GDGM81385).

Remarks. The distinctive morphological features of *Hygrocybe griseonigricans* are the following: white to dull yellow-colored pileus with black discoloration, white lamellae, white stipe base, and variable basidiospore shapes, from globose, subglobose to broadly ovoid. The ITS and LSU phylogenetic analyses support *H. griseonigricans* as a distinct species within a well-supported clade that includes *H. astatogala* (Figs 1–2).

Hygrocybe conica, originally described from Germany, is similar to *H. griseonigricans*. However, *H. conica* has a larger (up to 100 mm diameter) and somewhat fibrillose

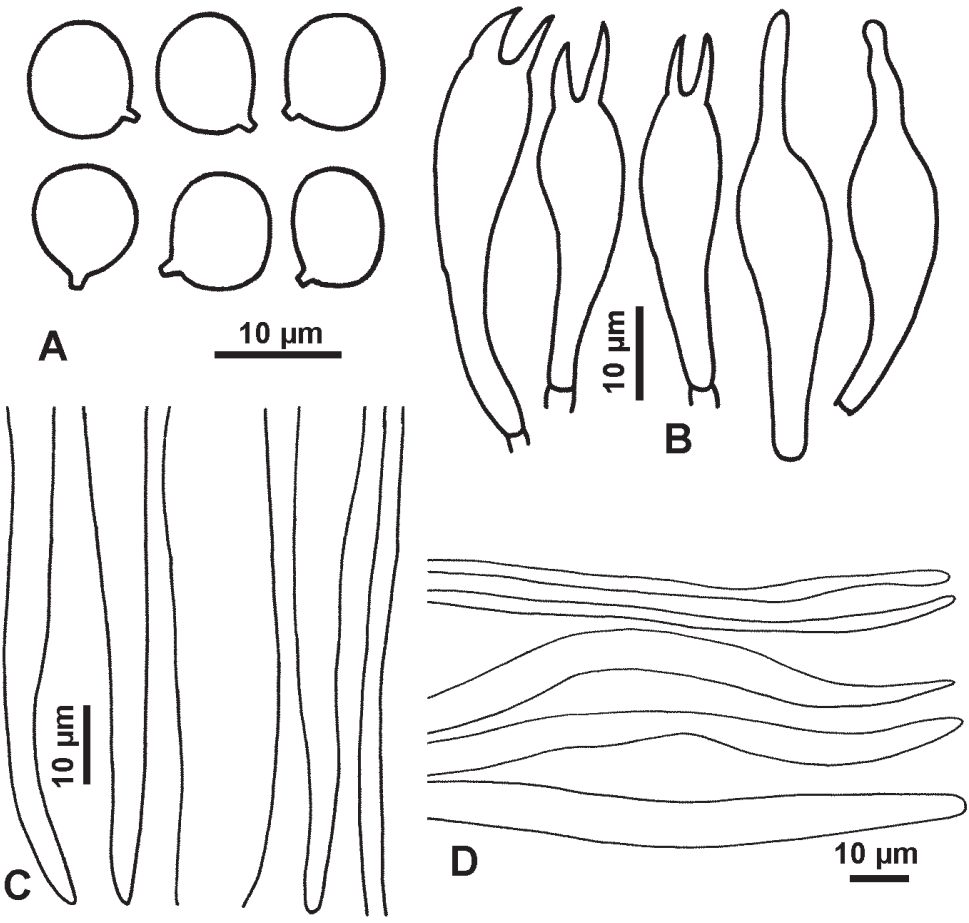

Figure 6. Microscopic features *Hygrocybe rubroconica* (GDGM45213) **A** basidiospores **B** basidia **C** Hymenophoral trama cells **D** terminal cells of pileipellis.

pileus, and usually grayish lamellae (Boertmann 2010). *Hygrocybe astatogala*, originally described from Madagascar, resembles *H. griseonigricans* in the black fibrils on the pileus. However, *H. astatogala*, has distinct and persistent conical and yellow to orange pileus, yellow to orange lamellae, and subglobose to ovoid basidiospores (Horak 1990; Leelavathy et al. 2006).

Hygrocybe rubroconica **C.Q. Wang & T.H. Li, sp. nov.**
MycoBank No:837541
Figures 3E, F, 6

Typification. China. Guangdong Province, Shaoguan City, Ruyang County, Nanling Natural Reserve, elev. ca 1180 m, 15 May 2015, Ming Zhang, Hao Huang and Jiang Xu (GDGM45213, Holotype!).

Sequences ex holotype. MW001786 (ITS), MW007881 (LSU).

Etymology. "*rubro-*": red, "*-conica*": conical. The species epithet "*rubroconica*" refers to its red pileus surface.

Diagnosis. *Hygrocybe rubroconica* differs from *H. conica* by having redder pileus, white to light reddish white and ventricose to broadly ventricose lamellae, simitranslucent stipe covered with white fibrils at first, and mainly 2-spored basidia.

Description. Pileus 5–25 mm broad, conical, conical when young, broadly conical, hemisphere to plano-convex when mature, sometimes with an umbo in center, red to vivid red (10A7–8, 10B7–8), usually darker at disc, translucently striate from the margin to about a half of radius, blackening when bruised or mature; margin incurved, white to light yellow to reddish yellow (4A5–6). Lamellae free, ventricose to broadly ventricose, white to yellowish white, blackening when bruised or mature, up to 4 mm broad, distinct, waxy, fragile, with 1–3 lamellula between two entire lamellae. Stipe 20–40 mm long, 1–4 mm thick, central, cylindrical, slightly enlarged towards the base, hollow, simitranslucent, pale yellow (4A3) to brownish orange (5C3–5), nigrescent when bruised or old, usually covered with white longitudinal fine fibrils when young.

Basidiospores (7.5)8–10.5(11) × (6.5)7–8.5 μm [mean length = 9 μm, mean width = 7.6 μm], Q = 1–1.47, Q_m = 1.2, globose, subglobose, broadly ellipsoid to ellipsoid, smooth, thin-walled. Basidia 25.5–45 × 8.5–12 μm, mainly 2-spored, rarely 4-spored, clavate, containing some black endochrome in KOH, with sterigmata up to 10.5 μm long. Pseudocystidia present. Pileipellis as a cutis, comprised of parallel hyphae 4–10 μm wide, occasionally with bend hyphae, with some black inclusions. Stipipellis made up of parallel hyphae, occasionally with some thick-walled haphae. Hymenophoral trama regular, of hyaline and thin-walled hyphae 8.5–17 μm wide, sometimes containing blackish brown materials.

Habit, habitat and distribution. Scattered to clustered on moist soil in forests; occurring from April to September. So far only known from Southern China.

Additional specimens examined. China. Guangdong Province, Ruyang County, Nanling Natural Reserve, elev. ca. 1400 m, 24°89'N, 113°01'E, 16 June 2014, M. Zhang & T. Li (GDGM45209); same location, 15 May 2015, M. Zhang, H. Huang & J. Xu (GDGM45214).

Remarks. *Hygrocye rubroconica* is characterized by the red pileus, ventricose to broadly ventricose lamellae, nearly translucent stipe covered with white fibrils at first, globose to ellipsoid basidiospores, mainly 2-spored basidia, and the presence of pseudocystidia.

Hygrocybe veselskyi Singer & Kuthan, originally described from Czechoslovakia, resembles *H. rubroconica* in its general appearance due to the red pileus and black staining reaction when touched or mature; however, *H. veselskyi* differs from *H. rubroconica* since it has yellow lamellae and bigger basidiospores measuring 10–12.5 × 5.3–6 μm (Candusso 1997).

Discussion

In this study, three new species of *Hygrocybe* subsect. *Hygrocybe* from Guangdong Province, China are described and compared with similar species based on mor-

phological and molecular data. More comprehensive phylogeny of genus *Hygrocybe* (focusing on subg. *Hygrocybe*) based on the LSU sequences and of sect. *Hygrocybe* based on ITS sequences are provided, including almost all the representatives in GenBank database and newly generated sequences. This study not only provides new species and genetic information of subsect. *Hygrocybe* from East Asia, but also provide some ideas on the species delimitation of subsect. *Hygrocybe* based on morphological and phylogenetic evidences.

Morphologically, the sizes of both fresh and dried basidiomata of *H. griseonigricans*, *H. rubroconica* and *H. debilipes* decrease in turns. The stipe of *H. debilipes* is especially more fragile than that of *H. griseonigricans* or *H. rubroconica*. Although the pileus color is variable within a species, the pileus color range, the pileus blackening rate and degree, and the lamellar color can be used as distinguishing features for distinguishing the three new species in southern China. For example, *H. debilipes* and *H. rubroconica* have a red to orange pileus, while *H. griseonigricans* has a white to yellow pileus. The pileus of *H. griseonigricans* mostly becomes black when mature, while the pileus of *H. debilipes* and *H. rubroconica* seldom becomes black when mature. The lamellar color of *H. debilipes* is orange, while *H. griseonigricans* and *H. rubroconica* have almost white lamellae. In contrast with the macro-morphology, limited micro-morphological features can be used to discriminate the species within subsect. *Hygrocybe*. The intraspecific variations in the basidiospore shape and in the number of basidum sterigmata are small in *H. debilipes*, but large in *H. griseonigricans* and *H. rubroconica*.

Molecular analyses seems to provide more stable information for species identification of subsect. *Hygrocybe*. Taking *H. singeri* as an example (Fig. 2), due to the release of the type specimen's ITS sequences in GenBank (NR_119897 and HQ185708), it is clear that the sequences retrieved from several samples that are labeled as "*H. singeri*" (KM248895, KC581351, MH062990 and MN089502) should be a different species. However, the shortage of released correctly identified sequences is a basic issue that needs to be urgently addressed. Within subsect. *Hygrocybe*, it is highly urgent to obtain the sequences from a well-identified *H. conica* specimen from the type location at Bavaria, Germany, since *H. conica* has undergone various interpretations in different continents (Figs 1–2).

To reach a point in which all validly published species names of blackening waxcaps are represented by pertinent DNA sequences, it is necessary to obtain sequences from well-identified specimens of existing species. These tasks may not be completed in a short time since specimens from the type location need to be found by the researchers, amateurs, or society citizens, and then carefully identified by fungal taxonomists with relevant research experience. In addition, new species should be published based on both morphological and molecular data.

Acknowledgements

The authors thank the editors and reviewers for improving the manuscript. All our colleagues who contributed collections are warmly thanked, especially X.N. Chen, H. Huang, Q.J. Huang, T. Li, L.Q. Wu, Y.W Xia, J. Xu and X.R. Zhong. The authors

thank Editage (www.editage.cn) for English language editing. This study is supported by the National Natural Foundation of China (Nos. 31800013, 31700021, 31770014, 31800014, 31970016), the GDAS' Special Project of Science and Technology Development (No. 2020GDASYL-20200104013), the Biodiversity Survey and Assessment Project of the Ministry of Ecology and Environment, China (No. 2019HJ2096001006), and the Science and Technology Planning Project of Guangdong Province, China (Nos. 2018B030324001, 2018B020205001).

References

Arnolds E (1986) Notes on Hygrophoraceae – VIII. Taxonomic and nomenclatural notes on some taxa of *Hygrocybe*. Persoonia 13(2): 137–160.

Babos M, Halász K, Zagyva T, Zöld-Balogh A, Szegö D, Bratek Z (2011) Preliminary notes on dual relevance of ITS sequences and pigments in *Hygrocybe* taxonomy. Persoonia 26: 99–107. https://doi.org/10.3767/003158511X578349

Boertmann D (2010) The Genus *Hygrocybe*, 2nd revised edition (Fungi of Northern Europe – vol. 1). Danish Mycological Society, Copenhagen, 200 pp.

Borgen T, Arnolds E (2004) Taxonomy, ecology and distribution of *Hygrocybe* (Fr.) P. Kumm. and *Camarophyllopsis* Herink (Fungi, Basidiomycota, Hygrocybeae) in Greenland. Meddelelser om Grønland Bioscience 54: 1–64.

Candusso M (1997) Fungi Europaei 6. *Hygrophorus* s.l. Libreria Basso, Alassio, 784 pp.

Cantrell SA, Lodge DJ (2000) Hygrophoraceae of the Greater Antilles: *Hygrocybe* subgenus *Hygrocybe*. Mycological Research 104(7): 873–878. https://doi.org/10.1017/S0953756299002142

Chen JL, Li Y (2013) The checklist of species in Hygrophoraceae from China and their distribution. Journal of Fungal Research 11: 3–13, 37.

Courtecuisse R (1992) Flore mycologique du littoral – 10 – *Hygrocybe cinereifolia* Courtecuisse & Priou sp. nov. et quelques hygrocybes sabulicoles noircissants. Documents Mycologiques 22(86): 69–73.

Deepnalatha KP, Manimohan P (2018) A new species of *Hygrocybe* from Kerala State, India. Phytotaxa 385(1): 13–22. https://doi.org/10.11646/phytotaxa.385.1.2

Gardes M, Bruns TD (1993) ITS primers with enhanced specificity for basidiomycetes – application to the identification of mycorrhizae and rusts. Molecular Ecology 2: 113–118. https://doi.org/10.1111/j.1365-294X.1993.tb00005.x

Griffith GW, Easton GL, Jones AW (2002) Ecology and diversity of waxcap (*Hygrocybe* spp.) Fungi. Botanical Journal of Scotland 54(1): 7–22. https://doi.org/10.1080/03746600208685025

Heinemann P (1963) Champignons récolétes au Congo par Madame M. Gossens-Fontana. V. Hygrophoraceae. Bulletin du Jardin botanique de l'État a Bruxelles 33: 421–458. https://doi.org/10.2307/3667377

Hesler LR, Smith AH (1963) North American Species of *Hygrophorus*. University of Tennessee Press, Knoxville, 416 pp. https://doi.org/10.5962/bhl.title.61976

Horak E (1990) Monograph of the New Zealand Hygrophoraceae (Agaricales). New Zealand Journal of Botany 28(3): 255–309. https://doi.org/10.1080/0028825X.1990.10412313

Kalyaanamoorthy S, Minh BQ, Wong TKF, von Haeseler A, Jermiin LS (2017) ModelFinder: fast model selection for accurate phylogenetic estimates. Nature Methods 14: 587–589. https://doi.org/10.1038/nmeth.4285

Katoh K, Rozewicki J, Yamada KD (2017) MAFFT online service: multiple sequence alignment, interactive sequence choice and visualization. Briefings in Bioinformatics 20(4): 1160–1166. https://doi.org/10.1093/bib/bbx108

Kornerup A, Wanscher JH (1978) Methuen Handbook of Colour (3rd edn). Eyre Methuen, London, 252 pp.

Kovalenko AE (1989) Definitorium fungorum URSS. Ordo Hygrophorales. Nauka 37, Leningrad, 176 pp.

Kühner R (1926) Contribution à létude des Hyménomycètes et spécialement des agaricacées. Le Botaniste 17: 1–224.

Kumar S, Stecher G, Li M, Knyaz C, Tamura K (2018) MEGA X: Molecular evolutionary genetics analysis across computing platforms. Molecular Biology and Evolution 35(6): 1547–1549. https://doi.org/10.1093/molbev/msy096

Kummer P (1871) Der Führer in die Pilzkunde. C. Luppe, Zerbst, 146 pp.

Lange JE (1923) Studies in the agarics of Denmark. V. Ecological notes. The *Hygrophorei*, *Stropharia* and *Hypholoma*. Supplementary notes to Parts I–III. Dansk Botanisk Arkiv 4(4): 1–55.

Leelavathy KM, Manimohan P, Arnolds EJM (2006) *Hygrocybe* in Kerala State, India. Persoonia 19(1): 101–151.

Letunic I, Bork P (2016) Interactive tree of life (iTOL) v3: an online tool for the display and annotation of phylogenetic and other trees. Nucleic Acids Research 44(W1): W242–W245. https://doi.org/10.1093/nar/gkw290

Lodge DJ, Padamsee M, Matheny PB, Aime MC, Cantrell SA, Boertmann D, Kovalenko A, Vizzini A, Dentinger BTM, Kirk PM, Ainsworth AM, Moncalvo JM, Vilgalys R, Larsson E, Lücking R, Griffith GW, Smith ME, Norvell LL, Desjardin DE, Redhead SA, Ovrebo CL, Lickey EB, Ercole E, Hughes KW, Courtecuisse R, Young A, Binder M, Minnis AM, Lindner DL, Ortiz-Santana B, Haight J, Læssøe T, Baroni TJ, Geml J, Hattori T (2014) Molecular phylogeny, morphology, pigment chemistry and ecology in Hygrophoraceae (Agaricales). Fungal Diversity 64: 1–99. https://doi.org/10.1007/s13225-013-0259-0

Malloch D (2010) Fleshy fungi (Basidiomycota) of the Atlantic Maritime Ecozone. Assessment of Species Diversity in Canadian Ecozones Series: 107–152.

Minh BQ, Nguyen MA, von Haeseler A (2013) Ultrafast approximation for phylogenetic bootstrap. Molecular Biology and Evolution 30(5): 1188–1195. https://doi.org/10.1093/molbev/mst024

Monthoux O, Röllin O (1993) Catalogue des champignons des zones xériques des environs de Genève. Candollea 48(1): 253–278.

Moser MM (1967) Kleine Kryptogamenflora von Mitteleruopa – Die Blätter –und Baupilze (Agaricales und Gastromycetes) Volume: IIb/2. G. Fischer, Stuttgart, 443 pp.

Murrill WA (1941) More Florida novelties. Mycologia 33: 434–448. https://doi.org/10.1080/00275514.1941.12020837

Nguyen LT, Schmidt HA, von Haeseler A, Minh BQ (2015) IQ-TREE: a fast and effective stochastic algorithm for estimating maximum-likelihood phylogenies. Molecular Biology and Evolution 32(1): 268–274. https://doi.org/10.1093/molbev/msu300

Orton PD, Watling R (1969) A reconsideration of the classification of the Hygrophoraceae. Notes from the Royal Botanical Garden Edinburgh 29(1): 129–138.

Pegler DN (1983) Agaric flora of the Lesser Antilles. Kew Bulletin Additional Series 9: 1–668.

Pegler DN (1986) Agaric flora of Sri Lanka. Kew Bulletin Additional Series 12: 1–519.

Singer R (1958) Fungi Mexicani, Series secunda – Agaricales. Sydowia 12: 221–243.

Singer R, Kuthan J (1976) Einige interessante europäische Hygrophoraceae. Zeitschrift für Pilzkunde 42: 5–13.

Valenzuela R, Guzmán G, Castillo J (1981) Descripción de especies de macromicetos poco conocidos en México. Boletín de la Sociedad Mexicana de Micología 15: 67–120.

Vizzini A, Picciola P, Battistin E, Ercole E (2015) *Hygrocybe rubroalba* (Hygrophoraceae, Agaricales), a new species of sect. *Firmae* from Brazil. Phytotaxa 226(1): 18–26. https://doi.org/10.11646/phytotaxa.226.1.2

Wang CQ, Li TH, Huang H, Xia YW (2019) *Hygrocybe pseudoacutoconica* (Hygrocybeae, Hygrocyboideae, Hygrophoraceae), a new species from a South China Sea island. Phytotaxa 400(1): 023–030. https://doi.org/10.11646/phytotaxa.400.1.3

Wang CQ, Li TH, Zhang M, He XL, Qin WQ, Liu TZ, Zeng NK, Wang XH, Liu JW, Wei TZ, Xu J, Li YQ, Shen YH (2020) *Hygrophorus* subsection *Hygrophorus* (Hygrophoraceae, Agaricales) in China. Mycokeys 68: 49–73. https://doi.org/10.3897/mycokeys.68.53264

White TJ, Bruns T, Lee S, Taylor J (1990). Amplification and direct sequencing of fungal ribosomal RNA genes for phylogenetics. In: Innis MA, Gelfand DH, Sninsky JJ, White TJ (Eds) PCR protocols: a guide to methods and applications. Academic Press, San Diego, 315–322. https://doi.org/10.1016/B978-0-12-372180-8.50042-1

Wood E, Dunkelman J (2017) Grassland Fungi: A Field Guide. Monmouthshire Meadows Group.

Young AM, Wood AE (1997) Studies on the Hygrophoraceae (Fungi: Homobasidiomycetes: Agaricales) of Australia. Australian Systematic Botany 10: 911–1030. https://doi.org/10.1071/SB96005

Zhang D, Gao FL, Jakovlić I, Zou H, Zhang J, Li WX, Wang GT (2020) PhyloSuite: an integrated and scalable desktop platform for streamlined molecular sequence data management and evolutionary phylogenetics studies. Molecular Ecology Resources 20(1): 348–355. https://doi.org/10.1111/1755-0998.13096